

1999

Laminated Sediments of Loch Ness, Scotland: Indicators of Holocene Environmental Change

Cooper, Michael Colin

<http://hdl.handle.net/10026.1/2030>

<http://dx.doi.org/10.24382/1538>

University of Plymouth

All content in PEARL is protected by copyright law. Author manuscripts are made available in accordance with publisher policies. Please cite only the published version using the details provided on the item record or document. In the absence of an open licence (e.g. Creative Commons), permissions for further reuse of content should be sought from the publisher or author.

**Laminated Sediments of Loch Ness, Scotland: Indicators of
Holocene Environmental Change**

Michael Colin Cooper

December 1999

A thesis submitted in partial fulfilment of the requirements for the degree of **Doctor of Philosophy** in the Department of Environmental Sciences, Faculty of Science, University of Plymouth, Drake Circus, Plymouth, PL4 8AA, UK. Material published in this work, and any information derived from it, remains copyright of the author and may not be republished without prior consent.

BHDSC number DX230725

REFERENCE ONLY

UNIVERSITY OF PLYMOUTH	
Item No.	900 4061337
Date	29 FEB 2000 S
Class No.	T 551.482 600
Contl. No.	X704074388
LIBRARY SERVICES	

STORE

90 0406133 7



Author's Declaration

At no time during the registration for the degree of Doctor of Philosophy has the author been registered for any other University award. This study was financed with the aid of a studentship from the Higher Education Funding Council for England, awarded through the University of Plymouth.

Relevant scientific seminars and conferences were regularly attended at which work was often presented; external institutions were visited for consultation purposes and several papers prepared for publication.

External Contacts:

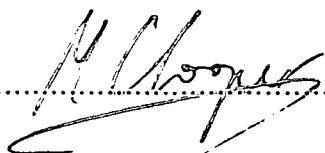
Dr K.M. Farr
School of Applied Sciences
University of Wolverhampton
Wulfruna Street
Wolverhampton
WV1 1SB

Dr A.E.S. Kemp
Department of Oceanography
University of Southampton
Southampton Oceanography Centre
European Way
Southampton
SO14 3ZH

Dr M.C. Bridge
Institute of Archaeology
University College London
31-34 Gordon Square
London
WC1H 0PY

Dr T.G. Acott
School of Earth and Environmental Sciences
University of Greenwich
Chatham Maritime
Kent
ME4 4TB

Signed



Date

3 December 1999

Contents

Declaration	i
Contents	ii
Figures	x
Plates	xvii
Tables	xviii
Acknowledgements	xxi
Papers submitted, and conferences attended	xxv

Abstract	1
-----------------------	----------

1. Introduction

1.1 Scope of research	2
1.2 Summary of aims	4

2. Literature Review

2.1 Introduction	5
2.2 Laminated sediments- origins, utilisation for chronology and as indicators of environmental change	
2.2.1 Introduction	5
2.2.2 Mechanisms of lamination formation	7
2.2.3 Laminated sediments as chronological tools	9
2.2.3.1 Use of geochronological terms within the thesis	11
2.2.4 Laminated sediments as indicators of environmental change	12
2.2.4.1 Elk Lake, Minnesota	12
2.2.4.2 Gosciarz, Central Poland	14
2.2.4.3 The sediments of Loch Ness as indicators of	

environmental change	15
2.3 Proxy climatic data- sources and dating	
2.3.1 Introduction	17
2.3.2 Types of proxy record	18
2.3.3 Dating of proxy records	19
2.3.3.1 Incremental records	19
2.3.3.2 Radiometric dating	21
2.3.3.3 Correlation with documentary evidence	23
2.3.3.4 Geomagnetic and orbitally-derived chronologies	24
2.3.4 Information gained from proxy data sources	25
2.4 Climatic context	
2.4.1 Present Climate of the British Isles	27
2.4.2 Lamb Weather types	28
2.4.3 Climate anomalies	30
2.5 Causes and nature of variability in the climate of the North Atlantic sector	
2.5.1 The North Atlantic Polar Front	30
2.5.2 Oceanic circulation	31
2.5.3 Summary of Holocene climates of NW Europe.....	33
2.5.4 Climatic teleconnections	36
2.5.4.1 The Younger Dryas cold event (YD)	38
2.5.4.2 The Holocene Hypsithermal	38
2.5.4.3 The Early Medieval optimum	40
2.5.4.4 The Little Ice Age (LIA)	40
2.6 The periodic nature of climatic and proxy-climatic time series	
2.6.1 Introduction	42
2.6.2 The nature and cause of climatic change	42
2.6.2.1 Variations in the orbit of the Earth	42
2.6.2.2 Planetary effects	43

2.6.2.3 Solar variability	45
2.6.2.4 Albedo variation	48
2.6.2.5 Quasi-Biennial Oscillation	49
2.6.2.6 North Atlantic Polar Front	51
2.6.2.7 North Atlantic Oscillation	51
2.6.2.8 Circumpolar vortex	53
2.6.2.9 El Niño Southern Oscillation (ENSO)	54
3. Site description	
3.1 Location	56
3.2 Tectonic setting	57
3.3 Morphology and Limnology	58
3.4 Climates of the North Atlantic Ocean & Loch Ness region	62
3.4.1 Major influences on the climate of the region	62
3.4.2 Deglacial climate of the Loch Ness region	63
3.4.3 Deglaciation	63
3.4.4 Deglaciation around Inverness	64
3.4.5 The present climate of the Loch Ness region	66
3.5 Description of catchment.....	68
3.5.1 Modern catchment	68
3.5.2 History and prehistory of catchment	69
3.5.2.1 The pollen record	69
3.5.2.2 Probable catchment history from the pollen record	69
3.6 Prehistoric and historic human impact upon the catchment of Loch Ness	71
3.6.1 General Chronology of settlement in Scotland from the Postglacial to present	71
3.6.2 Evidence of early settlement around Inverness and northern Great Glen.....	75
3.7 Previous research on sediments from Loch Ness	78

3.7.1 Catchment erosion studies	78
3.7.2 Atmospheric pollution	78
3.7.3 Eutrophication	79
4. Methods	
4.1 Coring	81
4.1.1 One-metre cores	81
4.1.2 Longer cores	81
4.2 Determination of percentage dry matter and percentage loss on ignition	
4.2.1 Introduction	83
4.2.2 General	83
4.2.3 Methods	83
4.2.3.1 Dry matter and water content	83
4.2.3.2 Ash content and percentage loss on ignition	84
4.3 Infrared photography	
4.3.1 General	85
4.3.2 Photographic Method	85
4.3.3 Sediment preparation	87
4.4 X-radiography	
4.4.1 Introduction	88
4.4.2 General	88
4.4.3 Exposure determination	89
4.4.4 Development of x-ray plates	90
4.5 Image analysis	
4.5.1 Introduction	91
4.5.2 Measurement and densitometry	92
4.5.3 Image enhancement	92
4.5.4 Smoothing and averaging	94
4.5.5 Histogram equalisation	95
4.5.6 Dilation and Erosion	95

4.6 Scanning Electron Microscopy (SEM)	
4.6.1 Introduction	97
4.6.2 Sample preparation	98
4.6.3 Imaging and elemental analysis.....	98
4.7 Acquisition and analysis of densitometric traces	
4.7.1 Introduction	99
4.7.2 Acquisition of densitometric data	100
4.7.3 Program operation	100
4.7.3.1 Program listing	101
4.7.4 Program structure	101
4.7.5 Analysis of densitometric traces	102
4.7.6 Computer program	103
4.7.7 Program operation	103
4.7.7.1 Program listing	103
4.7.8 Program structure	104
4.8 Compilation of datasets	
4.8.1 General	105
4.8.2 Sequencing of grey level determinations	105
4.8.3 Sequencing of lamination thickness determinations	106
4.9 Time series analysis	
4.9.1 Introduction	106
4.9.2 Estimation of randomness of extreme events	106
4.9.3 Fourier analysis	108
4.9.4 Methods	110
5. Results	
5.1 Sediment description	112
5.1.1 Core <i>LNR1</i>	112
5.1.2 Core <i>Ness 3</i>	114

5.1.3 Core <i>Ness 4</i>	116
5.2 Physical properties	
5.2.1 Percentage Dry Matter and Loss on Ignition	118
5.2.1.1 Core <i>Ness 3</i> Percentage Dry Matter	118
5.2.1.2 Core <i>Ness 3</i> Percentage Loss on Ignition	119
5.2.1.3 Core <i>Ness 4</i> Percentage Dry Matter	119
5.2.1.4 Core <i>Ness 4</i> Percentage Loss on Ignition	119
5.3 Imaging	
5.3.1 Photography of core sections	120
5.3.2 X-radiography	123
5.3.3 Scanning Electron Microscopy	123
5.4 Chronology	
5.4.1 Densitometry of x-radiographs	127
5.4.2 Core <i>Ness 3</i>	131
5.4.3 Core <i>Ness 4</i>	133
5.4.4 Core <i>LNRI</i>	134
5.4.5 Uncertainties in chronology	138
5.5 Time series analysis	
5.5.1 Sherman's statistic	139
5.5.2 Spectral analysis of the sediment record	139
6. Data Analysis	
6.1 Objectives	147
6.2 Sediment characteristics	148
6.2.1 General characteristics of Percentage Dry Matter (%DM) / Percentage Loss On Ignition (%LOI)	148
6.2.2 Core <i>Ness 3</i> , Percentage Dry Matter	149
6.2.3 Core <i>Ness 3</i> , Percentage Loss On Ignition	149
6.2.4 Core <i>Ness 4</i> , Percentage Dry Matter	150

6.2.5 Core <i>Ness 4</i> , Percentage Loss On Ignition	151
6.3 Microlithological examination	152
6.4 Photography and Image analysis	154
6.5 Chronology	157
6.5.1 Lamination counting	157
6.5.2 Radiocarbon dating	158
6.5.3 Lamination thickness	161
6.5.3.1 Lamination thickness record from core <i>Ness 3</i>	161
6.5.3.2 Lamination thickness record from core <i>Ness 4</i>	164
6.5.3.3 Lamination thickness record from core <i>LNRI</i>	168
6.6 Analysis of local climatic records	169
6.6.1 Precipitation record	170
6.6.2 Comparison of precipitation with streamflow	175
6.6.3 Occurrence of floods	176
6.7 The sedimentary record as a proxy of climatic variation	177
6.7.1 Comparison of the sediment record with precipitation	177
6.7.2 Comparison of the sediment record with temperature	178
6.7.3 The sediment record as a climatic proxy	178
6.8 Correlation with other time series	180
6.8.1 Other proxy palaeoclimate records	181
6.8.1.1 Sea ice, sea surface temperature (SST), NAO, and other climatic indices	181
6.8.1.2 Dendrochronological studies	190
6.8.1.3 Stable isotope record	195
6.8.1.4 Other isotope records	196
6.8.1.5 Other records	199
6.9 Spectral analysis	201
6.9.1 Spectral analysis of precipitation records	201
6.9.2 Spectral analysis of the sediment record	204

6.9.2.1 Core <i>Ness 3</i>	204
6.9.2.2 Core <i>Ness 4</i>	209
6.9.2.3 Core <i>LNRI</i>	210
6.9.2.4 Spectral characteristics of the NAO signal and its comparison with precipitation and lamination thickness records	211
6.9.2.5 Evolutive spectral analysis	212
6.10 Summary of analyses	216
6.11 Estimation of errors	217
6.11.1 Photography and x-radiography	218
6.11.2 Image analysis	218
6.11.3 Computer program	220
6.11.4 Chronology	221
6.11.5 Suitability of coring site	222
7. Conclusions	
7.1 Factors influencing the production of laminated sediments in Loch Ness.....	225
7.2 Summary	227
8. Further work	230
9. References	233
Appendix A X-radiographs. Core <i>Ness 3</i>	296
Appendix B X-radiographs. Core <i>Ness 4</i>	323
Appendix C X-radiographs. Core <i>LNRI</i>	352
Computer disk	Inside rear cover

Figures

1. Introduction

Figure 1.1 Organisation of the Loch Ness Research Group *ca* 1995 3

2. Literature review

Figure 2.1 Sediment dynamics within a lake and its catchment 6

Figure 2.2 Classification of laminated sediments by origin 7

Figure 2.3 Mechanism for the deposition of clastic varves 9

Figure 2.4 Record of lamination thickness from Elk Lake, Minnesota 14

Figure 2.5 Global oceanic thermohaline circulation involves the deep
waters of the North Atlantic Ocean 32

Figure 2.6 A warming trend revealed in recent Central England
temperature series 37

Figure 2.7 Variation in sunspot numbers 1750-1991 AD 45

Figure 2.8 The temperature record for Central England, compiled by
Manley (1974) 47

Figure 2.9 Correlation of solar activity, measured as flux of 10.7 cm
radiation with mean latitude of storm tracks in the North
Atlantic region 50

Figure 2.10 Location of the NAPF through the Early Holocene 51

Figure 2.11 North Atlantic Oscillation Index 52

Figure 2.12 Chronology of ENSO activity, 1860-1974 AD 55

3. Site Description

Figure 3.1 Site location (*Modified from Maitland, 1981*) 56

Figure 3.2 Seismicity of Scotland and the North of England 57

Figure 3.3 Echo sounding of transverse section of Loch Ness 59

<i>Figure 3.4</i>	Longitudinal section through Loch Ness, illustrating the basin-like structure of the profundal plain	60
<i>Figure 3.5</i>	Passage of a storm across Loch Ness.	61
<i>Figure 3.6</i>	Sites around Inverness displaying deglacial features	65
<i>Figure 3.7</i>	Frequency and strength of airflows across the Highland Region, Scotland.....	67
<i>Figure 3.8</i>	Mean monthly precipitation and temperature, Fort Augustus 1914-1994	67
<i>Figure 3.9</i>	The catchment of Loch Ness (<i>After Maitland, 1981</i>).....	68
<i>Figure 3.10</i>	Summary pollen diagram, selected taxa, from sediment core Ness 3, compared with that from Loch Tarff, Scottish Highlands	70
<i>Figure 3.11</i>	Distribution of northern tribes in the first century AD.....	73
<i>Figure 3.12</i>	Distribution of population in Scotland around the time of the first century AD.....	74
<i>Figure 3.13</i>	Distribution of Roman finds, first century AD.....	74
<i>Figure 3.14</i>	Archaeology - Inverness area.....	76
<i>Figure 3.15</i>	Archaeology - Drumnadrochit area.....	77
 4. Methods		
<i>Figure 4.1</i>	Elements of the Shine-designed 'long corer'	82
<i>Figure 4.2</i>	Spectral response of Kodak High-speed Infrared Film, with pass band of Kodak W10 filter and typical reflectivity curve for a clay mineral, montmorillonite	86
<i>Figure 4.3</i>	Diagram illustrating the method employed in order to ensure uniform illumination of the photographic field	87
<i>Figure 4.4</i>	Determination of resolution of x-radiographic technique	90
<i>Figure 4.5</i>	Densitometric trace derived from the x-radiograph in <i>Plate 4.1</i>	94

<i>Figure 4.6</i>	Densitometric trace derived from <i>Plate 4.1</i> after the application of median filtering.....	95
<i>Figure 4.7</i>	Densitometric analysis of a transect of an image after dilation	97
<i>Figure 4.8</i>	Confidence limits for interpretation of Sherman's Statistic	107
5. Results		
<i>Figure 5.1</i>	Log of core <i>LNR1</i> , indicating locations of prominent laminations	113
<i>Figure 5.2</i>	Percentage Dry Matter and percentage Loss On Ignition, core <i>Ness 3</i>	118
<i>Figure 5.3</i>	Percentage Dry Matter and percentage Loss On Ignition, core <i>Ness 4</i>	120
<i>Figure 5.4</i>	Variation of Grey Level throughout core <i>Ness 3</i> , determined from an Infrared image of the core	122
<i>Figure 5.5</i>	Variation of Grey Level throughout core <i>Ness 4</i> , determined from an Infrared image of the core.....	122
<i>Figure 5.6</i>	Screen dump of a typical EDS spectrum of material from core <i>Ness 3</i>	125
<i>Figure 5.7</i>	Typical densitometric trace obtained from analysis of x-radiographs	127
<i>Figure 5.8</i>	Variation of lamination thickness in core <i>Ness 3</i>	128
<i>Figure 5.9</i>	Variation of lamination thickness in core <i>Ness 4</i>	129
<i>Figure 5.10</i>	Variation of lamination thickness in core <i>LNR1</i>	130
<i>Figure 5.11</i>	Time/depth plot derived from lamination measurements from core <i>Ness 3</i>	135
<i>Figure 5.12</i>	Time/depth plot derived from lamination measurements from core <i>Ness 4</i>	136
<i>Figure 5.13</i>	Time/depth plot derived from lamination measurements from core <i>LNR1</i>	137

<i>Figure 5.14</i>	An example of the result from evolutive analysis of lamination thickness in core <i>LNR1</i>	146
6. Data Analysis		
<i>Figure 6.1</i>	Comparison of varve and ¹⁴ C calibrated ages from core <i>Ness 3</i>	158
<i>Figure 6.2</i>	Illustration of lamination thickness at the base of core <i>Ness 3</i>	162
<i>Figure 6.3</i>	Record of decadal totals of lamination thickness from core <i>Ness 3</i>	162
<i>Figure 6.4</i>	Record of centennial averages of lamination thickness from core <i>Ness 3</i>	163
<i>Figure 6.5</i>	Record of 200-year averages of lamination thickness from core <i>Ness 3</i>	164
<i>Figure 6.6</i>	Illustration of lamination thickness at the base of core <i>Ness 4</i>	165
<i>Figure 6.7</i>	Record of the moving average of thickness of ten laminae from core <i>Ness 4</i>	166
<i>Figure 6.8</i>	Record of centennial averages of lamination thickness, core <i>Ness 4</i>	167
<i>Figure 6.9</i>	Record of 200-year averages of lamination thickness, core <i>Ness 4</i>	168
<i>Figure 6.10</i>	Temporal variation of precipitation and temperature, Fort Augustus, 1914-1994 AD	170
<i>Figure 6.11</i>	Temporal variation of precipitation and temperature, Inverness, 1914-1994 AD	171
<i>Figure 6.12</i>	Comparison of precipitation at Fort Augustus with streamflow on the River Ness, 1974-1994	175

<i>Figure 6.13</i>	Comparison of monthly rainfall, Fort Augustus, 1992-1993, with amounts of seston collected by sediment traps	176
<i>Figure 6.14</i>	Annual lamination thickness in core <i>LNRI</i> , compared with the number of days sea ice was observed off the coast of Iceland over the period 1610 to 1963	182
<i>Figure 6.15</i>	Annual lamination thickness from core <i>LNRI</i> compared with the number of days when sea ice was observed in the Danish Sound, over the period 1764 to 1930	182
<i>Figure 6.16</i>	Annual lamination thickness from core <i>LNRI</i> compared with North Atlantic Sea Surface Temperature (NA SST), over the period 1864 to 1963	188
<i>Figure 6.17</i>	Comparison of the North Atlantic Oscillation index with lamination thickness from core <i>LNRI</i> , over the period 1890 to 1963	188
<i>Figure 6.18</i>	Comparison of annual lamination thickness from core <i>LNRI</i> with winter (JFM) NAO index	189
<i>Figure 6.19</i>	Comparison of annual lamination thickness from core <i>LNRI</i> with summer (JJA) NAO index	189
<i>Figure 6.20</i>	Regional tree ring records, AD 1300-1963 (<i>After Baillie</i>)	190
<i>Figure 6.21</i>	Record of normalised ring widths from European Larch located at Mar Lodge, Highlands, compared with annual lamination thickness from core <i>LNRI</i>	192
<i>Figure 6.22</i>	Spatial extent of correlation between dendrological datasets in Europe	193
<i>Figure 6.23</i>	Tree-ring chronology, 1940 AD to 800 AD, derived from German Oak growing in the Spessart Forest, Germany, compared with annual lamination thickness from core <i>LNRI</i>	194

<i>Figure 6.24</i>	GRIP $\delta^{18}\text{O}$ record compared with lamination thickness data from core <i>Ness 3</i>	196
<i>Figure 6.25</i>	Camp Century $\delta^{18}\text{O}$ record compared with lamination thickness data from core <i>LNRI</i>	197
<i>Figure 6.26</i>	Comparison of Grey level measurements in core <i>Ness 3</i> , atmospheric $\delta^{14}\text{C}$ and $\delta^{18}\text{O}$ in the GRIP ice core	197
<i>Figure 6.27</i>	Fort Augustus winter precipitation record compared with sunspot number, AD 1880 to AD 1990	200
<i>Figure 6.28</i>	Comparison of lamination thickness record from core <i>LNRI</i> with annual sunspot number, AD 1750 to AD 1963	200
<i>Figure 6.29</i>	Fast Fourier Transform spectrum of seasonal and annual precipitation Fort Augustus, 1886-1994	202
<i>Figure 6.30</i>	Fast Fourier Transform spectrum of seasonal and annual precipitation Inverness, 1890-1994	203
<i>Figure 6.31</i>	Fast Fourier Transform spectrum of lamination thickness data, core <i>Ness 3</i> , section 1 (<i>ca</i> 2.5 ka to 3.2 ka BP)	205
<i>Figure 6.32</i>	Fast Fourier Transform spectrum of decadal totals of lamination thickness, core <i>Ness 3</i> , section 1	206
<i>Figure 6.33</i>	Fast Fourier Transform spectrum of lamination thickness data, core <i>Ness 3</i> , section 2 (<i>ca</i> 3.2 ka to 4.9 ka BP)	206
<i>Figure 6.34</i>	Fast Fourier Transform spectrum of decadal totals of lamination thickness, core <i>Ness 3</i> , section 2	207
<i>Figure 6.35</i>	Fast Fourier Transform spectrum of lamination thickness data, core <i>Ness 3</i> , section 3 (<i>ca</i> 5.9 ka to 8.7 ka BP)	208
<i>Figure 6.36</i>	Fast Fourier Transform spectrum of decadal totals of lamination thickness, core <i>Ness 3</i> , section 3	208
<i>Figure 6.37</i>	Fast Fourier Transform spectrum of lamination thickness data, core <i>Ness 4</i>	209

<i>Figure 6.38</i>	Fast Fourier analysis of lamination thickness from core <i>LNRI</i> , over the period 1321-1963 AD	210
<i>Figure 6.39</i>	Fast Fourier Transform spectrum of the NAO index, 1876-1996 ...	212
<i>Figure 6.40</i>	FFT spectrum from core <i>LNRI</i> compared with that from analysis of the NAO index	213
<i>Figure 6.41</i>	Evolutionary Fourier spectrum of elements of periodicity contained within core <i>Ness 3</i>	214
<i>Figure 6.42</i>	Evolutionary Fourier spectrum of elements of periodicity contained within core <i>Ness 4</i>	215
<i>Figure 6.43</i>	Evolutionary Fourier spectrum of elements of periodicity contained within core <i>LNRI</i>	215
<i>Figure 6.44</i>	Graphical presentation of linearity check of image field of Quantimet image analyser	220

7. Conclusions

<i>Figure 7.1</i>	Flow chart summarising the factors influencing the formation of annually laminated sediments in the north basin of Loch Ness ...	228
-------------------	---	-----

Plates
4. Methods

- Plate 4.1* Image of an x-radiograph of a section of laminated sediment 93
- Plate 4.2* Image of a transect from *Plate 4.1*, after undergoing a series
of horizontal dilation transforms..... 96

5. Results

- Plate 5.1* Monochrome Infrared photograph of core *Ness 3* 115
- Plate 5.2* Monochrome Infrared photograph of core *Ness 4* 117
- Plate 5.3* Photograph, with monochrome Infrared sensitive film,
illustrating a section of core *Ness 3* 121
- Plate 5.4* Photomosaic of SESEM images illustrating the lack of change
in lithology between (upper images) dark clay-rich, and
(lower images) pale silt-rich, laminae 124

6. Data Analysis

- Plate 6.1* A photomosaic BSEI image of a section from core *Ness 4*.
The sediment is of Mid-Holocene age 155
- Plate 6.2* BSEI photomosaic of early-Holocene material, obtained
by Dean (Unpubl.). The general lack of contrast between
layers at the base of the section is well displayed 159

Appendix A

- X-radiographs of sections from core *Ness 3* 296

Appendix B

- X-radiographs of sections from core *Ness 4* 323

Appendix C

- X-radiographs of sections from core *LNR1* 352

Tables
2. Literature review

<i>Table 2.1</i>	Time resolution and duration of primary climatic proxy data sources	19
<i>Table 2.2</i>	Proxy sources - Ice cores	25
<i>Table 2.3</i>	Proxy sources - Tree rings	26
<i>Table 2.4</i>	Proxy sources - Marine.....	26
<i>Table 2.5</i>	Proxy sources - Lacustrine sediments	27
<i>Table 2.6</i>	General weather characteristics associated with Lamb "airflow types" over the British Isles	29
<i>Table 2.7</i>	Summary of Holocene climatic divisions	34

3. Site description

<i>Table 3.1</i>	Summary of morphological characteristics of Loch Ness	58
<i>Table 3.2</i>	Hydrological data for Loch Ness	59

4. Methods

<i>Table 4.1</i>	Techniques employed in this study, illustrating their purpose	80
<i>Table 4.2</i>	Sample designations for SEM analyses	99

5. Results

<i>Table 5.1</i>	Designation of sediment cores analysed in this study	112
<i>Table 5.2</i>	Subdimensions of core <i>Ness 3</i> . Designations are those used to describe x-ray images	114
<i>Table 5.3</i>	Summary of sectional lengths of core <i>Ness 4</i> . Section designations are those used to describe x-ray images	116
<i>Table 5.4</i>	Results of EDS analyses of unpolished, impregnated samples. Results of ZAF-corrected EDS analyses	126

<i>Table 5.5</i>	Typical output data produced by the lamination detection software	131
<i>Table 5.6</i>	Summary of radiocarbon age determinations from core <i>Ness 3</i>	133
<i>Table 5.7</i>	Summary of characteristics of samples submitted for ^{14}C analysis	134
<i>Table 5.8a</i>	Sherman's statistic for core <i>LNRI</i> maxima ($\geq \text{mean}+2\sigma$)	140
<i>Table 5.8b</i>	Sherman's statistic for core <i>LNRI</i> minima ($\leq \text{mean}-1\sigma$)	141
<i>Table 5.9a</i>	Sherman's statistic for core <i>Ness 3</i> , section 1	
	maxima ($>\text{mean}+2\sigma$)	142
<i>Table 5.9b</i>	Sherman's statistic for core <i>Ness 3</i> , section 2	
	maxima ($>\text{mean}+2\sigma$)	143
<i>Table 5.9c</i>	Sherman's statistic for core <i>Ness 3</i> , section 3	
	maxima ($>\text{mean}+2\sigma$)	144
<i>Table 5.10</i>	Summary of the periodicities found by FFT analyses of cores <i>Ness 3</i> , <i>Ness 4</i> , and <i>LNRI</i>	145
6. Data Analysis		
<i>Table 6.1</i>	Elements detected by EDS in sediments from Loch Ness, with their average abundance	153
<i>Table 6.2</i>	Correlation between annual and seasonal precipitation at Fort Augustus, 1886-1963 ($\nu=78$)	172
<i>Table 6.3</i>	Correlation between annual precipitation, and average and seasonal temperatures, Fort Augustus, 1914-1995 ($\nu=81$)	173
<i>Table 6.4</i>	Correlation between annual and seasonal precipitation at Inverness, 1890-1963 ($\nu=71$)	173
<i>Table 6.5</i>	Correlation between annual precipitation, and average and seasonal temperatures, Inverness, 1914-1995 ($\nu=81$)	174
<i>Table 6.6</i>	Correlation between annual and seasonal precipitation at Inverness and Fort Augustus, 1914-1994 ($\nu=78$)	174
<i>Table 6.7</i>	Correlation of annual lamination thickness from core <i>LNRI</i> with seasonal precipitation record,	

Fort Augustus, 1886-1963 ($v=78$)	177
<i>Table 6.8</i> Correlation of annual lamination thickness from core <i>LNRI</i> with seasonal precipitation record, Inverness, 1890-1963 ($v=74$)	178
<i>Table 6.9</i> Correlation between lamination thickness from core <i>LNRI</i> , North Atlantic sea surface temperature, and the persistence of sea ice around the coast of Iceland and in the Danish Sea	183
<i>Table 6.10</i> Results of correlation analysis between three-monthly-resolved NAO index and lamination thickness from core <i>LNRI</i> (decadal averages)	184
<i>Table 6.11</i> Correlation between monthly NAO index (N), and precipitation data for Fort Augustus (F), 1890 to 1993 ($v=103$)	185
<i>Table 6.12</i> Correlation between monthly NAO index (N), and precipitation data for Inverness (I), 1890 to 1993 ($v=103$)	186
<i>Table 6.13</i> Correlation between lamination thickness from core <i>LNRI</i> , and tree ring data from Scotland, Ireland, and the English Midlands	191
<i>Table 6.14</i> Pearson correlation coefficients for data plotted in <i>Figure 6.27</i>	198
<i>Table 6.15</i> Stages of analysis during which significant errors may have occurred	218
<i>Table 6.16</i> Linearity of image field of Quantimet 570 image analyser	219

Acknowledgements

Over the past five years I have felt extremely privileged to have been given the opportunity to study for a higher academic award. During this time I have had contact with numerous people, both at meetings and, again, on more informal occasions. Many have great academic standing, and I feel a sense of honour in meeting them all. I am very grateful for all their comments and advice.

Of immediate connection with this thesis, I would first and foremost extend my deepest thanks to my supervisors, Dr. Paddy O'Sullivan and Prof. Steve Rowland. Without their forbearance, perseverance and great encouragement from the beginning, I would not be at this stage now. In particular, Dr. O'Sullivan must be profusely thanked for his input to my many attempts at producing well-written reports and articles. His tireless reminders of the elements of good scientific writing have left a great impression upon me. Unfortunately, I am still wont to lapse from time to time. I am also grateful to him for displaying great patience and compassion throughout, but especially during the 'difficult' period of writing up. I would also like to thank my examiners, Prof. J.J.Lowe and Dr. Dan Charman, for a most interesting *viva voce*, and for their patience in waiting for me to prepare this final manuscript.

I would like to thank the other members of the Loch Ness Research Group, especially Adrian and Maralyn Shine, who have worked tirelessly, often with quite rudimentary equipment, in order to obtain sediment cores from what must be one of the most difficult on-shore sites in the UK. A warm thank-you also goes to John Minshull, in whose hands we entrust ourselves when we venture out onto the waters of the Loch. In addition, mention must also be made of the financial assistance provided by Swatch, of Switzerland, and input from Loughborough University, in connection with the construction of equipment by which the 'long' cores were recovered.

Members of other academic institutions, who have long-running projects studying the Loch, have also been a source of great encouragement and friendship. Anne Wheeler and Dr. Kate Farr (University of Wolverhampton), Dr Vivienne Jones (UCL), Dr. Sylvia Peglar (University of Bergen) and finally, Dave Bull, Dr. Jenny Pike, Jean Dean, Steve Hunt, Dr. Justin Dix and Dr. Alan Kemp (University of Southampton) merit special mention.

Throughout this project, daily journeys back and forth between University and Home were necessary, and would have been much more onerous without the regular companionship of a cohort of fellow passengers ('customers' in New Railspeak). I hold dear in my heart thoughts of Gareth Davey, Donna, Brian Fossey and Sir James Hill of Dawlish, who unfailingly managed to provide levity through breakdowns, delays, and the 'wrong type of rain'. Occasional on-train appearances by Dr. Malcolm Nimmo provided more academically-inclined journeys, in addition to Dr. Karen Stapleton, who furnished a lengthy overview of Fourier Transform techniques during one particularly slow trip. Regular travelling also enabled me to make friends with many of the train staff of Regional Railways and Inter-City, who often provided 'inside information'.

Friendships within the University were also forged, providing the camaraderie so often necessary when the going gets rough. Sharing an office with Dr. Helen Wilson and Derek Henon proved to be a great pleasure, and supplied hours of intense discussion about diverse topics, some even relevant to our respective projects. Dr. C. Anthony Lewis is to be thanked for the many times his droll sense of humour lightened the day. The other members of Dr. O'Sullivan's postgraduate team, Paula Powell, Tamsin Williams, Neil Salter, and Nina Matthews are also fondly remembered. I wish Martin Nicholson well as the latest member, who will concentrate some of his time in continuing this work.

The technical staff at Plymouth unfailingly provided first-class support. Betty Fox (now retired) is warmly thanked for her photographic expertise, which enabled many

fine images to be obtained from lengths of mud, and Paul Russell for introducing me to the pleasures and pitfalls of image analysis, both techniques, of course, essential to this project. I would also like to thank Dr. Roy Moate, Brian and Jane of the Electron Microscopy Unit for assistance, guidance, tea and biscuits. In addition, Brian and Adrian, who built (and re-built) a new type of freeze-sampler, and Trevor Parrot, Master of the University vessel 'Catfish', are to be acknowledged for their expertise. I would finally like to thank Ian Doidge, Andy Barker and Andy Tonkin for all their help, Ian proving invaluable on many occasions during the construction and testing of the freeze corer, often obviating the need for a winch or other such lifting device.

After I left Plymouth and gained remunerative employment at the University of Nottingham, others have provided elements of support. I would briefly like to thank Drs Mike Hey, Nick Miles, Brian Atkin, Douglas Brown, Trevor Jones, Chandhu Shah, Gareth Brown, and in addition, Tony Hollingworth, Brian Clarke, Dan Jackson, Piers Evershed, Channan Tiranarat, Alison Blackshaw, Chris Elverson, and Phill Windsor.

Friendships forged outside 'working' hours are particularly invaluable and help to provide a balance between the worlds of academia and 'real life'. I am indebted to Chris Jenkins, and his wife Jan, for their friendship now and throughout the past few years, sometimes through times of great personal distress. Warm thoughts of past times together will remain forever, and I wish them luck in their new life in Australia.

This would not be complete without thanks to my own family, who have had to endure nearly eight years of difficulty in order that I might have the opportunity to study for a higher degree. They have supported me financially, physically, emotionally and spiritually throughout that time. Amanda, Rowan and Oliver, I give you all my love and thanks. In addition, we have also been lucky to have had the support of our respective parents, who have been a great help when necessary.

Finally, the lyrics of a song come to mind, not only for their poignancy, but, as the title intimates, those who think that three years are more than sufficient to complete a PhD.....

Across the evening sky
All the birds are leaving...
But how can they know
It's time for them to go?
Before the winter fire
I will still be here
I have no thought of time
For who knows where the time goes?
Who knows where the the time goes?

Sad, deserted shore
Your fickle friends are leaving...
Ah, but then you know
Its time for them to go
But I will still be here
I have no thought of leaving
I do not count the time
For who knows where the time goes?
Who knows where the time goes?

And I am not alone
While my love is near me
I know it will be so...
Until it's time to go
So come the storms of winter
And then the birds in spring again
I have no fear of time
For who knows how my love grows?
And who knows where the time goes?

Lyrics of "Who knows where the time goes?" written by the late Sandy Denny, and published by NCB/Sandy Denny © Island Records Ltd. 1972.

Papers submitted, and conferences attended

During the programme of study, papers detailing work undertaken were submitted for publication, and conferences attended where oral presentations, or posters, were given.

a) Papers published, in press, or in preparation:

Acott T.G., Wells A.J., Bennett K., Cooper M.C. & Winterbottom S. (In proof). The use of digital image analysis in Environmental Science. *Progress in Physical Geography*.

Cooper M.C. 1998. The Use of Image Analysis techniques in the study of laminated sediments. *Journal of Paleolimnology*. **19**. 33-40.

Cooper M.C. & O'Sullivan P.E. 1998. The laminated sediments of Loch Ness, Scotland: Preliminary report on the construction of a chronology of sedimentation and its potential use in assessing Holocene climatic variability. *Palaeogeography, Palaeoclimatology, Palaeoecology*. **140**. 23-31.

Cooper M.C., O'Sullivan P.E. & Shine A.J. The record of climatic variability in the Holocene laminated sediments of Loch Ness, Scotland. Paper presented at the 2nd annual workshop of the European Lakes Drilling Program, Kraków, Poland. 23-26 October 1997. Submitted to *Quaternary International*.

Cooper M.C., O'Sullivan P.E., Shine A.J., Peglar S.M., Matthews N.M., Salter N.C.J., Henon D.N., Jones V.J., Williams T.S.C., Nicholson M.J., Sandford R.E. & Morris A. The environmental record in the Holocene laminated sediments of Loch Ness, Scotland- an outline. Submitted to *Journal of Paleolimnology*.

Cooper M.C., O'Sullivan P.E., Harkness D.D., Lawson E.M., Bull D.J., Kemp A.E.S., Peglar S.M., Matthews N.M., Jones R.I. & Shine A.J. 1998. ^{14}C dating of laminated sediments from Loch Ness, Scotland. Paper presented at the XVth International Radiocarbon Conference, Groningen, The Netherlands. 16-20th June, 1997. *Radiocarbon*. **40**. 781-793.

b) Conferences and workshops attended, seminars given.

University of Plymouth, Department of Environmental Sciences, Postgraduate Seminar series. One seminar given annually, 1993-1996.

First Workshop of the Loch Ness Research Group, University of Wolverhampton. 8-9 June 1994. Report presented:- *Use of digital image analysis for the investigation of Loch Ness sediments.*

15th International Radiocarbon Conference, Glasgow, Scotland. 15-19 August, 1994. Poster presented:- *Preliminary investigation of laminated sediments from Loch Ness-towards a lacustrine calibration.*

Inaugural meeting of IGCP Project 374-International Geological Correlation Programme between Marine and Lacustrine sediments. University of Southampton. 7-9 September 1994.

First International Limno-Geological Congress ILIC95, Copenhagen, Denmark. 21-25 August 1995.

IGCP 374 International Meeting. Burlington House, London. 14-18 October 1996. Report presented to Field Visit at the Loch Ness Field Centre, Drumnadrochit, Scotland:-

The laminated sediments of Loch Ness as indicators of climatic change.

University of Plymouth, Department of Geological Sciences. 31 October 1996. Research seminar programme. Presentation to staff and postgraduate students (*Co-presented with Dr. P.E. O'Sullivan*).

Abstract

Sediment cores, two approximately 6 metres and one about 1 metre in length, were recovered from the profundal plain of the northern basin of Loch Ness, Scotland. Examination revealed that the sediment is composed of irregular sequences of pale and dark laminations, most sub-millimeter in thickness, some *ca* 5 mm thick.

Enumeration of laminae, and determination of lamination thickness, was carried out using X-radiography and image analysis. A hypothesis was developed that the finer laminations represent varves. This was tested by means of lamination counting, and by radiocarbon dating of material from one 'long' core. Comparison of the two chronologies thus derived suggested that the hypothesis was correct, and that a non-continuous chronology had been obtained, spanning the period *ca* 9000 to 1500 BP.

Lamination thickness data derived from recent sediments was compared with meteorological data, especially rainfall, in order to test the hypothesis that prevailing climate, together with the alignment of the Loch with the predominantly southwesterly airflow, mediates in the production of the volume of allochthonous mineral material eroded from the catchment and its input to the water column. The result of this analysis has proved inconclusive, and a more complex relationship may be involved. Other proxy climatic data were utilised in order further to investigate this aspect of the study and correlations between the sediment record and several of these were shown to be statistically significant. Spectral analysis of the lamination thickness datasets was also employed in order to determine if patterns of sedimentation may be linked to periodic forcing processes. Cyclicities observed in recent sediments include those of *ca* 210 and *ca* 90 years, which are also present in many other climatically-related records. Analysis of lamination thickness in the 'long' cores has proved inconclusive, producing evidence of many periodicities, but few of significance. It is believed that this result may be attributed to the non-stationary behaviour of forcing agents through time.

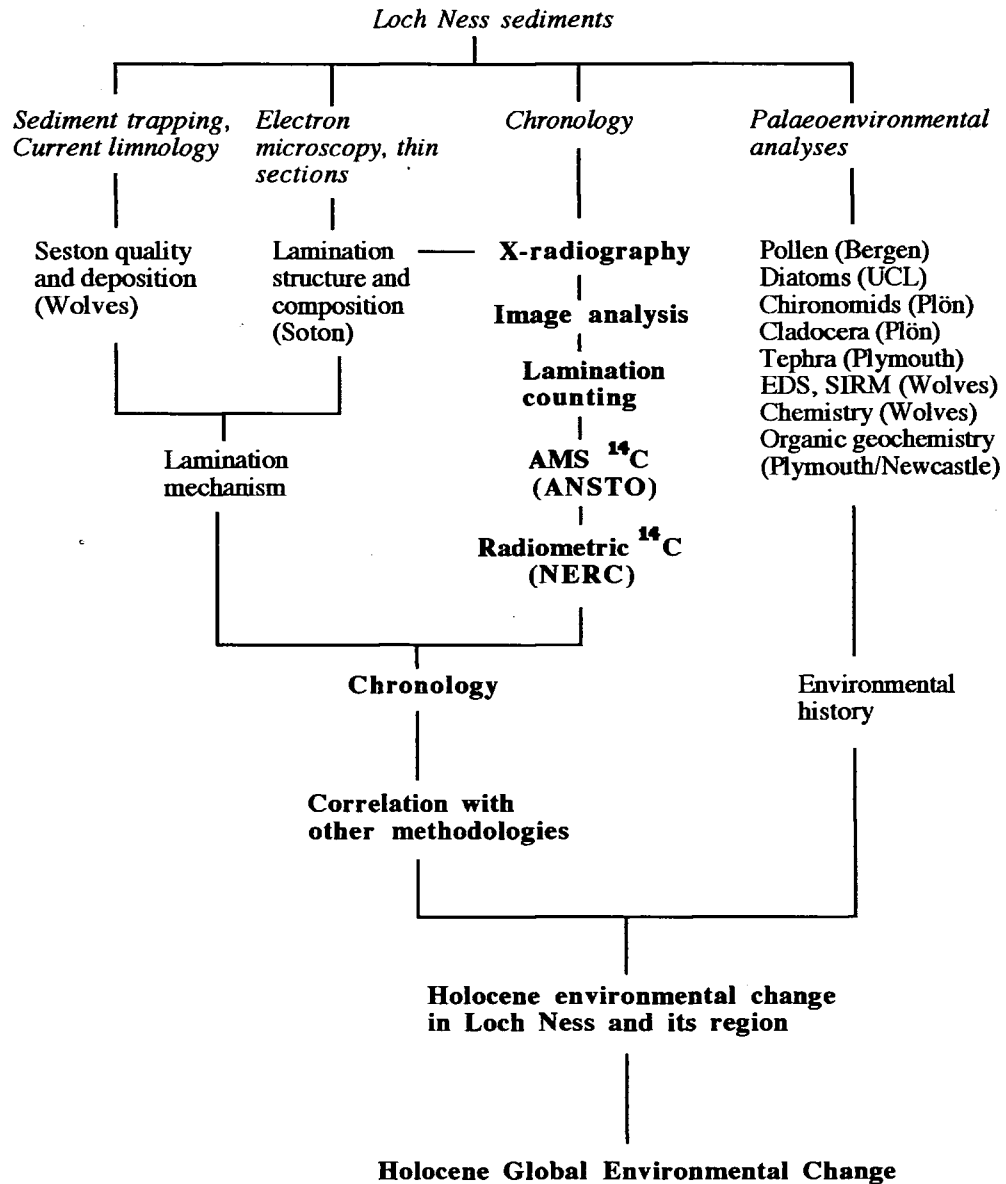
1.Introduction

1.1 Scope of research

Lake sediments provide a medium in which a record of past environments may be captured and stored (Pennington, 1981). Deposits which are, in addition, annually laminated may be utilised in order to impose a temporal framework on any observed variations in chemical or lithological properties arising from environmental change. Comparison of these proxy records with others from different natural systems, and from differing spatial locations enables a more complete synthesis of the effects of climatic forcing to be appreciated.

The investigations of this project were undertaken as part of a multi-institutional, multi-national group (*Figure 1.1*), formed with the purpose of analysing sediment cores recovered from Loch Ness, Scotland. When these sediments were discovered to be laminated, a hypothesis was formulated that the layers may represent annual laminae, or *varves*. If this proved to be the case, then other proxy records, such as those obtained by diatom and pollen analyses would be able to be dated to a high precision. Loch Ness would then represent a unique archive of data detailing palaeoenvironmental change in the North Atlantic region.

Recovery of cores proved to be difficult and time-consuming, but two *ca* 6 m and one *ca* 1 m long cores were obtained. Attempts to count laminae, both by visual inspection of freshly cut material and by photography, proved ineffective and it was decided that a combination of x-radiography and image analysis would prove suitable. Software was written in order to convert the results of image analysis into time series suitable for comparison with other palaeoenvironmental indices.



Topics highlighted in **bold** will be addressed by this study

Key to participating institutions:

ANSTO: Australian National Scientific and Technical Organisation

Bergen: University of Bergen, Department of Botany

Newcastle: University of Newcastle, Organic Geochemistry Research Group

Plön: Max Planck Institut für Limnologie

Plymouth: University of Plymouth, Department of Environmental Sciences

Soton: University of Southampton, Department of Oceanography

UCL: University College, London, Environmental Change Research Centre

Wolves: University of Wolverhampton, School of Applied Sciences

Figure 1.1 Organisation of the Loch Ness Research Group ca 1995 (After O'Sullivan, 1994a)

1.2 Summary of aims

To summarise, the aims of this study were fourfold:

- To utilise imaging techniques in order to enhance the sometimes indistinct lamination structure of the sediments.
- To count the laminations using image analysis techniques and subsequently produce a chronology of sedimentation relevant to the coring site.
- To utilise the data produced above to determine, by comparison with other proxy climatic datasets, whether or not the sediments have reflected changes in Holocene climatic conditions over the Scottish Highlands and the northeastern Atlantic Ocean.
- To analyse the spectral signature of the time series, in order to ascertain whether or not they contained periodicities which could be attributed to external forcing processes.

2. Literature Review

2.1 Introduction

The scope of this study has entailed the consideration of four main areas of research, in order to formulate a strategy by which the data from sediments recovered from Loch Ness may be analysed. These were i) the formation of laminated sediments and their utilisation as dating tools and palaeoclimatic indicators; ii) the concept of proxy data and their application to the investigation of past environments; iii) the study of climatic systems prevailing over the North Atlantic region, in order to appreciate the variability of meteorological data and to compare signals in sedimentary sequences with possible climatic origins; iv) a study of the periodic nature of natural systems, again with a view to understanding the nature and origins of any cyclic variation inherent in data gained from the study of sediments from Loch Ness.

2.2 Laminated sediments- origins, utilisation for chronology and as indicators of environmental change

2.2.1 Introduction

Lake sediments form a record of long- and short-term variations in both the quantity and quality of material entering a water body from its catchment. They consist of authigenic, allogenic and biogenic fractions (Engstrom & Wright, 1984; Battarbee, 1991; *Figure 2.1*). The effects upon sedimentation (in terms both of quantity and quality) caused by changes in the environment external to a lake, including variations in climate and changes to its catchment (Pennington, 1981), are complex and subject to many influences. These may act to vary both the quantity and quality of deposition either by effecting changes in the limnology of the lake so that sedimentation patterns may be disturbed, or by causing differing types and amounts of sediment to be deposited.

In laminated lake sediments, seasonal changes of deposition in lacustrine systems may be well preserved, giving rise to material exhibiting regular, rhythmic changes in lithology, texture or other physical and/or chemical characteristics. The term *varve* may be used for the sequence of laminations representing an annual cycle of variation in sedimentation (*Figure 2.2*). In passing, it may be noted that varved sediments are not confined to the lacustrine environment, but also occur both in marine (Jonsson *et al.*, 1990; Kennedy & Brassell, 1992; Kemp, 1990; Schimmelmann *et al.*, 1992; Pike & Kemp, 1996; Pokras & Winter, 1987) and riverine (Sonett *et al.*, 1992) environments. Discussion will focus here, however, on the origins and utilisation of lacustrine laminated sediments.

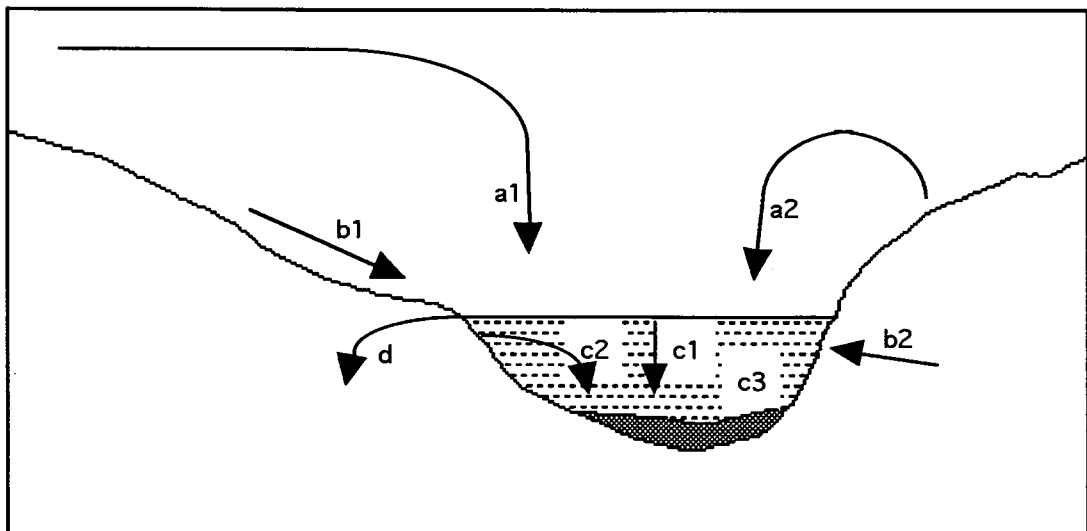


Figure 2.1 Sediment dynamics within a lake and its catchment, *a1*: sources beyond catchment; *a2*: sources within catchment; *b1* streams; *b2*: groundwater; *c1*: plankton; *c2*: littoral flora/fauna; *c3*: benthic flora/fauna; *d*: outflow losses (After Battarbee, 1991)

By carefully counting varves it is possible to date lacustrine deposits precisely (O'Sullivan, 1983; Zolitschka, 1991). Development of a such a chronology may aid in reconstruction of the palaeoenvironment of a lake and its catchment (Battarbee, 1991),

often over long periods and with high temporal resolution. Anderson and Dean (1988) have reviewed the variations in 'style' of varve throughout time and note that some elements of modern laminated sediments may be found even in the Precambrian. Changes in more recent examples, for instance from the Tertiary, reflect evolutionary processes involving the organic components.

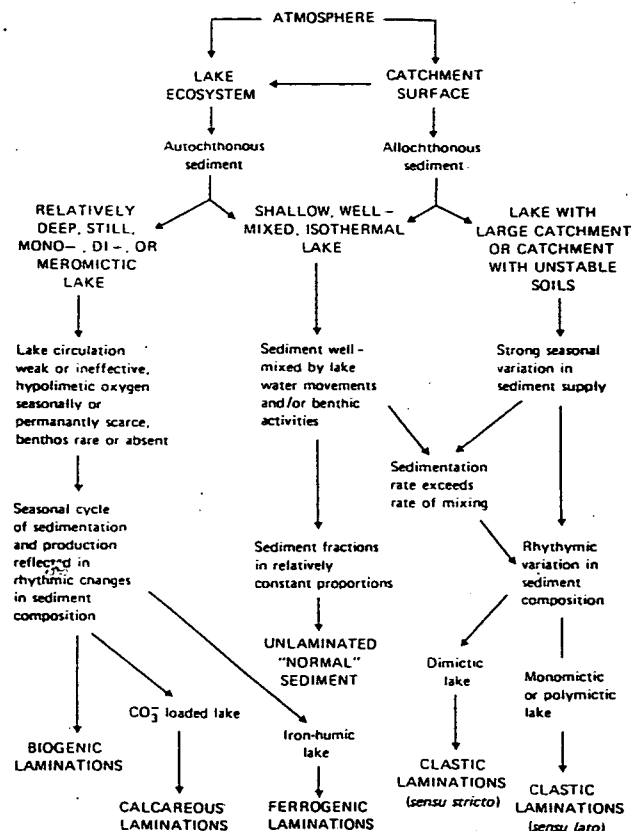


Figure 2.2 Classification of laminated sediments by origin (O'Sullivan, 1983).

2.2.2 Mechanisms of lamination formation

Laminated sediments occur where there is rhythmic variation in the amount and type of material delivered to the sediment/water interface. Generally, there is a difference in sedimentation between seasons, with laminae deposited in winter usually consisting of coarse detritus with a high mineral content, and summer layers often

containing diatom frustules (Håkanson & Jansson, 1983) or alternatively, a high proportion of calcium carbonate (Kelts & Hsü, 1978; Ludlam, 1979). Deposits from one season are usually pale in appearance and others, dark. Occasionally, however, only minor seasonal differences in sedimentation occur, and laminae may not be visible in a core when initially recovered. In this case, drying of a portion of the material may lead to spalling of laminae from each other, revealing the true structure (Ludlam, 1969). Alternatively, exposure to the air may lead to one or more components of the matrix being identified by oxidation, confirming seasonality (Renberg, 1981).

Laminations are often formed in anoxic or anaerobic environments, beneath a permanently, or semi-permanently deoxygenated hypolimnion, where bioturbation is negligible, and resuspension from wind-induced mixing absent (O'Sullivan, 1983). Thus many deep lakes may be found to contain laminated sediments (for example, Lake Malawi: Pilskałn & Johnson, 1991; Lake Van: Kempe & Degens, 1979). Meromixis is not a prerequisite, however (Dickman, 1979), since varves have been discovered in holomictic lakes where seasonal deoxygenation of the hypolimnion occurs (Renberg, 1981). In addition, morphometry of the water body is of importance, in order to permit the undisturbed sedimentation of material without slumping or lateral motion (O'Sullivan, 1983).

Varves may be produced in aerobic environments where sedimentation rate is high and faunal populations low (Lotter & Sturm, 1994). Sturm (1979) has suggested that for the formation of clastic (minerogenic) varves within an oligotrophic lake, deposition must be intermittent and matched to stratification (*Figure 2.3*). Miller (1994) has categorised the causes of lamination into four types, producing deposits which may be seasonal, occasional, lagoonal or brackish in origin. O'Sullivan (1983) has classified laminated lacustrine sediments by composition and includes those produced by detrital sedimentation, by organic processes and by chemical methods (*Figure 2.2*). Lotter and Sturm (1994) have utilised a simplified version of this scheme to categorise deposits

recovered from several Swiss lakes, including the Brienzensee (where clastic sedimentation predominates), and the biochemical deposits of the Greifensee, the Zürichsee, Baldegersee, Faulenseemoos and Soppensee. The last two are reported to contain long sequences of varves, in the case of Soppensee, some 15 000. Records of such duration and resolution provide the opportunity to investigate many aspects of environmental change with unprecedented accuracy.

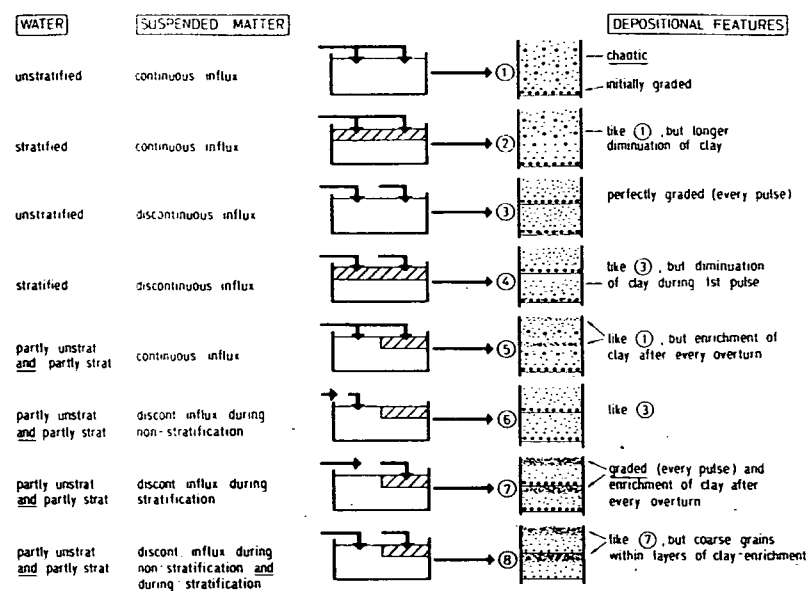


Figure 2.3 Mechanism for the deposition of clastic varves (After Sturm, 1979)

2.2.3 Laminated sediments as chronological tools

Of great importance in the study of laminated sediments is the identification of a signal of periodicity, and especially of the annual cycle of deposition. The counting of varves may produce a chronology which, ideally, is accurate to ± 1 year, and against which other data illustrating environmental change (pollen analysis: Allison *et al.*, 1986; diatom analysis: Battarbee, 1991; industrial pollution: Renberg & Wik, 1985) may be placed in historical context. Varves may thus be directly compared with tree-rings, and the

growth bands observed in corals.

Enumeration of laminations is, however, fraught with difficulty. Changing sedimentation patterns within a water body may lead to the formation of inter-annual layers, or of laminae which are indistinct, ill-formed or missing entirely. Processes within the lake cause diagenetic changes, bioturbation, or relocation of sediments out of sequence, as in the case of turbidites. Many techniques with which to investigate the structure, integrity and periodicity of laminated sediments (periodicity of pollen grains: Peglar *et al.*, 1984; succession of diatoms: Simola, 1977; Farr *et al.*, 1990; seasonality of chrysophyte cysts: Peglar *et al.*, 1984; organic geochemistry: Farr *et al.*, 1990; adhesive tape peels: Simola, 1977; light microscopy of thin sections: Merkt, 1971; scanning electron microscopy: Kemp, 1990, 1996; X-ray spectroscopy: Alapieti & Saarnisto, 1981; X-radiography: Koivisto & Saarnisto, 1978; Bodbacka, 1985) are available. Finally, without some means of independent calibration, for example radiocarbon dating, or without detailed comparison with other comparable time series (*eg* tree rings), the investigator can never be completely certain that the signal they are examining is annual in origin.

Other, parallel, dating techniques may also be utilised in order to test whether or not laminations are varves (e.g. ^{210}Pb : Appleby *et al.*, 1979; ^{14}C : Björck, 1987; $^{239,240}\text{Pu}$: Jaakkola *et al.*, 1983; ^{137}Cs : Stihler *et al.*, 1992; palaeomagnetism: Björck, 1987; Thompson, 1973; Sandgren, 1993; tephrochronology: Leonard, 1995). However, the reverse also applies, in that accurately-counted varved sediments may be used to provide time scales against which chronologies derived from radiometric and other dating techniques, may be calibrated (Hajdas *et al.*, 1993; Oldfield *et al.*, 1994; Wohlfarth *et al.*, 1993). Of current interest is the correlation of varve chronologies with those produced from dating by ^{14}C (Björck *et al.*, 1996; Goslar *et al.* 1992; Hajdas *et al.*, 1993; Zolitschka, 1991). It has been found that, owing to the variable rate of annual production of ^{14}C (Creer, 1988; Stuiver, 1980b), the tree-ring calibration curve for this technique

contains plateaux where multiple calendrical dates exist for a single radiocarbon age (Stuiver & Reimer, 1993).

The intention of de Geer to correlate his 'Swedish Chronology', derived from sequences of glacial laminations, with annual lamination sequences globally, ultimately failed owing to (a) lack of precision of the timescale then available, (b) understanding of the processes involved in the formation of laminae, and (c) the lack of sequences from sites elsewhere. Subsequent investigations have refined the Swedish Time Scale, but many difficulties need to be overcome before the realisation of an 'absolute' chronology for the Late Quaternary is achieved (Fromm, 1980; Tauber, 1980; Wohlfarth *et al.*, 1993).

2.2.3.1 Use of geochronological terms within the thesis

Discussion of laminated sediments as chronological indicators may involve use of different age scales when dating, for example, variations in determinands or events associated with these changes. Thus, documented events may conveniently be dated by reference to a calendar, usually the Christian one, and quoted as *x* AD or *y* BC (*or CE and BCE*). When referring to results obtained by ¹⁴C dating, uncalibrated radiocarbon dates are reported as *x* 14C yr BP (Before Present; 1950 AD) or, after calibration (for instance, Stuiver & Reimer, 1993), as *x* cal yr BP. Time periods obtained by lamination (varve) counting may be quoted as *x* varve years or, more properly in the case of a chronology determined from Loch Ness sediments, *x* Ness varve years. The equivalence of calendar and varve years must be proven before these terms may be considered interchangeable. The Loch Ness chronology is, at present, floating and the use of Ness varve years is implicit throughout this thesis when referring to data obtained from cores *Ness 3* and *Ness 4*. Core *LNRI*, however, contains a marker horizon which may be correlated with the occurrence of a flood event in the catchment (V.J.Jones *et al.*, 1997), and the chronology derived from this core may be considered fixed. Correlation of data from this core with other palaeoclimatic datasets indicates that Ness varve years are probably

equivalent to calendrical years.

2.2.4 Laminated sediments as indicators of environmental change

The utilisation of laminated sediments in the study of environmental change may be considered to have begun around the turn of the 20th Century, with the work of de Geer, who, from studying glacial deposits, compiled a chronology for the retreat of the Baltic Ice Lake at the end of the last Glaciation (Boyle, 1993). Many investigations, from many regions of the world, have used the accuracy inherent in laminated sediments in order to place indicators of palaeoecological change, from both natural and anthropogenic causes, within a temporal framework (Lotter, 1991a). It is clearly impossible to cite every such investigation, but it may be instructive to select two cases with which to illustrate the advantages of studying this type of sediment in connection with the quantification of change, both at catchment and regional levels.

2.2.4.1 Elk Lake, Minnesota

Elk Lake is, at present, situated in a climatic zone influenced by the position of the North Atlantic Polar Front (NAPF), which separates cold, dry Arctic airflows from the warmer, moister tropical Atlantic airstreams. In addition, the region is subjected to dry Pacific air masses, producing intense climatic gradients across the state of Minnesota (Anderson, 1993). Throughout the Holocene the region has undergone periods of profound climatic change as the position of the NAPF has varied, causing shifts in the location of the forest-prairie ecotone, and altering catchment vegetation cover, lake levels and water chemistry. These have consequentially affected sedimentation within the lake, which took place in three distinct phases. These are superimposed upon a continuous laminated sequence of some 10,400 varves, which record climatic changes as variations in thickness and composition (Anderson, 1993; *Figure 2.4*). It is postulated that the varve record is accurate to within ± 200 yr. Studies of modern sedimentation processes, lake

biogeochemistry, and indigenous flora and fauna, have enabled reconstruction of changing environments within the region throughout the Holocene (Bradbury & Dieterich-Rurup, 1993; Nuhfer *et al.*, 1993; Sanger & Hay, 1993; Whitlock *et al.*, 1993; Zeeb & Smol, 1993).

During deglaciation, coarse sediments, along with plant debris and Boreal aquatic ostracoda, accumulated in the newly-formed depression in the melting ice. When this had completely melted, varved sediments began to form in an environment of spruce and birch forest. Seasonal anoxia may have produced the alternating dark and pale, sharply defined laminae which persisted until, at *ca* 8 ka BP, forest was replaced by oak savanna. Then, from *ca* 8 ka until *ca* 4 ka BP (the Hypsithermal) prairie conditions prevailed, with an increase in clastic deposition, possibly from aeolian sources. Changes in lake level through this time, with release of nutrients from the sediment, led to the development of regular diatom blooms. After 4 ka BP, moist conditions returned, and allowed a forest of pine, birch and other hardwoods to become re-established. The volume of clastic input to the lake declined. Variations in water level, and lake chemistry, were accompanied by alterations to diatom and ostracod assemblages, and the production of more complex varve structures (Anderson *et al.*, 1993). Modern sediments from Elk Lake provide a record of fire frequency correlated with changes in forest type, which may in turn be compared with climatic variations (Clark, 1993).

The sediment record from Elk Lake also provides evidence for the periodicity of climate change and for its connection with variation in solar activity and the geomagnetic field (Anderson, 1993). Spectral analysis of time series formed from sequences of varve thickness reveals a number of periodicities, the spectral densities of which change in phase with the three stages in the development of the lake described previously. Early post-glacial varves exhibit periodicities of *ca* 22 yr, 40-50 yr and *ca* 200 yr, the former two values possessing a higher spectral density. In addition, 12.5- and 5 yr frequencies are identified within this time period. Sediments from the Prairie stage

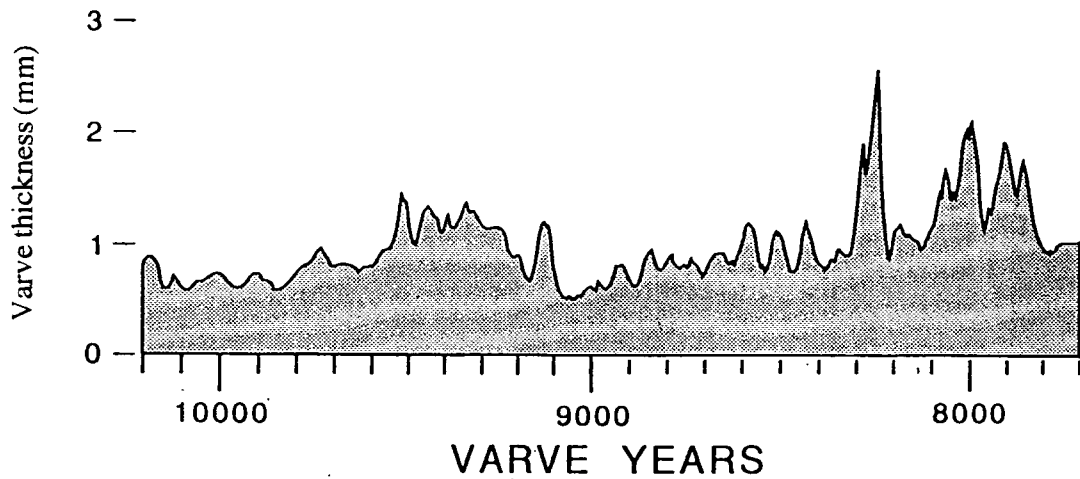


Figure 2.4 Record of lamination thickness from Elk Lake, Minnesota, over the period 10.2 to 7.7 ka BP (After Anderson, 1993)

display the same periodicities more strongly, although there are systematic changes within discrete time slices, especially within the 40-50 yr frequency band. Evolutive frequency analysis reveals similarities to that derived from $\delta^{14}\text{C}$ time series (Stuiver, 1980b), leading to the hypothesis of a connection between climatic variations and the flux of solar particles, which gives rise to the production of ^{14}C (Damon & Jirikowic, 1992).

2.2.4.2 Gosciadz, Central Poland

Gosciadz is one member of a group of lakes- the *Na Jazach* complex- fed by the Ruda river, a tributary of the Vistula, located in Central Poland. The lake is of glacial origin, with a maximum depth of *ca* 25 m. It is dimictic, ice-covered during the winter months, with significant groundwater input (Churski *et al.*, 1993)

Cores from the deepest part of the lake are composed of black, sulphuric-calcareous gyttja (Sandgren, 1993) and consist of an almost continuous sequence of laminations, terminating in basal layers of sand and peat, at a sediment thickness of *ca* 18 m (Goslar, 1993). Of note in these profundal cores, is the presence of a massive layer

composed of sand, which has prevented the recovery of a complete sequence (Ralska-Jasiewiczowa *et al.*, 1992). Shorter cores recovered from distal locations have, however, been observed to be entirely laminated to the basal peat layer and thus have been used to compile a composite varve chronology spanning *ca* 12 600 years (Goslar *et al.*, 1992). Thus, the sequence contains both Late Glacial and Holocene material, although it has been demonstrated that the varve style has not changed during this time. The record does not, however, reach the present.

The sedimentary record may, therefore, be utilised in order to facilitate study of the effects of rapid environmental change at the Allerød/Younger Dryas (YD) and YD/Preboreal boundaries (Ralska-Jasiewiczowa *et al.*, 1992), which are recognised by examination of the pollen and $\delta^{18}\text{O}$ records (Goslar *et al.*, 1993). In addition, the varve chronology from this site may be compared with the ^{14}C calibration curve, in order further to correct the latter where there exist multiple-age 'plateaux', and to extend the calibration into the Late Glacial (Goslar *et al.*, 1992). The construction of a chronology may also enable the duration and timing of the Younger Dryas in central Europe to be evaluated (Goslar *et al.*, 1995) and to date phases of early human influence within the catchment (Ralska-Jasiewiczowa & van Geel, 1992).

2.2.4.3 The sediments of Loch Ness as indicators of environmental change

Loch Ness is influenced by the climatic regime of the North Atlantic Ocean. Westerly and southwesterly airflows from the ocean are the main agents which impart a cool maritime climate to the region. The Loch is thus located in an ideal position to record climate change over the North-western Atlantic seaboard.

The North Atlantic Ocean is a major agent in the generation and maintenance of much of global climate (Berger & Labeyrie, 1987; Broecker *et al.*, 1988). Production of North Atlantic Deep Water (NADW) is crucial to the climatic system of northern Europe,

1993). Thus, the effect of the Late Devensian glaciation on the sediments within the Loch Ness basin, is of particular interest to the continuation of this study. Pennington *et al.* (1972), have detailed variations in pollen found in sediments from Loch Tarff (UK National Grid reference NH425100), a small loch in the south-west catchment of Loch Ness). Alternate phases of climatic deterioration and amelioration have been inferred, commencing at the time of the Late Glacial Interstadial. The Loch Lomond Stadial (Younger Dryas) is recorded in the catchment by many glacial and periglacial landforms, which suggest an extensive renewal of icefield activity in the Western Highlands. Glaciers flowed along the length of the Great Glen, but terminated at the location of Fort Augustus. Ice-dammed lakes were formed, the evidence of which may be observed in shoreline features, cross-valley moraines, and relict meltwater channels (Sutherland & Gordon, 1993). Sissons (1979) suggested that the catastrophic collapse, at the end of the Younger Dryas, of an ice-dammed lake in Glen Spean and Glen Roy was responsible for the production of a *jökulhlaup* which led to rapid changes loch level and in the formation of the Kessock narrows (NH475860), north-east of Inverness. Terrace and lacustrine shoreline features along the Great Glen indicate loch level changes over longer periods during the Younger Dryas, and have been utilised in demonstrating the effect of the renewal of glaciation upon isostatic recovery of the earth's crust following the melting of the main Late Devensian ice sheet (Sutherland & Gordon, 1993). Evidence of Holocene marine incursion into the loch (Merritt *et al.*, 1995) has so far not been detected by analysis of diatom taxa (V.J.Jones, pers. comm.), although Pennington *et al.* (1972) have reported increases in halide concentration in sediments recovered from the area of Dores Bay.

2.3 Proxy climatic data - sources and dating

2.3.1 Introduction

Studies related to palaeoclimates are conducted in many research disciplines.

Common sources of data include tree-rings, lake, bog and marine sediments, ice cores, and historical records, which may represent information spanning various periods of time. Palaeoclimatic records may be utilised as databases with which to validate climate models and to provide information in support of the study of climate change (for example, Holcombe, 1989). Until the advent of instrumentation, historical records provide the main source of verifiable climatic data (Ingram *et al.*, 1981; Ladurie, 1971). Before that time, information about palaeoclimates existed only in the form of proxy data, where natural phenomena have recorded and stored a record of climate.

2.3.2 Types of proxy record

Records of environmental change may be found throughout geological time, but many may be observed relating to climate variations during the Quaternary, and especially to the last 20 000 years. Data sources, with time resolution and duration are listed in *Table 2.1*. Climatically-related data from these sources may take many forms, including those based on oxygen isotope ratios, tree ring width, sediment lamination thickness, diatom, pollen and foraminiferal assemblages, dust concentrations, and atmospheric composition. Calibration of data, to produce time series suitable for analysis, may be performed by enumeration of seasonal or annual banding (Coral: Dunbar *et al.*, 1994; Tudhope, 1994; Speleothems: Shopov *et al.*, 1994; Tree-rings: D'Arrigo *et al.*, 1993; lake sediment laminae: O'Sullivan, 1983; Ice cores; Shoji & Langway, 1989), by correlation with historical records (Guiot, 1992; Pfister, 1992), by radiometric dating (Suess & Linick, 1990), by correlation with orbital cycles (Martinson *et al.*, 1987) or with variations in the geomagnetic field (Saarinen, 1994; Sprowl & Banerjee, 1985).

Once transformed into a time series, the primary data may then be subjected to both qualitative and quantitative analysis, in order to enhance and interpret the climatic signal contained within it. Many types of data require extensive calibration, usually by comparison with a modern signal, which enables the relationship of measured values to

Table 2.1 Time resolution and duration of primary climatic proxy data sources. (After Holcombe, 1989)

<i>Data source</i>	<i>Duration</i>	<i>Resolution</i>
Ocean sediments	>1 Ma	(<)100-5 000 yr
Tree rings	ca 10 ka	(<)1 yr
Lake sediments	100 ka	(<)1 yr
Bog sediments	100 ka	100-500 yr (¹⁴ C)
Ice cores	15 ka	1-10 yr
	100 ka	100-1000 yr

probable climatic conditions which gave rise to them, to be evaluated. One such method is the formulation of *transfer functions*, much utilised in the investigation of variations in water quality over time, by means of quantification of diatom assemblages (Battarbee *et al.*, 1995; Fritz *et al.*, 1991). Furthermore, elements of periodicity within the data (Berger, 1989; Hazen & Trefil, 1991) may be investigated by the application of, for example, Fourier (e.g. Press *et al.*, 1986), Maximum Entropy (e.g. Currie, 1995), or Wavelet (e.g. Edwards, 1996) analysis.

2.3.3 Dating of proxy records

Many techniques exist for the dating of proxy palaeoclimatic data. They may be classified into four main types: i) counting of annual or seasonal layers; ii) radiometric determinations; iii) correlation with documented events; iv) 'tuning' of data with orbital cycles or reversals of the Earth's magnetic field.

2.3.3.1 Incremental records

Many sources of proxy data originate from systems which are accumulative, in

that recent material is continually added to the archive. Where changes in the quality or quantity of material occur, owing to climatic variations over seasonal or yearly cycles, these may be utilised for dating purposes. For example, the rings of a tree consist of sequences of early growth, succeeded by layers of dense latewood (Schweingruber, 1987). Cross-sections through these are subjected to treatments in order to enhance the structure and thus enable counting of the annual layers. Similarly, lake sediments consist of laminae representing incremental seasonal sedimentation, enumeration of which enable an accurate chronology to be obtained (Simola, 1991). Similar structures are observed in ice cores, representing changes in the type of precipitation and ice formation (Shoji & Langway, 1989). In addition, annual dust layers and pulses of numerous chemical species aid the delineation of yearly cycles of deposition (Hammer, 1989).

Speleothems exhibit annual banding (Baker *et al.*, 1993) related to the kinetics of calcite deposition which is dependent upon many factors, including temperature, atmospheric concentration of carbon dioxide, water film thickness and drip rate, and concentration of calcite in vadose water (Baker *et al.*, 1995). The layers may be detected by luminescence at UV wavelengths, either by microscopy, photography or photodetector (Shopov *et al.*, 1994). Uranium series dating has been carried out in order to demonstrate the correlation of speleothem growth with glacial and interglacial periods (Gordon *et al.*, 1989).

Coral growth is strongly correlated with light intensity and water temperature, and occurs in the form of annual pairs of low- and high-density aragonite (CaCO_3) layers (Baumgartner *et al.*, 1989). These are observed by x-radiography or by illumination with UV radiation and therefore counted, and thus used in the construction of a chronology. Tudhope (1994) suggests, however, that formation of the growth bands is affected by many environmental factors, isolation of any single one of which has proven difficult. Thus density or thickness of banding may not represent an unambiguous environmental signal (Druffel & Griffin, 1993).

2.3.3.2 Radiometric dating

Many materials deposited in a physical system contain chemical elements which are naturally radioactive. These may be detected and, depending on half-life, utilised for dating purposes. All material containing carbon will incorporate small amounts of ^{14}C , an isotope produced by interaction of extra-terrestrial particles with the Earth's atmosphere. With a half life of *ca* 5730 years, it is thus suitable for the dating of material up to *ca* 50000 a. Presence of an excess in modern material owing to nuclear testing and the dilution of the global ^{14}C assay by fossil fuel combustion (the 'Suess effect'; Suess, 1970), however, makes this technique unsuitable for very recent dating. Typical materials that may be utilised by this method include bone (Arslanov & Svezhentsev, 1993; Hedges *et al.*, 1995), peat (Shore *et al.*, 1995), wood (for example, McCormac *et al.*, 1995; Zaitseva, 1995), shells (Heiarnielson *et al.*, 1995), organic-rich muds (for instance, Preece, 1995) and algae (MacIntyre *et al.*, 1996; Sartoretto *et al.*, 1996).

Three techniques are employed for the quantification of the amounts of ^{14}C present in a sample: gas-proportional counting (*GP*; Kromer & Münnich, 1992), liquid scintillation counting (*LS*; Polach, 1992), and accelerator mass spectrometry (*AMS*; Beukens, 1992). Gas counting and liquid scintillation are based upon the detection of β -particles emitted through the radioactive decay of ^{14}C to ^{14}N , the former technique by their immediate detection and the latter through their interaction with a chemical compound termed a scintillator, which fluoresces upon passage of energetic particles through it. Numbers of ^{14}C atoms present in a sample are determined by the AMS technique, which offers increased sensitivity (i.e. smaller sample size), and the ability to perform specific and often specialised chemical treatments on the components of a sample, prior to dating (Hedges, 1992). With each technique, however, problems exist which may act to yield incorrect or inconclusive dates, including the contamination of material under investigation by younger or older carbon (Hedges, 1992; Olsson *et al.*, 1983), the 'hard water' and

'reservoir' effects (Olsson *et al.*, 1983), the nature of sample pretreatment (Hedges, 1995), and from errors introduced by the variable nature of atmospheric ^{14}C production (Stuiver, 1989).

Decay of the near-ubiquitous isotope ^{238}U , to ^{210}Pb (Half life 22.26 years), may be used to date recent sedimentary material (Gale *et al.*, 1995). The ^{210}Pb detected may be classified as *unsupported* (out of equilibrium with its parent radionuclide, ^{226}Ra , and derived from catchment sources) or *supported* (produced from decay of *in situ* radionuclides, and in equilibrium with precursor ^{226}Ra). By quantifying total ^{210}Pb and ^{226}Ra , the amount of unsupported ^{210}Pb may be calculated. Thus, by assuming a constant rate of supply from the catchment, the age of the sediment may be determined (for instance, Appleby *et al.*, 1979; Appleby *et al.*, 1990; Rose *et al.*, 1995).

A further dating method utilises the decay of ^{10}Be (half life 1.6×10^6 a), a radioisotope which is produced in the atmosphere by cosmic ray-induced nuclear reactions. It is involatile, and is thus transported from the atmosphere by precipitation or dry deposition (Lorius, 1990). Much use is made of this technique in the analysis of ice cores, where the concentration of ^{10}Be may be considered an indicator of palaeotemperature and palaeoprecipitation (Yiou *et al.*, 1985). Correlation of this isotope with others of cosmogenic origin enables estimation of rates of production and thus solar activity (Beer *et al.*, 1994; Oeschger and Beer, 1990; Raisbeck *et al.*, 1990).

Many other isotopes may be utilised for dating, depending on the material under investigation. The decay of Uranium (^{234}U ; half life 250 000 a), Thorium (^{230}Th ; 75 000 a), and Protoactinium (^{231}Pa ; 32 000 a) may be monitored in samples of marine detritus (for example, Slowey *et al.*, 1996) and coral (Edwards *et al.*, 1997; Eisenhauer *et al.*, 1996; Hoang *et al.*, 1996). The half lives of these elements are considerable, enabling chronologies extending back over several glacial cycles to be compiled. In addition, dating by the potassium/argon (^{40}K ; half life 1.3×10^9 a) technique, applicable

to potassium-rich minerals, such as those of volcanic origin, enables a time frame over geological periods to be established (Sudo *et al.*, 1998).

The production of radioisotopes by nuclear testing, especially during the period 1954-1966, led to their incorporation into many physical systems. Many isotopes exhibit age/activity curves that display a bimodal distribution, with a pronounced maximum during 1962-1964 and a much less intense peak around 1958-1959 (Pennington *et al.*, 1973). Thus, detection of these may aid in the formation of a chronology spanning the past *ca* 50 years. Isotopes which have been utilised include ^{137}Cs and $^{239,240}\text{Pu}$ (Jaakkola *et al.*, 1983). The date of the accident at the Chernobyl nuclear power plant, Ukraine, in 1984 may be utilised as a convenient chronological marker, since an appreciable volume of radionuclides were released and are recorded in sediments over a large area of Northern Europe (Appleby, 1993; Battarbee & Allott, 1994; Callaway *et al.*, 1996; Pinglot & Pourchet, 1995).

2.3.3.3 Correlation with documented events

Recognition of a signal whose origin may be determined by documentary evidence may enable an unambiguous temporal reference point to be fixed within a proxy palaeoclimatic data series. Care must be taken, however, when interpreting historical records, since they often contain much subjective information, and much more reliance may be placed upon data which are documented independently by several reporters (Ingram *et al.*, 1981). Major climatic events often leave behind some evidence of their occurrence, such as a sudden change in tree-ring width or a unique sedimentary structure. Such *marker horizons* may be produced by events such as volcanic eruptions (Knox, 1994), extreme floods (Ely *et al.*, 1993), and severe storms (Liu & Fearn, 1993). Whilst these records are necessarily confined to recent times, they may enable the construction of chronologies with which to correlate for example, instrumental climate records, and to provide a framework within which to ascertain the periodic nature of the record under

investigation. In addition, the presence of a marker horizon in one time series provides a fixed point in time which may then be transferred to other data series which have been validated using other criteria.

2.3.3.4 Geomagnetic and orbitally-derived chronologies

Many lakes sediments retain a characteristic signal of the Earth's magnetic field prevailing at the time of deposition (Thompson & Oldfield, 1986). The recovery of cores of known alignment enables detection of changes of both declination and inclination in the geomagnetic field over time which may be correlated with reference magnetochronologies (Saarinen, 1994, Sprowl & Banerjee, 1985; Verosub, 1988). In addition, varves, where present, permit direct comparison of magnetic and incremental chronologies (Björck *et al.*, 1987). In addition, periodic reversals in polarity of the geomagnetic field occur over long time periods. These reversals, which have been dated utilising other techniques, enable a sequence of sediments, such as deep sea or long lacustrine cores to be independently dated against a master chronology (Langereis *et al.*, 1997).

The compilation of long chronologies, spanning hundreds of thousands of years, has been undertaken by analysis of lake sediments (Guiot *et al.*, 1989: Grande Pile and Les Echets, France, 140 ka; Hooghiemstra *et al.*, 1993: Funza, Colombia, ca 1420 ka), ice cores (Barnola *et al.*, 1987; Jouzel *et al.*, 1987: Vostok, Antarctica, 160 ka; Johnsen *et al.*, 1995: GRIP, 250 ka) or loess profiles (Tanaka *et al.*, 1995), and may be hindered by uncertainties of changes in sedimentation, compaction and, in the case of ice, towards the base of a sequence, lateral flow. In these cases, it is often necessary to correlate derived time series with the SPECMAP time scale (Imbrie & Imbrie 1986; Sowers *et al.*, 1993). Compilation of this long period chronology was originally effected by recognition of signals of correlated global events recorded in a suite of long deep-sea sediment cores, as variations in foraminiferal $\delta^{18}\text{O}$. Subsequently, these were radiometrically dated, or indirectly dated by correlation with the palaeomagnetic record,

Table 2.2 Proxy sources - Ice cores

<i>Phenomenon</i>	<i>Proxy</i>
Temperature	$\delta^2\text{H}$, $\delta^{18}\text{O}$
Precipitation	$\delta^2\text{H}$, $\delta^{18}\text{O}$, ^{10}Be
Humidity	$\delta^2\text{H}$, $\delta^{18}\text{O}$
Aerosols Natural	Al, Na^+ , Ca^{2+} , Na^+ , H^+ , SO_4^{2-} , NO_3^-
Aerosols Anthropogenic	SO_4^{2-} , NO_3^- , Pb, radionuclides
Atmospheric circulation	particulates
Atmospheric composition	O_2 , N_2 , CO_2 , CH_4 , N_2O , CH_3Cl †
Cosmogenic	$^{10}\text{Be}^*$, $^{26}\text{Al}^*$, $^{36}\text{Cl}^*$, $^3\text{H}^*$, $^{14}\text{C}^*$, $^{39}\text{Ar}^*$, $^{81}\text{Kr}^*$

Sources: Lorius, 1989a; * Lorius, 1989b, • Khalil & Rasmussen, 1989; ~ Dansgaard & Oeschger, 1989; > Legrand & Delmas, 1987; † Hammer, 1989.

and selected as control points. A chronology was then compiled by interpolating the radiometric dates of other events between these control points and submitting them to spectral analysis, tuning the sequence of dates to produce a signal phase-locked to Milankovitch orbital periods. It is considered that the resulting chronology is accurate to ± 3 ka over the past 400 ka (Imbrie *et al.*, 1989; Martinson *et al.*, 1987).

2.3.4 Information gained from proxy data sources

Proxy data take many forms, and encompass time series comprising data derived from micro- and macrofossil analysis, quantification of chemical species, stable and radio-isotopic analysis, sequences of lamination thickness, incidence of tephra layers and such bulk properties as colour, density and magnetic characteristics. It would therefore be fruitless to attempt to mention all incidences of the utilisation of proxy data series. Tables 2.2-2.5 outline many types of data which have so far been recovered and indicate the inferences derived from them. It is important, however, to note that many

Table 2.3 Proxy sources - Tree rings

<i>Phenomenon</i>	<i>Proxy</i>
Temperature	$\delta^2\text{H}^*$, $\delta^{18}\text{O}$, maximum latewood density* ring width#
Precipitation	$\delta^2\text{H}$, $\delta^{18}\text{O}$, ring width, ring density
Aerosols Natural	Al, Ca^{2+} , Na^+ , H^+ , SO_4^{2-} , NO_3^-
Aerosols Anthropogenic	SO_4^{2-} , NO_3^- , Pb, radionuclides
Cosmogenic	$^{14}\text{C}\dagger$
Atmospheric circulation	frost rings $^\wedge$

Sources: • Briffa *et al.*, 1988 ; # Briffa *et al.*, 1990 ; † Suess & Linick, 1990; * Feng & Epstein, 1995; $^\wedge$ LaMarche & Hirschboeck, 1984.

Table 2.4 Proxy sources - Marine

<i>Phenomenon</i>	<i>Proxy</i>
Temperature	$\delta^{18}\text{O}$, microfossil counts, alkenones $^\sim$, Mg/Ca‡ Sr/Ca $^\bullet$, ostracoda,
Salinity	$\delta^{18}\text{O}$
Rainfall	$\delta^{18}\text{O}$
ENSO	$\delta^{18}\text{O}$
Aerosols Natural	Al, Ca^{2+} , Na^+ , H^+ , SO_4^{2-} , NO_3^-
Aerosols Anthropogenic	SO_4^{2-} , NO_3^- , Pb, radionuclides, Cd $^\Delta$
Cosmogenic	Thermoluminescence*
Oceanic circulation	$^{14}\text{C}_{\text{benthic}}$ / $^{14}\text{C}_{\text{planktonic}}$ † $^{13}\text{C}_{\text{benthic}}$ / $^{13}\text{C}_{\text{planktonic}}$, $\delta^{14}\text{C}$, Sm/Nd $^\Delta$
Terrestrial input	$\delta^{13}\text{C}$
Atmospheric circulation	tephra
Productivity	$\delta^{13}\text{C}$, Cd/Ca, Ba/Ca $^\bullet$, diatoms, Cd#, $^{10}\text{Be} >$

Source: * Castagnoli & Bonino, 1988; • Tudhope, 1990; # Baumgartner *et al.*, 1989; > Rutsch *et al.*, 1995; $^\sim$ Eglinton *et al.*, 1992; † Wood *et al.*, 1993; $^\Delta$ Shen *et al.*, 1987; ‡ Dwyer *et al.*, 1995; Mitsuguchi *et al.*, 1996; Δ Innocent *et al.*, 1997.

Table 2.5 Proxy sources - Lacustrine sediments

<i>Phenomenon</i>	<i>Proxy</i>
Temperature	$\delta^2\text{H}$, $\delta^{18}\text{O}$, beetle assemblages [•] , pollen [^]
Precipitation	$\delta^2\text{H}$, $\delta^{18}\text{O}$, lamination thickness, pollen [^]
Palaeohydrology	$\delta^2\text{H}/\text{d}^{18}\text{O}\#$
Salinity	Mg/Ca _a
pH	diatoms
Erosion	Na _c , K _c , Mg _c , Fe _c , Mn _c
Redox	S _a , Fe _a , Mn _a
Productivity	C _b , N _b , P _b , Si _b , Monocarboxylic acids, Pigments
Eutrophication	C _a , N _a , P _a
Sediment source (organic)	Hydrocarbons, C/N, $\delta^{13}\text{C}$, Sterol/stanol
Aerosols Natural	Heavy metals _c
Aerosols Anthropogenic	PCBs Δ , PAHs [˘] , SCPs [†] , SO ₄ ²⁻ , NO ₃ ⁻ , Pb, radionuclides
Atmospheric circulation	tephra

Sources: O'Sullivan, 1995: _a - authigenic, _b - biogenic, _c - allogenic; # Ricketts & Johnson, 1996;

• Coope, 1987; ^ Vincens *et al.*, 1993; ˘ Sanders *et al.*, 1994; Δ Sanders *et al.*, 1993; † Rose *et al.*, 1995.

proxy series may be derived from more than one source and may thus provide opportunity for correlation between data sets, forming a cornerstone of palaeoenvironmental analysis.

2.4 Climatic context

2.4.1 Present Climate of the British Isles

The location of Scotland on the northwestern seaboard of Europe places it under the influence of one of the most powerful sources of climatic change- the North Atlantic Ocean. The common mechanisms which drive climate systems; deep water formation; oceanic upwelling; the Polar Front; Gulf Stream, and the northerly atmospheric

Jet Stream, all of which are subject to many external forcing factors, are all present in this area (Lowe, 1993). Westerly airflows derived from atmospheric systems above the North Atlantic are important in determining the climate experienced in the Scottish Highlands. In particular, the duration, quantity and frequency of precipitation are paramount in influencing the quantity and quality of sediment delivered to water bodies within the region. Thus, an understanding of the climatic regime which affects the region is of some importance to this study.

2.4.2 *Lamb Weather types*

Maps recording daily weather over the British Isles since 1873 have been classified by Lamb (1950), who concluded that seven major categories of weather type were prevalent, according to airflow direction or isobaric pattern (*Table 2.6*). The origin of the airflow, either maritime or continental, polar or tropical, controls the amount of moisture contained in it, and thus the likelihood of precipitation.

It has been determined that, annually, the most frequent airflow type over the British Isles is at present westerly (Barry & Chorley, 1992). The minimum for flows of this type occurs in May, when northerly and easterly types predominate. Cyclonic airflows are most frequent in July and August, while anticyclones are most common in June and September. Both occur at similar frequencies.

Smith (1995), in comparing rainfall data for the period 1869 to the present, suggests that Lamb's scheme does not entirely describe the nature of precipitation over Scotland. Westerlies are becoming rarer in frequency over the UK, especially during winter, and have been replaced by an increased incidence of cyclonic and anticyclonic systems (Briffa *et al.*, 1990; Jones *et al.*, 1993; Lamb, 1972). Mayes (1991), however, noted an *increase* in westerlies over Scotland in regional data from the mid 1970s, leading to increased precipitation which, again, is not represented in Lamb's more general scheme.

Makrogiannis *et al.* (1982) studied changes in atmospheric circulation over the North Atlantic during the period 1873-1972 by means of the zonal index, which may be defined as the mean pressure difference between latitudes 35° and 55°N. They identified three subperiods of differing characteristics. It was noted that the strength of winter westerly airflows had decreased in the period 1940 to present. Jones *et al.* (1993) found significant correlations with Lamb's weather types and long range precipitation series for England (positive r) and Wales (negative r).

Table 2.6 General weather characteristics associated with Lamb "airflow types" over the British Isles. (*From Barry and Chorley, 1992*).

<i>Airflow type</i>	<i>Weather type</i>
Westerly	Unsettled with variable wind directions as depressions cross country. Mild and stormy in winter, cool and cloudy in summer.
North-westerly	Cool, changeable. Strong winds and showers affect windward coasts.
Northerly	Cold in all seasons, often associated with polar lows. Snow and sleet in winter, especially in North.
Easterly	Cold in winter, sometimes severe in east and south. Warm in summer, dry in west. Sometimes thundery.
Southerly	Warm and thundery in summer. Mild and damp in winter when associated with Atlantic low. If high present over central Europe may be cold and dry.
Cyclonic	Rainy, often gales and thunderstorms. May be due to rapid or persistent depressions.
Anticyclonic	Warm and dry in summer. Cold and frosty in winter.

2.4.3 Climate anomalies

Although the types of airflow pattern described in the previous section occur regularly, such schemes provide an incomplete description of the climate over the British Isles. Some circulation patterns occur infrequently, but possess the ability to generate events which may be extraordinary, and thus need to be considered in relation to the possible occurrence of a climatic signal in lake sediments. The most common anomaly is formation of blocking conditions, associated with anticyclonic systems (Barry & Chorley, 1992), when the breakup of zonal (E-W) circulation in mid-latitudes causes meridional (N-S) circulation to occur. Blocking may occur over Fennoscandia, particularly in winter, when severe weather over mainland Europe and the British Isles is experienced. The winters of 1881, 1895, 1940 and 1947 were notable in connection with this type of anomaly. Location of the blocking system is important, as is illustrated by the occurrence in 1955 of anticyclonic activity over the North Sea, which produced a very fine summer. During the previous year blocking had developed over Fennoscandia, causing a very wet August. (Barry & Chorley, 1992)

2.5 Causes and nature of variability in the climate of the North Atlantic sector

2.5.1 The North Atlantic Polar Front

Arctic and Polar frontal systems are formed by differences in the characteristics of neighbouring air masses. Major zones of frontal development occur, especially in winter, where there is a difference between the warm air over the ocean, and cooler air over land. The location of the North Atlantic Polar Front (NAPF) is variable, extending across the Atlantic Ocean from the Scilly Isles to the Gulf of Mexico in winter but retreating northwards to about 50°N in the northern hemisphere summer (Henderson-Sellers & Robinson, 1987). The frontal system is the location for the genesis of families

of cyclones, which then move eastwards across the Atlantic. Successive members of each family travel on a more southerly path, the final one entering the zone of the Trade Winds, bringing cold Polar air to that circulation. Location of the NAPF is thus a critical factor in influencing the routes travelled across the Atlantic Ocean by these depressions, and consequentially the climate experienced by the British Isles, especially in terms of storm frequency and strength (Taylor, 1996). Evidence presented by Lamb (1979) suggests that, during the Little Ice Age in the northern hemisphere (*ca* 1100-1900 AD), changes in the direction, intensity and frequency of storms in the Atlantic sector may have been directly attributable to variations in the location of the NAPF.

2.5.2 Oceanic circulation

A further critical component of the climatic system over the British Isles, is circulation within the North Atlantic Ocean, which is part of a global system driven by changes in water temperature and salinity (*Figure 2.5. After Broecker, 1988*). In this sector, warm surface waters from the tropical and equatorial regions move northwards, losing energy and gaining salinity. The surface water mass then sinks at high latitudes and returns southwards as deep water (NADW), passing around Southern Africa and spreading into the Indian and Pacific Oceans. Here, it again warms, becomes more buoyant and flows back to the Atlantic as surface water (Broecker & Denton, 1990). Variations in this system throughout the last 18 ka BP (and beyond) have been detected, indicating its inherent variability and effect on the climate of the North Atlantic region (Keigwin and Jones, 1994).

There is evidence that, during the last glacial cycle, the above thermohaline circulation was 'switched off' (Broecker & Denton, 1990), or at least suppressed (Maslin *et al.*, 1995). By the examination of fossil assemblages, and the study of grain size in marine sediment cores, changes in oxygenation and current flow have been detected, which are indicative of variations in vertical oceanic circulation. This mechanism has been

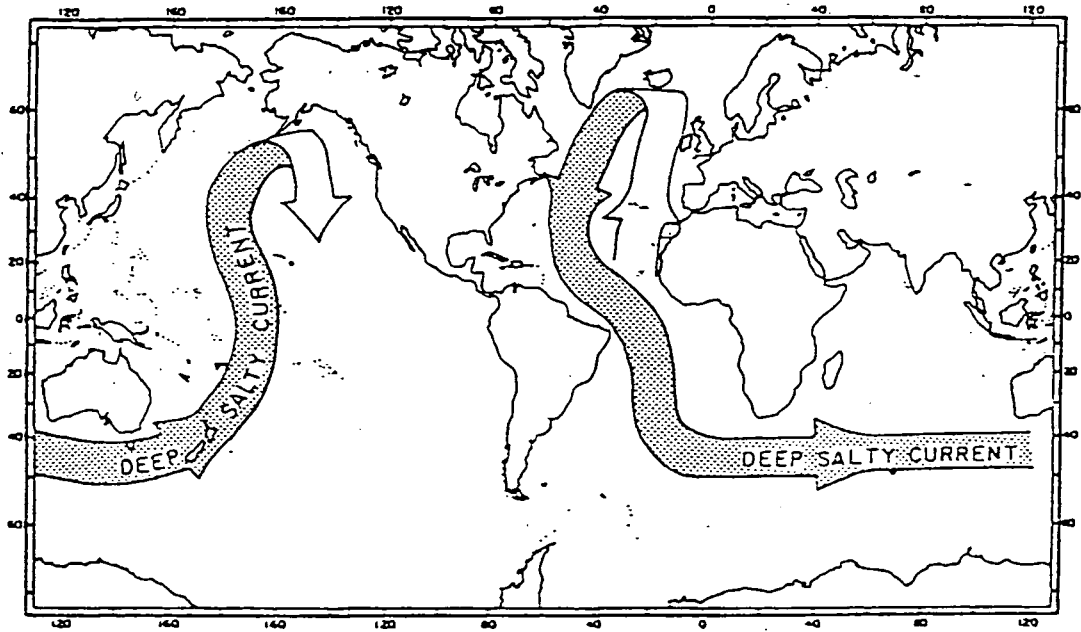


Figure 2.5 Global oceanic thermohaline circulation involves the deep waters of the North Atlantic Ocean (After Broecker, 1988)

adopted in order to account for short-term rapid changes in climate, such as those occurring throughout the glacial/Holocene transition, and for the origin of the Younger Dryas cold event. It has been proposed (Broecker *et al.*, 1989) that during deglaciation, meltwater released from the Laurentide ice sheet produced a cold, low-salinity 'pond' of water on the surface of the North Atlantic, preventing northward transport of heat and causing a temporary return to glacial conditions. Other investigators, however, have found evidence in sediments both from continental shelf and abyssal environments to suggest that such meltwater discharges were not as large as estimated, and doubt their efficacy in causing thermohaline disruption (Jansen & Veum, 1990; de Vernal *et al.*, 1996). Andrews *et al.* (1995) have investigated the provenance of detrital carbonate believed to have been discharged to the North Atlantic at the time of the YD (*ca* 11 ka ^{14}C BP). They have determined its origin to be within the region of Hudson Bay. They also propose, however, that this discharge did not precipitate cooling, but that, along with a similar, younger event (*ca* 8.2 ka BP), it merely represented the final collapse of the Laurentide ice sheet.

Evidence from deep sea cores suggests, however, that at other times throughout deglaciation, similar temperature fluctuations have occurred (Berger *et al.*, 1987), notably those during Heinrich events (major iceberg calving events from continental ice sheets; Andrews *et al.*, 1994; Broecker, 1994, Broecker *et al.*, 1992; Lehman, 1996), but also at times previous to these (Bond & Lotti, 1995). Analysis of the grain size of drift sediments from the eastern North Atlantic has indicated that changes in the rate of circulation of North Atlantic Deep Water (NADW) mirrors those of North Atlantic Middle Water (NAMW). This suggests that circulation does not halt, but switches mode, from that involving NADW (warm Atlantic) to one vigorously producing NAMW (cold Atlantic) (McCave *et al.*, 1995).

Indeed, recent research may support the concept of a constantly changing circulation system, variable even during warm periods. Mention may be made here of the 'Great Salinity Anomaly' of the late 1960s, 1970s and early 1980s, which caused a temporary decline in the production of cold deep water in the Greenland and Labrador Seas (Hay, 1993). Kellogg (1984) has demonstrated that, since the beginning of the Holocene, surface waters in the Denmark Strait have been affected by short-term oscillations in temperature. Koç *et al.* (1993) have postulated that the region encompassing the Greenland, Iceland and Norwegian (GIN) Seas, may respond rapidly to variations in insolation. They report changes in diatom assemblages indicative of differing sea surface temperatures in that area during six time slices throughout the Holocene. The implication for the global oceanic circulation system, in which the North Atlantic plays an important role as the origin of cold, oxygen-rich water, is stressed by Schäfer *et al.* (1995).

2.5.3 Summary of the Holocene climates of NW Europe

The change from a glacial Late-Pleistocene to an interglacial Holocene climate may be considered to have begun rather abruptly about 14 ka BP, with the rapid melting of

the Cordilleran and Fennoscandian Ice Sheets (Matsch, 1976). It has been demonstrated that, by 10 ka BP, both had disappeared, with the Laurentide Ice Sheet melting more slowly, lagging by *ca* 2 ka (Goodess *et al.*, 1992). Around 10.3 ka BP Scotland experienced increased airborne particulate transport from the south owing to a weakening in atmospheric circulation (Tipping, 1989).

Table 2.7 Summary of Holocene climatic divisions. (*After* (‡) *Lamb, 1982* & (*) *de Beaulieu et al., 1982*)

Younger Dryas	10700 bp*
Pre-boreal	10300 bp*
Boreal	9000 bp*
Atlantic	8000 bp*
Sub-boreal	4700 bp*
Sub-atlantic	2600 bp*
Medieval Warm Period	900-700 bp‡
Little Ice Age	500-300 bp‡

The period from complete glacial to more temperate conditions has been recognised as containing phases of widespread cooling occurring at intervals, the major example of which is the Younger Dryas. This was the final cooling event before complete deglaciation, which began about 10.8 ka BP, and was of less than 1 ka duration (Björck *et al.*, 1996; Goslar *et al.*, 1995; Lotter, 1991a). Evidence suggests that the onset of this event may have been extremely rapid, perhaps lasting only 100 years. Although the YD was initially considered to be a European phenomenon, evidence now suggests that it was a global event (Reasoner *et al.*, 1994).

The advent of high resolution analysis of proxy climatic data has made it possible to detect other transient cooling events which interrupted the process of deglaciation. These are also believed to have had a marked effect on the climate of the

North Atlantic region. The Amphi-Atlantic Oscillation (Levesque *et al.*, 1993), a *ca* 250-year event has been observed in the Dye 3, GISP and Summit ice cores from Greenland, in addition to lake sediments from Canada (Levesque *et al.*, 1993), and continental Europe (Broecker *et al.*, 1988). Alley *et al.* (1997) have suggested that signals observed from the GISP2 ice core indicate the occurrence of a Younger-Dryas type climatic perturbation at *ca* 8.2 ka BP, which may be correlated with similar events as distant as Tibet and north-west India.

By 8.5 ka BP, owing to continued weak atmospheric circulation, Europe was experiencing dry, anticyclonic warm summers. Climatic gradients were pronounced in an east-west direction, enhanced by the still extant Laurentide Ice Sheet, with zonal centres moving further North (Lamb, 1977b). During the period *ca* 8-6 ka BP, winter circulation over northwest Europe was similar to that of the present (Flohn & Fantechi, 1984) with variations in climate somewhat smaller (Lamb 1977b). Temperatures continued to rise, culminating over the period 7-5 ka BP in the Hypsithermal. Summer temperatures throughout Europe at this time are considered to have been *ca* 2-3°C higher than present, leading to a rise in global sea level as remaining ice, both on land and in the oceans, melted. Owing to the lag time between ice melt and sea level rise, sea levels reached a peak of 3m above present about 4.5 ka BP.

Around 6.5 ka BP, the North American atmospheric trough opened and moved further eastward, forcing westerly airflows, originating over the Atlantic Ocean, further into Europe (Lamb, 1977b). Reduced latitudinal climatic gradients around 6 ka BP produced warm summer temperatures in Central and Northern Europe, but with cooler winters throughout Northwestern, Central and Southern parts (Huntley & Prentice, 1988). Europe experienced a steepening in climatic gradients in both latitudinal and meridional directions following the Hypsithermal (Huntley & Birks, 1983), leading to increased storm frequency, as evidenced in Orkney around 5 ka BP (Keatinge & Dickson, 1979).

About 4.5 ka BP, a general westward shift of surface pressure patterns in Europe, coupled with a weak circulation system during the winter, led to a fall in annual temperatures (Lamb, 1977b). The renewed growth of peat bogs in northern Europe during the period 3-2.3 ka BP (the Iron Age) is thought to indicate the onset of generally wet conditions which culminated in a cold epoch, probably beginning around 2.5 ka BP (Lamb, 1977b).

Colonisation of Iceland and Greenland by Norse peoples around 1000-800 a BP is thought to be indicative of an amelioration in climate, with summer temperatures up to 1°C warmer than present (Lamb, 1977a). This Early Medieval warm epoch may not have been reproduced globally, however. The Little Ice Age began around 1430 AD and was characterised by two periods of harsh climatic conditions interrupted by more equable temperatures (Lamb, 1995). A general advance of glaciers throughout Europe, Asia and North America, and the limits of Arctic pack-ice expanded, suggesting that sea temperatures were some 3°C cooler than present. Sugden (1977) has suggested the development of glaciers in the Cairngorms between the seventeenth and nineteenth centuries. Evidence of a similar cooling in the Southern Hemisphere is not available although the period 1830-1900 AD is recorded to have been generally colder than today. More recently, a warming trend has been detected from 1880-1940 AD, especially in the Northern Atlantic, although this was replaced by a cooling from 1940 to the 1970s in the northern hemisphere (Lamb, 1995). The latest evidence suggests a renewed warming over the past few years (*Figure 2.6*; Parker *et al.*, 1992).

2.5.4 Climatic teleconnections

These may be described as extreme climatic events which occur at the same time in widely separated parts of the world, usually as a result of characteristic weather patterns, and which are related to flow patterns within the tropospheric westerlies (Barry & Chorley, 1992). They may be caused by shifts in position and number of the quasi-

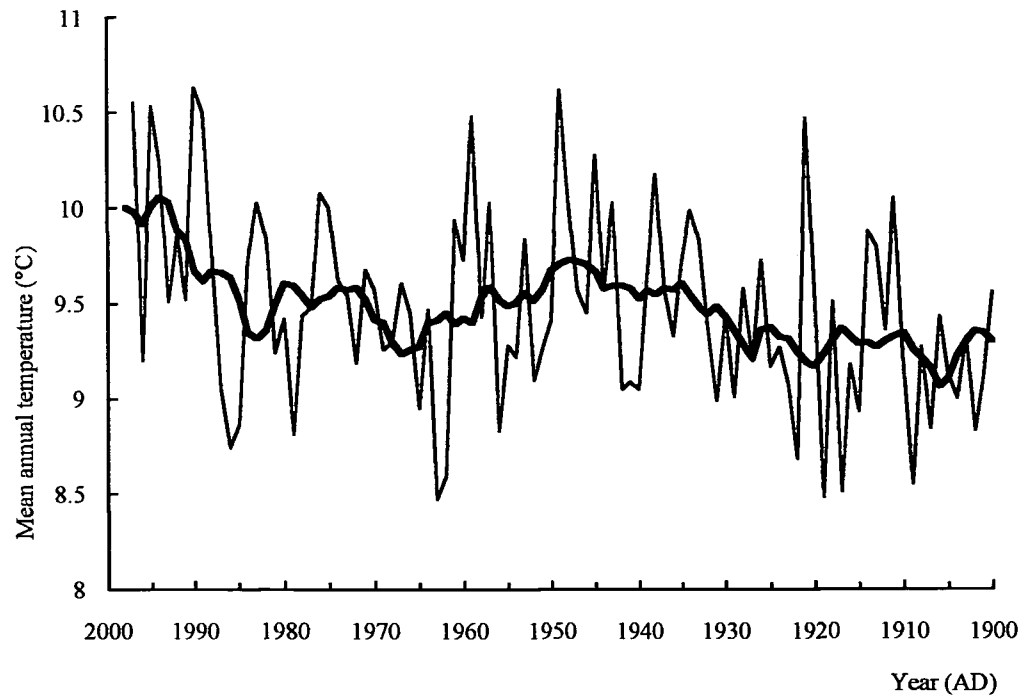


Figure 2.6 A warming trend revealed in recent Central England temperature series (After Parker *et al.*, 1992. Additional data from: <http://www.cru.uea.ac.uk/~mikeh/datasets/uk/cet.htm>)

stationary Rossby waves which penetrate into tropical latitudes and which are associated with blocking anticyclones (Henderson-Sellers & Robinson, 1987). Evidence for teleconnections in the rainfall belt of the tropics and subtropics is related to Walker circulation (Barry & Chorley, 1992). Of particular interest to palaeoclimatologists is the recognition of similar or identical climatic signals in proxy data obtained from sites throughout the globe. Bender *et al.* (1994) have correlated signals in both the GRIP and GISP2 ice cores with those recorded in the Antarctic Vostok core and have postulated that northern glacial and interstadial periods affect the Southern Hemisphere only if their duration is in excess of 2000 years.

Key events which occurred during the late Quaternary will now be examined in order to highlight the reasons behind the examination of the climatic signal in the

sediments of Loch Ness, and its comparison with other proxy climatic time series. Discussion of the Younger Dryas, the Holocene Hypsithermal, the Medieval Optimum, and the more recent Little Ice Age, will demonstrate that these episodes, initially detected in European records and assumed to be local in extent, have since been recorded globally.

2.5.4.1 *The Younger Dryas cold event (YD)*

The abrupt return to colder conditions which interrupted the rapid warming after the last glacial maximum, has been determined by numerous observations to have occurred at *ca* 12 ka BP. It is apparent in many other datasets from diverse locations in both Northern and Southern Hemispheres (Denton & Hendy, 1994: New Zealand (but see Singer *et al.*, 1998); Edwards *et al.*, 1993: New Guinea; Gasse *et al.*, 1991: Tibet; van Geel & van der Hammen, 1973: Colombia; Markgraf, 1993: South America, but see also Heine, 1993). Its signature, however, is recorded most strongly in environmental records from Europe (Goslar *et al.*, 1993; Lotter, 1991; Nesje & Dahl, 1993; Strömberg, 1994; Hajdas *et al.*, 1995), North America (Levesque *et al.*, 1993; Peteet *et al.*, 1990; Reasoner *et al.*, 1994) and the Arctic (Grootes *et al.*, 1993; Mayewski *et al.*, 1993; Taylor *et al.*, 1993). Jouzel (1994) highlights the lack of a comparable signal for this event in the Antarctic Vostok ice core, although other climatic fluctuations during the Pleistocene may be observed. Very recent data from an ice core collected at Taylor Dome, Antarctica, suggests that effects of the YD may have been felt over that continent (Steig *et al.*, 1998). Goslar *et al.* (1995) have attempted to correlate the cooling signal across a number of European datasets (German, Polish and Swedish lacustrine varves, German Pine chronology, GISP2 and GRIP ice cores) in order to ascertain whether or not the event was synchronous throughout the North Atlantic sector and Europe.

2.5.4.2 *The Holocene Hypsithermal*

The rapid rise in summer temperatures throughout northern Europe after the

Younger Dryas has been demonstrated, by the analysis of fossil beetle assemblages, to have been of the order of 7°C (Coope, 1987), leading to the establishment of modern climatic conditions within 1000 years from the beginning of the Holocene. This rise was not, however, experienced in the Americas, where decline of the Laurentide ice sheet lagged behind its Fennoscandian counterpart by *ca* 2000 years (Goodess *et al.*, 1992). Maximum temperatures were attained *ca* 8000 a BP and may have been of the order of 2°C in excess of modern summer values, which was sufficient to ensure the complete melting of many remaining polar ice caps and the retreat of many Alpine glaciers (Leeman & Niessen, 1994). Tree line limits lay *ca* 200 m higher than at present in the Alps and in Scotland, and coniferous forests extended up to 250 km further north than at present in Fennoscandia and Canada (Whyte, 1995).

The Hypsithermal appears to have been more easily detected in records from the Northern Hemisphere, although ice cores from Vostok in the Antarctic reveal slight temperature increases (Jouzel *et al.*, 1987). There appears to have occurred at the same time, however, a slight cooling of the Mediterranean region, owing to an increase in seasonality and continentality of climate. Increase of insolation elsewhere led to more intense heating of continental interiors and created a stronger monsoon circulation over Africa and Asia, bringing increased rainfall over regions further north (Gasse & van Campo, 1994).

The period of increased temperatures persisted until *ca* 5000 a BP when it was replaced by a cooler, less stable regime in mid-latitudes and by more arid conditions in the sub-tropics. Temperatures throughout the temperate regions of the Northern Hemisphere fell by *ca* 1°C, with consequent reduction in tree line elevation. Polar temperatures appear to have declined by some 3-4°C, leading to southwards movement both of coniferous forest limits and of the NAPF, which affected the paths of depression systems across the Atlantic Ocean and caused an increase in rainfall over the British Isles (Harding, 1982).

2.5.4.3 *The Early Medieval optimum*

A period of renewed warmth has been detected by an increase in elevation of the Alpine tree-line, by *ca* 150 m, and has been dated as occurring most strongly in the twelfth and thirteenth centuries (Lamb, 1965). At this time, a northward shift of both the NAPF and limits of pack ice permitted voyages into northern seas and prompted colonisation of the Arctic lands first by Irish peoples, in the Faroes and in Iceland, and then by Norse migrants, in Iceland, Greenland and America (McGovern, 1981). The change in climate has also been detected in palaeoclimatic archives from both hemispheres, and is observed in the Bristlecone Pine (*Pinus aristata* Engelm.) chronology from California (La Marche, 1974). In addition, investigation of the age distribution of drowned tree stumps from lakes located in the same region, reveals the existence of periods of lower water level, the dating of which, by dendrochronology, suggests two periods of intense drought, from *ca* AD 892-1112 and AD 1209-1350. The causal mechanism for variation in climate of this region is thought to be a contraction in the circumpolar vortex, with a probable change in its isobaric structure, owing to increased global temperatures.

2.5.4.4 *The Little Ice Age (LIA)*

This event has been demonstrated neither to have been (a) synchronous over a large area, or b) a period of continuously severe climate, but a more widespread and intermittent worsening of climate over a period of *ca* 500 years, with extreme conditions occurring more frequently than expected (Meese *et al.*, 1994). Records suggest the occurrence of a global event, with evidence in data from the Americas, China and Japan (Lamb, 1995). These indicate that the LIA may be considered to have been the most severe cold phase to have occurred during the Holocene since the YD. Indeed, some researchers have viewed the event as an aborted initiation of a new glacial cycle (Kullman, 1994; Whyte, 1995). In northern regions, the LIA may be considered to have begun at the end of the medieval optimum, around AD 1100, but evidence suggests commencement at a later

time in western Europe.

During this period settlements in Arctic regions were abandoned, because of crop and communication failures, and after many years of favourable harvests in Europe, wetter, colder conditions brought severe famine in the early fourteenth century. Glacier advances were noted throughout the Alps during the late thirteenth and early fourteenth centuries, with synchronous events in the Himalayas and New Zealand (Grove, 1988; Lamb, 1982). During this period, an expansion of both north and south circumpolar vortices occurred, causing a movement of depression tracks towards the equator (Kreutz *et al.*, 1997). The British Isles experienced more snow in winter, but generally, climate was drier than present. Stormier conditions over the regions bordering the North Sea brought a greater incidence of severe flooding, a trend which continued throughout the fifteenth century. Periods of amelioration occurred, before recommencement of more severe climate from the sixteenth to mid-nineteenth centuries. The most extreme phase for many parts of Europe came in the late seventeenth century, when crop failure brought famine to Scotland and to Fennoscandia. Sea ice limits lay close to the northern coast of Scotland, indicating temperatures some 5°C colder than present (Lamb, 1979). Glacial advances were noted in Alpine regions and permanent snow lay on the Scottish Highlands, with suggestions of the renewed formation of corrie glaciers (Whyte, 1995). In other areas, different phases of severe climate are recorded. In the Quelccaya ice cap (Peruvian Andes) a very cold period between AD 1490 and AD 1880, which both commenced and ended within three years, is recorded (Thompson, 1995).

Many writers have postulated possible causes for the LIA, but there is no unequivocal evidence (Whyte, 1995). Suggested mechanisms include atmospheric veiling owing to volcanic activity (Rampino *et al.*, 1988), variations in solar output (Kerr, 1996; *but see* Kreutz *et al.*, 1997) and changes in the circulation systems within the Pacific (McElroy, 1994) or the Atlantic Ocean (Grove, 1988).

2.6 The periodic nature of climatic and proxy-climatic time series

2.6.1 Introduction

Numerous studies of palaeoclimatic phenomena have demonstrated that the climatic system of the Earth responds, over a wide range of time scales, to various forcing mechanisms, originating both externally and internally. The time periods involved range from orbital forcing over thousands of years (for example, Hays *et al.*, 1976; Imbrie & Imbrie, 1979) to the passage of the seasons on a yearly basis. On shorter time scales, the signal may become blurred owing to the large noise component inherent in the processes which drive the global climatic system (Barnston, 1996).

In recent decades interest has been focused, for a number of reasons, upon the study and quantification of these climatic changes. First, recognition of periodic behaviour of the earth's climatic system may enable forecasting of large scale meteorological events (Mason, 1976), which would be advantageous for both economic and social reasons. Second, determination of past climatic regimes would aid the interpretation of the fossil record and, further back in time, the understanding of the evolution of the earth (Yiou *et al.*, 1994). Third, correlation of present climate with that of similar phases in the past would enable the separation of natural effects from those of anthropogenic origin, thus highlighting imminent, possibly catastrophic, changes wrought by human activities (Lane *et al.*, 1994).

2.6.2 The nature and cause of climatic change

2.6.2.1 Variations in the orbit of the Earth

The climatic evolution of the earth has been marked by a continuous change from glacial to interglacial conditions and back again. Duration and intensity of these

episodes has varied throughout the record. Over long periods changes are thought, in part, to be driven by the variable nature of the earth's orbit around the sun, where factors such as eccentricity, inclination and precession vary with different periodicities (respectively 96, 42 and 21/19 ka). Change of this type leads to variation in the amount of solar radiation received at the earth's surface. This theory was originally put forward in 1860 by James Croll, but was again brought to the attention of the scientific community by Milutin Milankovitch in 1920-30.

The Croll-Milankovitch orbital theory of ice ages has since been extensively used to explain many climatically-induced natural phenomena, such as the repetition of lithostratigraphic units in rock formations (Hinnov & Goldhammer, 1991) and changes in sedimentation type within deep sea cores (Imbrie *et al.*, 1989). In connection with the present study, it is noted that Quaternary sediments recovered from the North Atlantic Ocean have been shown to exhibit long-period variations of many physical properties, indicative of orbital changes in the Milankovitch wavebands (Mienert & Chi, 1995). Many researchers, however, believe that orbital effects alone may not be sufficient to drive glacial cycles. Indeed, changes in radiation over such long time scales affect only a fraction of the energy delivered by other possible agencies, such as changes in atmospheric composition and oceanic circulation (Berger, 1977; Broecker & Denton, 1990; Schäfer *et al.*, 1995; Whyte, 1995).

2.6.2.2 Planetary effects

The Earth is influenced by the gravitational attraction of the Moon, Sun and, to a lesser extent, the other planets of the solar system. The force exerted on the Earth by the first two is very much stronger than the combined effects of the others, but evidence suggests that certain planetary configurations may have affected the Earth's climate in the recent past. For example, a major grouping of the outer planets at opposition (a *syzygy*) around 1660 AD, caused the Earth to move more quickly in its orbit when it was

approaching them than when moving away (Burroughs, 1992). The effect of this was to shorten the duration of summers by about two days, with a corresponding lengthening of winters. Speculation suggests that this event may have precipitated the coldest spell of the Little Ice Age in the Northern Hemisphere.

The combined gravitational attraction of the Sun and Moon upon the Earth are far more powerful than that of the other planets, affecting crustal, oceanic and atmospheric systems. There also exists the possibility that the attraction of the Earth/Moon system, and that of the planets, may influence the circulation of the solar dynamo (Mörth & Schlamming, 1979). Difficulty arises in the quantification and prediction of solar-terrestrial gravitational effects because of the configuration and orbital periods of the Earth and Moon, long term changes occurring both in timing and relative position of perihelion and perigee, respectively. Evidence indicates that periodicities in climatic time series, resulting from orbital variations, exist, these being:

- i) 8.85 a period of advance of perigee of the Moon, which determines alignment with Earth's perihelion.
- ii) 18.61 a period of regression of lunar orbital nodes. This changes the accuracy of alignment of perihelion with perigee.

Both processes appear to produce physical effects in the atmosphere and thus would be expected to influence climate. In particular, the 18.61-year period is the most widely observed in many time series, including proxy data (for example, Currie, 1994a, 1994b, 1994c, 1994d; Mann *et al.*, 1995). The strongest effects are considered to be exerted at high latitudes when the angles of the Moon's orbit and the tilt of the Earth's axis are at extremes to the ecliptic (Burroughs, 1992).

2.6.2.3 Solar variability

The Sun is the primary energy source for many natural processes occurring on the Earth. Its radiation output is not constant, however, as luminosity has increased by some 30% over the past 4 Ga (Lamb, 1977a) and both visible and UV components of this output are known to vary significantly over timescales from 27 days to *ca.* 90 years (Stix, 1991; Willson & Hudson, 1988). The most easily observable phenomenon which indicates that the surface condition of the Sun is not constant, is the sunspot cycle, the past record of which extends for at least 300 years. The basic *ca* 11-year cycle exhibits a number of higher harmonics, *viz.* the 22-year Hale cycle, which represents the period between reversals of the solar magnetic dipole, and the 80-90 year Gleissberg cycle, which delineates the long term modulation of sunspot numbers (*Figure 2.7*).

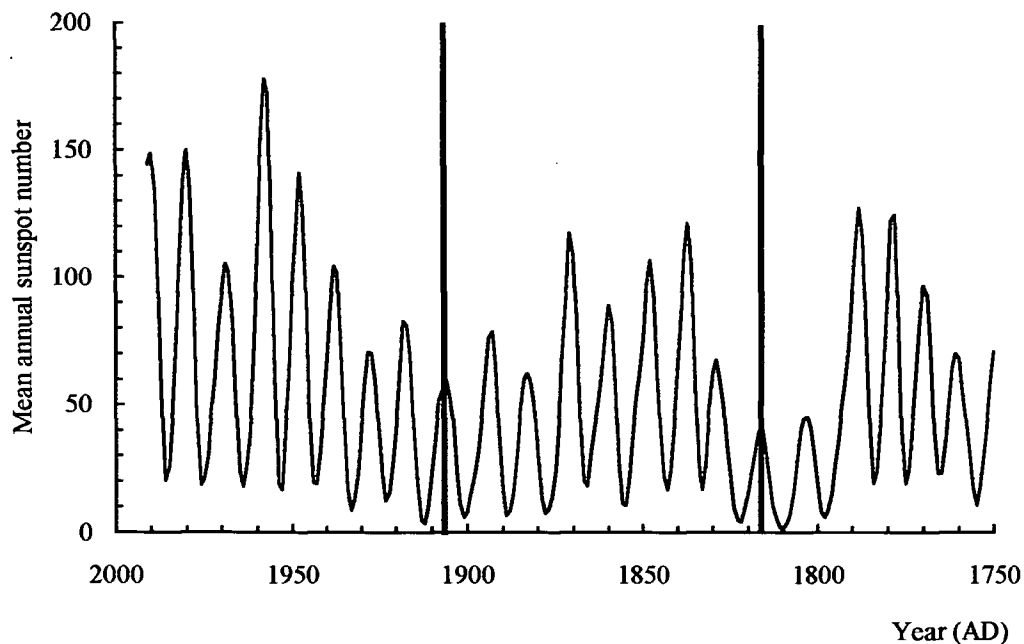


Figure 2.7 Variation in sunspot numbers 1750-1991 AD. The *ca* 11-year Hale cycle is illustrated by the many peaks and troughs, while *ca* 80-year Gleissberg cycles are delineated between the bold vertical lines (*Source: NOAA, WDC-A*)

Sir William Herschel, in the early nineteenth century, suggested that changes in solar output may influence the weather. Schwabe quantified, in 1843, historical

variations in sunspot number, fuelling further the speculation that the solar cycle and terrestrial climatic change may be linked by cause-and-effect. Sir Napier Shaw, in his *Manual of Meteorology*, published in 1926, mentioned that at least 100 different cycles had been discovered in weather records (Burroughs, 1992). The validity of solar-terrestrial relationships has been extensively studied during recent decades, and has invoked many possible mechanisms of action (Labitzke and van Loon, 1990; McIntyre, 1994; Reid and Gage, 1988; Tinsley, 1988). Although many apparent instances of correlations between climatic trends and solar activity have been identified, there still remains suspicion that such evidence may be circumstantial (Briffa, 1995).

Indication that changes in solar radiation may affect processes on the earth is most strongly observed in the production of atmospheric ^{14}C by cosmic ray bombardment of ^{14}N (Oeschger & Beer, 1990; Stuiver, 1994; Stuiver & Quay, 1980; Wigley & Kelly, 1990). Solar activity modulates the intensity of cosmic rays impinging upon the upper atmosphere, by causing alteration of the intensity of the geomagnetic field. Periods of high sunspot activity are correlated with low ^{14}C production and *vice versa*. Superimposed upon this signal are long term changes which may be the product of variation of the earth's magnetic field independent of other external factors.

Markson (1981) has postulated that modulation of cosmic ray intensity by solar activity leads to variations in the electric field which act to influence thunderstorm activity. He has also argued that changes in the flux of energy from the Sun are too weak to affect terrestrial weather systems, and that the sometimes rapid changes observed require an electromagnetic explanation. Markson suggests that at high latitudes a high positive correlation between solar activity and sunspot number indicates that the driving force is solar proton flux. At low latitudes, however, cosmic ray modulation by magnetic field variations provides the impetus. Together these produce a signal out of phase with solar activity.

Interest has long been focussed on the correlation of weather records with sunspot variability. With the application of recent advances in data manipulation and statistical analysis, many instances have been highlighted. One of the problems which has beset research in this area is the relatively short length of reliable climatic time series and the limited range of variables measured by historical solar observers. The longest reliable climatic time series available is the homogeneous temperature record, compiled by Professor Gordon Manley (1974), depicting Central England temperatures from 1659 to 1973 AD (*Figure 2.8*). During the same time period, the Sun underwent 28 sunspot and three Gleissberg cycles, with early observations being made during a quiet period of solar activity, termed the Maunder Minimum (Hoyt *et al.*, 1994; Mörner, 1993).

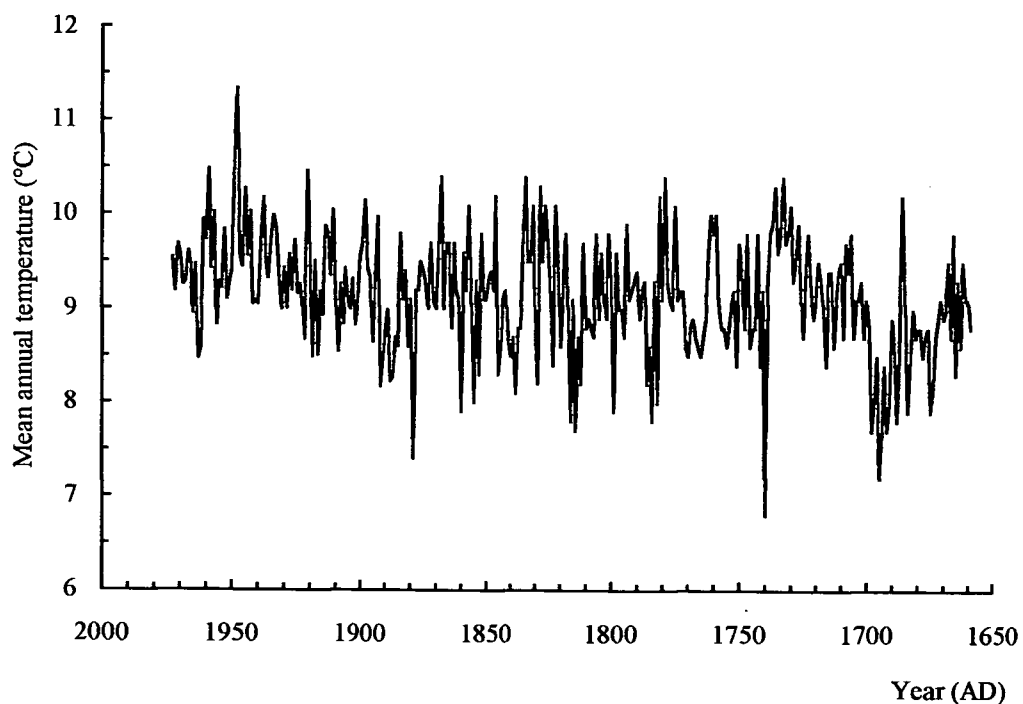


Figure 2.8 The temperature record for Central England, compiled by Manley (1974). This represents the longest reliable indicator of temperature variation available.

Mörner (1993) highlights a possible correlation between the length of the sunspot cycle and mean surface temperature in the northern hemisphere. Friis-Christensen & Lassen (1991) have determined that, for the last 130 years at least, shorter period sunspot cycles have occurred at times of relatively high surface temperature and *vice*

versa. The relationship fails, however, at times around the Maunder Minimum, where temperatures were severe although sunspot cycles were short.

2.6.2.4 Albedo variations

The Earth's atmosphere is generally opaque to solar radiation, except for those wavelengths representing the near-ultraviolet, visible light, near-infrared, radio waves, and extremely energetic atomic particles. Short wavelength radiation causes heating of the earth's surface, leading to re-radiation of longer wavelengths back into space. Certain components of the atmosphere selectively absorb this long wavelength radiation, leading to further warming. This is termed the *Greenhouse effect*, without which average global surface temperature would fall to *ca* -15°C (Whyte, 1995). Additional concentrations of these gases are thought to enhance this effect, causing the problem of *Global Warming* (Cline, 1992). Solar magnetic changes have been implicated in the variation in atmospheric concentrations of chemical species, notably O₃, NO₂, N₂O and CH₄, which alter the radiative balance of the atmosphere and thus the surface temperature. The effects are not uniform, but centred on the geomagnetic poles, which themselves are origins of atmospheric circulation. The correlation of variation in the temperature of the stratosphere (p 47) with sunspot cycle is consistent with this hypothesis.

The presence in the atmosphere of particulate matter has also been demonstrated to affect global temperatures (LaMarche & Hirschboeck, 1984). The most common source is volcanic eruptions. The link between past eruptions and disruption of climatic processes has hitherto been tenuous, partially because of the scarcity of reports of volcanic events from remote regions of the globe and also because of the difficulty of assessing their strength and nature. Recent studies have, however, demonstrated that several well-known eruptions have manifestly affected climate in subsequent years, and there is growing evidence that vulcanism may be responsible for short term climatic change in prehistory (Baillie & Munro, 1988).

Lamb (1970) compiled a quantitative chronology of past volcanic activity, albeit concentrated in the mid-latitudes of the northern hemisphere. This *Dust Veil Index* (DVI) considered climatic effects of vulcanism and observed that, compared with the preceding four centuries, there was little volcanic dust in the atmosphere during the late nineteenth and early twentieth centuries. This prompted speculation about the present warming trend, and the possible causes of the Little Ice Age. Recent analysis of these data by Currie (1994c) has highlighted a "possible periodicity", with elements of 18.6 and *ca* 11 year cycles inherent in the series.

An alternative to this index is one proposed by Newhall and Self (1982), and termed the *Volcanic Explosive Index* (VEI). This is an assessment, based entirely upon geological criteria, of the potential for the injection into the stratosphere of material from volcanic events, thus determining the power of respective eruptions to influence global climate. In addition, emission of volcanic gases, especially sulphur dioxide, may alter the opacity of the atmosphere and thus its radiation balance. Evidence of past vulcanism may be detected as tephra layers in sediments (Dugmore, 1989; Zolitschka *et al.*, 1995), or as acidic layers in ice cores (Hammer, 1980; Lorius, 1990).

2.6.2.5 *Quasi-Biennial Oscillation*

The most regular source of variation within the Earth's atmosphere is termed the Quasi-Biennial Oscillation (*QBO*). This may be defined as the regular reversal of stratospheric winds between east and west, which occurs with a period of about 28 months. The effect is most strongly observed at an altitude of *ca* 30 km, where the ambient pressure is *ca* 20 mb. The velocity of easterly winds is greater than those blowing from the west, the amplitude between extremes being about 50 ms^{-1} . As the cycle progresses, the winds move down into the denser, more turbulent atmosphere and weaken, but still appear to possess enough energy with which to influence climate, since a 28-month periodicity is apparent in many climatic time series (Burroughs, 1992).

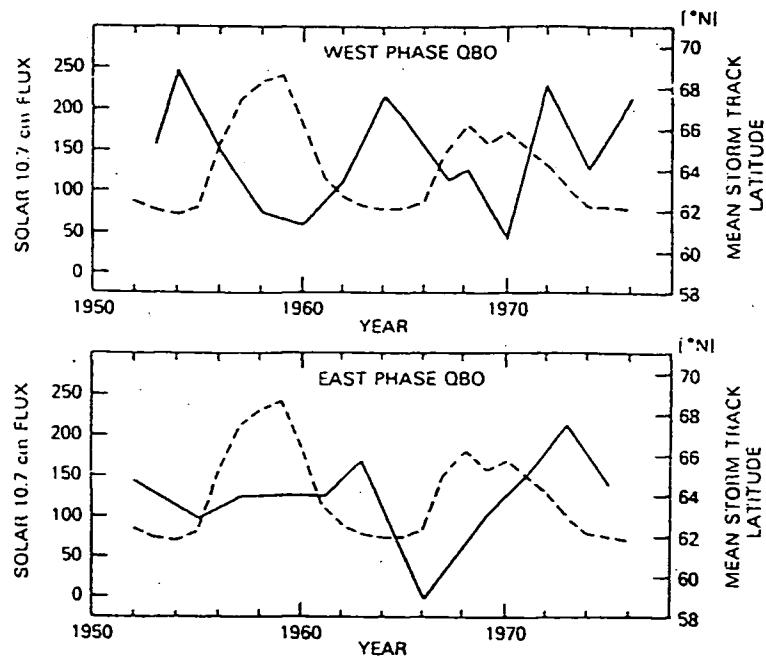


Figure 2.9 Correlation of solar activity, measured as flux of 10.7 cm radiation (dashed lines), with mean latitude of storm tracks in the North Atlantic region (solid lines), separated according to phase of the stratospheric Quasi-Biennial Oscillation (After Tinsley, 1988).

Labitzke and van Loon (1990) have demonstrated that if the two phases of the QBO are considered individually, a striking correlation between stratospheric temperature and solar activity is observed. Further research by Tinsley (1988; *Figure 2.9*) has highlighted the correlation between solar flux at a wavelength of 10.7 cm and latitude of winter storm tracks across the Atlantic Ocean, when these events are separated according to the phase of the QBO.

Variations in the upper westerly circulation are closely linked with average positions of weather systems at lower altitudes, especially in the North Atlantic sector which marks the boundary between warm tropical waters flowing poleward (Gulf Stream) and cold polar currents. Taylor (1996) has reported that the position of the north wall of

the Gulf Stream and the summer abundance of zoöplankton recorded in Windermere (in the English Lake District; 54.5°N, 3°W) appear to be correlated. He infers that this may be caused by variations in ocean-atmosphere heat exchange and subsequent effects on weather systems over the region.

2.6.2.6 North Atlantic Polar Front

The position of the North Atlantic Polar Front has been shown to have been variable throughout the last glacial cycle, when it advanced southwards to the Azores at the height of the glaciation, and then moved northwards as climate ameliorated (*Figure 2.10; Ruddiman & McIntyre, 1981*). At the time of the Hypsithermal, the Polar Front lay between Greenland and Iceland, although during the late seventeenth century it advanced south of Iceland, almost into Scottish waters (Lamb, 1977a; Whyte, 1995).

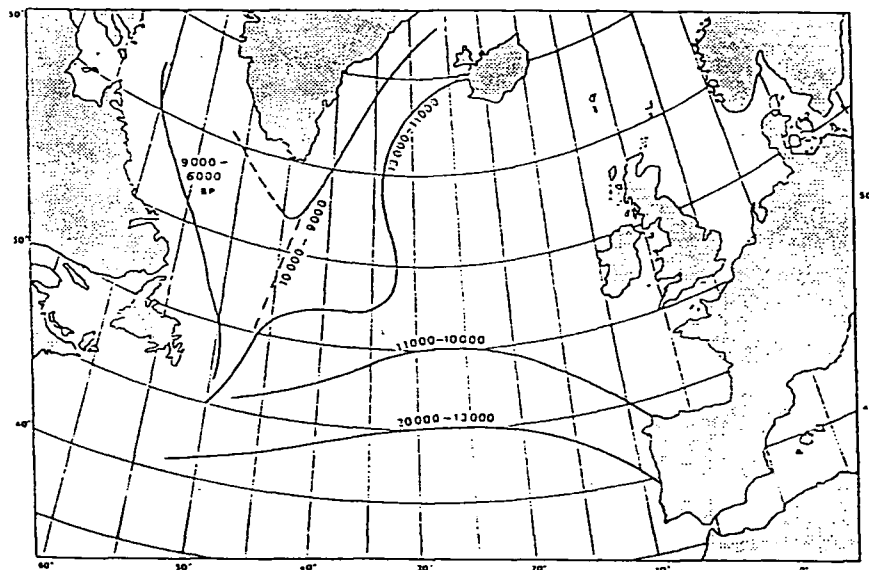


Figure 2.10 Location of the NAPF through the last glacial cycle and Early Holocene (*After Ruddiman & McIntyre, 1981*).

2.6.2.7 North Atlantic Oscillation

In addition, interest has recently focussed on quantification of the North

Atlantic Oscillation (NAO), which is itself a major source of interannual climatic variability within the region (Hurrell, 1995). It is associated with changes in direction and strength of the surface westerly winds across the North Atlantic and affects airflows over Europe, North America, Fennoscandia, and the Arctic. The NAO has been observed since 1864 and is quantified by an index, calculated by determining the difference in atmospheric pressure over Iceland and the Azores (*Figure 2.11*). A high value indicates low pressure over Iceland and high pressure over the Azores, a situation that results in the formation of strong westerly airstreams over the North Atlantic Ocean.

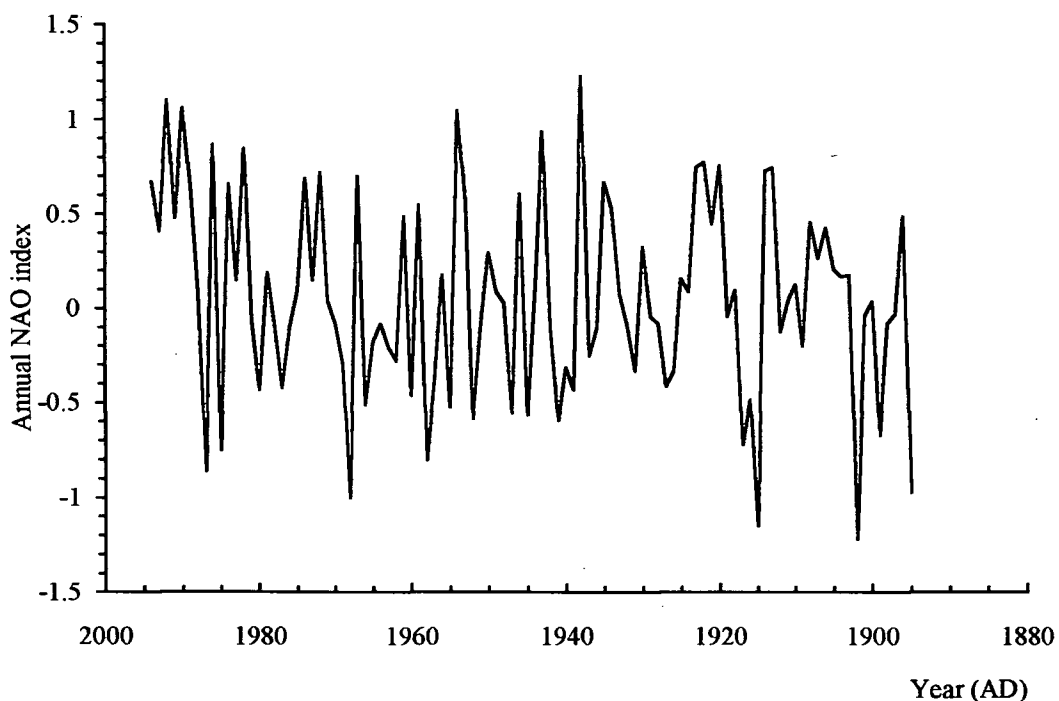


Figure 2.11 North Atlantic Oscillation Index, based on the difference in atmospheric pressure between the Azores and Iceland, for the period 1895-1994 AD (*After Mann & Lazier, 1996*)

Analysis of the NAO index has revealed that, in addition to interannual variability, longer term trends are manifest, which are correlated with the persistence of anomalous weather patterns over the continental United States and the Mediterranean region, and the incidence of winter storms over the UK. Moulin *et al.* (1997) have utilised satellite observations in order to conclude that the atmospheric export of dust from the

Sahara Desert is also correlated to NAO activity. Reid *et al.* (1998) have demonstrated a connection between phytoplankton density in the North Atlantic Ocean and the North Sea, with changes in NAO index. D'Arrigo *et al.* (1993) have utilised dendrochronological data from Scandinavia and Northeast Canada in order to reveal correlations between tree growth, temperature and NAO index. Recent investigations suggest that the NAO may not solely be an atmospheric phenomenon. Variations in deep oceanic convection, especially in the Greenland, Labrador, and Sargasso Seas may be implicated in the propagation of the atmospheric signal (Curry *et al.*, 1998; Talley, 1996).

2.6.2.8 Circumpolar Vortex

The circumpolar vortex is a further source of climatic variation over the North Atlantic. This is a belt of rapid air movement located in the upper troposphere, circulating around the north polar region at altitudes of *ca* 10 km. Topographic barriers such as the North American Rocky Mountains act to steer the jet streams associated with the vortex, creating wave formations which are variable over many time scales. Lamb (1979) explained the variation in circumpolar vortex in connection with the onset of the Little Ice Age.

Two extreme configurations of the vortex, one in which it contracts around the polar region and the flow within it is streamlined, the other where large meanders form and the flow is less rapid, exist. In the second state, ridges of warm air may move polewards or troughs of polar air equatorwards. In addition, meanders in the vortex become severed, creating blocking anticyclones which persist for long periods, bringing to western Europe dry summer conditions in summer or extremely cold weather in winter. The presence of blocking anticyclones over Britain often results in wetter conditions in Scotland, as storm tracks are diverted to the north around the high pressure zone (Barry & Chorley, 1992). Davis and Benkovic (1994) have studied variations in both temporal and spatial extent of the January circumpolar vortex and observed that from 1944 to 1990, the

size of the vortex expanded, leading to enhanced meridional flow over W.Europe. There has also been an increase in ridging over W.Europe and Fennoscandia, producing a strengthening in the Icelandic Low.

2.6.2.9 *El Nino Southern Oscillation (ENSO)*

Under normal conditions, the direction of the flow of air at altitude over the tropical and sub-tropical Pacific Ocean is eastwards, from an area of low pressure over Indonesia, returning at a lower level westwards. Regions beneath the descending air remain dry, with rainfall occurring under the moist, rising air mass in the east. The persistent, returning, air mass creates warm currents in the ocean, sending water westwards towards Australia and causing cold deep water upwelling off the coast of South America (the Peru Upwelling Zone). Periodically, the westerly airflows weaken or fail, creating a backwash of warm surface water moving eastwards. The associated low pressure atmospheric systems then also move eastwards, bringing heavy rainfall to the mid-Pacific region, or even to the normally dry western coast of South America.

There is some evidence that the ENSO system represents the most powerful source of yearly climatic variability, with attributable effects detected in rainfall records of the continental United States (Keppenne & Ghil, 1992), the occurrence of monsoon rains over Zimbabwe (Cave *et al.*, 1994) and India (Meehl, 1994), and possibly in weather anomalies over Europe (Fraedrich, 1994; Fraedrich & Müller, 1992). Taylor *et al.* (1998) have reported that variation in the annual mean latitude of the Gulf Stream may be partly attributable to ENSO activity. Decreased ice cover over the Laurentian Great Lakes has been determined to have occurred during recent ENSO events (Assel, 1998). Signals have also been detected in the laminated sediments from East African lakes (Johnson *et al.*, 1993) and from locations on the Iberian peninsula (Rodo *et al.*, 1997). The effect of ENSO variability has been invoked in the amelioration of the expected severe winter in the USA during 1988/89, which was forecast employing sunspot/QBO variations.

The phenomenon does not appear to have been a permanent feature of postglacial climate, however, and may have commenced only some 4500-5000 years ago (Diaz & Markgraf, 1992; Sandweiss *et al.*, 1996; Shulmeister & Lees, 1995). Other studies have concluded, however, that an ENSO-like feature may have existed in the atmosphere of the Earth as early as the Eocene, as recorded in the lacustrine oil shales of the Green River formation, Colorado (Ripepe *et al.*, 1991). The timing and strength of the modern signal appears to be variable, with events occurring on average every four years, but with intense episodes only every nine years (*Figure 2.12*). In recent years, severe El Niño events have become more frequent, with consequent concern from those societies most exposed to their effects.

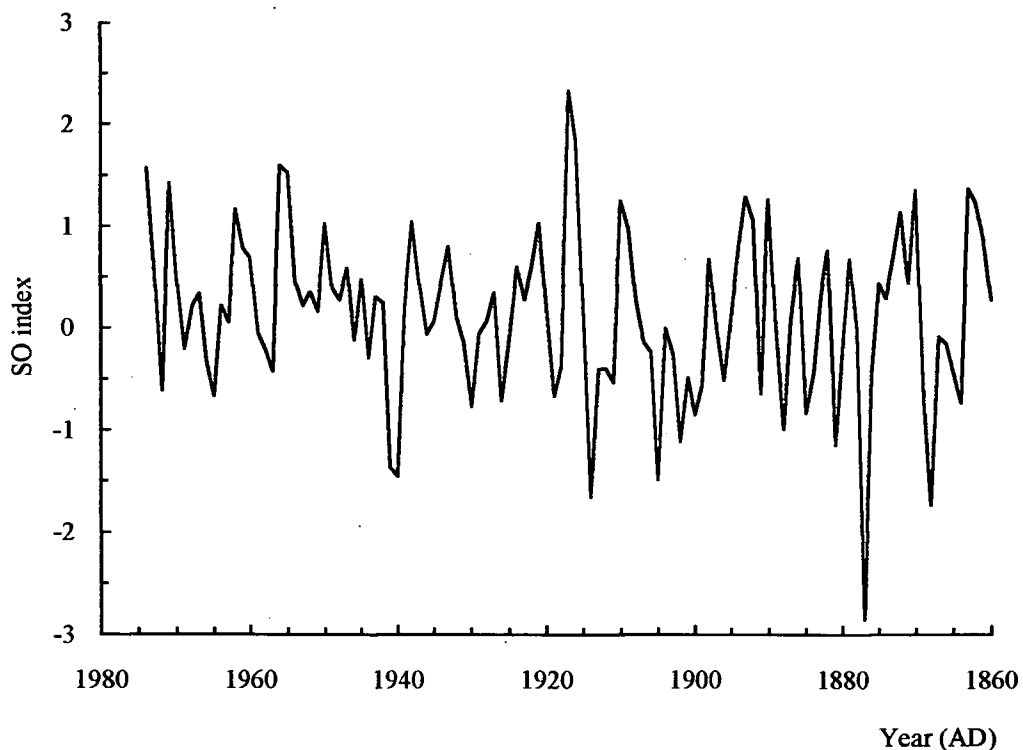


Figure 2.12 Chronology of ENSO activity, 1860-1974 AD (Source: NOAA, WDC-A)

3. Site description

3.1 Location

Loch Ness (Latitude $57^{\circ} 15' N$, Longitude $4^{\circ} 30' W$, UK National Grid Reference NH 285 429) is located in the Highland region of Scotland to the southwest of Inverness (*Figure 3.1*). The loch forms nearly one half the total length of the Caledonian Canal, which crosses the Scottish Highlands from Fort William to Inverness.

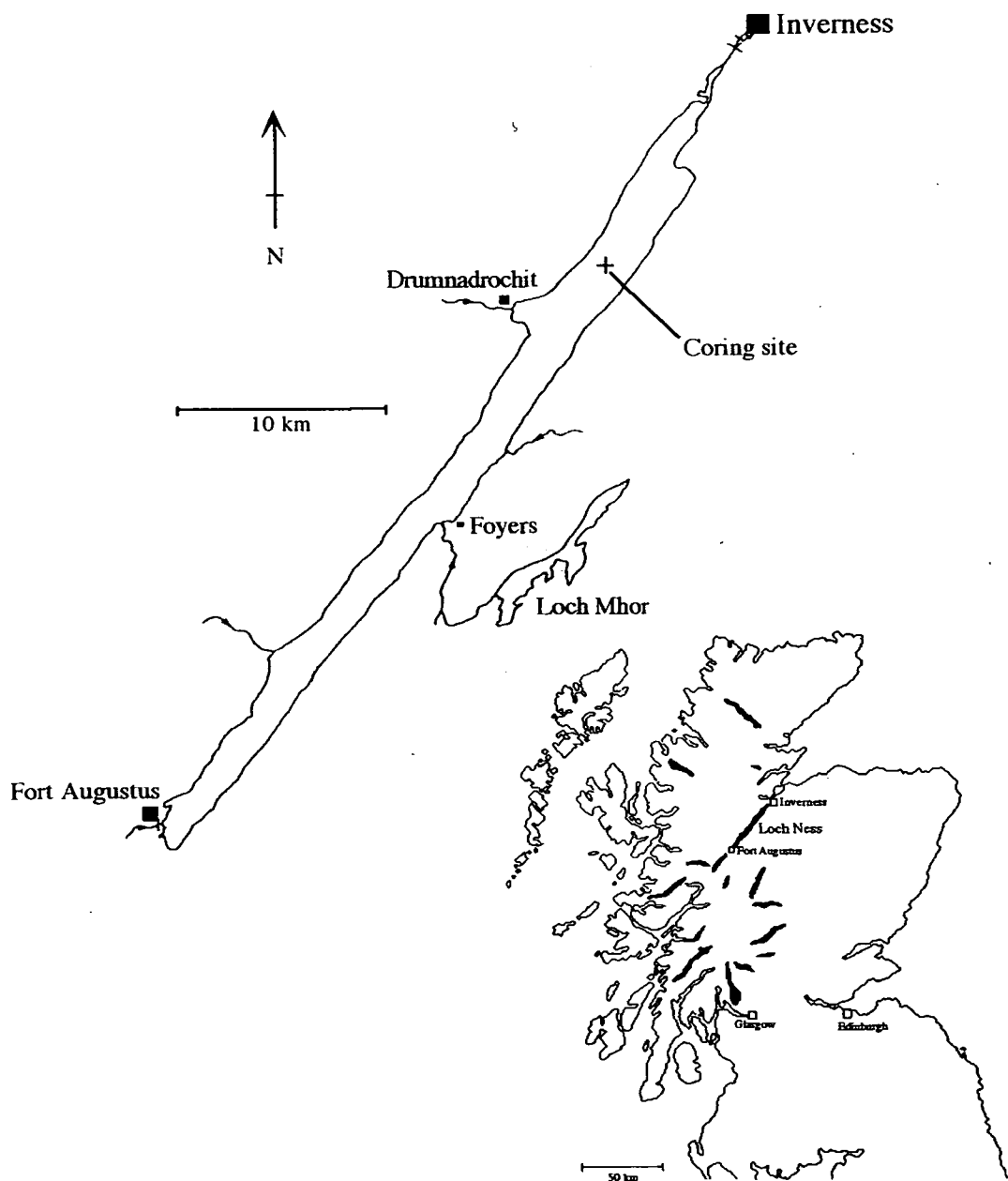


Figure 3.1 Site location (Modified from Maitland, 1981).

3.2 Tectonic setting

The Loch occupies a glacially-scoured valley trending southwest/northeast, the physical form of which is related to its alignment along the Great Glen Fault, a major tectonic feature of the Scottish Highlands (Canning *et al.*, 1998) and part of the larger Great Glen Fault Zone (Harris, 1991). The area is noted as a modern source of seismic activity (British Geological Survey. *Seismicity of the UK. Figure 3.2*).

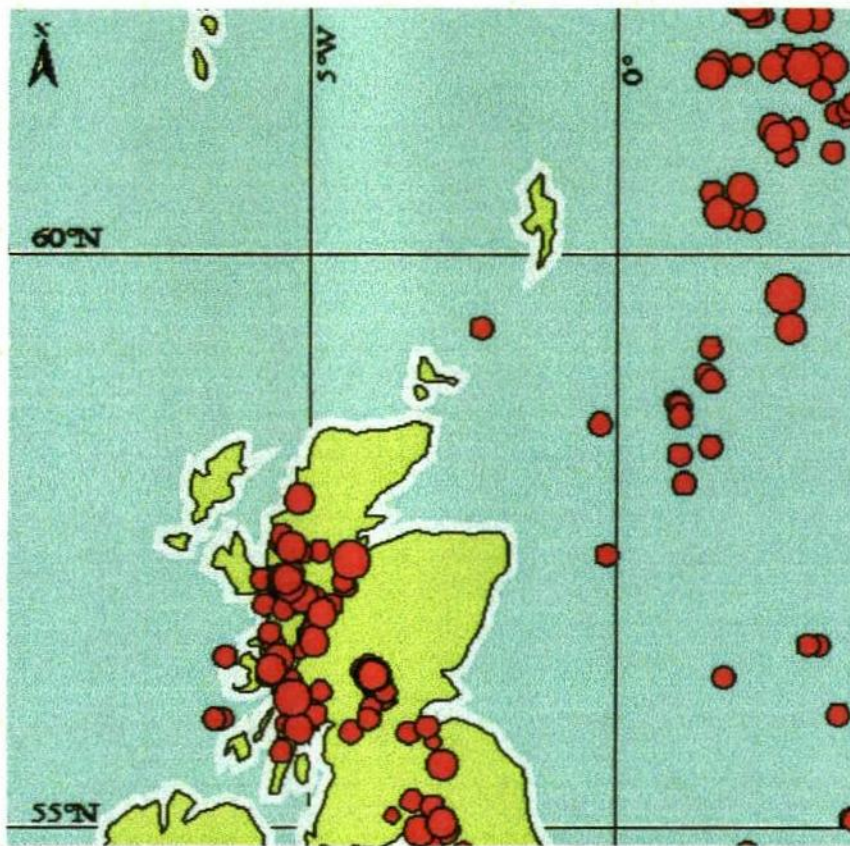


Figure 3.2 Seismicity of Scotland and the North of England. Red circles represent foci of seismic activity, scaled according to magnitude. The largest represent events of local magnitude (m_l) 3, and the smallest, less than magnitude 1.

(Source: <http://www.gsrn.nmh.ac.uk/~phoh/seismap2.gif>. Accessed Sept 15, 1998).

3.3 Morphology and Limnology

Loch Ness is the largest body, by volume, of lentic water in the UK (Maitland, 1981). Its major morphological characteristics are listed in *Table 3.1*. A recent bathymetric and seismic survey has revealed a maximum depth of 226.96 m with the possibility of sediments *ca* 40 m deep in some locations (Young & Shine, 1993). In cross section, the sides of the Loch are very steep (*Figure 3.3*) and the large, flat profundal plain is divided into two basins to the northeast and southwest of Foyers (*Figure 3.4*).

Table 3.1 Summary of morphological characteristics of Loch Ness (*After Smith et al., 1981*).

Area (km ²)	56.4
Volume (m ³ x 10 ⁶)	7452
Length (km)	39.0
Mean breadth (km)	1.5
Max. depth (m)	227
Mean depth (m)	150.7
Shoreline length (km)	85.3
Shore slope (m / m water fall)	3.7
Mean elevation (m amsl)	15.8

Loch Ness is temperate, monomictic, and oligotrophic (Maitland, 1981). Hydrological data are given in *Table 3.2*. Chemical analysis indicates that the water of the Loch is slightly acidic (pH 6.55), with low base cation concentrations (Ca²⁺, 81 fEq l⁻¹; Jones *et al.*, 1994). Nutrient concentrations (1992 values) are extremely low, below 500 µg (NO₃)²⁻ l⁻¹ and 200 µg (PO₄)²⁻ l⁻¹ (V.J.Jones *et al.*, 1997), although the equivalent unit loadings of solid and dissolved matter are greater than those of other large Scottish lochs, presumably because of the large catchment and the great number of streams flowing into the main body of water (Maitland, 1981). Concentrations of dissolved silicon are seasonally variable, but exceed 1 mg Si l⁻¹ during spring. The brown waters of the loch

(>15 Hazen units) indicate that total organic carbon levels in the water column are high (3 mg C l⁻¹). Secchi disc transparency is noted to be highest for red light (*ca* 630 nm wavelength), the 1% transmission depth being 4.7 m (Bailey-Watts & Duncan, 1981), which is comparable with other northern brown-water lakes (*e.g.* Pääjärvi, Finland; Jones & Ilmavirta, 1978).

Table 3.2 Hydrological data for Loch Ness (After Maitland, 1981; Thorpe, 1977)

Mean annual inflow (m ³ s ⁻¹)	84.1
Unit loading (t a ⁻¹)	2655
Eq. unit loading (g m ⁻² a ⁻¹)	47
Retention time (a)	2.8
Water level variability monthly (m)	0.27
Seiche depth (m)	132
Seiche period (hrs)	52

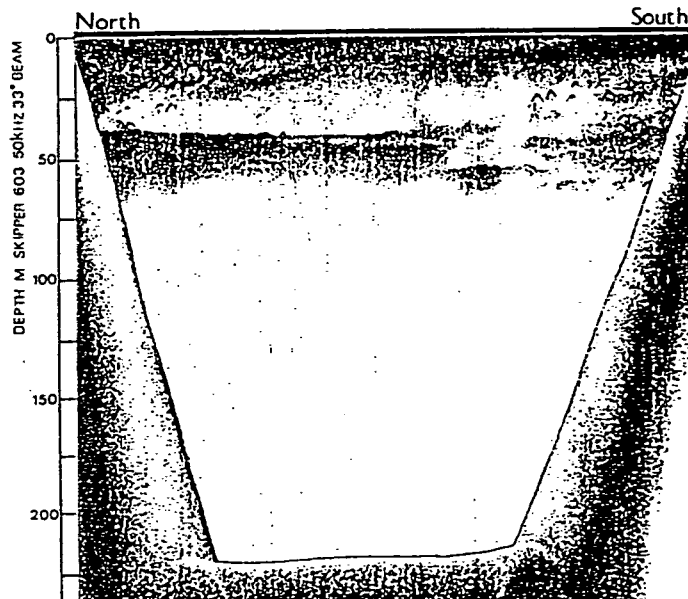


Figure 3.3 Echo sounding of transverse section of Loch Ness, illustrating the steepness of the sides of the basin. The mottled area at the top of the profile represents acoustic returns from fish and the developed thermocline. (After Shine & Martin, 1988).

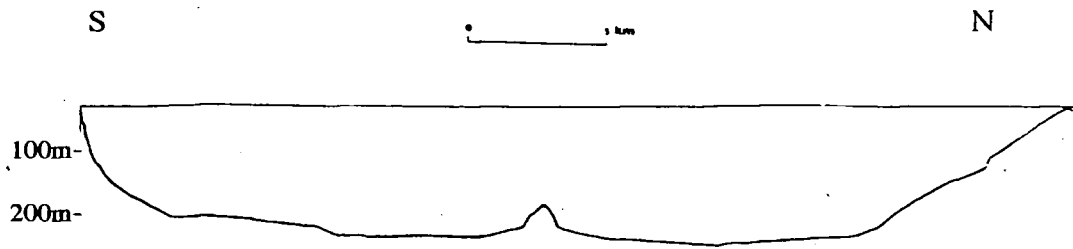


Figure 3.4 Longitudinal section through Loch Ness, illustrating the basin-like structure of the profundal plain (After Maitland, 1981).

The water column remains isothermal from late autumn until spring when a weak thermocline forms, descending to *ca* 50 m when fully developed, and possessing a thermal microstructure (Simpson & Woods, 1970). In comparison with other lochs in the region, stratification is delayed and the intensity reduced, presumably owing to the large volume of the basin. The theoretical water retention time has been calculated as 2.8a, but it is recognised that wind-induced currents may increase the volume of water transported through the loch and that the rapid discharge of 'recent' water may occur with appropriate combinations of inflow and wind speed (Thorpe, 1977; *Figure 3.5*). The construction of the Caledonian Canal, completed in 1822 and the Ness pumped-storage hydroelectric scheme, operational since 1975, are presumed to have had an effect on the limnological characteristics of the loch, especially in terms of the quality and quantity of inputs. Although no long-term records exist with which to test this hypothesis, it appears that flood prevention in the Inverness area has been enhanced owing to the impoundment and control of excessive flows through the Ness hydro-electric scheme (Johnson, 1994).

Loch Ness is aligned in the direction of the prevailing south-westerly winds, the nature of the surrounding terrain ensuring that low level air movements are directed along the major axis of the water body. Thus, circulation within the loch takes place in the

same direction, causing the formation of internal waves or *seiche* (Thorpe, 1971; Thorpe *et al.*, 1972; Thorpe, 1977) and a strong wind-induced mixing (R.I.Jones *et al.*, 1995). Indeed, R.I.Jones *et al.* (1995) have determined that the distribution of seston within the loch is dependent on recent wind history and conclude that this mechanism is the primary source of variability of plankton within the water column.

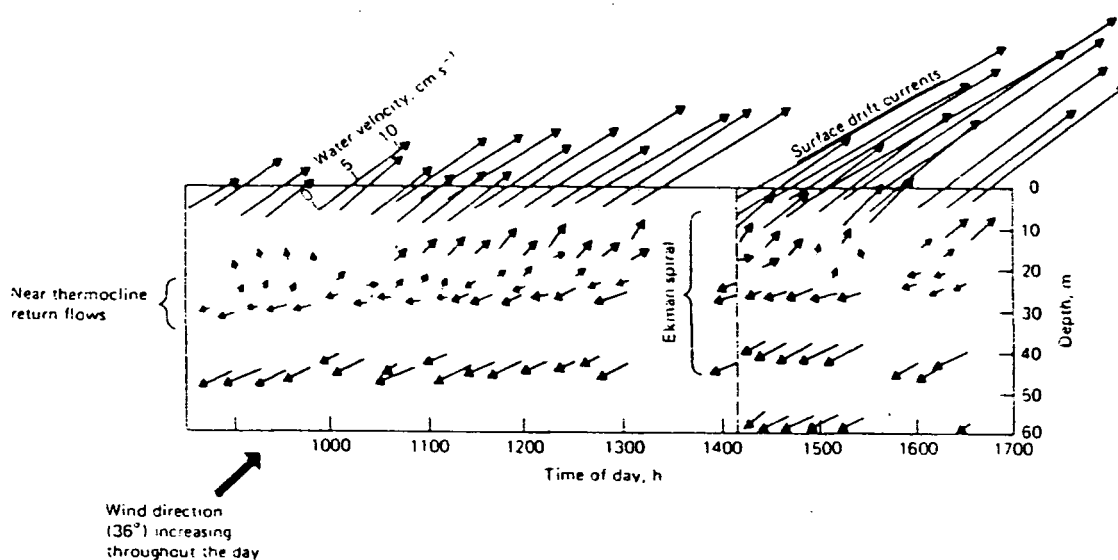


Figure 3.5 Passage of a storm across Loch Ness. Length of arrows indicate the magnitude of water flow. (After Thorpe, 1977).

A suite of sediment cores, collected in 1993, reveals that sedimentary patterns vary throughout the loch. At the southern end, coarse, mainly riverborne sediments are found (Bennett & Shine, 1993), whereas laminated lacustrine deposits appear mainly to be confined to the northern basin. This is probably because of the smaller number of rivers entering that part of the Loch directly, and the effect of SW winds on the seasonal and spatial distribution of seston. Sediments recovered from the profundal plain of the northern basin possess subtle colour differences between laminae, the contrast increasing in cores from the shallower areas towards the northern end of the loch

(Bennett, 1992). Laminated sands have been retrieved from the floors of both north and south basins adjacent to the mid-loch rise which exhibit iron staining, indicating a well-oxygenated environment. Sediments from close to the inflows of the rivers Moriston, Oich and Tarff contain organic debris-rich sands, silts and muds, an observation reinforced by investigation of the floor around Urquhart Bay by underwater camera, which has revealed abundant organic debris, including both decomposed and whole vegetable matter, twigs and branches (Bennett, 1992).

A submerged two-point mooring has been established at the coring site (UK National Grid Reference NH 256779.286 832203.627) by members of the Loch Ness Project. (*Figure 3.1*; Shine *et al.*, 1993). Cores were recovered from beneath 204 m of water. The site was chosen for its proximity to existing quay facilities, its mid-loch location above the profundal plain of the north basin and its relative distance from major riverine inputs (Shine, 1993). A submerged mooring is necessary owing to the recreational and navigational nature of the loch, whilst a two-point station proved to be economical to construct, yet provide the stability needed for coring and water sampling.

3.4 Climates of the North Atlantic Ocean & Loch Ness region

3.4.1 Major influences on the climate of the region

As discussed in *Section 2.4*, the location of Scotland on the northwestern seaboard of Europe places it under the influence of one of the Earth's most powerful sources of climatic regulation- the North Atlantic Ocean (Lowe, 1993). Here a distinct boundary, termed the North Atlantic Polar Front (NAPF), separates cold sub-arctic water to the north from temperate regions to the south. The front is marked, approximately, by the southern limit of iceberg survival, and generates an active zone of ocean-atmosphere interaction by which frontal systems are guided eastwards across the Atlantic. The location of the NAPF is thus a critical factor in determining the paths travelled by depressions, and

consequentially the climate experienced by the British Isles, especially in terms of storm frequency and strength (Keigwin & Jones, 1994; Kelly, 1979). Its position has been variable throughout the Pleistocene and Holocene (Ruddiman & McIntyre, 1981).

A second critical component of the climatic system of the region, is ocean thermohaline circulation, especially the 'North Atlantic Conveyor' (Broecker *et al.*, 1988). This is part of a global system driven by changes in water temperature and salinity. In the Atlantic sector, warm surface waters from the tropical and equatorial regions move northwards, losing heat and gaining salinity. This cold water mass then sinks at high latitudes and returns southwards at depth. The system is thus responsive to variations in water temperature and salinity, such as those experienced by the melting of the northern ice sheets at the end of the last glaciation, and by rates of production of deep, cold water in the northern seas.

3.4.2 Deglacial climate of the Loch Ness region

Fossils of land mammals have not been found at any of the late glacial interstadial sites but radiocarbon dating of deposits containing coleoptera indicate that the climate at about 13000 bp was very similar to that of the present time (Coope, 1977). At Redkirk Point species dated at about 11000 bp were found to be typical of more northern climates, indicating a marked deterioration of climate. This has been identified as the Loch Lomond stadial. Ice to the west of the Great Glen moved down Glens Arkaig, Lochy and Garry to fill the Great Glen with ice as far north as Fort Augustus (Sissons, 1979).

3.4.3 Deglaciation

The major phase of ice melting, named by Broecker & van Donk (1970) Termination 1A, and of about 1000 years duration, commenced about 15150 BP ($\pm 270y$) and is recorded in marine sediments as a period of low foraminiferal production in the

northern Atlantic. The signals for the abundances of two benthic taxa, *Neogloboquadrina pachyderma* (sinistrally coiled), which is a circumpolar species, and *Globigeroides bulloides*, found in more temperate waters, indicate changes in sea temperature with input of large amounts of glacial meltwater, mainly from the Laurentide ice sheet but probably also from Scottish glacial regions. The Allerød interstadial is marked by the reappearance of *G. bulloides* and the sudden total disappearance of *N. pachyderma*. Terrestrial evidence as to the rapid onset of this period may be found in the changes wrought in coleopteran populations throughout the UK (Coope and Brophy 1972). At the onset of the Younger Dryas cold period at about 10700 BP, the abundances of the foraminifera are again reversed, with the increase of *N. pachyderma* indicating falling sea temperatures. Termination 1B, which marked the period of transition from periglacial conditions to present climatic regimes, began after about 10500 BP and ended *ca.* 6000 BP. By 9500 BP the temperatures may have been as warm as at present (Osborne 1975, Bishop and Coope 1977).

Ruddiman *et al.* (1977) have suggested that, at that time, the movement of the Atlantic Polar Front was about 1500 m/yr southwards, followed by a retreat of *ca.* 1650 m/yr northwards at the termination of glaciation. Precipitation was high in the NW Highlands during the Younger Dryas, related to the location of the NAPF, which influenced the tracks of storm depressions, forcing them to a more southerly track than at present. These regions were ice-covered at that time and precipitation probably fell as snow (Lowe and Walker, 1984).

3.4.4 Deglaciation around Inverness

The effects of deglaciation in the area may be observed at a number of sites in the area, especially Alturlie and Ardersier (*Figure 3.6*). At the former location, a marine delta consisting of well sorted sands and beach gravels may be found in an ice-

proximal setting. Some of the features have been modified by marine action and some slumping has been caused by the melting of submerged blocks of ice (Firth, 1993).

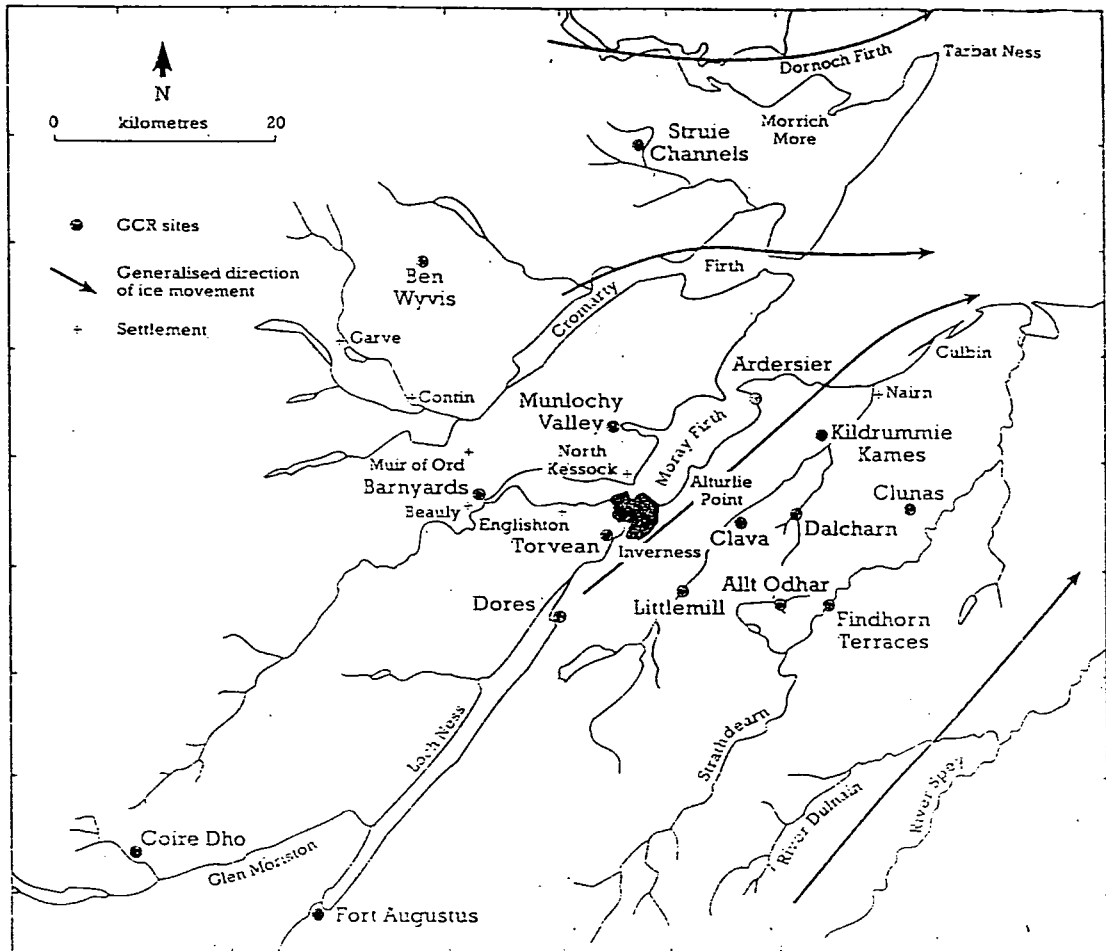


Figure 3.6 Sites around Inverness displaying deglacial features. (After Sutherland & Gordon, 1987. p 150)

The Ardiersier silts, consisting of folded and faulted sand/silt beds, have been explained by the glacial action of a readvancing ice sheet at *ca* 13000 BP (Synge 1977, Synge and Smith 1980), although Firth (1989), has suggested that the sediments represent *in situ* glaciomarine deposits. It may be possible that the sediments were deposited rapidly in an ice-free area surrounded by stagnant ice, formed by a retreating ice

front. The disrupted silts are overlain by the Hillhead beds of sands, formed in a high energy, probably littoral, environment. There are no faunal remains to produce positive evidence of the provenance of these features.

Other locations in the area exhibit other features which may illustrate other phases of deglaciation. At Redcastle, a degraded cliffline may be observed, cut into late-Devensian kame and kettle topology. There is no evidence of marine incursion (Firth, 1993). The Coulmore/Letlock area may have been occupied by ice until the relative sea level had fallen below 20 m AOD. The narrows in the Inverness Firth at Kessock (*Figure 3.6*) are thought to have been formed by deposits washed through the Great Glen by the *jökulhlaup* of the ice dammed lakes in Glens Roy and Gloy (Sissons, 1981).

3.4.5 The present climate of the Loch Ness region

The present climate is characterised by prevailing southwesterly airstreams, and possesses a pronounced maritime bias (*Figure 3.7*). Rainfall is greater over more westerly catchments than in the east, owing to topographic effects (Werrity *et al.*, 1994). Typical distribution of precipitation and temperature throughout the year, calculated from data collected at Fort Augustus during the period 1961-1994, is illustrated in *Figure 3.8*. As may be observed, temperatures only fall below 5 °C during December-February, with a broad maximum of *ca* 13 °C during June-August. Precipitation is high during autumn, winter and part of spring with average values of *ca* 100 mm month⁻¹. Low rates of evapotranspiration from the widespread moorland flora ensures that more than 75% of precipitation is converted into direct runoff, and snowmelt may additionally significantly increase flows in watercourses (Werrity *et al.*, 1994).

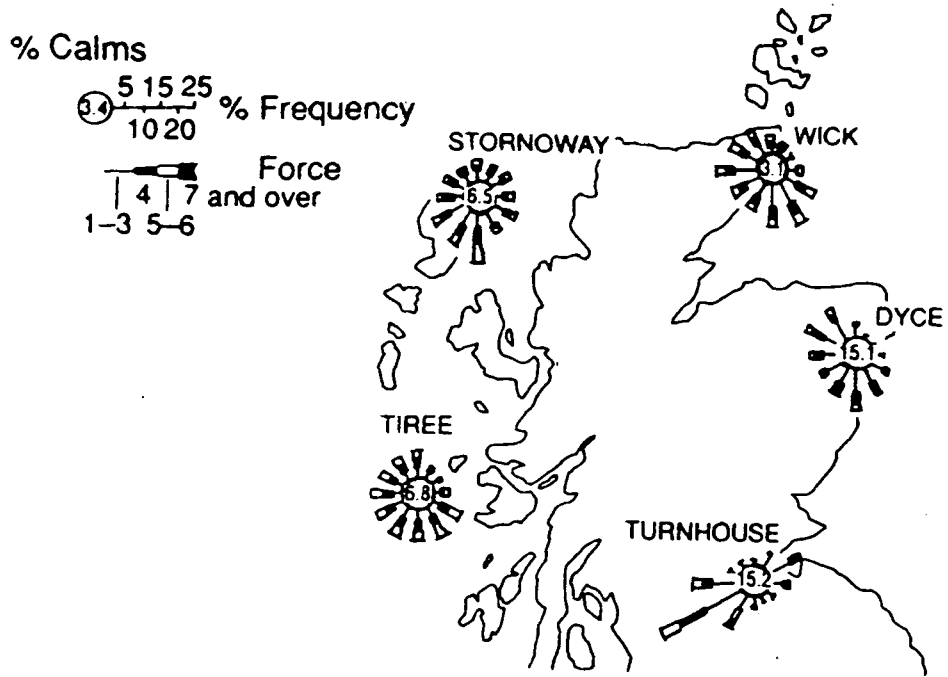


Figure 3.7 Frequency and strength of airflows across the Highland Region, Scotland.

(After Goudie and Brunsden, 1994).

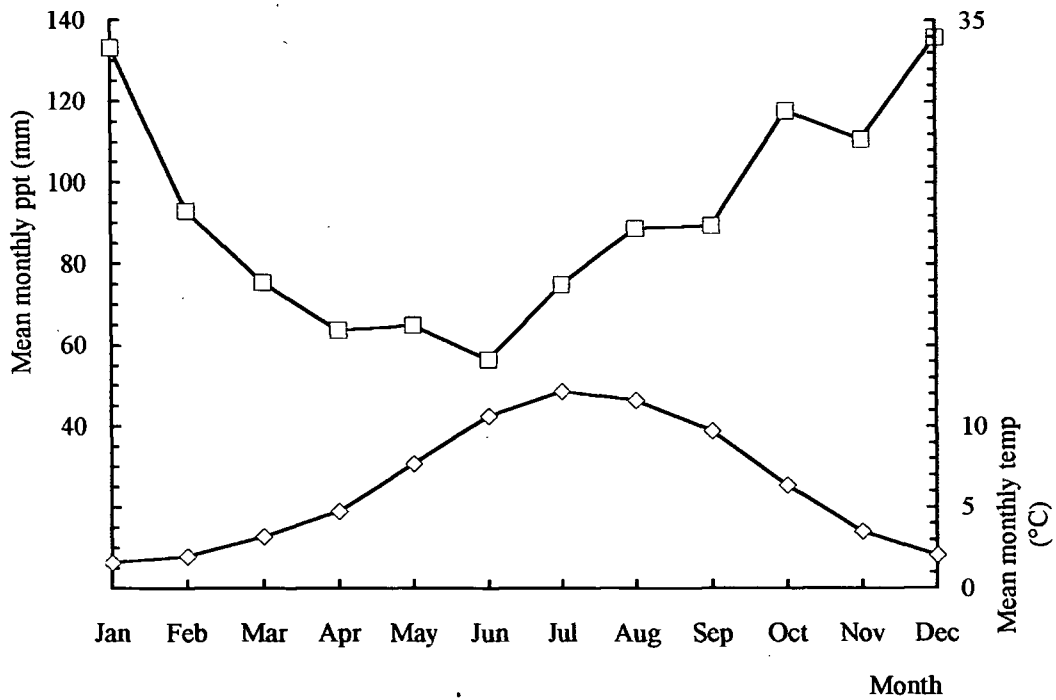


Figure 3.8 Mean monthly precipitation and temperature, Fort Augustus 1914-1994. (Data supplied by the UK Meteorological Office).

3.5 Description of catchment

3.5.1 Modern catchment

The catchment of Loch Ness (mean elevation >360 m; *Figure 3.8*) covers some 1800 km^2 and, at present, consists mainly of mountain and moorland, with some arable land to the north and east. The general geology of the area is composed of rocks of the Moine series, although both Lower- and Middle-Devonian sandstones outcrop in some areas along the edge of the loch. Small granite intrusions are located to the south.

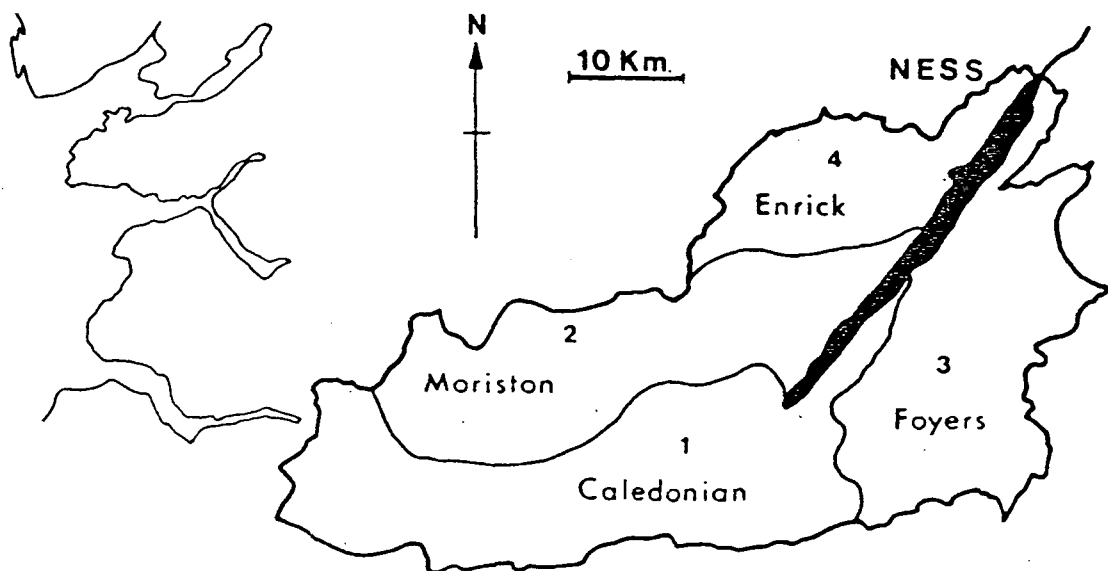


Figure 3.9 The catchment of Loch Ness (After Maitland, 1981).

Maitland (1981b) divided the catchment into four (*Figure 3.9*), based upon the watersheds of four major watercourses: the Caledonian canal, and the Rivers Enrick, Foyers and Moriston. It may be noted that the differences between modern catchments are slight with the greatest contrasts lying between the two northerly (Enrick and Foyers) and the two southerly (Caledonian and Moriston) basins, the former containing richer (more basic) soils, and relatively more arable land.

3.5.2 History and prehistory of catchment

3.5.2.1 The pollen record

A preliminary pollen diagram by Peglar (*Figure 3.10, upper*) from sediment core *Ness 3*, indicates that environmental changes in the catchment of Loch Ness may not have been very different from those recorded at other sites in this part of the Scottish Highlands. Indeed, the diagram from core *Ness 3* most closely resembles that by Pennington *et al.* (1972; *Figure 3.10 lower*), from Loch Tarff, a small (area *ca* 1 km², maximum depth 29 m) loch situated to the southeast of the Great Glen within the Caledonian catchment (Maitland, 1981). Peglar (pers. comm.) has commented upon the poor state of preservation of the pollen from core *Ness 3*, which she considers to indicate that waterborne transport of grains is a major pathway from the catchment into the loch. Other water bodies along the course of the rivers may act as sediment sinks, preventing pollen from a wider area reaching the loch via the fluvial route and restricting it to airborne dispersion over a limited area.

3.5.2.2 Probable catchment history from the pollen record

The landscape immediately after deglaciation (*ca* 9500 BP), was largely occupied by shrub and herbaceous taxa such as *Empetrum*, then *Ericaceae*, *Artemisia* and *Armeria*, growing on immature soils. Successive colonisation by *Salix*, *Juniperus*, *Betula*, and *Corylus/Myrica* was quickly followed by a rapid influx of Scots Pine, *Pinus sylvestris*. L. Investigations of the spread of this tree at other sites by Pennington *et al.* (1972; Lochs Clair, Wester Ross, and Sionascaig, Assynt), Birks (1972; Loch Maree, Wester Ross) and O'Sullivan (1976; Loch Pityoulish, Speyside) indicate that it took place during the period *ca* 9300-8500 BP, although it is recognised that the pines around Loch Maree are genetically different from those of other areas in the Scottish Highlands (Birks, 1996).

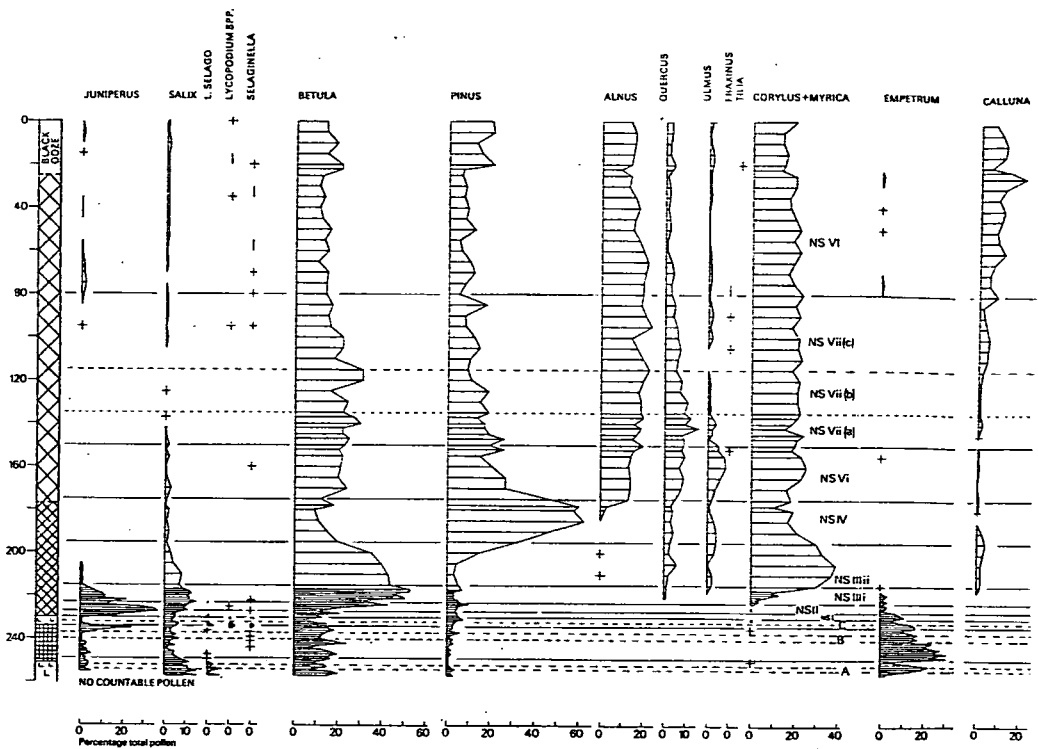
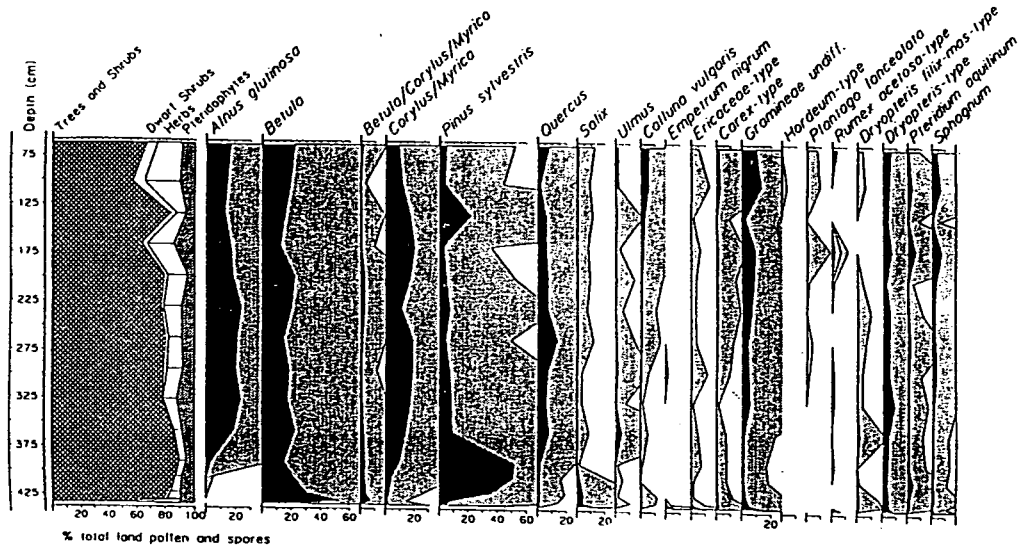


Figure 3.10 (Upper) Summary pollen diagram, selected taxa, from sediment core *Ness 3* (After Peglar, pers comm.), (Lower) compared with that from Loch Tarff, Scottish Highlands, (After Pennington et al., 1972).

At the time of the hypsithermal, *ca* 7000 aBP, it is estimated that 50%-60% of the landscape, up to the treeline at *ca* 800 m was under woodland (Smout, 1995). The expansion of other species from *ca* 4400 BP onwards, led to the retreat of pine to approximately its modern distribution, although in some areas expansion occurred. This decline has been attributed to many causes, the most likely being a deterioration in climate (Bennett, 1995; Birks, 1972). Decline of *Pinus* was followed by an increase in *Quercus*, *Ulmus* and *Alnus*, which in turn may have suffered decline owing to utilisation by early settlers (Edwards, 1993). O'Sullivan (1976), however, suggests that, at Loch Pityoulish, the decline in *Ulmus* pollen may represent a decrease in the general contribution of the taxon to the pollen spectrum of the Highlands, possibly because of a decline in populations further south. As tree species declined, an increase in taxa typical of upland moor (eg *Calluna*) occurred, in addition to those indicative of peat bog formation (*Sphagnum* sp.).

The preliminary pollen diagram from core *Ness 3* is insufficient to determine changes over short time scales and therefore may not indicate periods of recent woodland clearance and regeneration typical of the Neolithic/Early Bronze Age. Pennington *et al.* (1972) remark that the general zonation of succession in the Northwest Highlands may be compared with that of upland areas further to the south, for instance, the English Lake District. Recent analysis of core *Ness 4* has yielded the same result (Cooper *et al.*, in press).

3.6 Prehistoric and historic human impact upon the catchment of Loch Ness

3.6.1 General Chronology of settlement in Scotland from the postglacial to present

Knowledge of the human occupation of the Scottish Highlands has increased over the recent few years (Price, 1983) and, primarily through pollen analytical data, it is

possible to reconstruct changes to the environment brought about by human activity during the Holocene. Evidence of the earliest human habitation in Scotland has been found at Kinloch, on the island of Rhum, and has yielded radiocarbon dates in the region of 8590-7570 aBP, placing it in the Mesolithic (Edwards, 1993). Pollen analytical data from the site suggests that changes in flora were possibly caused by the forager lifestyle of the population, and an abundance of charcoal implies the use of fire, probably to clear woodland. It should be noted, however, that in remote areas, Mesolithic cultures survived long into what is chronologically, further south, the Neolithic, blurring the boundary between the two periods, but may be considered to have occurred from 6700-6300 aBP (Castleden, 1992; O'Sullivan, 1974).

The population of Mesolithic Scotland as a whole, based upon analysis of 100 known sites, is suggested to have been of the order of 60-70 persons (Atkinson, 1962). The distribution of settlements at this time was markedly coastal, possibly indicating the inhospitable nature of the interior of the country, although it may only reflect the ease of discovery of artefacts in beach and dune environments. It is also probable that any earlier sites of settlement around the coast may have been lost during the eustatic Postglacial marine transgression (Price, 1983).

Arrival of farming marked the change from foraging to agriculture, utilising domesticated livestock and cereal crops. Major changes to the environment would have ensued from a rapid rise in population, supported by a more plentiful supply of food, enabling the construction of the earliest permanent structures in the region. Evidence, in the form of pottery, suggests that by the Middle Neolithic, major ceremonial sites (for example, Cairnpapple Hill Henge, Lothian, Castleden, 1992; Ring of Brodgar, Mainland, Orkney, Longworth, 1985) were in use by worshippers both from Scotland and England, indicating that travel over long distances had become feasible. It is also from this period that the strikingly geometric cup-and-ring markings, found on a large number of standing stones and cists, originate. Evidence of large-scale forest clearance in northern Scotland

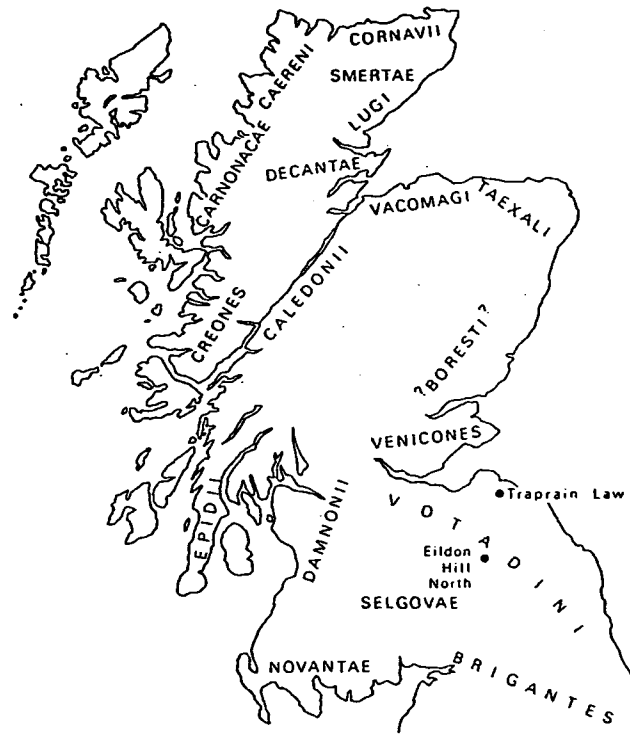


Figure 3.11 Distribution of northern tribes in the first century AD.

prior to the Iron Age (*ca* 2500 aBP; MacKie, 1975) is limited, however (Tinsley & Grigson, 1981).

The earliest historically dated event in the human occupation of Scotland is the arrival of the first expedition of the Roman army, in *ca* 80 AD (MacKie, 1975). Similarity of artefacts discarded by the invaders with those found at sites around the Mediterranean, enables the construction of a cross-dated chronology for the region, and one which may be extended, to a limited extent, both backwards and forwards in time. The distribution of the northern tribes at the time of the first century AD may be noted in *Figure 3.11*. No data exists as to population numbers, although Price (1983) suggests that they were certainly less than 250,000. Distribution may be estimated from the concentrations of monuments dated from this time and still displays a marked coastal bias (*Figure 3.12*). The spread of Roman culture over the period 200-500 AD may be illustrated by *Figure 3.13*, which

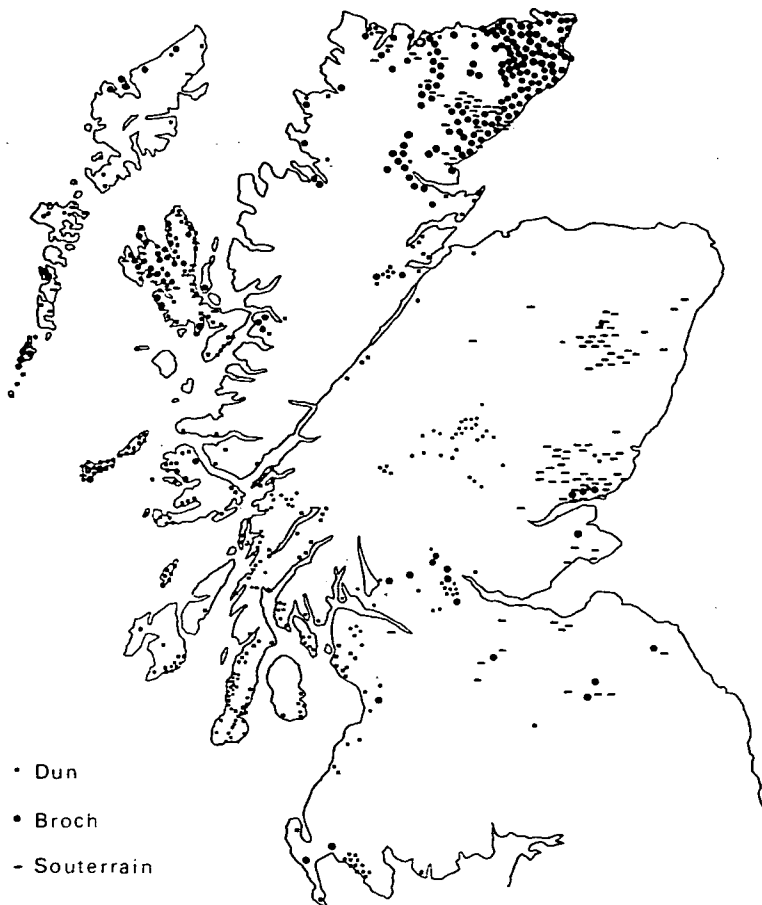


Figure 3.12 Distribution of population in Scotland around the time of the first century AD.



Figure 3.13 Distribution of Roman finds, first century AD.

depicts finds of Roman origin from non-military sites. These also delineate the extent of Roman military incursions into the region. Contemporary reports describe the native Picts as "half-naked enemies" and, indeed, part of the fourth century was marked by a series of wars between Picts and Romans (Breeze, 1982).

3.6.2 Evidence of early settlement around Inverness and northern Great Glen

The area around Inverness contains many archaeological features, which may be observed on the accompanying UK Ordnance Survey map extract (*Figure 3.14*). These include Neolithic/ Bronze age burial mounds at Caiplich (UK National Grid reference *NH 543386*, Ordnance Survey, 1993), a vitrified fort at Dun More Cabrich (*NH 535429*), and possible broch at Castle Spynie (*NH 541421*). The burial cairns at Clava (*NH 756443*), consisting of three chambers surrounded by stone circles, date from Late Neolithic/Early Bronze Age (*ca 4800-4700 aBP*; Castleden, 1992), indicating that the region was occupied at that time, and probably earlier (*Figure 3.14*). Castleden (1992) estimates that the community which constructed the cairns may have numbered no more than 30-40 adults. The vitrified fort of Craig Phadrig (*NH 640453*), situated on a prominent hilltop above Inverness, was once believed to have been a Pictish capital, but dating of material from the walls places its construction as earlier. Artefacts found by excavation suggest traces of Dark Age occupation (MacKie, 1975).

In the area around Drumnadrochit (*Figure 3.15*), cairns (*NH 383303*, *NH 495315*), forts (*NH 500295*, *NH 491236* and *NH 452298*), settlements and field systems (*NH 510321*) and a cup marked rock (*NH 500312*) record occupation at various times since the retreat of the ice. In particular, the presence of cup-marked stones illustrates that the area was inhabited around the early Bronze age, *ca 4000 aBP*. The siting of two forts, Dun Dearduil and Dun Garbh (*NH 530240*) above Inverfarigaig, on the south-eastern fringe of the Loch indicates settlement in the catchment during the Iron Age. At Urquhart Castle, on Strone Point (*NH 531286*) continuing occupation of the area, from the Late

3. Site description

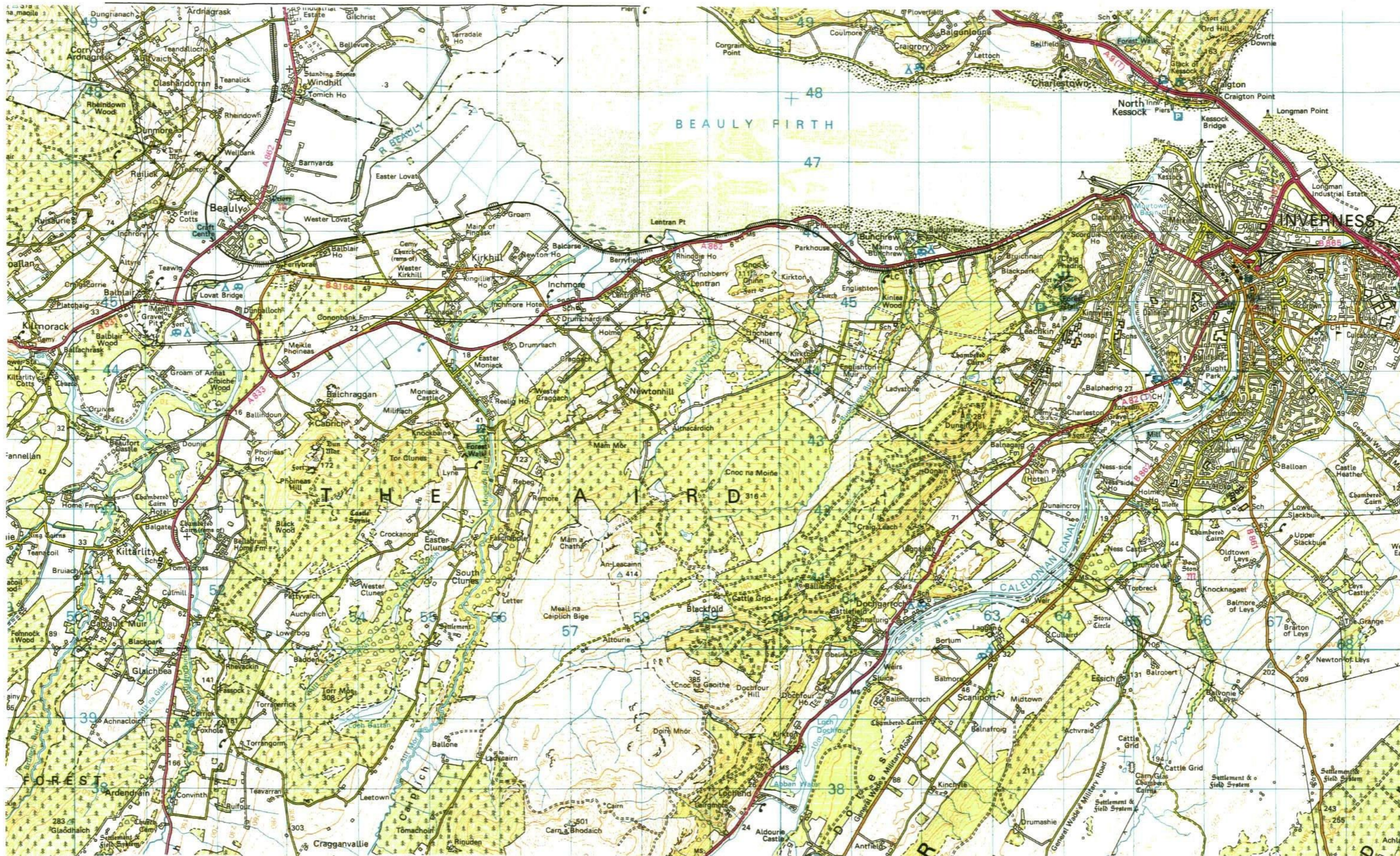


Figure 3.14 Archaeology- Inverness area

Ordnance Survey map © HMSO

3. Site description

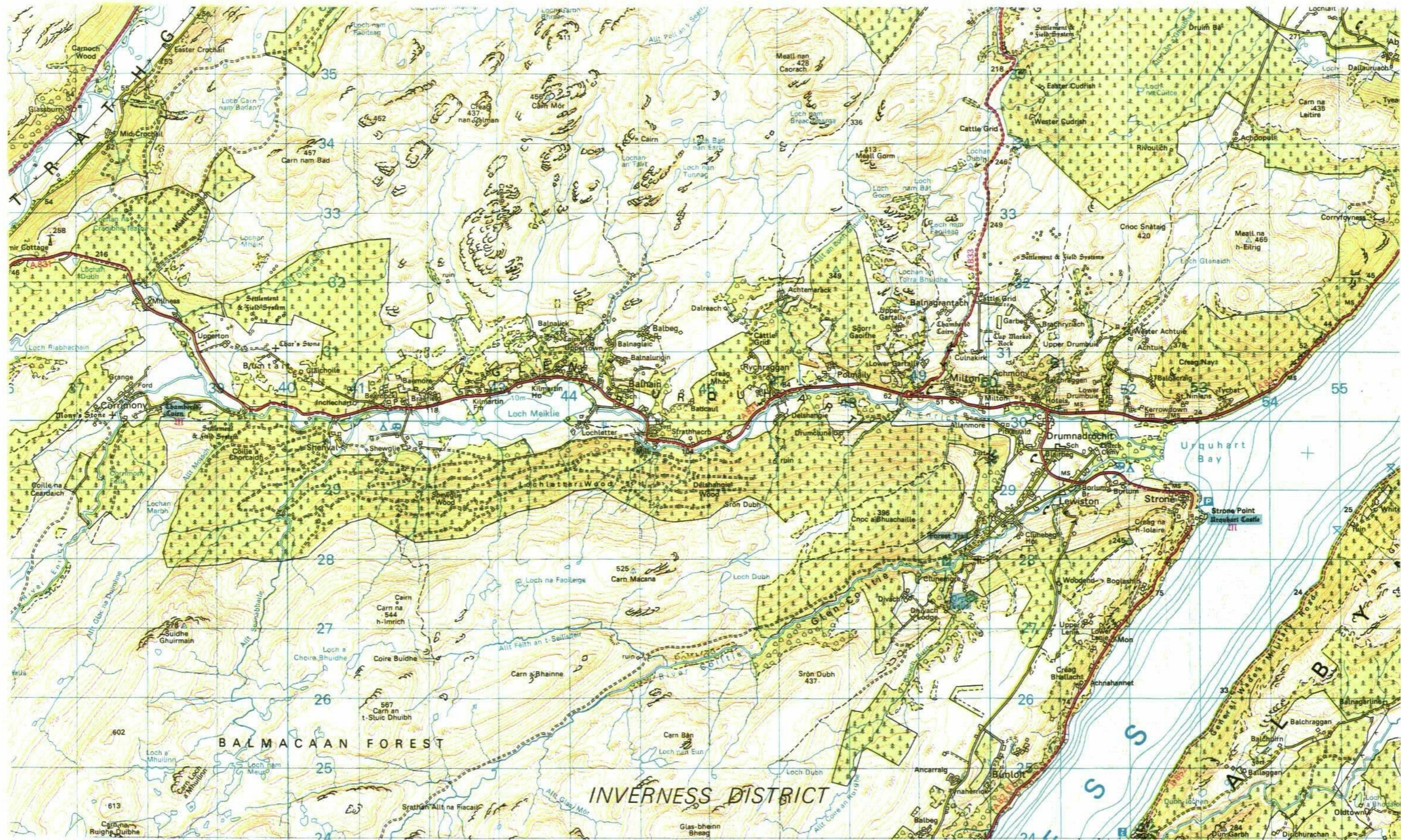


Figure 3.15 Archaeology - Drumnadrochit area.

Ordnance Survey map © HMSO

Bronze Age, represented by the remains of a vitrified fort, through a motte of Norman age, to a 14th century stone castle, possibly one of the largest in Scotland (MacKie, 1975), is recorded.

3.7 Previous research on sediments from Loch Ness

Several investigations have been undertaken in recent years, on both the sediments and the water column of Loch Ness, in order to characterise this important body of water and to further understand the processes occurring within it. Some aspects of investigations into the limnology and biology of the loch have been mentioned briefly earlier in this chapter. Current research into sediment characteristics will now be described.

3.7.1 Catchment erosion studies

A one metre core has been analyzed for mineral magnetic and single element bulk geochemical properties (Jenkins, 1993). The data are thought to indicate an increase in catchment erosion during the Little Ice Age (500-300 aBP; Lamb, 1979), and the additional input of lead to the sediments from the modern burning of fossil fuels. At present, conclusions are speculative, since no dating has been carried out on this material.

3.7.2 Atmospheric pollution

A separate one metre core has been dated by ^{210}Pb in order to produce a recent chronology by which to date the incidence of atmospheric radionuclide contamination. The record of artificial radioisotopes (^{137}Cs , ^{134}Cs and ^{241}Am) in the sediment indicates that Loch Ness and its catchment has received contamination from global weapons testing over the last 40 years, and from the Chernobyl nuclear accident (Battarbee & Allott, 1994).

Spheroidal carbonaceous particles (SCP) are indicators of industrial contamination (Renberg & Wik, 1991), and the combustion of coal (Rose *et al.*, 1995). The SCP profile for Loch Ness reflects national and regional trends in fuel burning over the last 150 years. Polychlorinated Biphenyls (PCBs) and Polycyclic Aromatic Hydrocarbons (PAHs) (Sanders *et al.*, 1993) have also been detected in recent sediments recovered from the Loch and their concentrations over the last 60 years have been determined. These exhibit an initial increase which may be related to industrial activity and burgeoning fossil fuel consumption, followed by a decrease in very recent material, which is thought to result from the global restrictions on their production and use.

The diatom record of recent sediments may be utilised in this case in order to determine whether or not a water body has been acidified by increased sulphur loads (Battarbee *et al.*, 1988; V.J.Jones *et al.*, 1993). Results from Loch Ness suggest that there have been recent species changes, but that taxa sensitive to acidification have not significantly declined. Reconstruction over the whole length of a core, probably spanning in excess of 400 years, shows that pH lay consistently at about 6.5 over this period (V.J.Jones *et al.*, 1997).

3.7.3 Eutrophication

Variations in the diatom population may also be indicative of eutrophication. Analyses of sediments from Loch Ness indicate that nutrient levels within the Loch are still extremely low but that over the last 10 years, planktonic taxa have expanded to account for approximately 50% of the diatoms in the sediment, indicative of increasing nutrient enrichment (V.J.Jones *et al.*, 1997).

4. Methods

Many techniques have been utilised for the analysis of the material recovered from Loch Ness (*Table 4.1*), and these will now be described in detail. The utilisation of image transforms in order to facilitate rapid characterisation and measurement of laminae (Cooper, 1998) is believed to be a unique facet of this study.

Table 4.1 Techniques employed in this study, illustrating their purpose.

Determination of dry matter & loss on ignition	Determination of lithological variation with time and estimation of organic content of core material.
Infrared photography	Enhancement of surface features of vertically sliced sediment cores.
X-radiography	Enhancement of lamination structure. Visualisation of internal structure of laminae.
Densitometry	Quantification of lamination characteristics. Construction of time series.
Image analysis	Enhancement of lamina structure. Determination of lamination thickness, construction of chronology and time series.
SEM analysis	Visualisation of microlithology of laminae. Determination of variations in elemental composition between layers.
Radiometric and AMS ^{14}C dating	Estimation of age of core material. Testing of hypothesis that laminae are varves.
Statistical analysis	Identification of degree of randomness of values within time series. Determination of variation in deposition rates.
Fourier analysis	Estimation of periodicity of time series.

4.1 Coring

Recovery of sediment cores was carried out by members of the Loch Ness Project, based at Drumnadrochit, Scotland. Equipment used was dependent on the length of core required, and consisted of hybrid versions of Mackereth (Mackereth, 1958; Mackereth, 1969), Kullenberg (Kullenberg, 1947), and piston corers. One-metre cores were recovered using PVC drain pipe as the coring barrel, and six-metre cores with stainless steel tubing. Each corer has been designed to be deployed from a small boat by a small number of operators.

4.1.1 One-metre cores

These were recovered by means of a 'bucket corer', designed by Adrian Shine to accommodate coring tubes of up to two metres in length. The equipment may be deployed from a small boat. Its basis, as the name implies, is a galvanised steel bucket, modified to enable core tubes to be passed through its base and fixed. The corer is weighted by the addition of small rocks to the bucket, in order to achieve slight negative buoyancy to provide the coring effort. The equipment is lowered through the water column until a messenger weight, which is attached to a spring-loaded shackle holding the bucket to the support cable, touches the sediment/water interface. Bucket and coring tube are then released from the cable, to fall under gravity into the sediment. The entire corer is then recovered. It is reported that, with care, it is possible to recover an intact sediment/water interface (SWI) with this device (A.J. Shine, pers. comm.). This equipment was used to recover core *LNRI*. No drawings are available for this device.

4.1.2 Longer cores

Cores *Ness 3* and *Ness 4* were recovered by use of a hybrid Mackereth corer, originally designed to penetrate up to 12 m of sediment. This device utilises the anchor

chamber design of the Mackereth corer, in order to provide stability while coring, while other elements of the design may be compared to the Kullenberg corer.

Briefly, operation of the device is as follows. The corer is towed to the coring station by small boat, utilising the coring tube rotated into a horizontal position between the anchor chambers. Water is then admitted to these, causing the device to submerge and enabling the core barrel to be swung to an upright position, in preparation for coring. The anchor chambers are then flooded and the corer allowed to settle on to the lake bed. A vertical position is maintained by means of auxiliary floats attached to the corer. Water is then pumped out of the anchor chambers, causing them to settle further into the sediment and preventing the device lifting when the core barrel enters the sediment. An airlift bag of one-tonne capacity is then inflated to propel the core barrel into the sediment and to also provide an element of lift in order to recover the device to the surface after coring. *Figure 4.1* illustrates a simplified representation of this device.

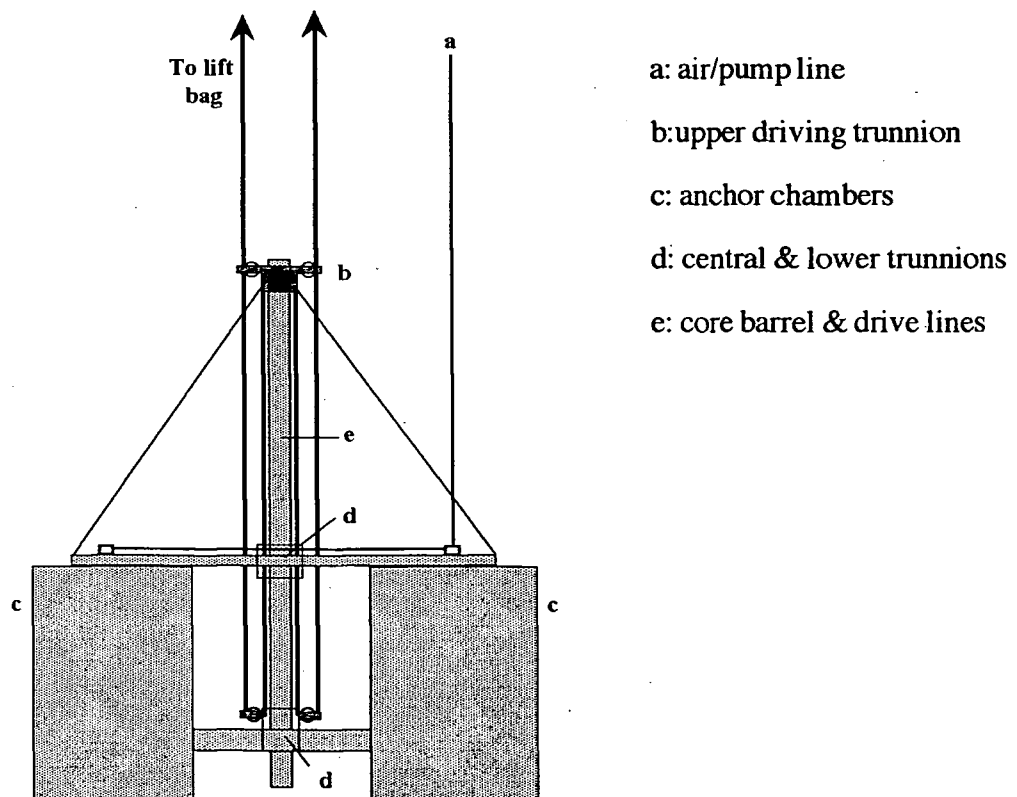


Figure 4.1 Elements of the Shine-designed 'long corer' (After A.J.Shine, pers. comm.)

4.2 Determination of percentage dry matter and percentage loss on ignition

4.2.1 Introduction

Percentage dry matter (%DM) and percentage loss on ignition (%LOI) may be conveniently determined together after the method of Engstrom & Wright (1984). Knowledge of the value of %DM throughout the length of a core enables lithostratigraphic variations to be identified through the detection of changes in the type of material deposited, which may result in variation in the porosity of the sediment. %LOI values may be employed in order to ascertain changes in the amounts of organic or mineral matter present, which may indicate variation in such processes as biological productivity or catchment erosion.

4.2.2 General

Samples for %DM and %LOI analyses were taken from both core *Ness 3* and *Ness 4*, and consisted of *ca* 4 cm lengths of sediment removed from the surface of each core. It was decided to sample at closer intervals in the upper and lower sections of both cores as it was thought that these sections might record evidence of more rapid changes in catchment and climate.

4.2.3 Methods

4.2.3.1 Dry matter and water content

Samples of wet sediment were placed in pre-weighed, labelled porcelain crucibles, which were then re-weighed. The weight of each sample was then determined. The samples were placed in an incubator at 105°C for 24 hours, after which they were

checked in order to ensure full dryness. The combined weight of crucible plus dry sample was then determined, and the dry mass and water content of each sample calculated by the formulae:

% dry matter

$$\frac{(\text{dry sample +crucible}) - (\text{weight of crucible})}{(\text{wet sample +crucible}) - (\text{weight of crucible})} \times 100 \quad (4.1)$$

% water content

$$1 - \frac{(\text{dry sample +crucible}) - (\text{weight of crucible})}{(\text{wet sample +crucible}) - (\text{weight of crucible})} \times 100 \quad (4.2)$$

4.2.3.2 Ash content and percentage loss on ignition

Dry samples and crucibles from previous determination were re-weighed and placed in a muffle furnace. A careful note of the relative positions of each sample was taken, since all labelling was removed by the high temperature of the operating furnace. Samples were ignited at 550°C for four hours, after which the furnace was allowed to cool to 120°C before they were removed and re-weighed. The weight of remaining sample, representing refractory inorganic material ('ash'), and percentage loss on ignition were determined by the following:

% ash

$$\frac{(\text{ashed sample+crucible}) - (\text{weight of crucible})}{(\text{dry sample +crucible}) - (\text{weight of crucible})} \times 100 \quad (4.3)$$

%LOI

$$1 - \frac{(\text{ashed sample} + \text{crucible}) - (\text{weight of crucible})}{(\text{dry sample} + \text{crucible}) - (\text{weight of crucible})} \times 100 \quad (4.4)$$

4.3 Infrared photography

4.3.1 General

Infrared radiation may be generally classified as that electromagnetic radiation with a wavelength of between *ca* 10^{-6} - 10^{-4} m, and may be generated by a number of processes. Detection of infrared radiation may be carried out by the exposure of photographic film sensitive to those wavelengths (*Figure 4.2*), although an optical filter allowing only a narrow band of wavelengths to pass through is additionally placed between subject and film in order to diminish extraneous radiation. Normal photographic techniques may be employed and the resultant image indicates the efficiency of the subject in reflecting or emitting infrared radiation. For this study, sediment cores were illuminated with photographic flash lighting. The images obtained indicate the emissive or the reflective properties of the sediment material in the wavebands under consideration (*Figure 4.2*) and may be correlated with lamination structure viewed in visible light.

4.3.2 Photographic Method

Sections of core, *ca* 1m in length, were imaged at various magnifications, utilising studio flash equipment synchronised with a tripod-mounted 35mm SLR camera loaded with Kodak High-Speed Infrared film (*Eastman Kodak Corp., Rochester, USA*). Test photographs were initially taken in order to ascertain the homogeneity of lighting, film response and development time. Critical determination of the distribution of light from

the flash units was carried out by measuring the deviation of exposure time determined at fixed points across the photographic field, from that at the centre of the field (*Figure 4.3*). Gross deviations (>0.5 f-stop) were addressed by the repositioning of one or both of the heads of the flash units and the process repeated until all points within the photographic field were determined to be equally (<0.5 f-stop) illuminated. This procedure was followed at the beginning of each photographic session to ensure continuity between different sets of images.

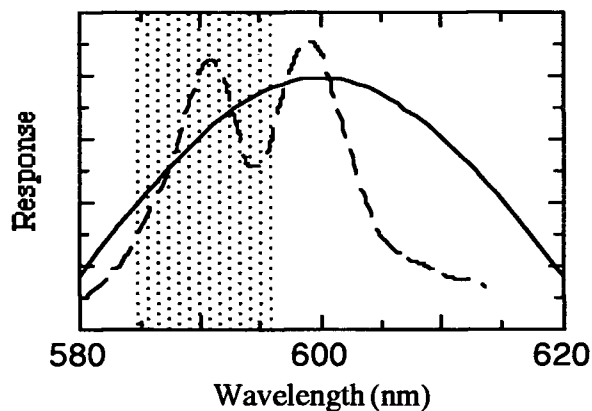


Figure 4.2 Spectral response of Kodak High-speed Infrared Film, with (solid line) pass band of Kodak W10 filter, and (dashed line) typical reflectivity curve for a clay mineral, montmorillonite (After Eastman Kodak, 1972; Drury, 1988).

Images were obtained using a 50mm lens utilising various subject-camera distances, depending on the type of image required (wide-angle or close-up). A series of macro images were obtained but were deemed unsatisfactory owing to spurious reflections from the irregular surface of the sediments, even following extensive preparation. Images were obtained in all cases with an indication of scale by the positioning of a white ruler alongside each core section. Development and printing of the images was carried out in accordance with the manufacturers recommendations.

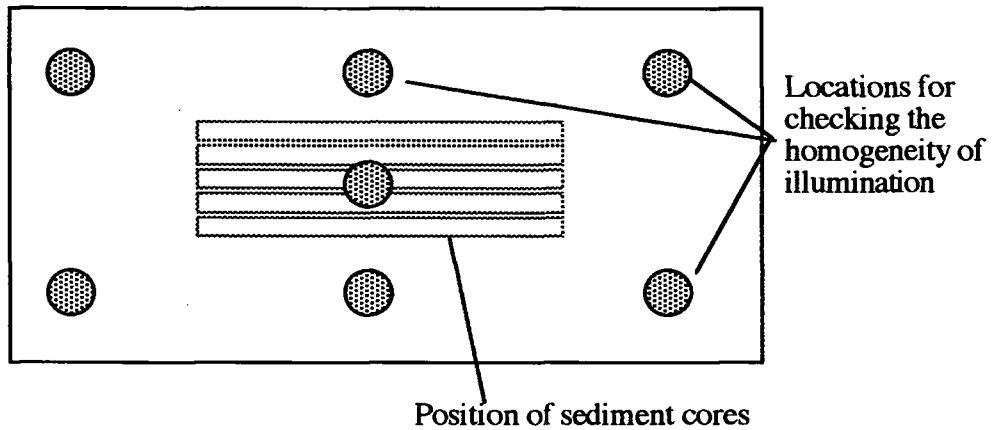


Figure 4.3 Diagram illustrating the method employed in order to ensure uniform illumination of the photographic field.

4.3.3 Sediment preparation

Prior to each photographic session, sediment cores were removed from cold storage, unwrapped and allowed to warm slightly in the laboratory. For each initial session, *ca* 1-2mm of sediment was removed from the surface of each core by means of a taut stainless steel wire pulled across each section in the direction of the laminae. The freshly cut surface was then carefully smoothed, again in the direction of the fabric of the sediment, by dragging over it the edge of a glass microscope slide (Renberg, 1981). Water (a powerful absorber of Infrared radiation) present on or just beneath the surface of the material was demonstrated not to affect the imaging process by photographing, in close-up, a section of sediment of which half the surface remained untreated. The other half was maintained in a moist state by allowing water to stand on it for *ca* 10 minutes before taking the photograph. No differences were detected.

4.4 X-radiography

4.4.1 Introduction

X-radiography has been employed in many studies in order to reveal the internal structure of sediment cores, and offers high resolution (of the order of 0.1mm; Algeo *et al.*, 1994) when comparatively thin sections (cm-scale) of material are analysed. It may be utilised to determine rates of accumulation, variation in lithology, gas content, onset of eutrophication and to illustrate variation in sedimentary style, for example, from laminated to non-laminated sediments (for examples of these applications see, for instance, Axelsson, 1983; Bodbacka, 1985; Boespflug *et al.*, 1995; Koivisto & Saarnisto, 1978; Schimmelmann *et al.*, 1992).

4.4.2 General

X-ray plates (AGFA Curix, *blue sensitive type C. Agfa-Geveart AG, Leverkusen, Germany*) were stored according to manufacturers recommendations (<10°C) and loaded into a light-proof film cassette under darkroom conditions (*Safelight filter type 206*). The cassette employed contained scintillation screens comprising an organic fluorescing agent producing visible blue radiation upon absorption of x-ray quanta. This mechanism generates a latent photographic image upon the x-ray plate, which may be then developed by conventional photographic techniques.

Orientation of the sediment sections was achieved by the adoption of a consistent work pattern, aided by the labelling of the clingfilm wrapping of each section and the marking of each section during x-ray exposure by an identification number made from x-ray opaque material, which was always placed at the base of each section.

4.4.3 Exposure determination

Test exposures were carried out with a random selection of pre-sampled sediment sections to ascertain the optimum conditions for x-ray imaging. It was found that while small (*ca* 10 kV) changes in x-ray energy had a very marked effect on the detection of the structure of the laminae, exposure times were not so critical. Source-sample distance was also varied and observations of changes in resolving power, based upon fine detail visible, were noted. An exposure time of *ca.* 0.4 s, at a source-sample distance of 1.9 m, produced good lamination detail and a wide range of photographic density from an x-ray energy of 40kV. This latter value was the lowest obtainable from the unit used. After examination of the x-radiographs by image analysis, however, it was decided that images of sections near to the tops of the sediment cores were perhaps a little over-exposed (too much radiation), while those near the base were under-exposed. Repeat images were then obtained from these sections by adjustment of exposure times by -0.1 s and +0.05 s, respectively.

Increasing the distance of the x-ray source from the sediment did not result in an increase in photographic resolution as might be expected (Algeo *et. al.*, 1994). This was attributed to possible interference of the transmission of the x-radiation by the collimating baffles at the exit window of the x-ray unit. Whilst it is realised that, from the geometry of the equipment, a theoretical resolution of only 0.26 mm (section length 10 cm, allowing for 5cm overlap between sections; *equation 4.5*) is possible at the specified source-sample distance, it was decided that owing to the contrast between laminations, the finest detail observable from the plates did indeed delineate the darkest (and often the thinnest) laminae in the sediments and that only in the lowest, early Holocene, section of the core, may x-radiography not prove conclusive.

$$\text{resolution} = t \cdot \tan(a) \quad (4.5)$$

where: t = thickness of section
 α = angle of radiation normal to the sediment surface

with reference to *Figure 4.4*.

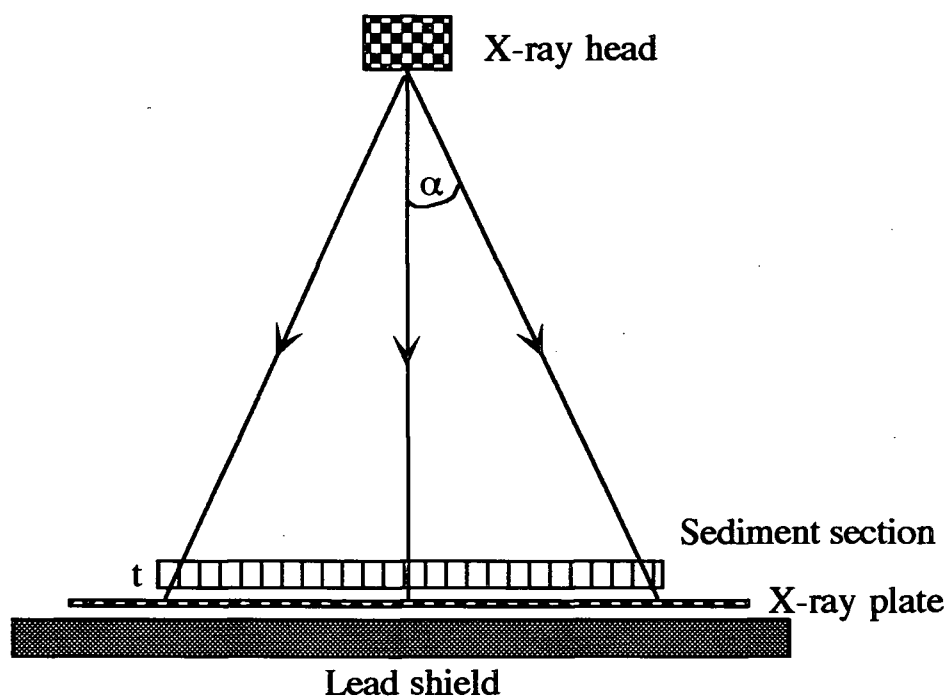


Figure 4.4 Determination of resolution of x-radiographic technique. Distance between film plane and sediment section is negligible compared with that between x-ray source and section.

4.4.3 Development of x-ray plates

After exposure, the plates were returned to a darkroom for photographic development, again under safelight conditions. Plates were prewashed in water to aid uptake of developing solution prior to immersion, with constant agitation, in developer (*Agfa G150, Agfa-Geveart NV, Belgium*) at 22°C for 3min. They were then removed to a stop bath, in this case water, to halt development before immersion in fixer for a further

1.5min. After rinsing, they were finally washed in surfactant solution. Plates were air dried at 60°C for 30min, after which contact prints were produced for illustrative purposes.

4.5 Image analysis

4.5.1 Introduction

The use of image analysis for the examination of the structure of unlaminated sediments and soils is well documented (Dartnell & Gardner, 1993; Glasbey & Horgan, 1995; McBratney *et al.*, 1992). Walanus & Goslar (1993), working with varved sediments from the Polish lake Gosciaz, have demonstrated that it is possible to count laminations using image transforms. Ripepe *et al.* (1991) have utilised densitometric analysis of tape peels from oil shales of Eocene age in order to detect ENSO and sunspot cycles. More recently, Schaaf and Thurow (1994) have employed the technique in order to produce high resolution time series from drill cores and rock samples.

For this study it was decided to obtain primary images of sediment from Loch Ness which exhibited unambiguous lamination detail and to further submit these to image analysis in order to count the layers. Details of this stage, utilising X-radiography, may be found in *Section 4.4*. A dedicated image analyser (*Quantimet 570, Leica, Cambridge, UK*) was employed in order to digitise the primary images, and enabled the application of transforms to each (Cooper, 1998), prior to densitometric measurement and lamination counting, in order to facilitate:

- i). delineation of the laminated structure of the sediment
- ii). measurement of the mean thickness of each lamination
- iii). measurement of the average grey level of each lamination.

4.5.2 Measurement and densitometry

Perhaps the simplest technique of image analysis to perform is direct measurement of features from the digitised image. The technique has been widely applied to the study of laminated sediments (for example Boespflug *et al.*, 1995; Dean *et al.*, 1994; Koivisto & Saarnisto, 1978; Schimmelman & Lange, 1996; Schimmelman *et al.*, 1992) and allows calibration of distances within an image to correspond to the actual distance in the real world. Within the Quantimet environment, this procedure is performed by invoking a movable line profile which is positioned between two points whose actual distance apart is known. Other distances in that image may then be easily computed. For laminated sediments, this procedure may be utilised in order to measure lamination thickness, although where many laminae are to be quantified, this would be very time consuming.

An alternative approach was utilised in this study, which simultaneously furnished both lamination thickness and mean Grey Level (GL), that of densitometric analysis. Here a transect, shown as a slim rectangular frame superimposed on the sediment image and perpendicular to the laminae (*Plate 4.1*), was selected and the grey level of each pixel in the profile determined. A trace such as *Figure 4.5* was produced, where large grey values represented pale laminae and small values, dark ones. Examination of rates of change of grey values, large values of which occurred where there were lamination boundaries, enabled the calculation of lamination position and thickness.

4.5.3 Image enhancement

Several processing techniques were employed in order to enhance images, and to facilitate detection of weak or ill-defined laminae. A major source of error in counting was uncertainty in the unequivocal detection of laminae caused by insufficient perceived

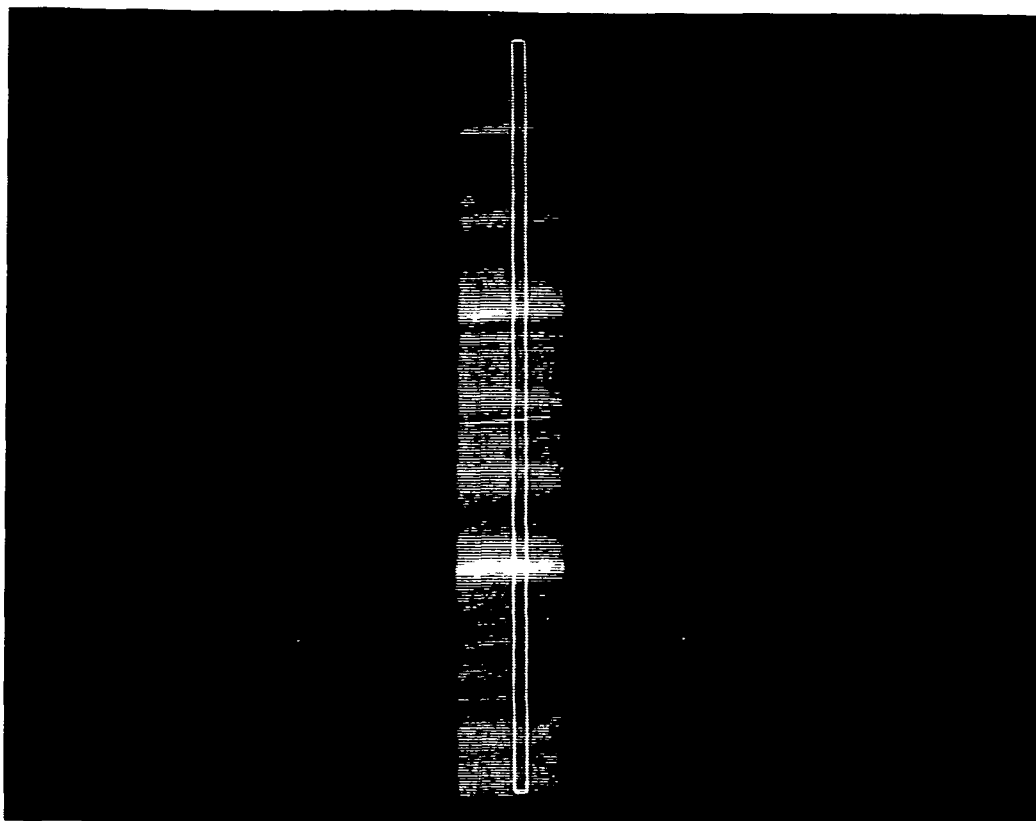


Plate 4.1 Image of an x-radiograph of a section of laminated sediment. Pale areas represent more radio-transparent material. The white frame superimposed upon the x-radiograph is an 8-pixel-wide window within which grey level measurements are taken.

spatial or grey level resolution upon digitisation. Images of laminated sediments, whether obtained by photography or x-radiography, consist of areas of varying tones of grey level, each characterised by a quantifiable set of parameters. Of particular interest was characterisation of laminae in terms of grey level, thickness and location in the stratigraphic sequence. Measurement of these values was aided either directly or indirectly by the application of one or more image processing operations. Of particular interest was the use of smoothing algorithms, and of filter matrices (kernels), in order to enhance lamination perception.

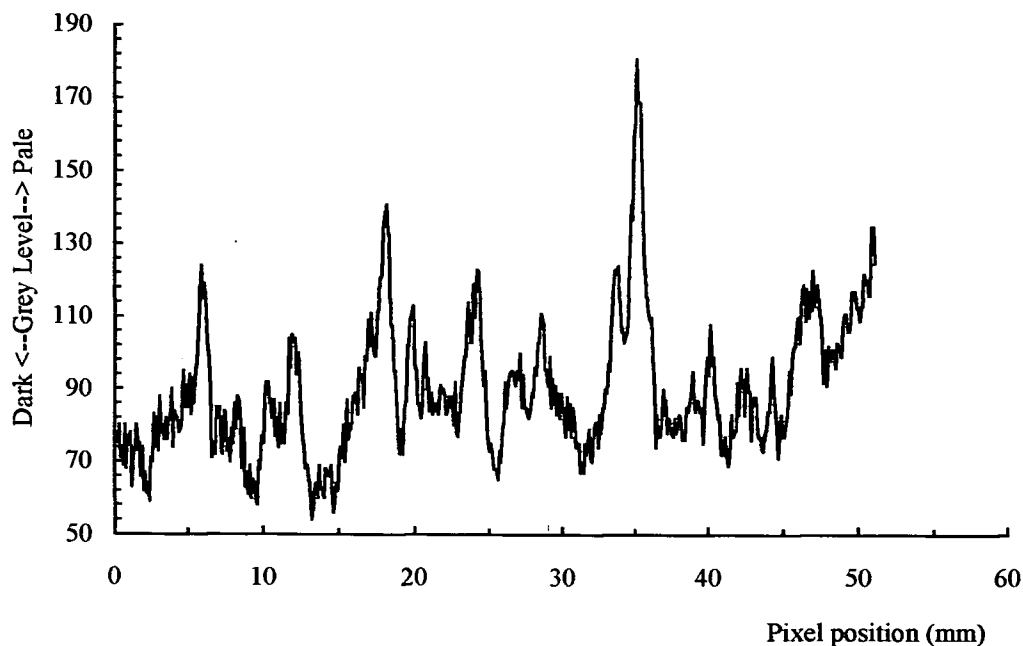


Figure 4.5 Densitometric trace derived from the x-radiograph in *Plate 4.1*, data being taken from within the 8-pixel-wide measurement frame. Note that a conspicuous noise component, manifest as a high frequency, low amplitude signal, exists within the data.

4.5.4 Smoothing and averaging

Random noise produced by electronic circuitry (Marion, 1991) was decreased by averaging eight frames of the same image during acquisition, but these still contained minor defects owing to, for example, detector noise, as well as to those features inherent in the subject, such as photographic grain. A smoothing transform was thus applied to each image in order to remove, or at least greatly to decrease, these defects. Median filtering was found to be well suited to this purpose, since the nature of the filter ensured that boundaries were not moved and that grey level differences across them remained. Densitometry of this image revealed that the noise levels had decreased (*Figure 4.6*) after application of this transform.

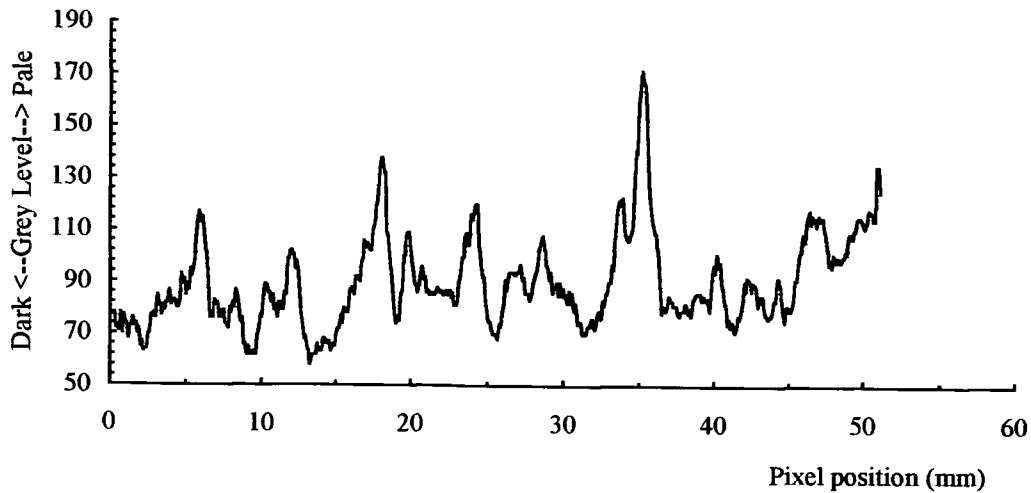


Figure 4.6 Densitometric trace derived from *Plate 4.1*, after the application of median filtering, illustrating the diminution of high frequency noise within the image.

4.5.5 Histogram equalisation

Many images did not contain a full range of all possible grey level values and histogram equalisation was employed in order to spread grey levels more evenly (Russ, 1992). With this technique, differences in brightness between pixels was maintained, but GL values were shifted, leading to the enhancement of detail indiscernible in the original image. Although useful generally, it was found in many cases to degrade image quality to the point where densitometry was deemed unreliable, and was thus only sparingly utilised.

4.5.6 Dilation and Erosion

Dilation is the addition of pixels of the same GL to the boundaries delineating an object from its background. The operation thus replicated pixels around the periphery of, and also tended to remove 'holes' within, an object. Dilations performed parallel to the fabric of the laminae were found to be the most useful in the context of this study.

In practice, a transect, a few pixels wide and aligned parallel to the frame of

the image analyser, was copied into another image memory, producing a narrow image containing information about GL changes along that transect caused by the lamination structure. The image was then dilated parallel to the laminae, enlarging the transect. No extra information was added by this operation, the only effect being to replicate the data contained within the original transect (*Plate 4.2*). Thus all positional, GL and dimensional information was retained. The process was then repeated utilising another transect, leading to formation of another dilated image. One was then subtracted from the other, resulting in the production of a null image (or nearly so) and acted as a test to ensure that the original image was aligned with the image frame and that the laminae within each transect were identical. Individual transects were then averaged in order to produce an further image for densitometric analysis (*Figure 4.7*).

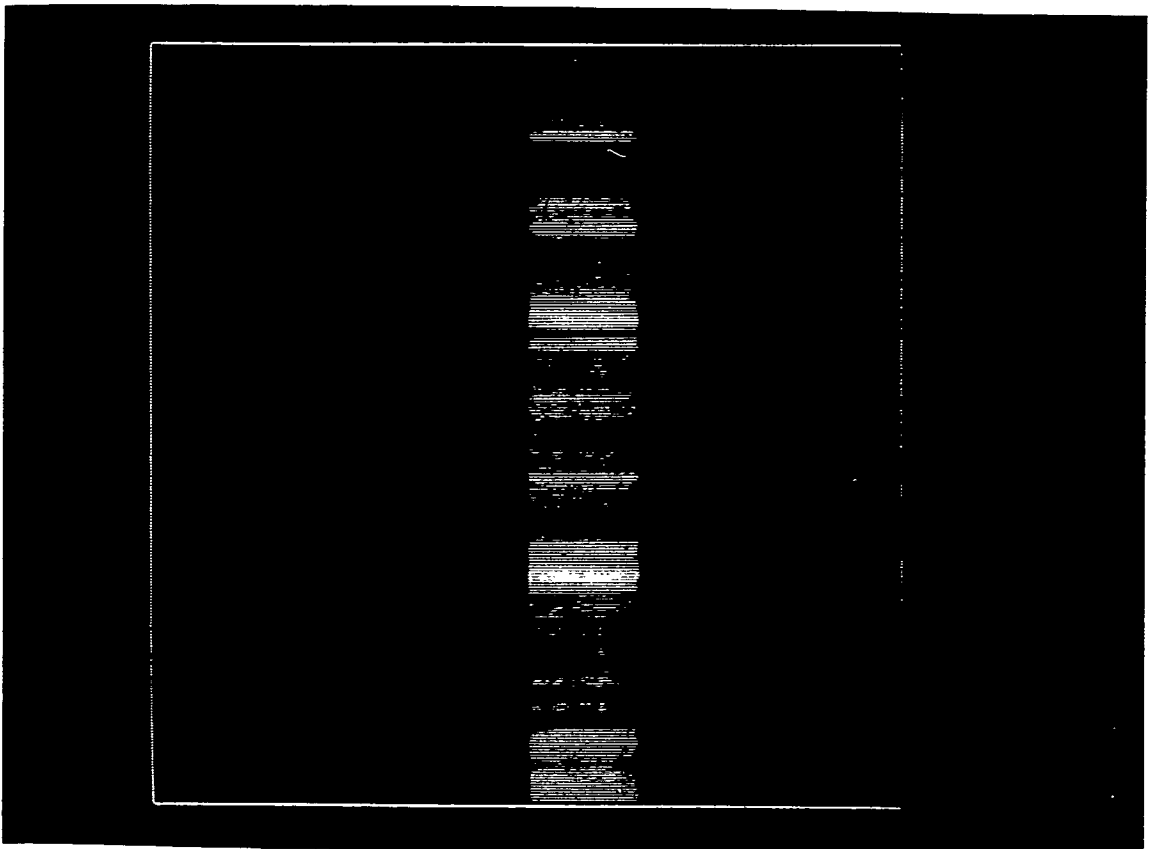


Plate 4.2 Image of a transect from *Plate 4.1*, after undergoing a series of horizontal dilation transforms. Each lamina is now homogeneous across the width of the image.

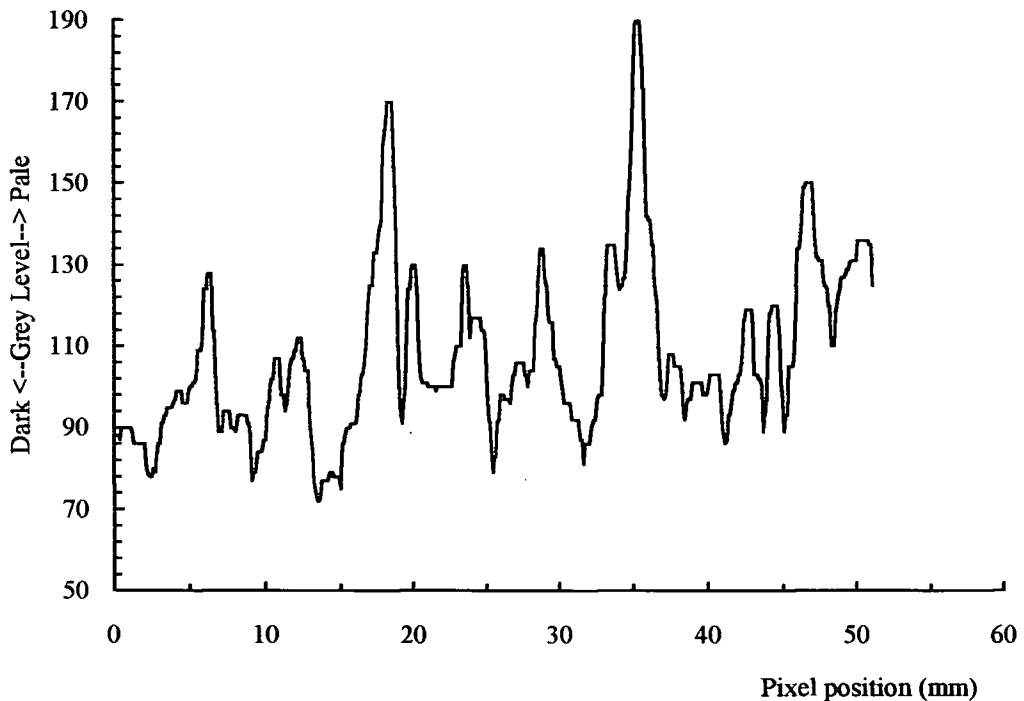


Figure 4.7 Densitometric analysis of a transect of an image (*Plate 4.2*) after dilation

4.6 Scanning Electron Microscopy (SEM)

4.6.1 Introduction

Many texts describe the principles of operation of this technique, both as a tool for imaging, utilising both secondary and backscattered electrons, and for the determination and quantification of chemical elements present (see, for example, Coldstream *et al.*, 1992). The application of SEM to the study of laminated sediments may be divided between that of imaging in order to determine microlithological variations (for example, Brodie & Kemp, 1994; Kemp, 1990; Kemp *et al.*, 1996), observation of fossil microfauna (for example, Dean *et al.*, 1984; Schimmelmann *et al.*, 1992), and elemental analysis, which may ascertain changes in chemical composition (Alapieti & Saarnisto, 1981), between layers.

4.6.2 Sample preparation

Eight sections of sediment, representing material deposited at different times within the last *ca* 8.5 ka, and consisting of *ca* 20 laminae were removed from both long cores. Each section was divided vertically into two and material in each prepared for analysis by different procedures. All samples were air dried in ambient conditions, and one from each section was impregnated with epoxy resin (Pike & Kemp, 1996; *Spurr's resin*; Polysciences Inc., 1993). Several sections were rough polished but others remained unimpregnated and unpolished. All were vacuum-coated (VG Isogas, Horsham, UK) with gold or carbon in order to improve the electrical conductivity of the specimen.

4.6.3 Imaging and elemental analysis

Sections were examined by SEM (JEOL 6100, JEOL Ltd., Tokyo, Japan), at 20 KV electron energy, and at various magnifications. Both secondary and backscattered electrons were detected, with additional Electron Dispersive X-ray analysis, utilising the EDS detector attached to the instrument and associated software (Link Analytical Ltd., High Wycombe, UK; Oxford Instruments Ltd., Oxford, UK). Identification of sediment samples is listed in *Table 4.2*. Transects of each sample, perpendicular to the fabric of the laminae, were scanned in order to ascertain whether or not there appeared to be any variations in microlithology between layers, or if there existed visible changes in number or type of microfossils within laminae.

Elemental analysis was carried out by scanning the primary electron beam over a small (*ca* 3000 μm^2) area of the sample, in order to average the signal. For each analysis, sample stage height within the instrument remained constant at 17mm and integration time of the analysis was 100 seconds. A beam intensity appropriate for *ca* 25% detector dead time was maintained. Examination of both pale and dark laminae was undertaken. Preliminary examination of the samples was initially carried out in order to

Table 4.2 Sample designations for SEM analyses.

<i>Sample</i>	<i>Approx. age (ka BP)</i>	<i>Impregnated</i>	<i>Polished</i>	<i>Coating</i>
c1	2	✓	✓	C
c2	4	✓		C
c3	5	✓	✓	C
c4	7			C
g1	2	✓	✓	Au
g2	4	✓		Au
g3	5	✓	✓	Au
g4	7			Au

ascertain which elements were present, and variation in composition between samples was determined by calculating the ratios of those elements. Detection software was then configured to quantify those elements present. Samples coated with gold were analysed utilising the detector covered with a thin window, allowing elements as light as carbon to be quantified. Results from the analysis of polished sections were corrected using the ZAF method in order to negate effects due to atomic number, absorption and fluorescence (Coldstream *et al.*, 1992).

4.7 Acquisition and analysis of densitometric traces

4.7.1 Introduction

X-radiographs of sections of sediment were produced by methods previously detailed in *Section 4.4*. They were then digitised, enhanced utilising image analysis transforms, and densitometrically analysed as described in *Section 4.5*. A software routine

was written in order to facilitate conversion of the densitometric data contained within the digitised X-radiographs into a form which could then be processed by further software specifically written for the purpose of detecting the position of laminae within the sedimentary sequence and for quantifying their characteristics. Lamination thickness data were then assembled into chronological sequence in order to produce time series for investigation by Fourier Transform spectral analysis, and for comparison with other palaeoclimatic datasets.

4.7.2 Acquisition of densitometric data

A computer program, written by the author in the QuicBasic programming language (*Version 2.1. Leica, Cambridge, UK. 1995*), was utilised in order to acquire and quantify grey level values along a longitudinal transect of an image. The rationale behind the method may be found in *Section 4.5*, and it is only intended here briefly to discuss the program and explain its structure.

4.7.3 Program operation

An array of 512 elements was set up, the maximum allowed by the image analyser, which was utilised as data space for the densitometric measurements. Array elements not filled were set to zero. The program stores calibration data, and time/date stamps the output in order to provide a record for the user. Measurements in either vertical or horizontal directions were accommodated by altering the aspect ratio of the measuring frame. User input consisted of identification of the image frame to be measured, and enabled a suite of images to be consecutively quantified at one time.

4.7.3.1 Program listing

```
10 REM**** nessmeas - measurement of greyscale ****
20 REM**** values from photos/radiographs of Loch Ness
   sediment cores ****
30 REM**** 1994 February 24. Mick Cooper. Env Sci ****
40 REM*
50 input 'Enter data file name:',ifile$
60 ifile$='B:'+ifile$
70 open#1 ifile$
80 riasettings      'cal_value' k
90 PRINT 'Calibrated (Y/N)?';
100 INPUT cal$
110 IF cal$ = "N" OR cal$ = "n" THEN k = 0
120 print #1: date$,time$
130 print #1:'pixel size:',k
140 riasettings      'mframex' x1
150 riasettings      'mframey' y1
160 riasettings      'mframeh' h1
170 riasettings      'mframew' w1
180 mframe x1 y1 w1 h1
190 s1=0
200 input 'Enter image for measurement: ',p1
210 DIM x(512)
220 if w1<h1 then s1=h1:goto 240
230 if w1>h1 then s1=w1:goto 260
240 vprof p1 x1 y1 w1 h1 x(1)
250 goto 270
260 hprof p1 x1 y1 w1 h1 x(1)
270 for n=1 to s1
280 print #1: x(n)
290 NEXT n
300 close#1
310 END
```

4.7.4 Program structure

The basic structure of the program may be summarised as follows:

- 1) Set up variables and dimension data storage.
- 2) Ask user for file name
- 3) Ask user if data is calibrated. Set calibration to zero if not.
- 4) Ask user for image number to measured
- 5) Check on aspect ratio of measurement frame and select appropriate greyscale measuring routine- vprof: vertical profile; hprof: horizontal profile.

6) Write data to output file

The program was configured to measure only one image at a time, since the Quantimet operating system does not allow for the background operation of QuicBasic. Thus, the program needed to be re-run for each image to be measured, which incidentally alleviated the need to include reinitialisation routines since all variables are declared and cleared each time. The inclusion of the request for image identification does, however, enable the user to acquire many images, manipulate them, and then perform densitometric analysis without returning to the Quantimet operating system between each set of measurements.

4.7.5 Analysis of densitometric traces

The task of determining the position of 'highs' and 'lows' within a series of sequential digital measurements is a problem common to many disciplines. The quantification of the signal from a detector affixed to a gas or liquid chromatograph as it responds to the elution of different chemical compounds, and the location and translation of bar code markings by a checkout scanner at a supermarket are two examples. Many mathematical techniques may be utilised in order to standardise the perceived signal and extract the required data (peak location, intensity and width in the former example, and bar thickness and sequence in the latter), but most employ algorithms which define, in the signal stream, points of rapid change in intensity and thus the location of the digital 'peaks and troughs'. Mathematically, many procedures involve the calculation of the first derivative of the signal, although calculation of the second derivative has been shown to be advantageous where poorly-defined peaks are prevalent (Grant & Bhattacharyya, 1985). For simplicity of programming, however, it was felt that utilisation of image processing techniques, prior to densitometric analysis, would obviate the requirement of second differential arithmetic and thus it was decided to calculate the first differential of the signal over four consecutive pixels within a sliding data window.

4.7.6 Computer program

The computer program, written by the author in Microsoft QBasic (*Version 1.1. Microsoft Corporation, Seattle, USA. 1987-1992*), quantifies densitometric data and produces sequences of lamination thickness, average greylevel and lamination position. The root algorithm has been designed to recognise the portions of a densitometric trace where large, rapid changes in greylevel occur. These are invariably related to the boundaries between laminae. Quantification of their characteristics may then be determined by flagging these and calculating thickness, average greylevel and position of the laminae by the simple summation of the qualities of intervening pixels.

4.7.7 Program operation

Routines are included to recognise the range of greylevels in a dataset and to adjust the lamination recognition parameters to compensate. Peripheral to the main calculation algorithm is the ability to select input and output devices and filenames in order to enable the user to output results directly to a printer or via an intermediate file in tab-delimited format, which may be exported to commercial statistical packages for further processing. Data may be input from files residing on both floppy and hard disks.

4.7.7.1 Program listing

The program is necessarily complex. It consists of some 750 lines of code, and for brevity will not be reproduced here. A copy (Macintosh format) may be found on the 3.5 inch disk included on the rear cover of this thesis. The file may be viewed by loading into any word processor, after first setting the input file type to 'text'.

4.7.8 Program structure

The basic structure of the program may be summarised as follows:

- 1) Set up variables and dimension data storage. Display introduction if program has just loaded.
- 2) Ask user for input device
- 3) Ask user for data file name
- 4) Load file and display file header information
- 5) Calculate differences in greylevel between successive pixels
- 6) Flag large differences
- 7) Determine the greylevel range of dataset and set tolerance for lamination detection accordingly
- 8) Display results, calculating thickness, location and average greylevel of each lamination.
- 9) Ask for output destination
- 10) Write data to output device. If printer, maintain page numbering and line format information
- 11) Clear data store and associated variables. Keep input and output environments
- 12) Return to step 3)

At present, the program is configured to run in a linear fashion from data input to output of results. Many of the variables relating to the discrimination of laminae are preset and hence unalterable during run-time.

The algorithm has been tested against both contrived and genuine data sets, with satisfactory results. A contrived densitometric trace, consisting of four 'peaks' was constructed with Microsoft Excel (*Version 4, Microsoft Corp. Seattle, USA*), and

subjected to analysis by this method. A further test involved the digitisation and densitometric analysis of an image of laminated sediment from Holzmaar, Germany. Laminae in the original image were counted visually and the result compared with that derived from application of this algorithm.

4.8 Compilation of datasets

4.8.1 General

At this point it should be made clear that the study necessitated the compilation of two sets of data. One set is represented by sequences of grey level determinations derived from the densitometric analysis of X-radiographs, and the other by lamination thickness measurements calculated from those data. The values contained within the first dataset possess units of 'per pixel' and those in the second set, 'per year'.

4.8.2 Sequencing of grey level determinations

The Quantimet image analyser possesses an image frame of 512x512 pixels. Thus, only 512 grey level measurements may be determined at one time. At the image scale employed in this study, it was found necessary to acquire and measure several images, each offset by *ca* 4 cm, of every 15 cm core section. Following each analysis, raw grey level data was input to Microsoft Excel and a densitometric curve plotted. Exact matching of overlapping sections was achieved by moving each 512-pixel dataset relative to the others until a good visual fit was achieved. GL data for the entire section was then written to a file for processing by lamination detection software. Similar procedures were employed for data which spanned overlapping 15 cm core sections.

4.8.3 Sequencing of lamination thickness determinations

After processing by lamination detection software, lamination data derived from individual 15 cm core sections were again sequenced utilising Microsoft Excel. Since adjustment of data owing to overlapping sections had already been carried out in the previous step (*Section 4.7.1*), further processing was deemed unnecessary and measurements were simply ‘stacked’ in chronological order. Excel was then utilised to calculate core distance, mean lamination thickness, and estimated (‘varve’) age from the data inputted.

4.9 Time series analysis

4.9.1 Introduction

Standard statistical techniques may be utilised for the analysis of time series derived from many physical processes, and include the determination of the mean, mode, standard deviation and variance, tests for normality and correlation between different series. Of particular interest, however, is the extent to which the signal exhibits elements of periodic behaviour, the evolution of the signal over time, and the determination of the magnitude of ‘randomness’ inherent in it.

4.9.2 Estimation of randomness of extreme events

The apparent cyclicity of climatic events may be conveniently expressed in the repetition of extreme events. The assessment of the statistical significance of the spacing of these may be performed by employing Sherman’s statistic (Burroughs, 1993).

If n extreme events occur at dates $d_1, d_2, d_3, \dots, d_n$, in chronological order, and that d_0 and d_{n+1} are the start and end dates of the complete time series under

consideration, then the total time covered by the series, D , is

$$D = (d_{n+1} - d_0) + 1 \quad (4.6)$$

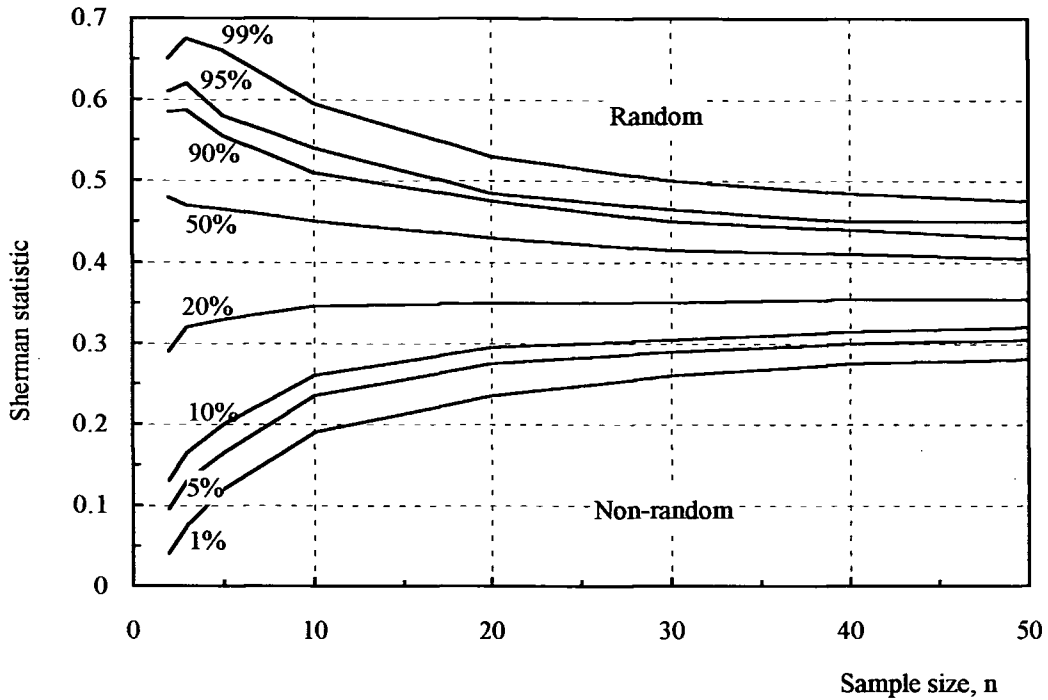


Figure 4.8 Confidence limits for interpretation of Sherman's Statistic (*After Burroughs, 1993*). Increasing values indicate a greater likelihood of extreme values from a time series being a product of chance, rather than from some underlying periodicity.

The average time between extremes may be expressed as $D/(n+1)$ and Sherman's statistic may then be defined as:

$$\omega = 0.5D \sum_{j=1}^{j=n} |(d_j - d_{j-1}) - D/(n+1)| \quad (4.7)$$

This provides a measure of the difference between each of the actual intervals between extremes and the average interval. The probability of ω being the product of chance, for n extreme events, may be determined by reference to *Figure 4.8*. For this study, intervals between extreme values of lamination thickness ($>2\sigma$, $<1\sigma$ from the mean), from each of the cores, were determined and subjected to this test.

4.9.3 Fourier analysis

A physical process may be described either in terms of change as a function of time or by change in terms of frequency (Chatfield, 1989). Thus, the same function may be thought as being represented in both the time and the frequency domains and conversion between the two may be carried out by utilisation of the Fourier transform equations (4.8 and 4.9).

$$H(f) = \int h(t) e^{-2\pi i f t} dt \quad (4.8)$$

$$h(t) = \int h(f) e^{-2\pi i f t} df \quad (4.9)$$

This method may be described as the ‘classical’ technique for the analysis of underlying periodicity in time-resolved data sets. The rationale may be found in most texts dealing with the analysis of data in the frequency domain (for example, Chatfield, 1989), and will be explained only briefly here.

The technique seeks to resolve data into a series of sine expressions, from which the original series may be recreated by an inverse procedure. Thus it is possible to determine elements of periodicity within a time series, and to assign values of significance to them. A variation of the classical Fourier method (which is also termed a Discrete Fourier Transform), and which permits more rapid calculation, is the Fast Fourier Transform (FFT). This method is used for the preliminary investigation of periodicity

within the time series considered in this study.

With the advent of fast, powerful computers, other techniques have been recently developed to improve on many of the shortcomings of the classical method of determining periodic trends. These have been utilised by many researchers, but are only recently being included in commercially available statistical analysis applications. Specific improvements embodied in newer techniques may be classified into the main groups of i). reduction of spectral leakage; ii). the increase of resolution at high or low frequencies; iii). the improvement to spectral density estimates; and, iv). the reduction of artefact signals. To these ends, the following techniques have been applied to the problem by various researchers:

Blackman-Tukey analysis (BTA)

Maximum entropy spectral analysis (MESA)

Thomson multitaper spectral analysis (TMT)

Minimum cross-entropy spectral analysis (MCESA)

Discrete Wavelet transforms (DWT)

Of interest here is the study by Berger *et al.* (1990), which sought to compare six methods of spectral analysis, in order to elucidate the most significant periodicities in the time series derived from the observation of sunspot numbers from AD 1700 to AD 1986. Evolutive analysis was also carried out in order to illustrate changes in the phase of calculated periodicities within the data. It was noted that although each method enhanced different features of the power spectrum, most detected the same periodicities as the initial, classical, Fourier transform.

It was decided therefore to confine spectral analysis to the determination of the FFT spectrum, with fine tuning of transform parameters dependant upon the time series under consideration. A number of commercial statistics packages were evaluated and it

was decided to employ SPSS (*SPSS Inc.1990. Chicago, USA*), which contains a wide selection of customisation parameters for FFT, in addition to a full set of descriptive statistical routines. Output from Fourier analysis was further manipulated in Microsoft Excel. For initial screening of the spectral properties of time series, the software package ProFit (*QuantumSoft, 1990-1994. Zürich, Switzerland*), was utilised. This is extremely user-friendly and simple to configure for rapid analysis.

4.9.4 Methods

Time series were constructed as detailed in *Section 4.7* and submitted to preliminary spectral analysis using Pro-Fit. Examination of the spectral characteristics of the data then enabled the parameters of SPSS to be adjusted according to the criteria of Chatfield (1989), in order to produce the optimal spectral analysis. In the case of *Core Ness 3*, where continuous data were not available, analysis was optimised for each individual section.

Confidence limits were calculated for each spectrum by considering the number of degrees of freedom of the window utilised to process the data and applying *equation 4.10* (Chatfield, 1989; Koopmans, 1974) to each of spectral density estimates.

For the 100(1-a)% confidence interval:

$$\frac{nf(w)}{\chi^2_{n,a/2}} \quad \text{to} \quad \frac{nf(w)}{\chi^2_{n,1-a/2}} \quad (4.10)$$

Evolutionary spectral analysis was performed by first dividing time series into discrete subseries, each of 128 data points (years), and subjecting each to Fourier analysis. Results

were then 'stacked' in chronological order into a Microsoft Excel spreadsheet and plotted as a contour diagram, where regions which share common spectral density estimates in a 2-dimensional time/frequency space are linked. The resultant diagram illustrates changes in the periodic nature of sedimentation as exhibited in cores *Ness 3*, *Ness 4* and *LNRI*.

5. Results

5.1 Sediment description

In this investigation three cores, two almost 6 m in length, one *ca* 0.8 m long, were studied (*Table 5.1*). All three are laminated dark brown/black, with paler shades of olive/brown, almost throughout. Both long cores are laminated to *ca* 4.3 m and terminate, with sharp contact, in a basal grey clay. A distinctive section, consisting of blocks of chaotically-arranged, laminated sediment, surrounded by unlaminated dark brown *gyttja*, was observed at *ca* 1.5 m in both long cores. As the position of these features *vis a vis* the sediment/water interface is uncertain, measurements are given in distance from the top of each core.

Table 5.1 Designation of sediment cores analysed in this study.

<i>Designation</i>	<i>Length (m)</i>	<i>Notes</i>
<i>LNRI</i>	0.787	Utilised to investigate recent sediments.
<i>Ness 3</i>	5.67	Initial 'long core'. Laminae distorted in some places.
<i>Ness 4</i>	5.37	Better quality laminations.

5.1.1 Core LNRI (*Figure 5.1*)

The total length of sediment recovered was 0.787 m. Many prominent pale laminae were noted. Of particular interest is a layer, *ca* 5 mm thick at 0.153 m, which is believed to represent material deposited during the well-documented flood of AD 1868 (*Inverness Courier*, 1868). Below, two further pale laminae, at 0.157 and 0.16 m, may be observed,

another pair at 0.286 and 0.289 m, and a further three at 0.584, 0.603 and 0.616 m. No further prominent layers were noted below about 0.65 m. A number of dark laminae, at 0.333, 0.413, 0.417, 0.514, and 0.565 m, were also identified. None of these were as thick as the paler laminations.

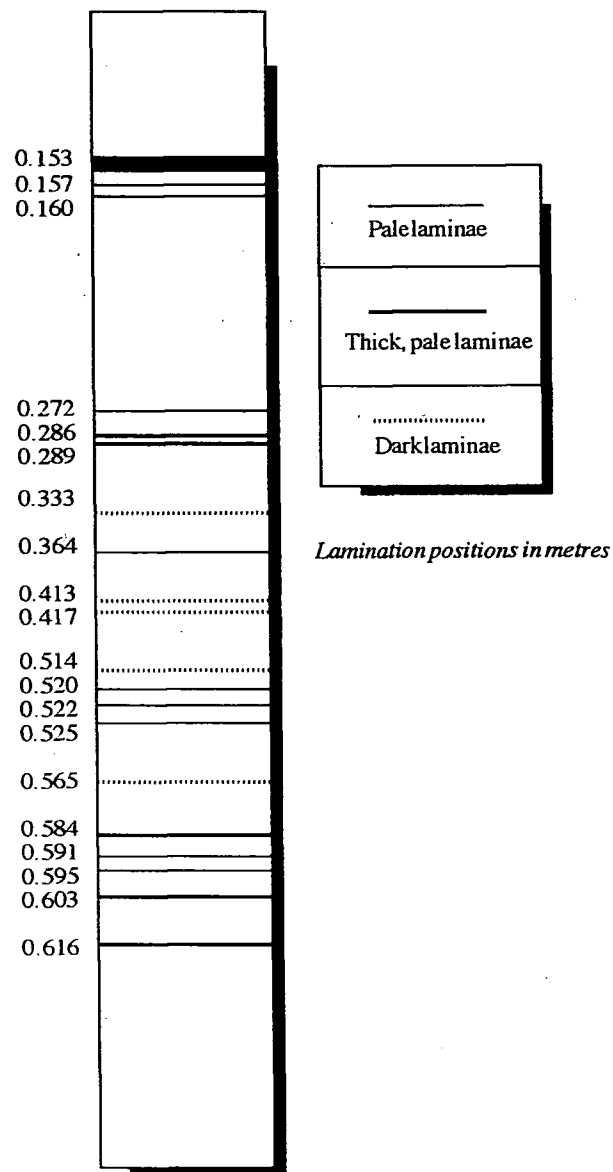


Figure 5.1 Log of core LNR1, indicating locations of prominent laminations.

 5.1.2 Core Ness 3 (Plate 5.1)

The total length of core recovered was 5.67 m. The distance to the contact between *gyttja* and basal clay was 4.315 m. The sediment was extruded into six, one meter sections (Table 5.2). Above 0.61 m, they were very soft and contained much water. Upon extrusion and sectioning, these tended to flow, causing destruction of the laminations. Below 0.61 m, the sediment became much firmer, retained good lamination detail, and consisted of brown (Munsell code 5YR7/1) *gyttja* interspersed with pale cream/olive (10YR7/2-3) and dark brown/black (2GR3/2) laminations of varying thickness. Below *ca* 3.15 m the predominant colour became paler (10YR3/2), changing to 10YR5/2 below 3.83 m. The basal clay was pale grey, and estimated to be 7YR7/1.

Table 5.2 Subdimensions of core Ness 3. Designations are those used to describe x-ray images.

<i>Section</i>	<i>Length (m)</i>	<i>Cumulative length (m)</i>
3/1	0.96	0.96
3/2	0.99	1.95
3/3	0.94	2.89
3/4	0.94	3.83
3/5	0.91	4.75
3/6	0.92	5.67

At 0.66 m a prominent brown band was observed. The core continued to be well laminated to 1.14 m, where severe disruption of the stratigraphy began, persisting to 1.53 m. This section appeared to consist of blocks of laminated sediment chaotically arranged within a non-laminated matrix. Appearance of the matrix was identical to that of the brown *gyttja* found throughout the rest of the core. Between 1.14 and 1.38 m, the sediment was

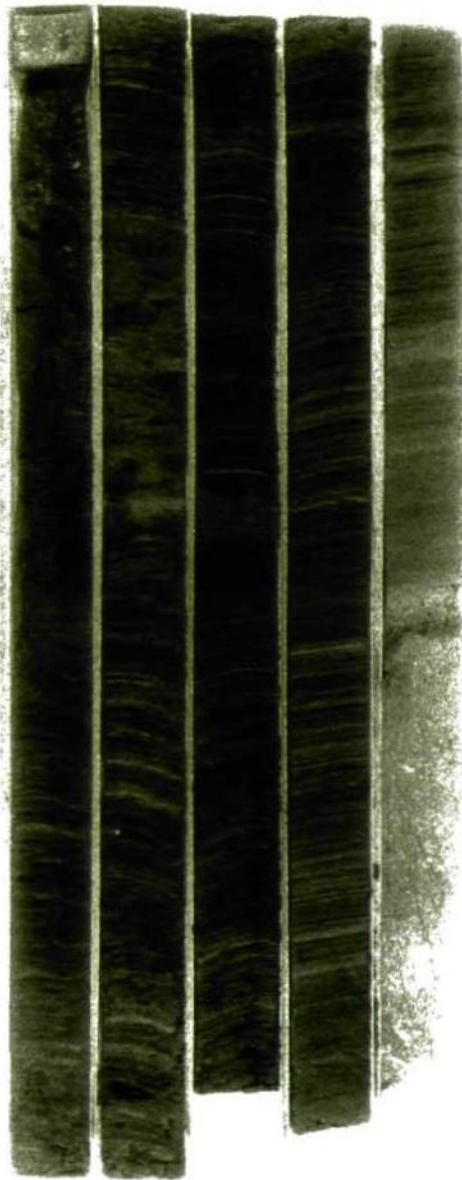


Plate 5.1 Monochrome Infrared photograph of core *Ness 3*. The base of the core is located at the bottom right of the image, the upper section to the top left.

more gritty in texture than the remainder of the core. From 1.53 m, laminations continued to 2.35 m, with prominent pale layers at 1.82 and 2.34 m. A change in lithology at 2.35 m, taking the form of homogeneous, fine-grained sediment, marked the location of the join between the coring tubes. It was presumed that this material leaked into the core barrel

under pressure during coring. Laminations recommenced at 2.42 m and continued, with good definition, to the clay/*gyttja* boundary at 4.31 m. A sand layer, consisting mainly of quartz grains, was observed between 4.36 and 4.37 m. Homogeneous grey clay then continued to the base of the core.

5.1.3 Core Ness 4 (Plate 5.2)

The total length recovered was 5.15 m, with a distance of 4.08 m to the clay/*gyttja* contact. The material was again extruded into six, one metre, sections (*Table 5.3*) and consisted of brown *gyttja* laminated with pale olive/cream layers. Laminations existed from the top of the core, the texture of the material there being very firm, although above 0.14 m they were noted to be indistinct. An air gap in the core, some 4 mm thick, was observed at 0.33 m. Prominent olive coloured laminae (Munsell 10YR7/2) were noted at 0.48, 0.50, 0.52 m, the last some 0.75 mm thick and discontinuous across the section. Weak bands of the same colour were observed at 0.82, 0.88 and 0.93 m. A chaotic section, similar to that observed in core *Ness 3*, occurred between 1.4 and 1.57 m.

Table 5.3 Summary of sectional lengths of core *Ness 4*. Section designations are those used to describe x-ray images.

<i>Section</i>	<i>Length (m)</i>	<i>Cumulative length (m)</i>
4/1	0.95	0.95
4/2	0.96	1.92
4/3	0.97	2.89
4/4	0.95	3.84
4/5	0.97	4.82
4/6	0.33	5.15

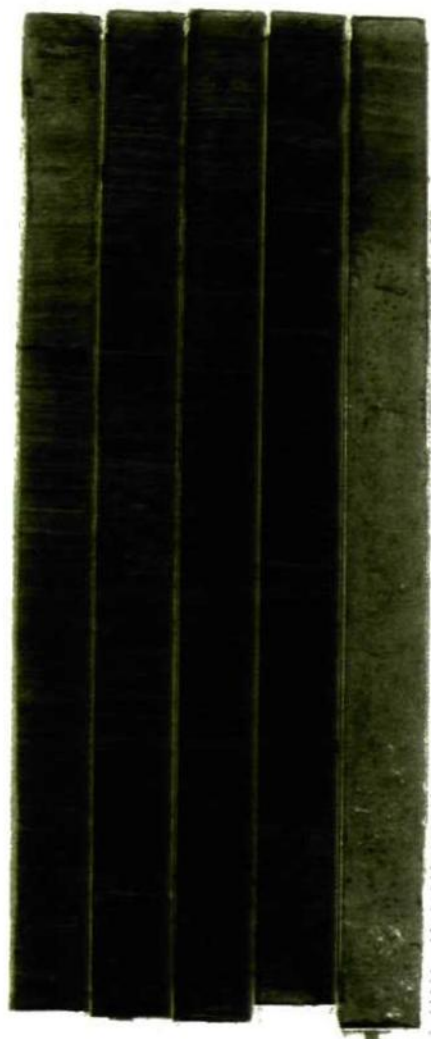


Plate 5.2 Monochrome Infrared photograph of core *Ness 4*. The base of the core is located at the bottom right of the image, with the uppermost sections towards the top left.

Fragments of wood, conformable with the bedding of the laminae, were recorded at depths 1.57 m, 2.67 m, and 3.12 m. Many olive-coloured laminations were observed, as were black layers. A small pebble, diameter *ca* 4 mm, was discovered at 3.403 m. Laminae were noted to be distinct and undistorted throughout the remainder of

the core, the boundary between the *gyttja* and basal clay occurring at 4.08 m. A coarse-grained sand layer was again noted, at *ca* 4.1 m.

5.2 Physical properties

5.2.1 Percentage Dry Matter and Loss on Ignition

5.2.1.1 Core Ness 3 Percentage Dry Matter (Figure 5.2)

Percentage Dry Matter (%DM) remains low almost throughout the entire length of core *Ness 3*, but decreases from 32% at the contact between basal clay and *gyttja*, to about 20% at the top. Typical results from the grey basal clay are of the order of 80%. Values of 28% are recorded at 3.25 and 2.4 m, which represent increases of the order of 10% above those figures obtained from the surrounding sediment. A slight peak (to *ca* 27%) may also be observed in the section from *ca* 1.1 m to 1.4 m, which contains the chaotic layer.

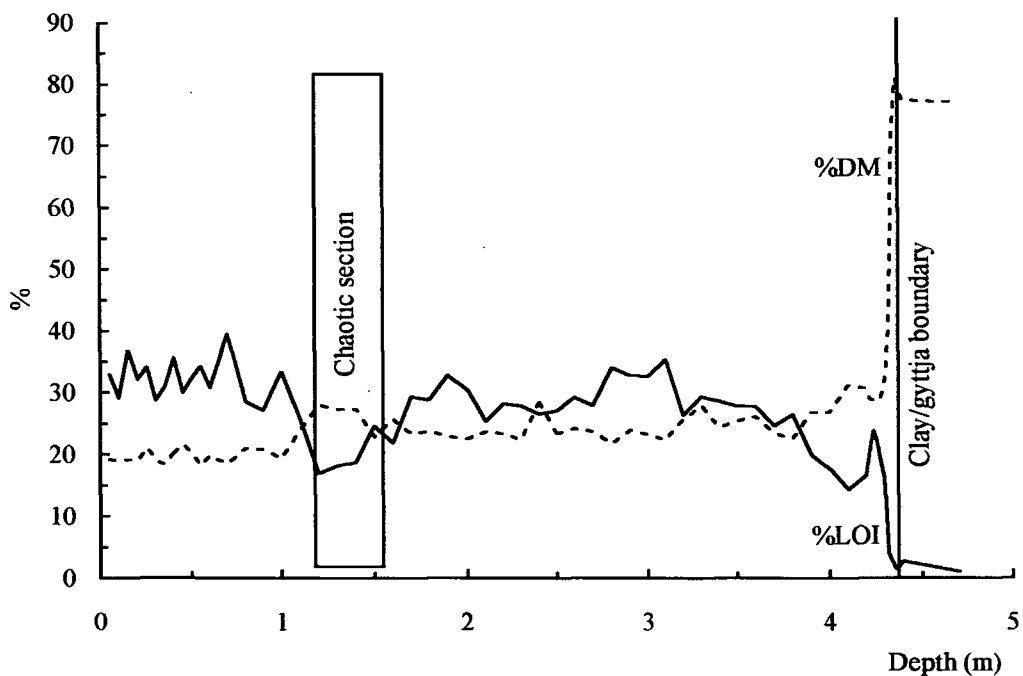


Figure 5.2 Percentage Dry Matter and percentage Loss On Ignition, core *Ness 3*.

5.2.1.2 Core Ness 3 Percentage Loss on Ignition (Figure 5.2)

Loss on ignition (%LOI) for core *Ness 3* exhibits a trend from small values (ca 20%) at the base of the gyttja, to about 30-40% at the top. The signal contains larger fluctuations, many at the same horizons, than for %DM. In general, decline in %LOI is matched by an increase in %DM. The grey basal clay exhibits very little loss on ignition (ca 2-3%), values increasing steeply across the clay/gyttja contact. An immediate decline to 15% is observed at 4.1 m, but is rapidly followed by an increase to ca 30% at 3.7 m. A prominent 'plateau' in values may be observed in the section from 3.8 to 2.7 m. The signal declines to ca 20% at two sampling points within the chaotic section from 1.6 to ca 1.0 m. Values in the topmost one metre of the core remain around 30-40%, with minor fluctuations, which may be artefacts of the sampling process.

5.2.1.3 Core Ness 4 Percentage Dry Matter (Figure 5.3)

The %DM content of core *Ness 4* is similar to that of core *Ness 3*, but the profile is much more complex. Values of %DM from the basal grey clay are again high, some 60-70%, which decline rapidly across the clay/gyttja boundary at 4.08 m. The signal continues to fall, less quickly, until large increases in %DM occur at ca 2.8 m, and again at ca 2.3 m. Core *Ness 4* does not display a pronounced increase in %DM within the chaotic section at 1.57-1.39 m, as was noted for core *Ness 3*. A decline in %DM is measured at 1.0 m but this is transitory, and in the uppermost 0.5 m of the core %DM rises with only minor fluctuations towards the top, where a comparatively large value of 46% is observed.

5.2.1.4 Core Ness 4 Percentage Loss on Ignition (Figure 5.3)

Similar values of %LOI were found in core *Ness 3*, but many fluctuations occur in core *Ness 4* which are not observed in the former. Very low levels are

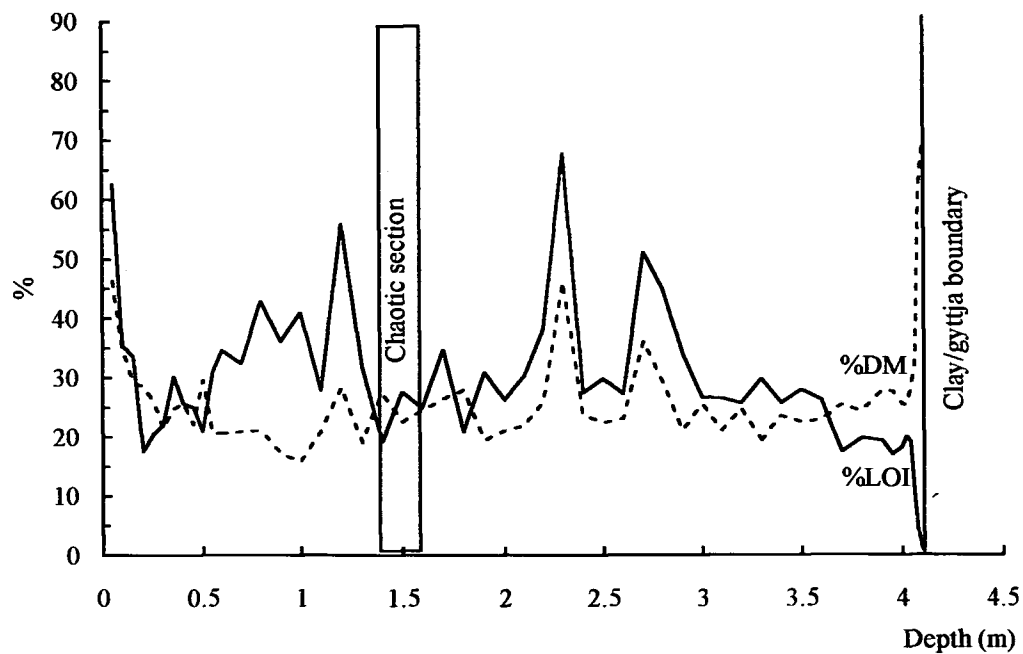


Figure 5.3 Percentage Dry Matter and percentage Loss On Ignition, core *Ness 4*

observed within the grey clay, with subsequent rapid increase across the clay/*gyttja* contact. Values remain fairly low, however, (less than 20%) until 3.6 m, where they increase to *ca* 27%. Large fluctuations in %LOI, notably at 2.75 and 2.3 m, are observed, the values of which increase from *ca* 30% to 50%-70%. %LOI declines to *ca* 20% within the chaotic section, and increases rapidly to *ca* 60% in the region of 1.2 m. A 'plateau' of values of *ca* 35-40% are measured from 1.0 to 0.5 m, declining to *ca* 20% from 0.5 to 0.2 m. Large values, *ca* 60%, are observed at the extreme top of the core.

5.3 Imaging

5.3.1 Photography of core sections

A black-and-white, infrared image of a section of core *Ness 3* is shown in *Plate 5.3*. The general fabric of the sediments and lamination structure are better delineated in infrared photographs than in colour, but reveal a noticeable 'graininess'

within each lamina. This is presumably owing to the 'plucking' of individual grains during the smoothing of the sediment surface. This effect was found very difficult to avoid, and could not be alleviated by use of plastic film or rigid plastic sheet (Renberg, 1981). Thus this was eventually abandoned as a method for the counting of laminations.

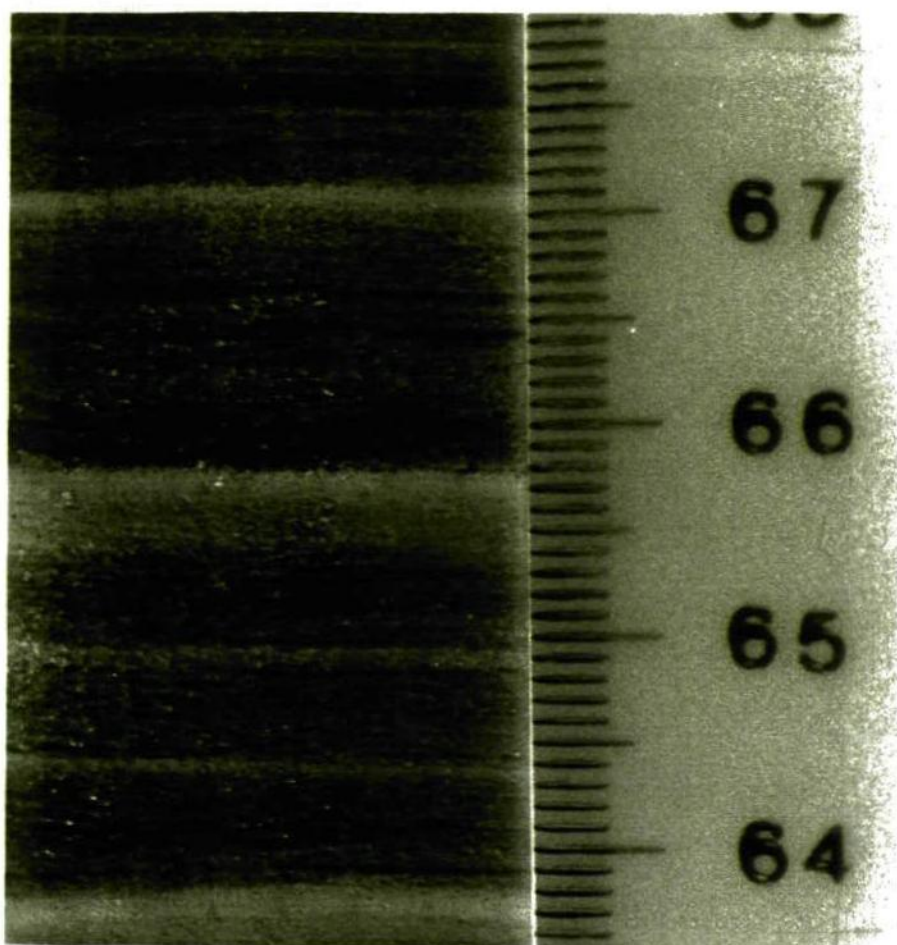


Plate 5.3 Photograph, with monochrome Infrared sensitive film, illustrating a section of core *Ness 3*.

Infrared photographs of long core sections are shown in *Plates 5.1* and *5.2*. The negatives were carefully exposed in order to ensure uniform illumination and printed with regard to producing a near-uniform background. The images obtained were then subjected to image analysis, in order to quantify variation in greylevel throughout each core (*Figures 5.5* and *5.6*)

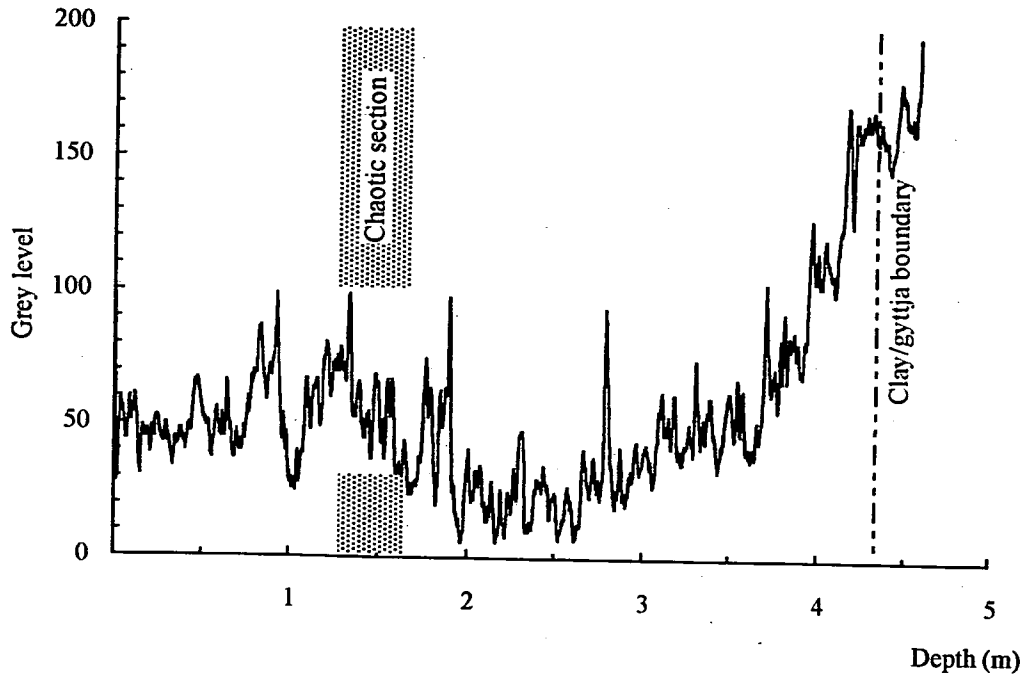


Figure 5.4 Variation of Grey Level throughout core *Ness 3*, determined from an Infrared image of the core.

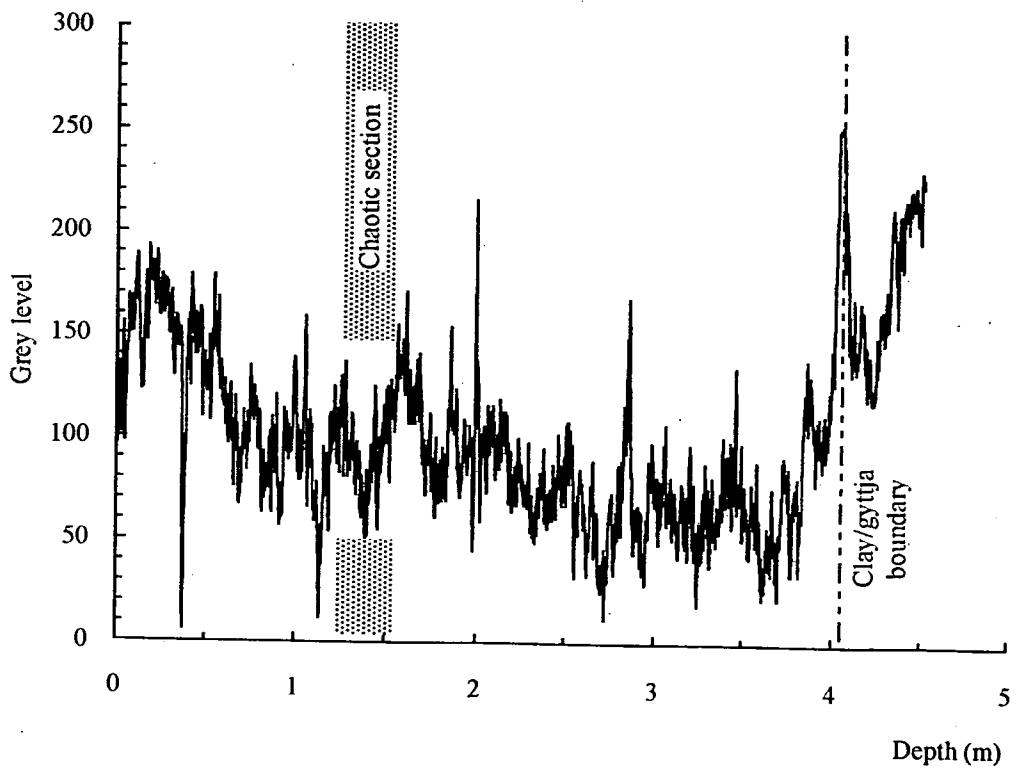


Figure 5.5 Variation of Grey Level throughout core *Ness 4*, determined from an Infrared image of the core.

5.3.2 X-radiography

X-radiographs were obtained of 0.15 m sections from Cores *Ness 3*, *Ness 4* and *LNR1*. Contact prints made from these are illustrated in Appendices A, B, and C. For reproduction, the prints were processed on to a 'hard' grade of photographic paper (Ilford Multi-grade, Ilford Photographic Ltd., Mobberley, UK) in order to accentuate subtle detail as much as possible. This has given, however, a 'grainy' appearance to each plate.

Radiographs from core *Ness 3* illustrate the variable quality of laminae, which was also noted in the infrared images. Many layers appear distorted and some sections exhibit a diffuse, undefined structure, where contrast between laminations is indistinct. Infrared photography, however, suggested that these features are genuine, resulting, perhaps, from lack of contrast in bulk density between laminations. These indistinct sections were not included in the chronology, since it was not possible in these cases to enhance the structure by image analysis.

5.3.3 Scanning Electron Microscopy

SEM analysis employed both secondary (SESEM) and backscattered (BSEI) electrons in order to form an image. In addition, elemental analysis was performed by Energy Dispersive X-Ray Spectroscopy (EDS). Attempts to distinguish between pale and dark laminae by examination of microlithology, both by qualitative estimation of variation in grain size, and by distribution of diatom frustules, generated images typified by *Plate 5.4*, and proved inconclusive. This image illustrates part of a clay-rich lamina (*upper*), grading into silt-rich (*lower*). No changes in appearance of the lithology, or of diatom type or number, are seen.

Elemental analysis of a number of samples, extracted from different sections of core *Ness 3*, and thus representing sediments deposited during different periods of the

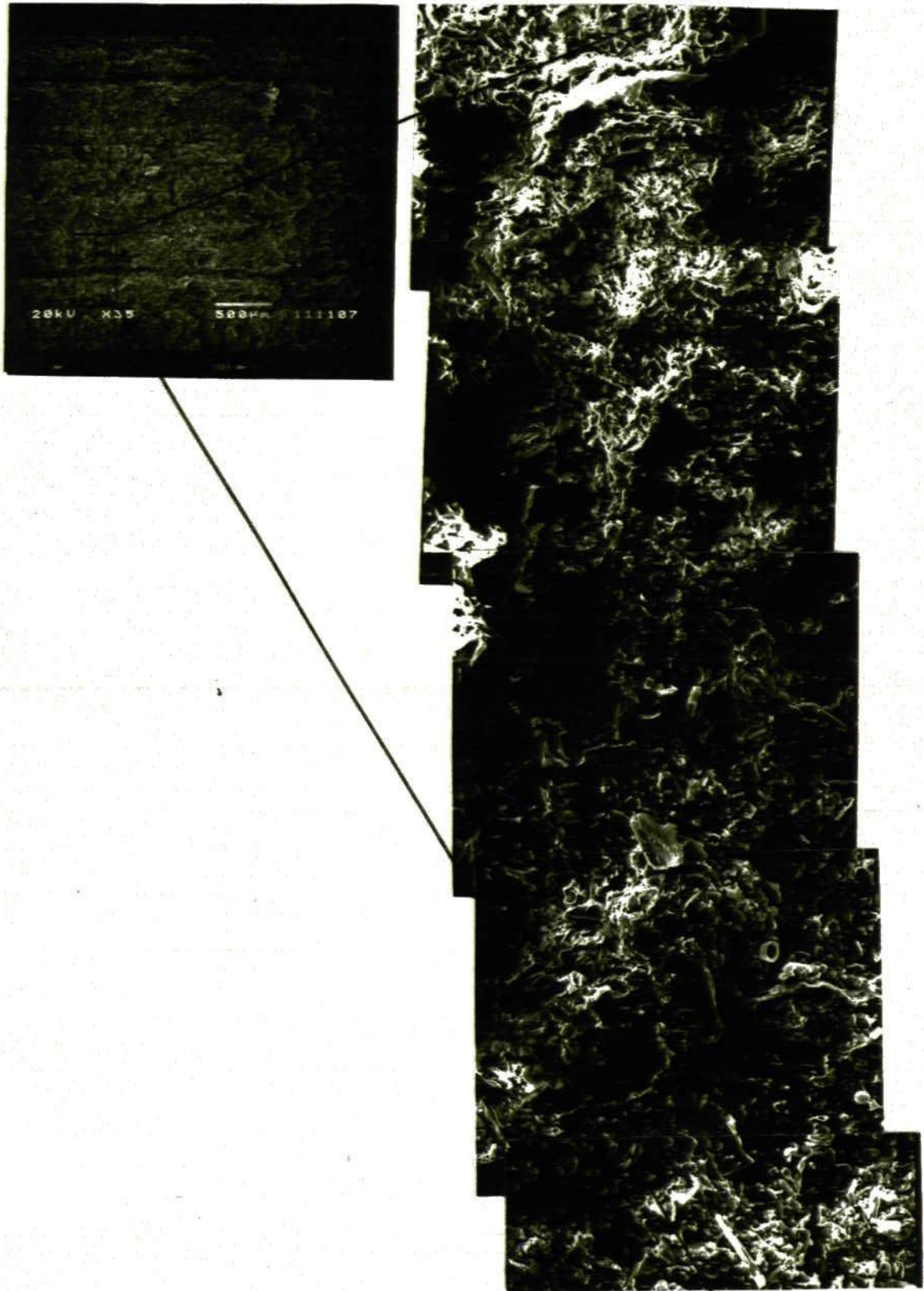


Plate 5.4 Photomosaic of SESEM images illustrating the lack of change in lithology between (upper images) dark clay-rich, and (lower images) pale silt-rich, laminae.

Holocene, were carried out by EDS. Both pale and dark laminae were included in the analyses, in order to test for variations in ratios of elements and differences in absolute quantities, between pale and dark laminae. Both rough-surfaced and semi-polished sections were analysed, ratios of elements calculated from data gained from the former. Results from polished sections were subjected to correction by ZAF (ZAF-4B; Link Analytical, 1992). *Table 5.4* illustrates results of EDS analyses. Little difference in spectra obtained from pale and dark laminae were noted. A typical spectrum, acquired as a screen dump directly from the SEM, is illustrated in *Figure 5.6*. In addition, ZAF-corrected EDS analysis was carried out on material collected from dried, dissected individual laminae, on behalf of Ms L.A. Wheeler, of the University of Wolverhampton (Unpubl. PhD thesis).

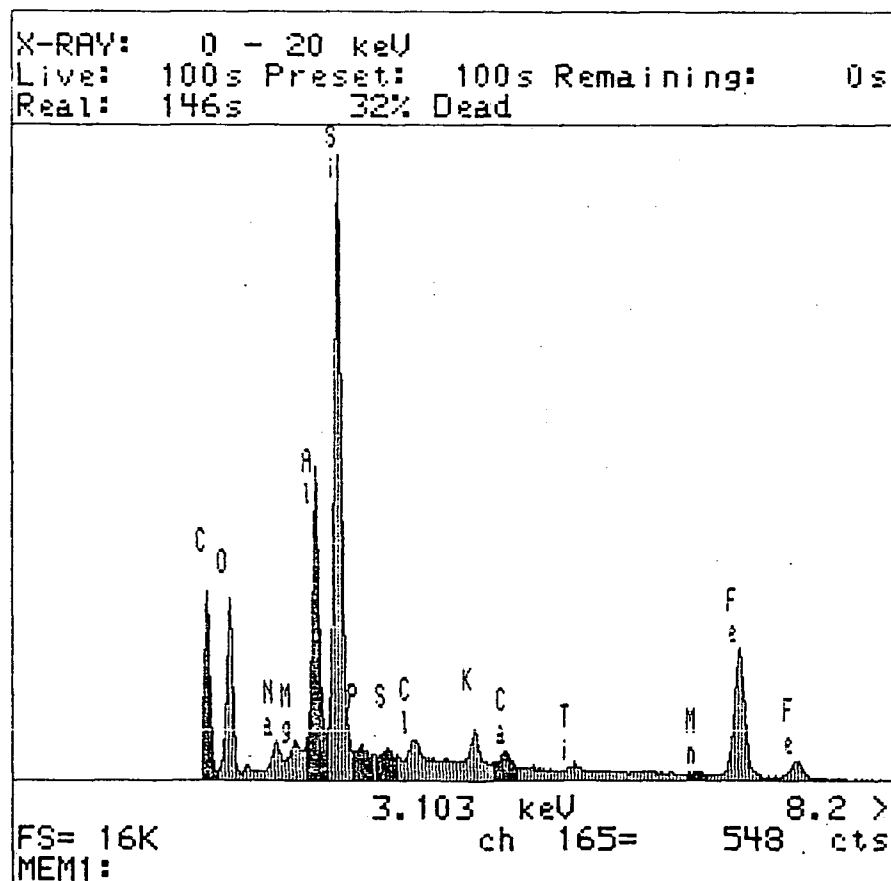


Figure 5.6 Screen dump of a typical EDS spectrum of material from core *Ness 3*.

Elements detected are annotated.

Table 5.4 (Left) Results of EDS analyses of unpolished, impregnated samples. (Right)

Results of ZAF-corrected EDS analyses.

Sample	Al	Si	K	Ca	Fe	Si/Al	Si/K	Si/Ca	Si/Fe	Al/K	Al/Ca	Al/Fe	K/Fe	K/Ca	Ca/Fe
		Gross integral								Elemental ratio					
c2 pale	2066	8639	1133	652	3380	4.18	7.62	13.25	2.56	1.82	3.17	0.61	0.34	1.74	0.19
c2 dark	2417	9523	1378	990	2151	3.94	6.91	9.62	4.43	1.75	2.44	1.12	0.64	1.39	0.46
c4 pale	2214	10612	787	509	1350	4.79	13.48	20.85	7.86	2.81	4.35	1.64	0.58	1.55	0.38
c4 dark	1818	9655	982	547	1644	5.31	9.83	17.65	5.87	1.85	3.32	1.11	0.60	1.80	0.33
g2 pale	2268	10245	921	998	1633	4.52	11.12	10.27	6.27	2.46	2.27	1.39	0.56	0.92	0.61
g2 dark	1541	8307	936	617	2398	5.39	8.88	13.46	3.46	1.65	2.50	0.64	0.39	1.52	0.26
g4 pale	1796	6518	772	571	2288	3.63	8.44	11.42	2.85	2.33	3.15	0.78	0.34	1.35	0.25
g4 dark	1713	6921	1311	621	2432	4.04	5.28	11.14	2.85	1.31	2.76	0.70	0.54	2.11	0.26

Sample	Na	K	Mg	Ca	Mn	Fe	Al	P	Si
					atom %				
c1 pale	1.81	3.27	1.31	4.74	1.24	30.67	15.71	1.05	40.19
c1 dark	1.96	3.97	1.56	5.57	1.38	34.21	17.90	0.00	45.29
c3 pale	2.43	5.28	1.88	1.93	0.47	19.09	16.99	0.48	51.43
c3 dark	2.88	4.58	1.78	2.36	0.61	21.19	15.64	0.85	50.10
g1 pale	3.04	6.01	1.57	2.13	0.46	23.15	17.10	0.58	45.95
g1 dark	2.74	5.70	1.82	1.68	0.00	15.68	15.40	1.11	45.40
g3 pale	3.13	5.10	1.82	2.44	0.54	18.63	17.29	0.39	50.66
g3 dark	2.69	4.12	1.38	2.20	0.56	21.49	15.47	0.23	50.51

5.4 Chronology

5.4.1 Densitometry of x-radiographs

Analysis of each X-radiograph produced curves representing variation of image density, exemplified in *Figure 5.7*. Further processing of these data by custom-written software, described previously, yielded data on lamination thickness and varve counts, such as those displayed in *Table 5.5*. For core *Ness 3*, these were put together in order to compile an intermittent, floating chronology comprising a total of 5546 lamination pairs (*Figure 5.8*). Only a discontinuous chronology could be assembled, owing to the presence of sections of laminations not amenable to x-radiography and image analysis. Core *Ness 4* yielded 6155 laminae pairs and produced a continuous, floating, chronology (*Figure 5.9*). Correlation between the two cores is, however, at present uncertain.

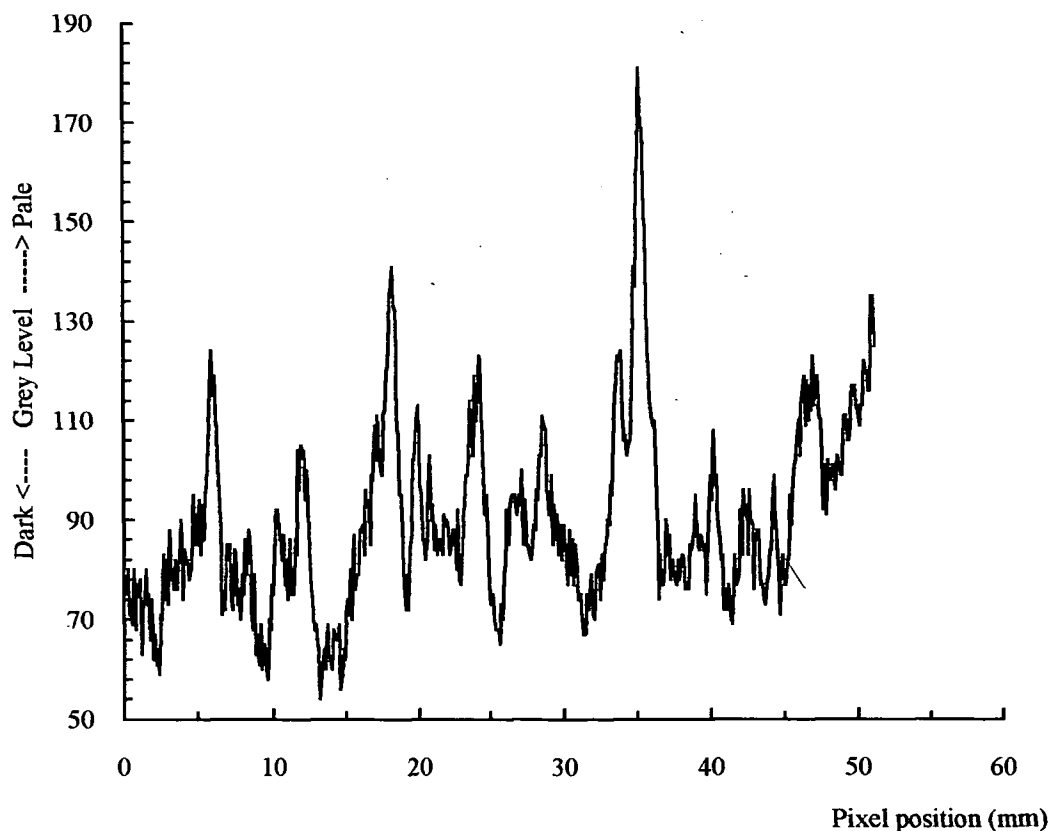


Figure 5.7 Typical densitometric trace obtained from analysis of x-radiographs.

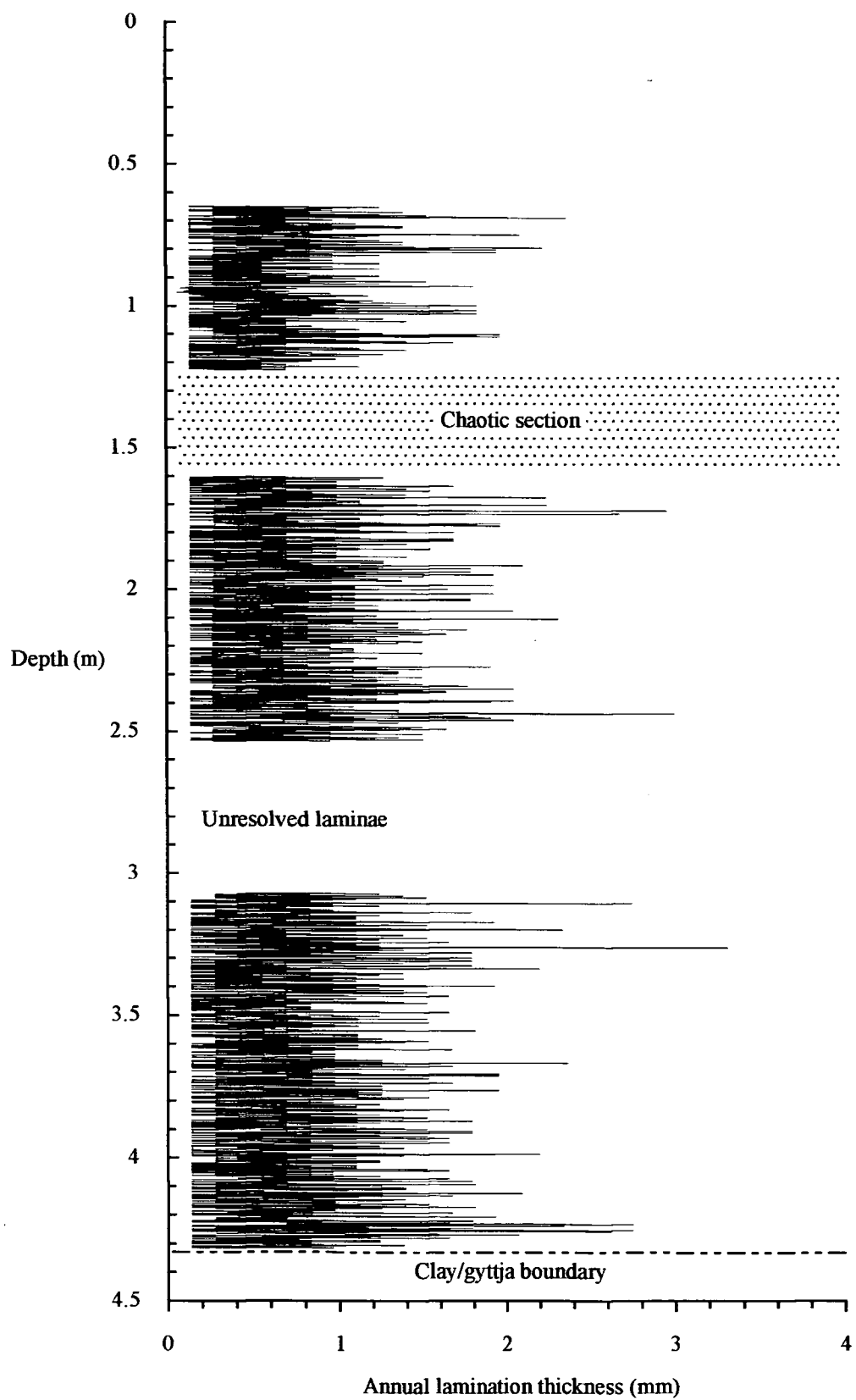


Figure 5.8 Variation of lamination thickness in core Ness 3.

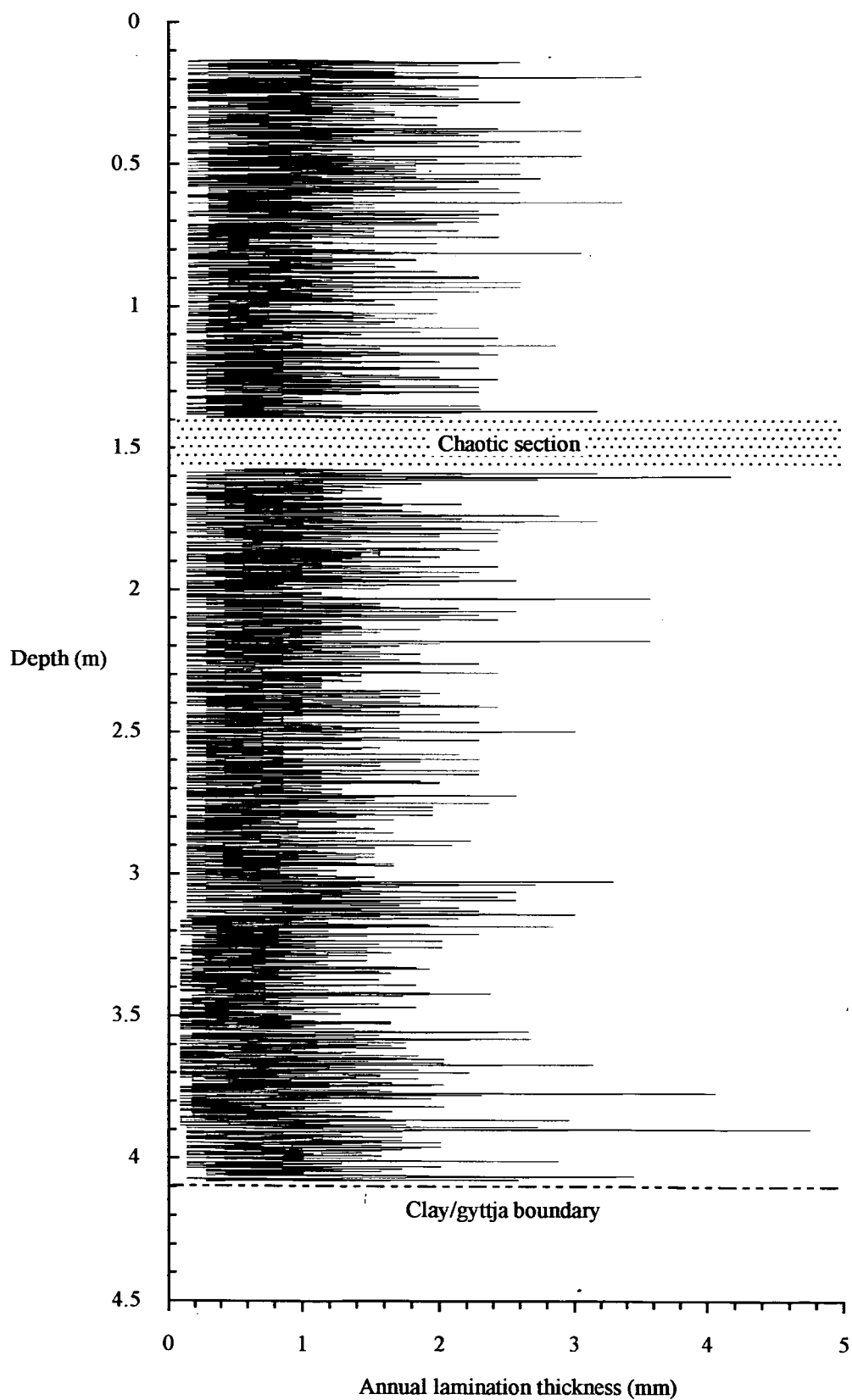


Figure 5.9 Variation of lamination thickness in core Ness 4.

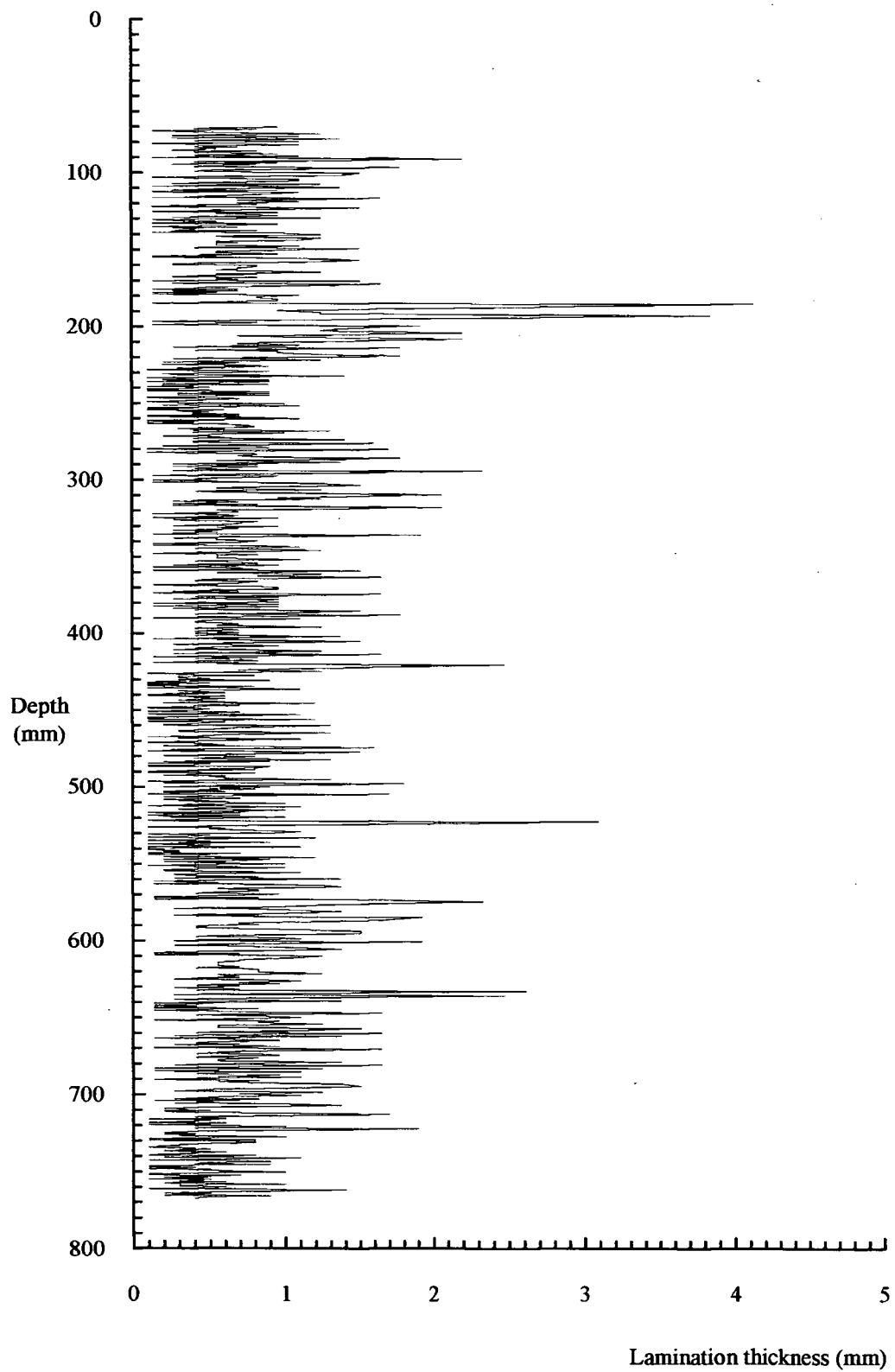


Figure 5.10 Variation of lamination thickness in core LNRI.

Table 5.5 Typical output data produced by the lamination detection software.

Analysis of file: a:4143
 Analysis date: 03-05-1996 17:17:15
 Pixel size (mm): .152672
 Frame size (pixels): 199
 No. of laminations: 31

Lamination data

Lamination number	Position mm	Thickness mm	Ave. Grey
1	0.31	0.31	110
2	0.92	0.61	88
3	1.53	0.61	123
4	3.21	1.68	86
5	4.73	1.53	99
6	5.65	0.92	69
7	6.56	0.92	105
8	7.33	0.76	91
9	7.48	0.15	136
10	7.63	0.15	93
11	9.47	1.83	106
12	10.08	0.61	94
13	11.45	1.37	98
14	11.76	0.31	76.....

Average lamination thickness for both long cores were found to be different; in core *Ness 3*, 0.45 mm a^{-1} , and in core *Ness 4*, 0.61 mm a^{-1} . Laminae in short core *LNRI*, recovered from the same site as the long cores, were also examined and counted, in order to develop a more recent record (*Figure 5.10*). A complete suite of data for all cores analysed may be found, as text files, on the floppy disk inside the back cover of this thesis.

5.4.2 Core *Ness 3*

The lamination record from this core was found to be very variable, enabling only a discontinuous, segmented chronology to be determined. This is presented as a time/depth curve illustrated in *Figure 5.11*. Since no definitive datable reference horizons existed within the long cores, the following method was adopted in order to facilitate the construction of the diagram (Cooper *et al.*, in press). The average, annual, lamination

thickness was determined over the three sequences analysed and plotted on the depth/time chart. This line did not pass through the origin, but was positioned as if a loss of 0.5 m from the top of the core had occurred. It has been observed that the long corer does not recover topmost sediments, although the absolute value of this loss is uncertain. Individual sequences of laminae were then plotted along this average line, in the appropriate positions.

Two suites of ^{14}C dates were obtained, the first a series of three determined by AMS and kindly donated to the study by Dr Ewan Lawson of ANSTO, Menai, Australia; the second, six radiometric dates, determined by Dr. D.D. Harkness of the NERC Radiocarbon Laboratory and one AMS date, determined by the Radiocarbon Laboratory at the University of Tucson, Arizona. These latter dates were supported by the NERC Steering Committee. In *Figure 5.11* the dates are superimposed upon the depth/time curve. The dates prefixed 'OZB' represent the ANSTO data, and those labelled 'SRR' the results from the NERC laboratory. AA-21852 was measured at the AMS facility, University of Tucson, Arizona. The data are summarised in *Table 5.6*.

Samples submitted for radiocarbon dating consisted of bulk sediment taken from core *Ness 3*. Particular care was taken to avoid sampling sediment which had been in contact with the storage container, in order to minimise possible inclusion of particles of plastic which by possessing an infinite radiocarbon age, may have biased the determinations. Similarly, the core from which the samples were removed had been primarily wrapped with aluminium foil, and then overwrapped with plastic cling film, again in order to obviate contact between sediment and plastic. Each sample comprised about 50 lamination pairs, in order to minimise additional errors in age determination associated with sampling. This strategy, however, resulted in only small amounts of carbon present for dating, necessitating lengthy analysis times. Sample characteristics are noted in *Table 5.7*.

Table 5.6 Summary of radiocarbon age determinations from core *Ness 3*.

<i>Laboratory Reference</i>	<i>Average Depth (m)</i>	<i>Age (¹⁴C Years BP)</i>	<i>Cal Age (Years BP)</i>	<i>2σ range (Cal yr BP)</i>	<i>δ¹³C (‰)</i>
SRR-5735	1.03	2730±50	2776	2880-2744	-28.7
SRR-5736	1.98	3350±60	3620, 3585	3723-3460	-26.6
OZB260U*	2.26	4000±90	4499	4625-4373	-26.9
SRR-5737	3.26	5305±60	6170, 6143	6211-5981	-25.6
SRR-5738	3.58	6050±70	6899	7092-6775	-25.1
OZB259U*	3.83	7600±110	8484	8587-8381	-26.9
SRR-5739	3.90	6715±70	7547	7667-7470	-25.0
OZB258U*	4.07	8580±220	9495	9649-9340	-26.9
SRR-5740	4.30	8435±85	9437	9526-9206	-27.2
AA-21852*	4.33	9450±110	10424	10918-10279	-26.6

* denotes an AMS determination. Calendrical dates were calculated using the Radiocarbon Calibration program 3.0.3c (Stuiver & Reimer, 1993), utilising calibration file INTCAL93.14C, and are expressed as a 2σ range. Italics denote dates calculated using the program calibETH, expressed as a 1σ range. δ¹³C analyses of samples dated by ANSTO were undertaken by Dr. Martin Jones at the University of Newcastle, UK.

5.4.3 Core *Ness 4*

The lamination sequence from core *Ness 4* proved to be complete, although examination of lamination counts and thickness reveals discrepancies between this core and core *Ness 3*. Densitometric analysis of X-radiographs from this core suggests that the average annual lamination thickness is 0.61 mm and that there are 6651 lamination pairs, generating the depth/time plot illustrated in *Figure 5.12*, construction was by the same method as described for core *Ness 3* in *Section 5.3.2*.

Table 5.7 Summary of characteristics of samples submitted for ^{14}C analysis.

<i>Laboratory Reference</i>	<i>Average Depth (m)</i>	<i>Wet weight (g)</i>	<i>LOI (ave) (%)</i> *	<i>Carbon available (%)</i> †
SRR-5735	1.03	45.25	32	9.3
SRR-5736	1.98	30.64	30	12.0
OZB260U	2.26	-	27	§
SRR-5737	3.26	32.89	28	12.0
SRR-5738	3.58	33.93	29	11.1
OZB259U	3.83	-	27	§
SRR-5739	3.90	35.45	18	9.3
OZB258U	4.07	-	18	§
SRR-5740	4.30	41.30	10	4.9
AA-21852	4.33	47.92	5	0.1

* Determined at University of Plymouth † Determined at radiocarbon laboratory, expressed as percentage of weight of dried material after sample pretreatment. § Data not available.

5.4.4 Core LNRI

Laminae were counted throughout the interval *ca* 0.07 m to 0.75 m, yielding a total of 1284 individual layers (642 varves). Although no SWI was recovered, a prominent pale lamination (the thickest in the core) was assumed to represent deposition by the 1868 flood, dated to 1868 by ^{210}Pb by V.J.Jones *et al.* (1997), from a third, independently recovered, short core, *NESS90*. This date enabled an absolute chronology between the years 1963 and 1321 AD to be constructed. Average annual lamination thickness for this core was calculated to be 1.08 mm a^{-1} . The depth/time curve for this core is illustrated in *Figure 5.13*.

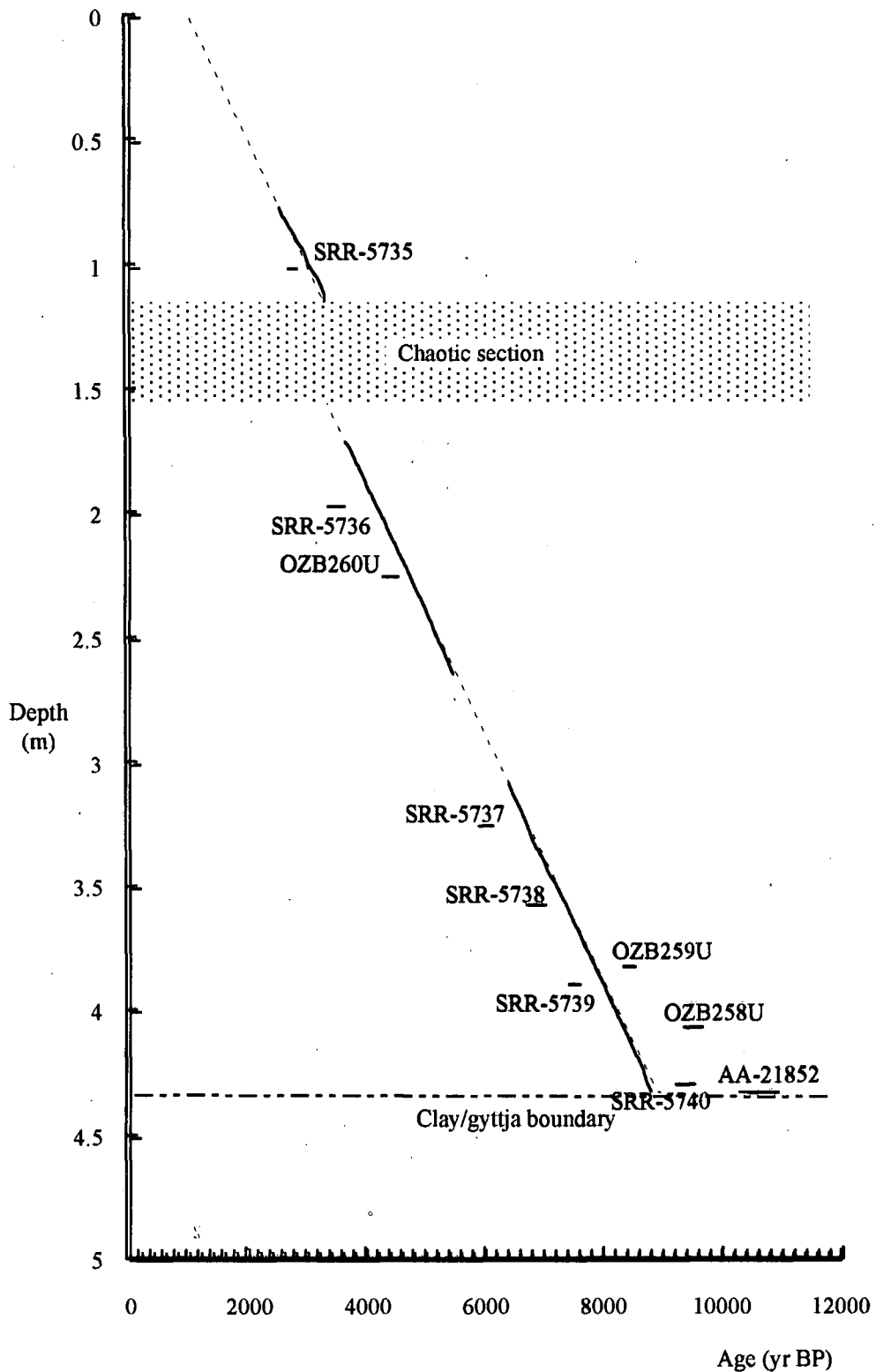


Figure 5.11 Time/depth plot derived from lamination measurements from core Ness 3.

The overlay illustrates the results of ^{14}C dating. Italic titles indicate AMS dates. Calibrated ages are presented.

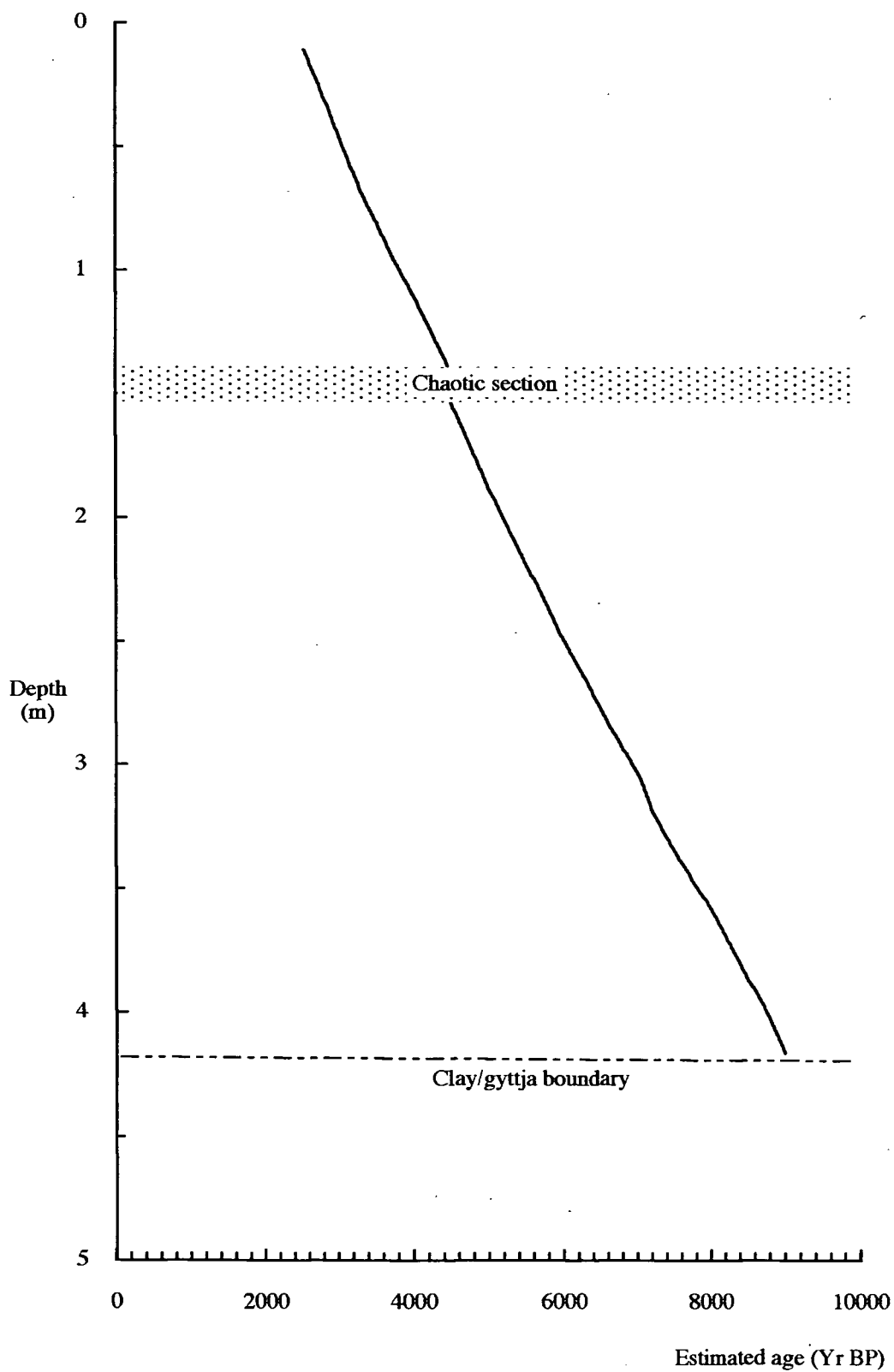


Figure 5.12 Time/depth plot derived from lamination measurements from core *Ness 4*.

Age estimates are fixed to that of the clay/*gyttja* boundary in core *Ness 3*.

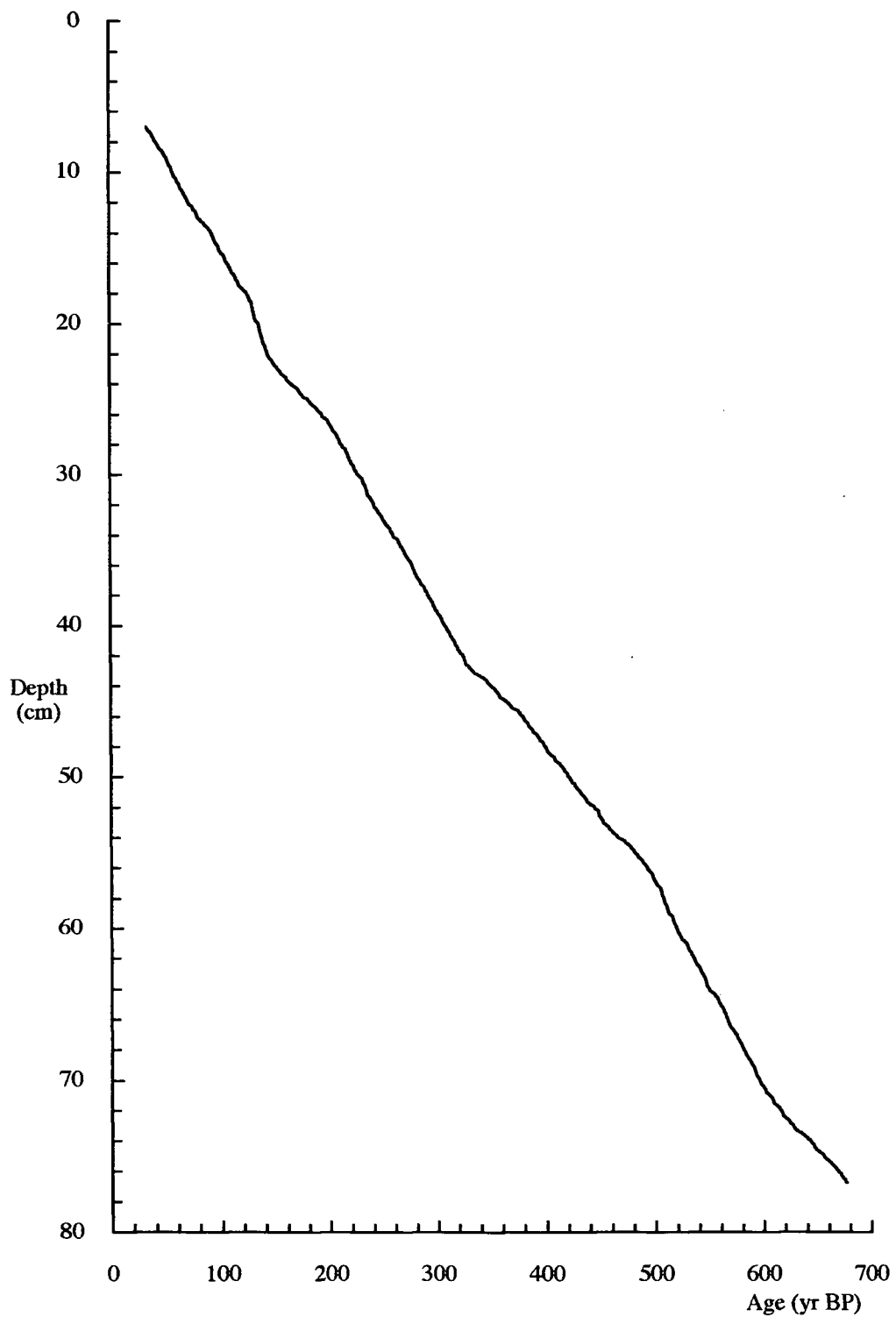


Figure 5.13 Time/depth plot derived from lamination measurements from core *LNR1*.

Age estimates are based on a prominent layer dated by ^{210}Pb by V.J.Jones *et al.*, 1997.

5.4.5 Uncertainties in chronology

Sources of error pertaining to the techniques employed in this study, and to the site, are discussed in Chapter 6, but it is useful to briefly describe here other considerations which may need to be taken into account when compiling a varve chronology. Since the laminae in Loch Ness have been deduced to be of a clastic origin, processes relating to biogenic varve formation will not be discussed.

Varves contain two types of information (Zolitschka, 1996). By counting, an internal chronology may be constructed, but since the sediment-water interface is often recovered only with difficulty, some external method of absolute dating is usually required. This may include radiometric methods, and the correlation of marker horizons. Thickness variations and composition of yearly laminae provide information on the response of the sedimentological system to a variety of forcing processes. Climatic variation is important but may also control catchment processes, such as erosion, transportation of material and growth of vegetation. The study of the entire system is required in order to fully characterise and understand the dataset obtained (Bradley *et al.*, 1995). For example, the record from Skilak Lake, Alaska (Perkins & Sims, 1983) contained anomalous depositional events which were originally misinterpreted as annual laminae. In addition, correlation of a climatic signal with varve thickness may only hold good if the boundary conditions of the catchment are constant throughout the time period studied. Furthermore, anthropogenic influences over the last 3000 years may be superimposed over the climatic signal (Zolitschka, 1996).

The signals of grey level variations throughout the cores recovered from Loch Ness are complex, and on this basis alone it is not possible to ascertain with certainty that anomalous layers do not exist in the sedimentary record from this site. The close correlation of lamination thickness with NAO signal indicates, however, that over the past *ca* 100 years few, if any, laminae are missing or are intra-annual. Comparison of the

time/depth curve obtained from core *Ness 3* with that derived from ^{14}C dating supports this theory, as does the comparison of pollen zone data with those from other sites in the region. Correlation of cores *Ness 3* and *Ness 4*, and closure of the Loch Ness chronology will enable an accurate assessment of the errors involved, but at present these are considered to be less than 10%. It is noted that Zolitschka (1996) has estimated the error in the Holzmaar chronology to be less than 2%, based on the study of multiple cores.

5.5 Time series analysis

5.5.1 Sherman's statistic

This test was employed in order to determine whether or not the observed distribution of very thick and very thin laminae in the sedimentary record may be considered random. Data employed in this test, for core *LNRI*, may be found in *Tables 5.8a* and *5.8b*. Lamination thickness greater than ($mean+2\sigma$) and less than ($mean-1\sigma$) were considered, resulting in 24 events conforming to the former criterion and 90 to the latter. Both were recorded from within a total time period of 643 years. Similar analyses for core *Ness 3* are illustrated in *Tables 5.9a*, *5.9b*, and *5.9c*.

5.5.2 Spectral analysis of the sediment record

FFT spectra were obtained from analysis of entire sequences of lamination thickness determinations from all cores, and are presented in Chapter 6, *Figures 6.31-6.40*. A summary of the results from these analyses may be found in *Table 5.10*. Periodic elements within core *Ness 3* are illustrated by three spectra, representing the three separate sequences determined from that core. No attempt has been made to isolate any perceived forcing agent by 'windowing' of the data, apart from the utilisation of a Parzen window inherent in the FFT procedure.

Table 5.8a Sherman's statistic for core *LNR1* maxima ($\geq \text{mean}+2\sigma$)

<i>Year (AD)</i>	<i>Difference</i>	<i>Year(AD)</i>	<i>Difference</i>	<i>Year(AD)</i>	<i>Difference</i>
1945		1859	2	1548	123
1939	6	1854	5	1499	49
1892	47	1773	81	1491	8
1868	24	1766	7	1480	11
1867	1	1762	4	1476	4
1866	1	1756	6	1451	25
1862	4	1718	38	1450	1
1861	1	1671	47	1404	46

Average period (a) = 26.79

$\omega = 0.438$ (significant at 95%)

In addition, evolutive spectral analysis was carried out on lamination data from all cores, by 'stacking' individual FFT spectra derived from sequences of 128 years and displaying these as a contour plot (for example, *Figure 5.14*). Thus, time runs vertically, with spectra derived from more recent sediments toward the tops of the figures, while the frequency domain exists horizontally, with low frequency events represented by regions to the left of the page and higher frequency events to the right. Again, results of these analyses are presented in Chapter 6 (*Figures 6.41-6.43*).

Table 5.8b Sherman's statistic for core *LNRI* minima ($\leq \text{mean}-1\sigma$)

<i>Year(AD)</i>	<i>Diff.</i>	<i>Year(AD)</i>	<i>Diff.</i>	<i>Year(AD)</i>	<i>Diff.</i>	<i>Year(AD)</i>	<i>Diff.</i>
1938		1730	6	1618	3	1522	4
1923	15	1703	27	1607	11	1514	8
1920	3	1697	6	1601	6	1472	42
1916	4	1673	24	1600	1	1471	1
1913	3	1669	4	1591	9	1446	25
1910	3	1661	8	1587	4	1444	2
1895	15	1660	1	1585	2	1436	8
1846	49	1658	2	1562	23	1423	13
1838	8	1657	1	1558	4	1386	37
1833	5	1656	1	1556	2	1372	14
1830	3	1655	1	1555	1	1365	7
1828	2	1654	1	1551	4	1364	1
1819	9	1652	2	1550	1	1363	1
1818	1	1645	7	1549	1	1356	7
1813	5	1635	10	1547	2	1355	1
1810	3	1631	4	1543	4	1348	7
1801	9	1629	2	1540	3	1347	1
1799	2	1627	2	1538	2	1345	2
1785	14	1626	1	1534	4	1344	1
1783	2	1625	1	1530	4	1339	5
1772	11	1624	1	1529	1	1327	12
1751	21	1623	1	1528	1		
1736	15	1621	2	1526	2		

Average period (a) = 7.14 $\omega = 0.412$ (significant at 95%)

Table 5.9a Sherman's statistic for core Ness 3, section 1 maxima ($>\text{mean}+2\sigma$)

Case	Value	Case _n - Case _{n-1}	Case	Value	Case _n - Case _{n-1}	Case	Value	Case _n - Case _{n-1}
6	1.25		308	1.95	17	772	1.41	1
7	1.11	1	326	1.25	18	773	1.69	1
9	1.11	2	329	1.11	3	776	1.13	3
38	1.39	29	397	1.25	68	788	1.83	12
53	1.25	15	442	1.25	45	834	1.27	46
60	1.53	7	509	1.25	67	836	1.27	2
68	2.37	8	532	1.11	23	862	1.41	26
131	1.11	63	557	1.53	25	949	1.13	87
148	1.25	17	568	1.25	11	954	1.13	5
149	1.39	1	573	1.11	5	977	1.27	23
152	1.39	3	592	1.81	19	982	1.97	5
156	1.39	4	594	1.11	2	983	1.41	1
160	1.11	4	678	1.15	84	987	1.83	4
201	2.09	41	682	1.18	4	990	1.97	3
212	1.25	11	716	1.21	34	994	1.13	4
213	1.11	1	722	1.13	6	1017	1.13	23
221	1.11	8	727	1.27	5	1023	1.41	6
241	1.25	20	728	1.41	1	1030	1.69	7
252	1.39	11	735	1.13	7	1080	1.13	50
265	1.39	13	740	1.27	5	1096	1.41	16
274	1.11	9	742	1.83	2	1136	1.27	40
281	2.23	7	753	1.55	11	1148	1.13	12
286	1.67	5	759	1.13	6	1262	1.13	114
291	1.95	5	771	1.83	12			

Average period (a) = 18.25

$\omega = 0.442$ (significant at 98%)

Table 5.9b Sherman's statistic for core Ness 3, section 2 maxima ($>\text{mean}+2\sigma$)

Case	Value	Case _n - Case _{n-1}	Case	Value	Case _n - Case _{n-1}	Case	Value	Case _n - Case _{n-1}
14	1.27	0	665	1.27	13	1375	1.5	13
92	1.27	78	672	1.79	7	1390	1.36	15
95	1.69	3	679	1.38	7	1402	1.36	12
110	1.41	15	692	1.79	13	1424	1.5	22
128	1.55	18	704	1.51	12	1447	1.36	23
151	1.41	23	708	1.93	4	1470	1.5	23
171	2.25	20	717	1.51	9	1477	1.77	7
223	2.25	52	747	1.38	30	1492	2.05	15
231	1.27	8	787	1.93	40	1495	1.5	3
263	2.96	32	812	1.65	25	1500	1.64	5
289	2.68	26	842	1.93	30	1507	1.64	7
293	1.27	4	845	1.79	3	1514	1.36	7
346	1.27	53	874	1.79	29	1568	2.05	54
351	1.97	5	884	1.51	10	1573	1.91	5
352	1.41	1	885	1.79	1	1578	1.36	5
356	1.83	4	967	2.05	82	1625	1.36	47
359	1.97	3	1023	2.32	56	1632	1.36	7
392	1.41	33	1046	1.36	23	1647	1.36	15
399	1.69	7	1051	1.36	5	1650	3	3
455	1.69	56	1077	1.36	26	1667	1.77	17
469	1.69	14	1098	1.77	21	1676	1.91	9
486	1.27	17	1110	1.5	12	1689	2.05	13
487	1.41	1	1127	1.64	17	1704	1.36	15
489	1.27	2	1140	1.36	13	1736	1.5	32
519	1.55	30	1174	1.36	34	1746	1.64	10
584	1.41	65	1175	1.5	1	1781	1.5	35
616	1.27	32	1185	1.36	10	1800	1.36	19
630	1.27	14	1262	1.5	77	1812	1.5	12
652	2.11	22	1362	1.91	100			

Average period (a) = 9.62

 $\omega = 0.348$ (significant at 50%)

Table 5.9c Sherman's statistic for core Ness 3, section 3 maxima ($>\text{mean}+2\sigma$)

<i>Case</i>	<i>Value</i>	<i>Case</i> _{<i>n</i>} <i>Case</i> _{<i>n-1</i>}	<i>Case</i>	<i>Value</i>	<i>Case</i> _{<i>n</i>} <i>Case</i> _{<i>n-1</i>}	<i>Case</i>	<i>Value</i>	<i>Case</i> _{<i>n</i>} <i>Case</i> _{<i>n-1</i>}
14	1.38	0	818	1.65	80	1804	2.2	44
27	1.52	13	866	1.52	48	1807	1.93	3
61	2.75	34	897	1.53	31	1811	1.38	4
120	1.79	59	958	1.81	61	1907	1.52	96
191	1.38	71	1027	1.53	69	1925	1.65	18
193	1.93	2	1033	1.39	6	1974	1.65	49
218	1.52	25	1088	1.67	55	1985	1.79	11
245	2.34	27	1177	2.37	89	2012	1.81	27
283	1.38	38	1198	1.67	21	2037	1.39	25
302	1.52	19	1217	1.39	19	2040	1.39	3
329	1.65	27	1251	1.95	34	2044	1.39	4
353	3.31	24	1258	1.95	7	2075	2.09	31
359	1.38	6	1273	1.53	15	2090	1.67	15
360	1.38	1	1311	1.67	38	2117	1.39	27
367	1.38	7	1363	1.95	52	2148	1.39	31
381	1.79	14	1409	1.53	46	2149	1.53	1
392	1.52	11	1423	1.38	14	2160	1.39	11
410	1.79	18	1497	1.52	74	2162	1.81	2
411	1.38	1	1500	1.65	3	2203	1.67	41
412	1.65	1	1503	1.38	3	2231	1.93	28
427	1.79	15	1550	1.52	47	2261	1.79	30
444	1.38	17	1556	1.52	6	2278	1.65	17
467	1.79	23	1564	1.38	8	2282	2.75	4
490	2.2	23	1574	1.79	10	2286	1.79	4
532	1.38	42	1627	1.38	53	2288	2.34	2
569	1.38	37	1632	1.52	5	2297	1.79	9
616	1.93	47	1645	1.79	13	2301	1.65	4
620	1.52	4	1646	1.38	1	2307	2.75	6
645	1.38	25	1654	1.79	8	2313	2.62	6
656	1.52	11	1677	1.52	23	2330	2.07	17
661	1.38	5	1691	1.65	14	2345	1.65	15

Columns continued on next page

Table 5.9c Sherman's statistic for core *Ness 3*, section 3 maxima ($>\text{mean}+2\sigma$) *contd.*

<i>Case</i>	<i>Value</i>	<i>Case</i> _{<i>n</i>} <i>Case</i> _{<i>n-1</i>}	<i>Case</i>	<i>Value</i>	<i>Case</i> _{<i>n</i>} <i>Case</i> _{<i>n-1</i>}	<i>Case</i>	<i>Value</i>	<i>Case</i> _{<i>n</i>} <i>Case</i> _{<i>n-1</i>}
682	1.65	21	1705	1.52	14	2399	1.38	54
729	1.38	47	1720	1.65	15			
738	1.52	9	1760	1.38	40			

Average period (a) = 24.21
 $\omega = 0.347$ (significant at 50%)

Table 5.10 Summary of the periodicities found by FFT analyses of cores *Ness 3*, *Ness 4*, and *LNRI*.

<i>Ness</i> 3/1	3/1 (10)*	<i>Ness</i> 3/2	3/2 (10)*	<i>Ness</i> 3/3	3/3 (10)*	<i>Ness</i> 4	<i>LNRI</i>
342	343	609	167	161	161	2197	214
205	206	166	80	93	93	550	92
31		79	64	43	78	200	46
22		54	54	34	45	183	27
6		44	42	27	36	137	9.5
5.2		33	37	23	35	129	
3.9		29	33	20	28	115	
3.75		22	21	16		96	
2.8		20		15		84	
2.5		19					
2.4		17					
2							

* (10) represents periodicities calculated from decadal totals of annual lamination thickness

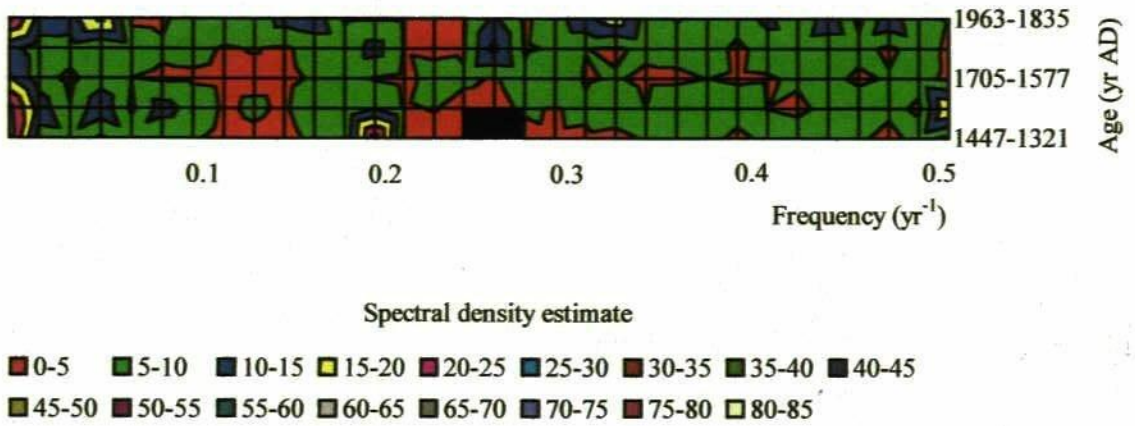


Figure 5.14 An example of the result from evolutive analysis of lamination thickness in core *LNRI*.

6. Data Analysis

6.1 Objectives

Analysis of the data was performed in order to provide answers to the following questions:

- i). Did couplets of pale and dark laminae represent annual deposition? If so, over what time period did the long and short cores represent? What were the compositions of the layers? Could the subtle variations in shade, observed within each long core, be quantified by digital image analysis and could this signal be correlated with long-term proxy records?
- ii). Was it possible to correlate lamination thickness measurements with modern meteorological records, in order to determine whether or not local climatic variation was a forcing agent of deposition? Could the analysis be extended to a regional synthesis, and could the sediment record from Loch Ness be compared with other published regional proxy records? Could analysis of lamination thickness data reveal elements of periodicity within the time series?

In order to answer question i), lithological and microlithological analyses of sediment material were performed, in order to record changes in the moisture and organic content, and to determine the nature of the differences between pale and dark laminae. Techniques employed included the determination of loss on ignition, Backscatter Scanning Electron Microscopy, and Energy Dispersive Spectroscopy. Digital image analysis was employed as a tool with which the laminae could be counted, and radiocarbon dating was utilised as a framework against which the success of the resultant chronology could be judged. DIA was also used in order to measure variations in grey level throughout the long cores.

Question ii) was addressed by the construction of time series of lamination thickness and grey level by digital image analysis. Lamination thickness data were compared with local meteorological records, in order to determine the response of sedimentation in the loch to variations in local climate. Palaeoclimatic datasets derived from areas around the north-eastern Atlantic seaboard were also compared with Loch Ness data in order to ascertain whether or not these regional climatic changes were recorded by variations in sedimentation. Proxy data relating to longer-period forcing processes were also correlated with both lamination thickness and grey level data, in order to determine the possible effects of these on both quantity and quality of sedimentation. Spectral analyses of variations in lamination thickness were performed in order to detect the presence of periodicity which may indicate further the nature of forcing processes acting on sedimentation.

6.2 Sediment characteristics

6.2.1 General characteristics of Percentage Dry Matter (%DM) / Percentage Loss On Ignition (%LOI)

Both dry matter and loss on ignition values exhibit variations throughout each *ca* 6 m core, although there is some difficulty in correlating between them. %DM values are consistently low in each core, indicating that the sediments remain high in moisture, even at depth. For both cores the average value of %LOI is of the order of 30%, indicating an abundance of organic material. Loch Ness is classified as an unproductive lake, and most organic matter found in the water column has been determined to be of terrestrial origin (R.I.Jones *et al.*, 1997) Increases in %LOI in core *Ness 4* at *ca* 2.7 and 2.3 m may be comparable to those observed in core *Ness 3* at *ca* 3 and 1.9 m, although the magnitude of increase in *Ness 4* is much greater. Variations at the base of each core, representing possibly the first 2ka after deglaciation, denote increasing organic content of

the sediment, probably relating to changing inputs from a maturing catchment and lake system. Both cores exhibit a slight increase in %LOI at the location of the boundary between the laminated *gyttja* and basal clay.

6.2.2 Core Ness 3, Percentage Dry Matter (Figure 5.2)

Variations in this determinand may reflect compression of the sediments towards the base, since they generally decline towards the top of the core. Velde (1996) has suggested, however, that for most clay-rich sediments compaction is complete within the uppermost 20-30 cm. An alternative hypothesis is that there exists a change in sediment composition with depth, resulting in fewer voids containing water. This explanation may be borne out by considering the image of the core acquired in the Infrared (Plate 5.1), where a gradual lightening of the tone of the core material towards the base may be observed, indicating perhaps a higher silt content during the Early Holocene, when soils would have been less mature and erosion facilitated by the lack of vegetation. An abrupt increase occurs at the contact between brown laminated *gyttja* and the grey basal clay, which contains only about 20% water. The prominent excursion at *ca.* 1.25 m, to values typical of the lower sections of sediment, coincides with the chaotic section described in Section 5.1. Other, smaller, increases in %DM may be explained by presence of numerous pale, silt laminae which, because of their low porosity, would be expected to contain less water.

6.2.3 Core Ness 3, Percentage Loss On Ignition (%LOI; Figure 5.2)

Again, this relationship may be understood by suggesting that changes in %LOI are indicative of variations in lithology of the sediment and that the depositional regime of silt particles is sufficiently different from that prevalent during clay/organic particle sedimentation. Indeed, the premise that the fine laminae recorded through the cores represent seasonality of sedimentation, where silts are washed into the loch during

winter causes the corollary that organic particles would be less numerous in those layers deposited at other times of the year.

The decrease in %LOI from the clay/*gyttja* boundary to a maximum at *ca* 3.0 m would be consistent with growing maturity of catchment soils after deglaciation and perhaps an increase in nutrient status of the water body with time. The initial input of allogenic material, which would have followed the melting of the ice, has also been recorded by an increase in in-lake organic productivity by Ms J.M. Dean (unpubl.), in that greater numbers of diatoms have been observed in early Holocene sediments than in more recent ones. Values then rise steadily to a maximum of *ca* 34% at 3 m. This section of core has been dated as containing material deposited during the Hypsithermal and may thus indicate a true rise in in-loch productivity consequent upon increased water temperature, or an increase in vegetation cover in the catchment. A decline in %LOI is then observed, with a brief return to larger values at 1.9 m (3.7 ka BP) and corresponding to a period within the European Neolithic and Bronze Ages (*ca* 4.5 to 3 ka BP), until a minimum is reached within the chaotically-laminated section at *ca* 1.3 m. This contains little organic material, and may consist of rebedded material of Early Holocene age, since pollen analysis (Ms S.M. Peglar, pers. comm.) demonstrates an abundance of Pine.

Values rise in the topmost 1m of the core, with slight fluctuations which may reflect changes in the loch and/or catchment during the past two millennia, a time scale which indicates that human influence may be the root cause.

6.2.4 Core Ness 4, Percentage Dry Matter (Figure 5.3)

This exhibits several large variations which are not repeated in core *Ness 3*. The base of the core, from *ca* 3 m to the *gyttja*/clay boundary, exhibits few deviations, with water content increasing slightly from the boundary itself to 3.0 m. An increase at *ca* 2.8 m may be explained by this sample being taken from the end of a guttering section,

from sediment which may have suffered dehydration from evaporation or drainage. The apparent decrease in water content is mirrored, however, by an *increase* in loss on ignition. This observation is contrary to the relationship noted in core *Ness 3* and to the notion that low water content is related to porosity, silt-rich sediment being of low porosity and clay/organic *gyttja*, highly porous. A large increase in dry matter at *ca* 2.3 m does not correlate with any prominent feature depicted in infrared photographs, although a sequence of faint pale laminae occurs in this segment of core. An increase in loss on ignition also may be observed at this point. Core *Ness 4* does not display the pronounced decrease in water content within the chaotic section at 1.39-1.57 m, previously noted for core *Ness 3*. The uppermost 50 cm of core exhibits an increase of %DM towards the top, which may again indicate that moisture has been lost, possibly by drainage through the endcaps of the storage guttering. This is not observed, however, in core *Ness 3*, although both cores were wrapped and stored in similar conditions.

6.2.5 Core *Ness 4*, Percentage Loss On Ignition (Figure 5.3)

%LOI values are low at the base of this core, within the grey unlaminated clay, owing to the barren nature of the material. A narrow, positive 'peak' in %LOI, also present in the record for core *Ness 3*, is observed from material situated at the boundary of *gyttja* and clay, and suggests that an influx of nutrients may have led to increased productivity, following deglaciation. This hypothesis has been corroborated by lamination thickness measurements and by observations of diatom numbers by SEM, and will be discussed in the relevant sections. Values rise steadily, indicating increasing organic content with time, from *ca* 20% at 4 m to some 30% at 3.5 m, with a subsequent large increase to 50% at 2.7 m. The steady rise is also observed in core *Ness 3* at *ca* 3 m and may thus indicate a genuine increase in organic material in the water column. A further rapid increase and decline at *ca* 2.25 m is not satisfactorily explained in terms of productivity or increased inwash of organic matter, since no distinct sedimentary structures or variations in colour of the sediments are observed. It may thus result from

sediment deterioration due to oxidation at the end of a section of storage guttering. Values fall slightly within the chaotic section, but not to the same extent as observed in core *Ness 3*.

Variations above the chaotic section of the core indicate a decline in organic matter content from about 40% at 1 m to a minimum of 19% at 0.2 m, which may be connected with catchment changes in recent times, leading to decreased erosion and reduced input of nutrients to the loch. It remains to be seen, however, whether this represents a genuine effect in the amount of organic material in the water column or is an artefact of sampling. Of further note is the increase in %LOI at the extreme top of this core, which is not observed in *Ness 3*. A possible explanation is that the equivalent section of core *Ness 3* is not complete, consisting of an unlaminated ooze which appears to have broken up during extrusion, whereas this core appears completely laminated.

6.3 Microlithological examination (Plates 5.4 and 6.1)

Microscopic examination of sediment structure was carried out using SEM techniques described in *Section 4.6*. Additional analyses, by BSEI and optical microscopy, on thin sections from various ages from each of the three cores under discussion, have also been carried out, by Ms J.M. Dean at the Southampton Oceanography Centre.

It was observed, by secondary electron scanning electron microscopy (SESEM) of air-dried bulk material, that there is little obvious difference between pale and dark laminae in terms of grain size and general appearance. Observations carried out, by the author at Plymouth, along random transects perpendicular to the fabric of the sediment failed to reveal appreciable changes in diatom taxa between laminae, although particles of mica were found to be more abundant within the pale silt-rich laminae, than in the darker clay-rich layers. Dean has also observed that some of the micas are deposited conformably

with laminae and others not. Presumably, this is indicative of the energy of the environment of deposition and/or evidence of resuspension.

Table 6.1 Elements detected by EDS in sediments from Loch Ness, with their average abundance.

<i>Element</i>	<i>Abundance %</i>
Si	47.5
Fe	23.0
Al	16.4
Ca	2.9
Na	2.6
Mg	1.6
Mn	0.7
P	0.6

Attempts, by the author at Plymouth, to test for periodicity via changes in elemental composition, as determined by Energy Dispersive X-ray Spectroscopy (EDS) on bulk sediments, were unsuccessful, indicating that the most abundant chemical elements in the fabric of the sediments are continuously deposited throughout the year. These elements are typical of those contained within detrital clay minerals derived from the catchment (*Table 6.1*). Thin window EDS was also employed, in order to test for variations in abundance of light elements such as carbon, but did not produce significantly different spectra. ZAF-corrected spectra from gold-coated polished bulk specimens, and from material collected from the dissection of individual laminae, reinforce this conclusion.

BSEI, carried out on sediments in thin section by Dean, provided the most informative images (*for example, Plate 6.1*), illustrating the contrasts between pale and

dark laminae. Investigations indicate that four styles of lamina predominate, identified as

- a). silt-rich
- b). silt-poor
- c). clay
- d). storm deposits -
 - i). graded bedding, with coarse base
 - ii). without coarse base.

The subdivision of case d) is believed to illustrate the variability of the energy of the depositional environment, and thus may act as an indication of storm intensity, duration, or location. Observation of the orientation of mica particles within laminations indicates that they are bedded conformably within 'normal' laminae but not within storm layers, suggesting that the latter were deposited by events of higher energy.

Although diatom frustules exist throughout the sediment column (Cooper *et al.*, submitted; L.A. Wheeler, Unpubl.), Dean has determined that Early Holocene sections contain a greater abundance than recent sediments, and that laminae from the Early Holocene are thicker than those from the Late Holocene. This may be indicative of initially larger amounts of detrital mineral input to the loch, providing a correspondingly large influx of nutrients to the water column, which then subsequently declined when catchment vegetation and soils matured.

6.4 Photography and Image analysis

Colour photographs of cores failed to enhance the fine-scale lamination structure, although they may be utilised to illustrate the contrast between the pale, thick flood-derived laminae, and the more abundant, brown-coloured *gyttja*. The numerous fine, black layers are not well recorded, except in close-up photographs.



Plate 6.1 A photomosaic BSEI image of a section from core *Ness 4*. The sediment is of Mid-Holocene age (*J.M. Dean, pers. comm.*).

Photographs taken with film sensitive in the infrared reveal, however, a host of features not readily visible in real colour images. In addition, reflections from the surface of the material are greatly reduced, further increasing contrast. It is uncertain whether the final image represents an indication of the true thermal emissivity of the components of the sediment, or merely the reflectivity of each of the laminations in those wavebands.

Analysis of images of both long cores (*Plates 5.1 and 5.2*) reveals a non-linear change in 'Grey Level' (GL) with depth. On a scale of 0 (black) to 255 (white), basal sediments possess GLs *ca* 150, which decreases to minimum of *ca* 25 at about 2.50 m. More recent sediments exhibit a GL of *ca* 45 which indicates that paler sediments exist at the base of each core, with darker material at the top. Mid Holocene deposits appear quite dark in comparison. Very high GL readings are obtained from the pale grey, basal clay. Thus, it may be presumed that infrared GL values are indicative of variations in lithological composition of the sediment, with low values indicating dark, organic-rich clays and large readings, pale organic-poor clays and silts.

X-radiography offers a convenient method for visualisation of the laminated structure of sediments. Features such as irregular boundaries between layers may be detected (which may be indicative of erosion), in addition to the internal structure of some of the thicker laminae. Densitometry of digitised x-radiographs of sections of sediment from each core, using image analysis, has enabled the determination of lamination thickness. In addition, utilisation of image transforms has facilitated quantification of laminae within sections where visual quality was observed to be poor, and where x-radiography alone proved unsuccessful at optimising contrast between layers. The application of image transforms to analysis of laminated sediment has served to enhance perception of structural units, and produced images which are more amenable to analysis and contain fewer errors which may have compromised accuracy and reproducibility (Cooper, 1998). The technique was thus utilised as a method for rapid quantification of

visual characteristics of laminated sediments, although there remained sections, especially within core *Ness 3*, where reliable densitometric measurements could not be performed. These sections were thus omitted from the development of a chronology (*Appendices A, B, and C*).

In addition, digital image analysis could not by itself, for example, identify turbidite layers where they were not already visually apparent. It is therefore recognised that investigators still need an intimate knowledge of the material under analysis and may even require recourse to other techniques, such as the production of tape peels (e.g. Simola, 1977) and thin sections (for instance, Mehl & Merkt, 1990), in order fully to characterise a sediment core.

6.5 Chronology

Construction of a chronology may be discussed in terms both of lamination counting and radiocarbon dating of the sediments. It was hoped to: a) test the hypothesis that the laminae present in the sediments from Loch Ness are varves; b) demonstrate that the deficiencies of the methods utilised, (which have been previously outlined), have not seriously compromised accuracy; c) verify inconsistencies between cores.

6.5.1 Lamination counting

Figure 5.11 illustrates a tentative time/depth relationship for core *Ness 3*. Construction of the line, utilising ten-year averages of lamination thickness has been described previously (*Section 5.3.2*). The line has not been plotted through the origin, since it is known that, owing to the mode of operation of the corer, the uppermost sediments were not sampled. The amount of loss is not known with any certainty, but photographs by A.J.Shine (unpubl.) of the corer in position on the bed of the loch prior to sampling, may indicate that it is driven into the sediment *ca* 0.5 m. This value has

therefore been employed as representing the approximate distance between the top of core *Ness 3* and the SWI. The lithological composition of the chaotic layer present in both cores *Ness 3* and *Ness 4* suggests that it may have been deposited as an instantaneous event. It is therefore represented on the plot by a vertical line.

6.5.2 Radiocarbon dating

A close correspondence between the chronology derived from lamination counting and the radiocarbon dates may be observed. Differences between the two sets of dates are quantified in *Figure 6.1*. It may be observed that varying the assumed depth of settling of the corer in the sediment, by moving the intersection of the line and the abscissa, would enable a much closer relationship to be obtained, especially in the

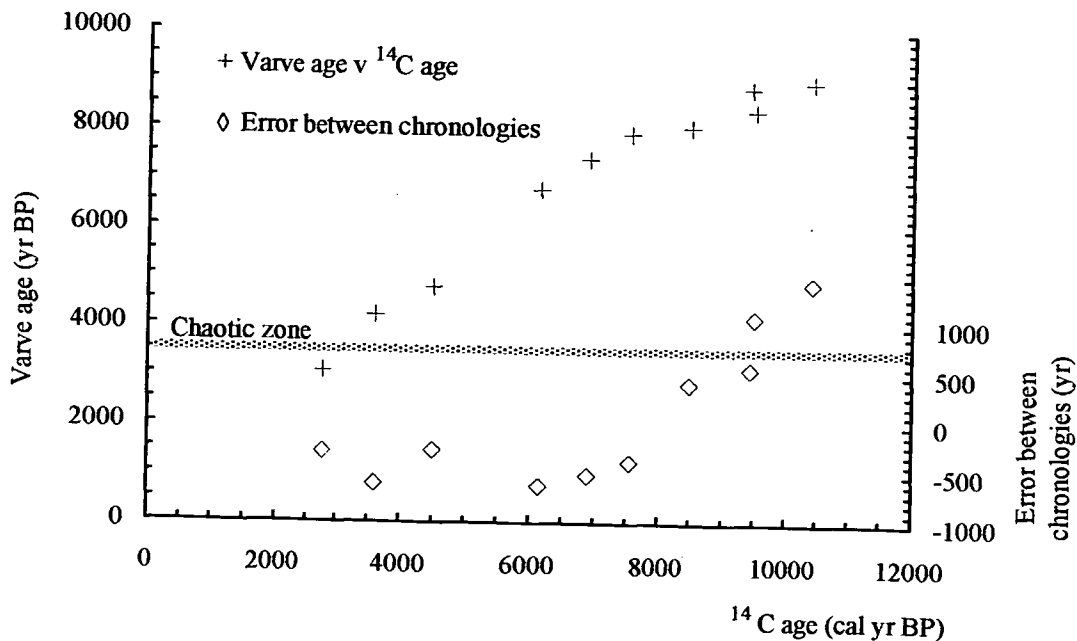


Figure 6.1 Comparison of varve and ^{14}C calibrated ages from core *Ness 3*.

section representing the Mid-Holocene. Differences between the two sets of dates increase at the base of the core, probably owing to lack of resolution of the X-radiographs, and to the decreasing contrast between adjacent laminae in the early Holocene. Both of these factors may be instrumental in causing large errors when counting by image analysis,



Plate 6.2 BSEI photomosaic of early-Holocene material, obtained by Dean (Unpubl.).
The general lack of contrast between layers is well displayed.

since laminae will be ill-defined. The lack of contrast between laminae from the early Holocene is well displayed in *Plate 6.2*, a BSEI photomosaic obtained by J.M. Dean (Unpubl.). The type of sediment deposited in the loch may have been more or less constant throughout the seasons during this period, owing to the presence of still-melting ice in the catchment, and increased erosion owing to immaturity of the soils. In addition, movement of the time/depth line would cause sample *SRR-5735* (consisting of material taken from the upper section of this core) to exhibit an older date, which, considering that this material originated after human occupation of the catchment, may indeed contain reworked, radiometrically 'old' carbon (O'Sullivan *et al.*, 1973).

Of further note are the differences between AMS and 'conventional' dates, particularly at the base of the core. These may merely be due to sample pretreatment processes, which differed between laboratories (Cooper *et al.*, 1998). Samples dated at ANSTO (*OZB-* prefix) were subjected to two alkaline extractions, which probably removed humic material and therefore produced slightly older dates. In contrast, samples indicated by an *SRR-* prefix were treated by acid extraction only, thus retaining those compounds. $\delta^{13}\text{C}$ values for all samples, irrespective of laboratory, lay in the range *ca* -25 to -29‰, which indicates, especially in view of the comparative lack of primary productivity in the water column, that the material dated was probably obtained from terrestrial sources (Boutton, 1991).

Core *Ness 3* was chosen as the primary material from which to derive a time/depth relationship by lamination counting, since sub-sampling for pollen and diatom analyses had also been performed upon the same core. These analyses were carried out prior to radiocarbon dating, and simultaneously with digital image analysis. The results from preliminary pollen analysis were employed in deciding the sampling strategy for radiocarbon dating. Thus, the fragmented nature of the lamination record in this core was not discovered until after pollen and diatom analyses were completed, and samples already submitted for radiocarbon dating.

Dating of core *LNR1* was carried out by lamination counting from X-radiographs, and correlation of the thickest layer present in the most recent sections with the 1868 flood. A chronology was then constructed from this datum, with each year defined by two laminae. The total period represented was thus calculated to be 1321 to 1963 AD.

6.5.3 Lamination thickness

Lamination thickness is representative of the amount of sediment deposited within a year and may thus indicate variations from year to year in environmental conditions within and over the catchment of the loch. These factors may be considered over many time scales but will be discussed here in terms of annual, decadal, and centennial changes. It may again be noted that the record from core *Ness 3* appears fragmented, owing to the presence of the chaotic layer at *ca* 1.2 to 1.5 m and the inability to resolve laminae in x-radiographs of sections at *ca* 2.9 m.

6.5.3.1 Lamination thickness, core *Ness 3* (Figure 5.8)

Determinations of annual thickness of laminae reveal that following deglaciation, deposition rates were high. Thick layers (*ca* 1.5 to 3.5 mm) occur at the base of the core, above the clay/*gyttja* boundary (Figure 6.2). Sedimentation rates in the core then declined, although there were brief intervals where increases occurred, in addition to sustained periods of higher deposition. Many large 'spikes' in the record exist, notably those at *ca* 3.3, 3.1, 2.65 and 1.8 m, corresponding, respectively, to ages of *ca* 6.4, 5.5, 4.8, and 2.3 ka cal BP. Closer inspection reveals periodicities within the record, and that average sedimentation rates seem to have declined over the period represented by the core, especially in the most recent section.

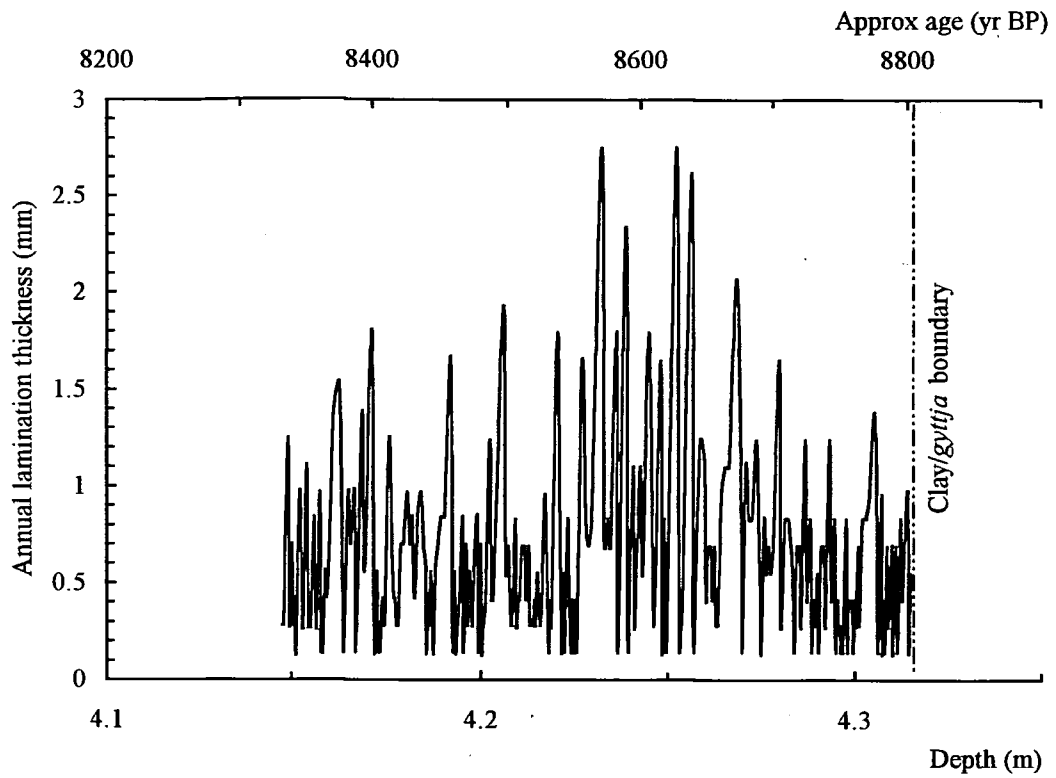


Figure 6.2 Illustration of lamination thickness at the base of core *Ness 3*.

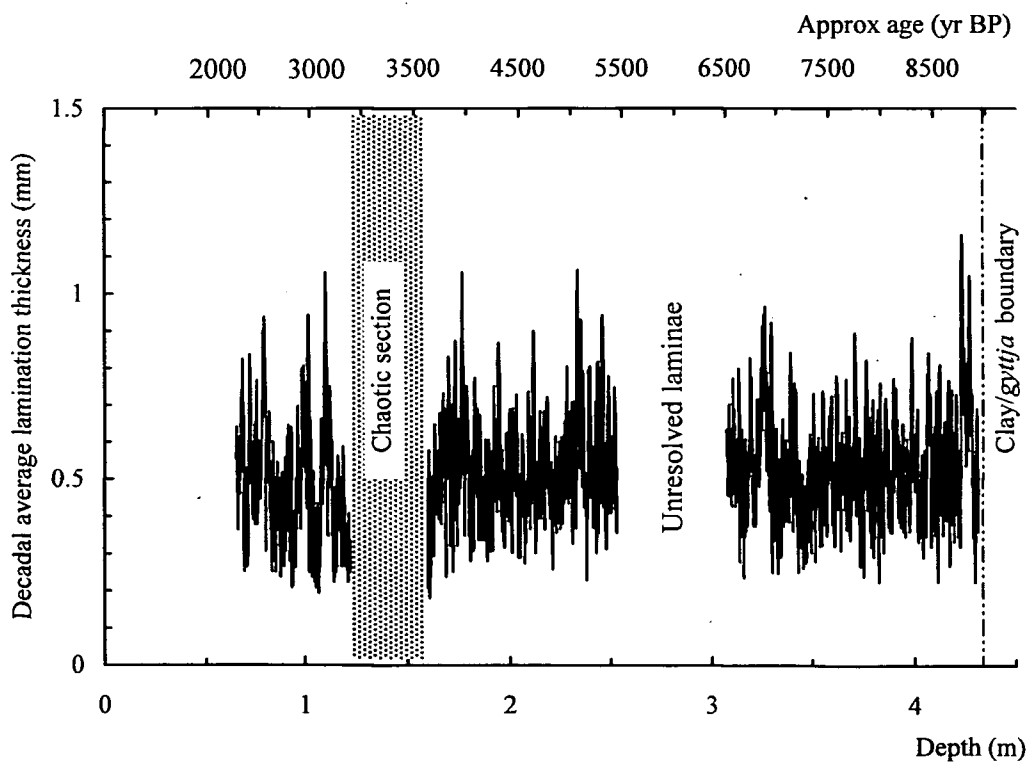


Figure 6.3 Record of decadal averages of lamination thickness from core *Ness 3*.

Decadal lamination thickness data reveal long-term variations in sedimentation over time (*Figure 6.3*). Of immediate note are the large values (*ca* 1.1 mm) at the base of the core, at about 9.5 ka cal BP, persisting for nearly a century before terminating abruptly in a shorter period of near-average deposition with very little variation. There then follows a further phase of near-average sedimentation, lasting from 8.5 to 6.5 ka BP, which is punctuated by abrupt (decadal-scale) extremes. Periods of alternate low and high sedimentation then take place from *ca* 6.5 ka to 5.7 ka BP, including an extended period of higher than average sedimentation at *ca* 6 ka BP.

Data for the Mid-Holocene again exhibit near-average values but also display abrupt variations on a decadal scale. Of note are the large 'spikes' denoting increased lamination thickness at *ca* 5 ka and 4.2 ka BP, and the trend to lower values towards the beginning of that section. More recent sediments (from *ca* 3 ka to 2.2 ka BP) exhibit generally below-average values, but with pronounced cyclic variations of *ca* 200-300 years, which are easily detected by Fourier analysis (*Section 6.8.2, Figure 6.31*).

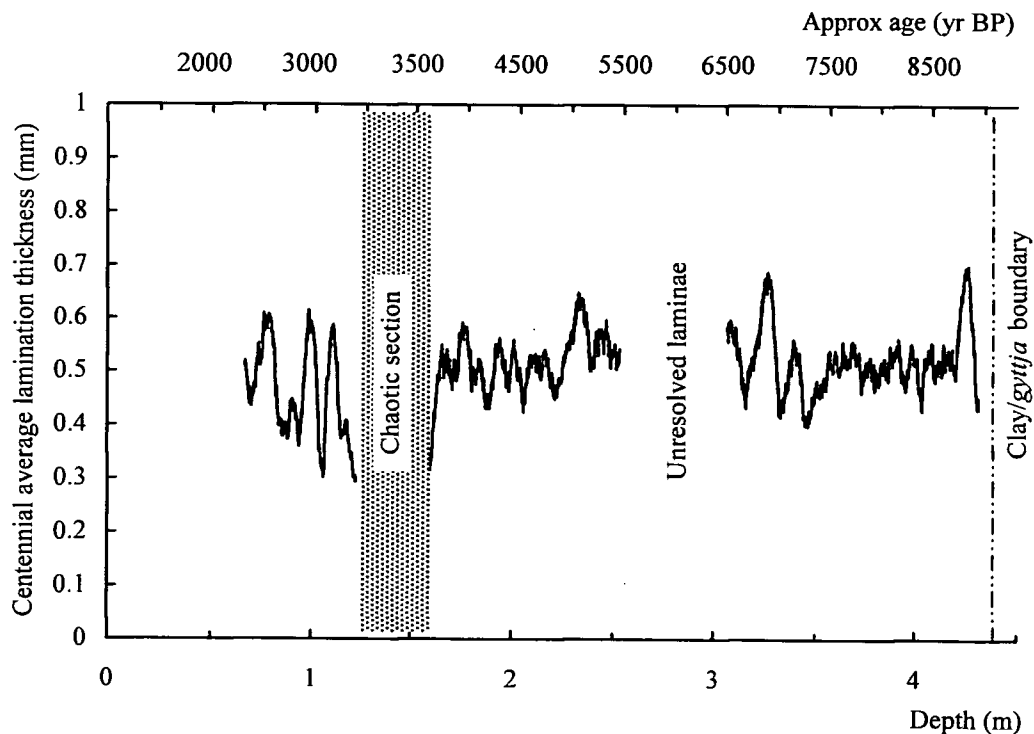


Figure 6.4 Record of centennial totals of lamination thickness from core *Ness 3*.

Averaging of lamination thickness over centennial timescales enhances the perception of periodicity (*Figure 6.4*), revealing maxima at *ca* 8.5, 6, and 4.5 ka BP, in addition to the trend towards generally smaller, but more variable, values around 2.8 ka BP. This increase in variability might be considered as being less of an indicator of climatic change than, perhaps, of anthropogenic influence, since this period marks the beginning of the British Iron Age. If average lamination thickness is calculated over 200-year timeslices, instead of by determining running means, a more graphic representation of variability is obtained (*Figure 6.5*). Here the 200-year periodicity, previously discussed, is well observed, in addition to a period from *ca* 7 ka to 4 ka, when lamination thickness was consistently greater than the average calculated for the entire core. This section is considered to represent deposition throughout the Hypsithermal (Whyte, 1995).

6.5.3.2 Lamination thickness record in core *Ness 4* (*Figure 5.9*)

Owing to the present uncertain chronology of this core is not possible to comment on the pattern of variation of sedimentation with age, with any certainty.

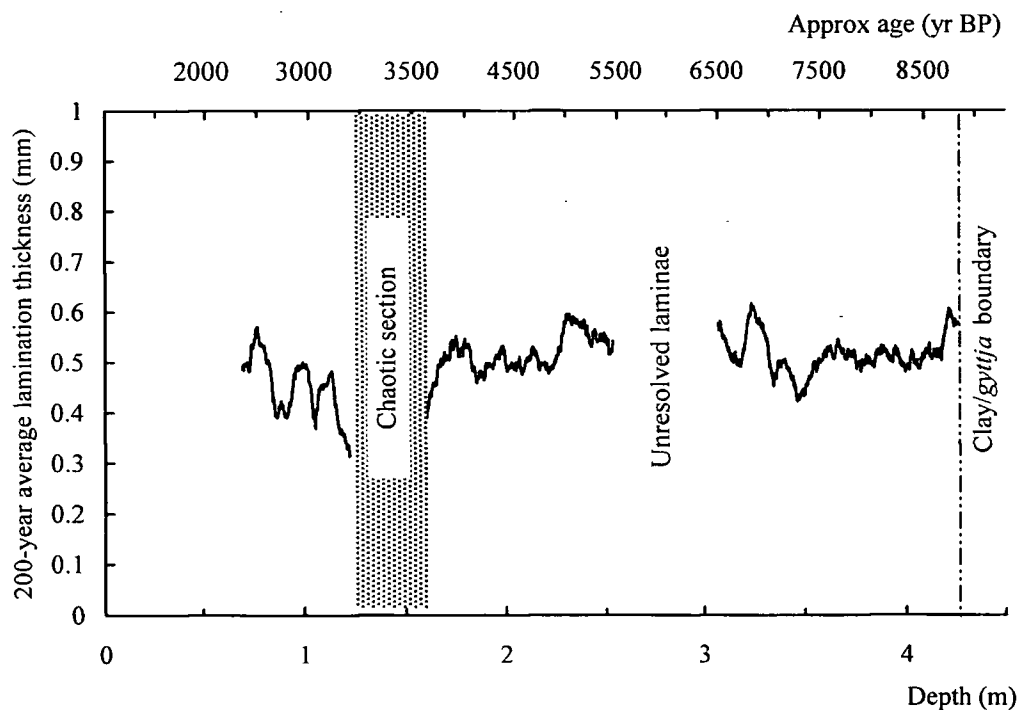


Figure 6.5 Record of 200-year averages of lamination thickness from core *Ness 3*.

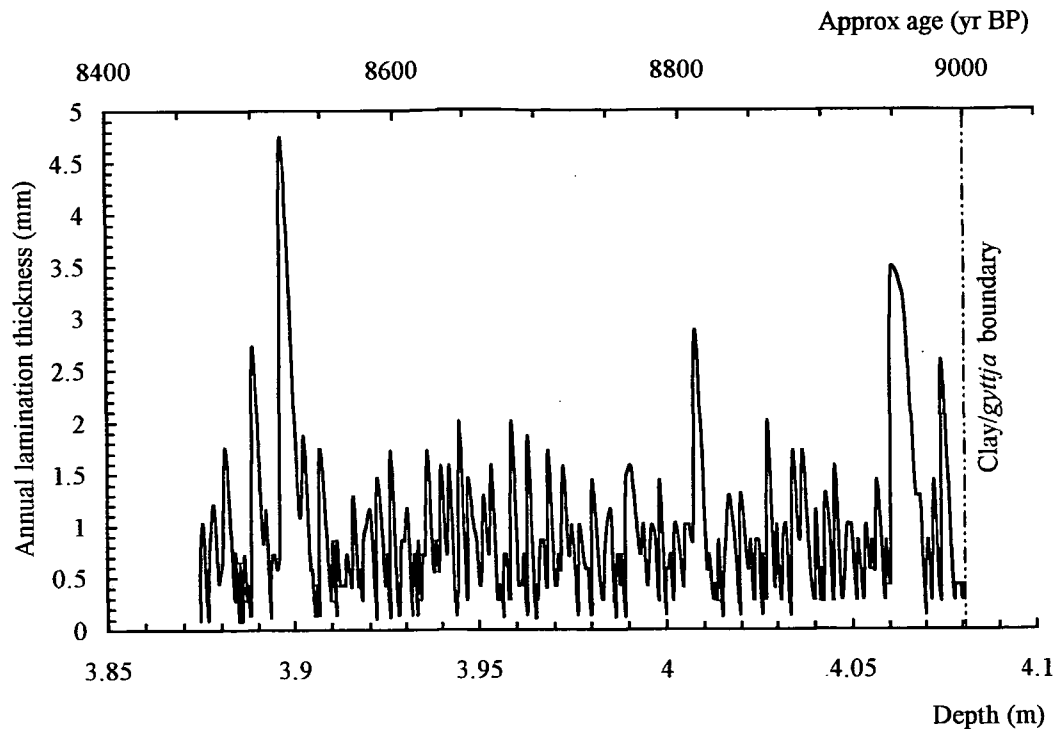


Figure 6.6 Illustration of lamination thickness at the base of core *Ness 4*.

Discussion will thus focus upon changes in lamination thickness with depth, although the timescale derived from core *Ness 3* may still be used as an approximate guide, by utilising the chaotic zone and clay/*gyttja* boundary as markers. There exist, however, extremes of deposition, as with core *Ness 3*, including the presence of similarly thick laminae at the base of the clay/*gyttja* (*Figure 6.6*). The record from this core appears to be more 'spikey' than that from core *Ness 3*.

Averaging over ten-laminae intervals aids the interpretation of trend within the signal (*Figure 6.7*). Lamination thickness from the clay/*gyttja* contact to *ca* 3.9 m is of the order of 0.8 mm, with large values occurring at *ca* 3.9 m. For the next 10-15 cm (3.9- 3.75 m) thickness declines to *ca* 0.5 mm, before increasing to *ca* 0.8 mm, briefly, at 3.65 m. Decreasing lamination thickness follows over the section 3.55 - 3.15 m, recording only *ca* 0.5 mm. The signal expands again at *ca* 3.1 m, where average measurements of over 1 mm are recorded. A sustained interval of thinner laminae is then

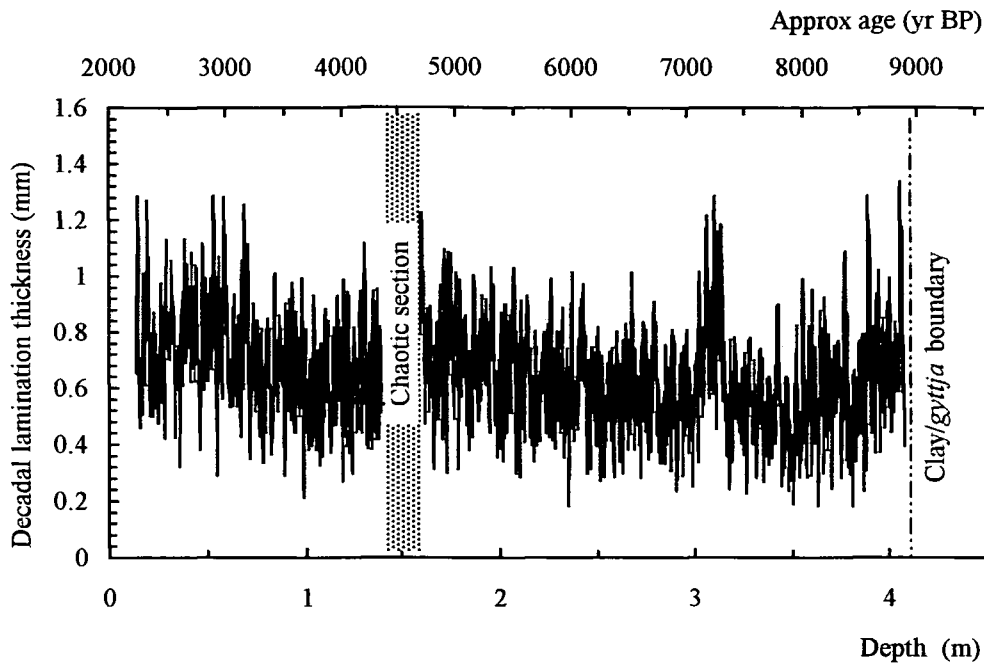


Figure 6.7 Record of the moving average of thickness of ten laminae from core *Ness 4*.

observed in the section 3.0-2.75 m, with typical values of 0.5-0.6 mm, followed again by a brief increase at 2.4 m. Further episodes of increased lamination thickness are observed at 1.8 m and 1.6 m, before the record is interrupted by the chaotic section at 1.5-1.4 m.

A similar pattern emerges in the upper 1.5 m of core with alternating periods of rapid and slow sedimentation, the average upper values of lamination thickness being of the order of 1 mm and the lower, 0.5 mm. Average values in the top 0.5 m are *ca* 0.8 mm, which suggests an increase in the rate of deposition, a trend not observed in core *Ness 3*. Pollen analytical data suggests, however that core *Ness 4* contains more recent material than core *Ness 3*, and thus may contain evidence of human impact, namely increasing erosion, within the catchment of the loch.

Further averaging of lamination thickness data from core *Ness 4*, employing windows of 100 and 200 laminae, begins to highlight features which may possibly be

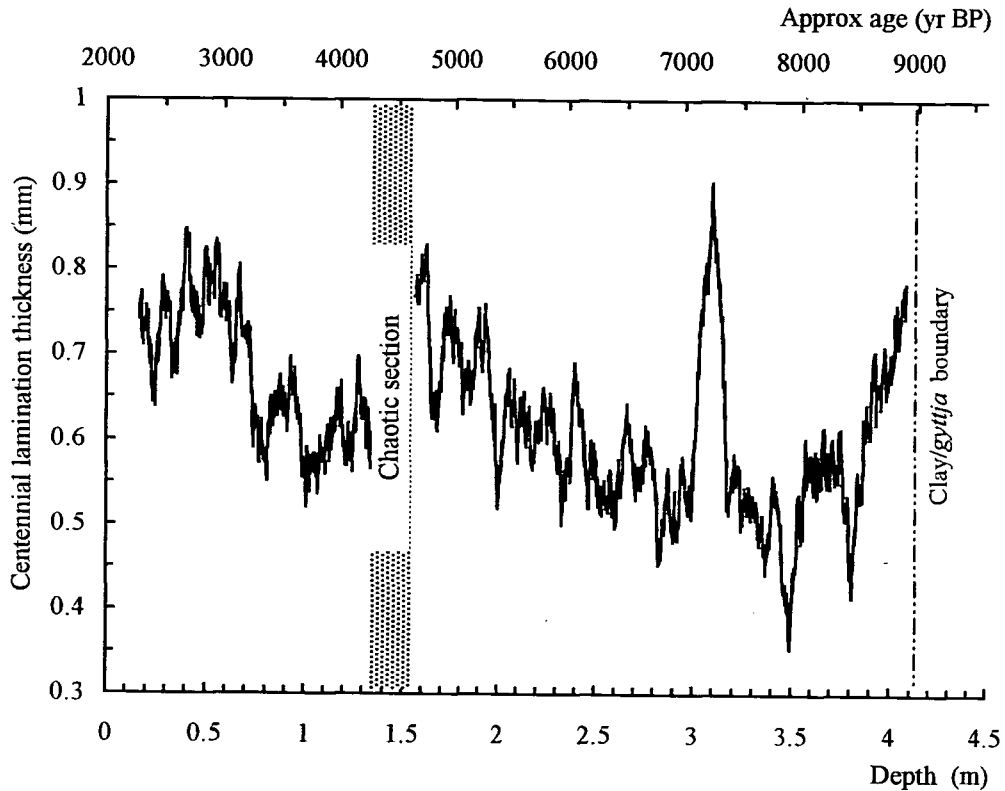


Figure 6.8 Record of centennial averages of lamination thickness, core *Ness 4*.

used for correlation between this core and *Ness 3*. For example, the large 'peak' in lamination thickness at *ca* 3.1m, and enhanced by averaging over 200 laminae (Figure 6.9) may be correlated with a similar, but less intense, feature appearing in the core *Ness 3* data at *ca* 3.2 m (Figure 6.6). Further features which may be employed for correlation are missing from *Ness 3*, owing to the fragmented chronology. It is noted that, however, there exists a trend of increasing lamination thickness, from *ca* 3 m to the base of the chaotic zone, in core *Ness 4*, whereas the same segment of core *Ness 3* exhibits no such trend. A decrease in lamination thickness after the deposition of the chaotic layer, followed, in more recent sediments, by oscillations in deposition rate, occur in both long cores.

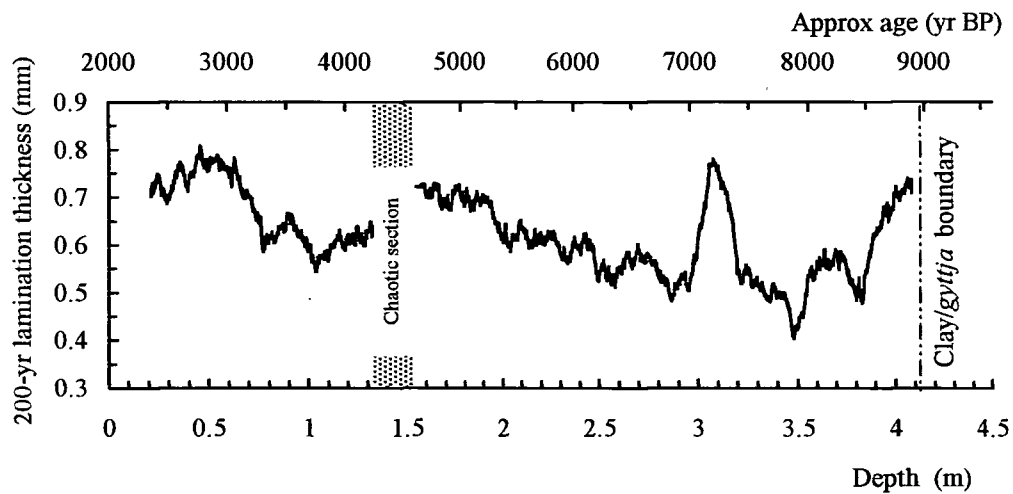


Figure 6.9 Record of 200-year averages of lamination thickness, core *Ness 4*.

6.5.3.3 Lamination thickness record in core *LNRI* (Figure 5.10)

Lamination thickness in this core exhibits many variations which may be correlated with climatic events recorded in other studies, and from instrumental and historical records. Of prime importance is the presence of extreme values during the 1850s and 1860s AD, including material thought to be from the Great Flood at Inverness of 1868 (Inverness Courier, 1868).

The record in core *LNRI* spans both the Medieval Warm Period (MWP; *ca* AD 1400 to 1550) and the Little Ice Age (LIA; various periods from AD 1550 to *ca* AD 1900; Bradley, 1994). The effect of these episodes on sedimentation in the loch may be observed by considering variations in lamination thickness. Above average values are encountered from AD 1400 to 1500, followed by a period from AD 1520 to 1660, when laminae are persistently thin. These may represent response to climatic variation owing, respectively, to the MWP and the LIA. The decline in thickness values observed in the section dating from AD 1800 to 1840 may be due to a further LIA cool episode. Similar variations have been detected in the varve record from the Finnish lake Pyhäjärvi (Itkonen

& Salonen, 1994), where thick layers are observed between the 14th and 16th Centuries (MWP), and thinner laminae from AD 1600 to 1800 (LIA). This pattern is also displayed in the accumulation record of the GISP2 ice core and is believed to be indicative of a lowering of temperature (Meese *et al.*, 1994). Lamb (1988), also reports a lowering of North Atlantic sea surface temperature during the 17th Century. There then follows a short (*ca* 40 year) period of much increased average lamination thickness, from about the mid-AD 1840s almost to 1880, which includes the 1868 Inverness flood. The Potato Famine in Scotland occurred at about this time, a period characterised by warmth and wetness, which encouraged the growth of spores of the potato blight, borne on easterly winds from continental Europe (Roberts, 1995).

Overpeck *et al.* (1997), who describe variation in Arctic climate over the last 400 years, have found that many records indicate that 1600 to *ca* 1680 AD, and 1800 to 1900 AD, were cold, with the intervening period, and especially 1730 to 1800 AD, warmer. Comparison of these results with the record from core *LNRI*, again suggests that low temperatures equate with thin laminations, and warmer temperatures with increased lamination thickness.

6.6 Analysis of local climatic records

Rainfall patterns over the Scottish Highlands are affected by weather systems prevalent within the North Atlantic (Barry & Chorley, 1992). The derived proxy record may thus be indicative of variations in these systems. Of particular importance is the location of the North Atlantic Polar Front (NAPF), which controls movement of frontal systems across the Atlantic Ocean (Taylor & Yates, 1967).

Analysis of precipitation (1886-1995) and temperature (1914-1995) records for Fort Augustus and Inverness (Meteorological Office, Scotland) has been performed, in order to test whether they correlate with the sedimentary record obtained from Loch Ness,

and whether, therefore, lamination thickness represents a proxy record of climate in general, and of precipitation in particular. The two sites were chosen because they represent weather conditions prevailing at the northern and southern extremes of the loch. Of immediate note, however, are the many gaps in the data from both sites, especially for the early and mid- 1920's, the period 1947-1951, and surprisingly, half of the record for the 1970's.

6.6.1 Precipitation record

Examination of a five-year running mean of data from Fort Augustus (*Figure 6.10*) reveals that precipitation falls into three phases, with values prior to 1915 slightly above average, those between 1915 and 1978 generally below, while the period from 1978 to present is continually wetter. These trends are representative of those described by Smith (1995), which record the temporal variability of precipitation over Scotland in general. Analysis of data from Inverness (*Figure 6.11*) indicates quasi-periodic variations of above- and below-average precipitation of *ca* 20 year duration. Both locations, however, appear to have experienced a decline in precipitation around 1970, followed by an increase leading to a maximum around 1990.

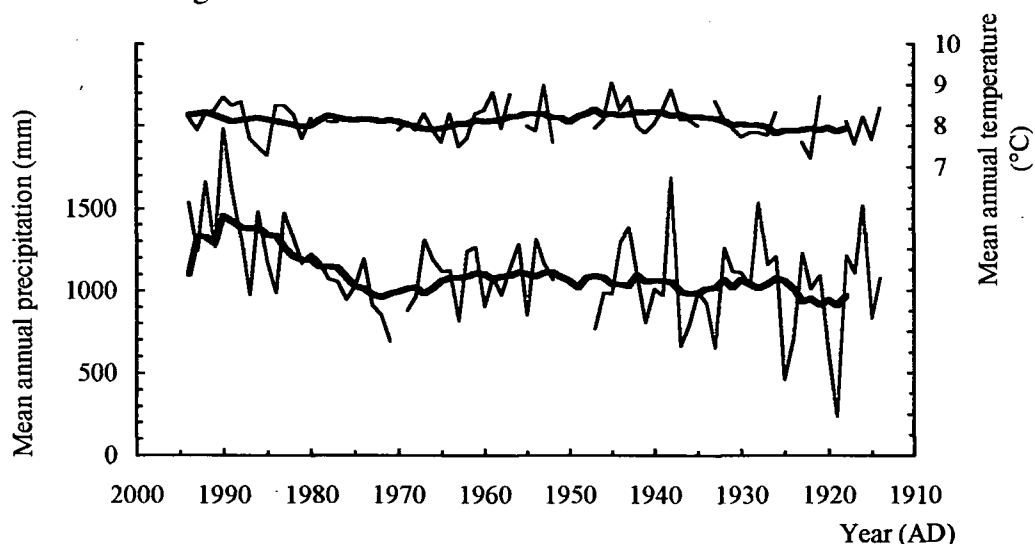


Figure 6.10 Temporal variation of precipitation and temperature, Fort Augustus 1914-1994 AD.

For Fort Augustus, significant positive correlations between winter (December, January, and February; DJF) and spring (March, April, May; MAM) data, and between summer (June, July, August; JJA) and autumn (September, October, and November; SON) precipitation data, have been calculated, (Table 6.2), although no others yield similar results. Comparison between annual and seasonal figures reveals that winter and spring precipitation are more representative of annual data than are summer and autumn. Figures for Inverness (Table 6.4) indicate a high degree of correlation between annual precipitation and that of winter, spring and autumn, the latter exhibiting the highest value of r . Summer precipitation is inversely correlated with spring.

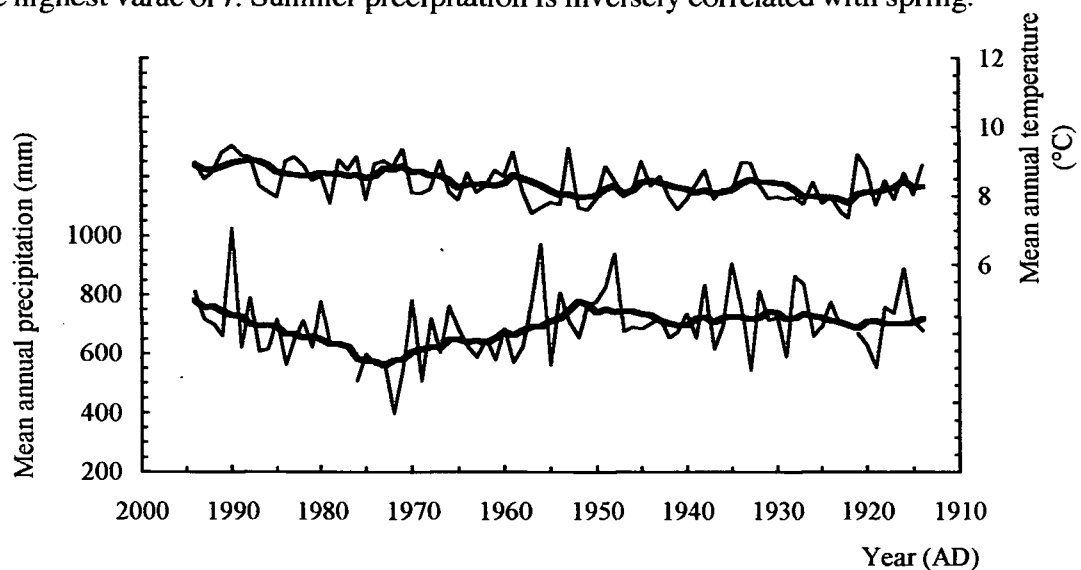


Figure 6.11 Temporal variation of precipitation and temperature, Inverness 1914-1994 AD.

Correlations have also been calculated *between* the two sets of data (Table 6.6) revealing that variations in precipitation at the two locations are strongly positively correlated when considering both annual and seasonal values. Only summer precipitation over the two sites appears not to be correlated. Annual, winter, spring and autumn figures yield very high correlations at the 1% significance level.

Comparison of data on precipitation with annual temperature for Fort Augustus for the period 1970-1994, yields a correlation coefficient, $r=0.3288$ ($v=24$,

signif. 10%). When this is extended over periods suffering from a lack of data (for example, the 1920s), the coefficients decrease but attain greater significance levels (1914-1994, $r=0.2765$, $v=81$, signif. 5%; *Table 6.3*). The highest correlation exists between spring precipitation and annual temperature (0.7355; significant at <1%). Thus, warm years appear associated with increased precipitation, and colder years with less.

Table 6.2 Correlation between annual and seasonal precipitation at Fort Augustus, 1886-1963 ($v=78$)

	<i>DJF</i>	<i>MAM</i>	<i>JJA</i>	<i>SON</i>	<i>Ann. ppt</i>
<i>DJF</i>	-				
<i>MAM</i>	0.2693*	-			
<i>JJA</i>	0.1098	0.0691	-		
<i>SON</i>	-0.0076	-0.0123	0.3230**	-	
<i>Ann. ppt</i>	0.5593**	0.5124**	0.3684**	0.4496**	-

* - significant at less than 5%

** - significant at less than 1% (2-tailed)

Analysis of unfiltered data from Inverness, 1914-1995, indicates the existence of only a weak negative correlation between average precipitation and temperature ($r=-0.1330$, not significant, $v=81$), the highest correlation being between summer temperature and annual precipitation ($r=-0.3067$, significant at 1%, $v=81$; *Table 6.5*). Hence, these data exhibit characteristics opposite to those from Fort Augustus, presumably because of the lower altitude of the site, its near-coastal location, and to possible rain shadow effects.

Table 6.3 Correlation between annual precipitation, and average and seasonal temperatures, Fort Augustus, 1914-1995 ($v=81$)

	<i>AvTemp</i>	<i>DJF</i>	<i>MAM</i>	<i>JJA</i>	<i>SON</i>	<i>AnnPpt</i>
<i>AvTemp</i>	-					
<i>DJF</i>	0.1826	-				
<i>MAM</i>	0.7355**	0.1080	-			
<i>JJA</i>	0.5402**	-0.1825	0.1247	-		
<i>SON</i>	0.3451**	-0.2045	0.0209	0.0773	-	
<i>AnnPpt</i>	0.2765*	0.2416*	0.1452	0.0472	0.0125	-

* - significant at less than 5%

** - significant at less than 1% (2-tailed)

Table 6.4 Correlation between annual and seasonal precipitation at Inverness, 1890-1963 ($v=71$)

	<i>DJF</i>	<i>MAM</i>	<i>JJA</i>	<i>SON</i>	<i>Ann. ppt.</i>
<i>DJF</i>	-				
<i>MAM</i>	0.1675	-			
<i>JJA</i>	-0.0761	-0.2486*	-		
<i>SON</i>	0.0284	-0.0087	-0.0126	-	
<i>Ann. ppt.</i>	0.3793**	0.4120**	0.1020	0.4542**	-

* - significant at less than 5%

** - significant at less than 1% (2-tailed)

Table 6.5 Correlation between annual precipitation, and average and seasonal temperatures, Inverness, 1914-1995 ($v=81$)

	<i>AvTemp</i>	<i>DJF</i>	<i>MAM</i>	<i>JJA</i>	<i>SON</i>	<i>AnnPpt</i>
<i>AvTemp</i>	-					
<i>DJF</i>	0.3369**	-				
<i>MAM</i>	0.6478**	-0.2517*	-			
<i>JJA</i>	0.5305**	0.0876	0.2458*	-		
<i>SON</i>	0.5409**	-0.2185	0.1463	0.2542*	-	
<i>AnnPpt</i>	-0.1330	0.0168	-0.1450	-0.3067**	-0.1514	-

* - significant at less than 5%

** - significant at less than 1% (2-tailed)

Table 6.6 Correlation between annual and seasonal precipitation at Inverness and Fort Augustus, 1914-1994 ($v=78$)

	<i>I'ness</i>	<i>Ann.ppt.</i>	<i>DJF</i>	<i>MAM</i>	<i>JJA</i>	<i>SON</i>
<i>Fort Augustus</i>						
<i>Ann.ppt.</i>		0.5467**	0.2065	0.2070	0.0262	0.2937*
<i>DJF</i>		0.2950*	0.7715**	0.3009*	-0.0430	-0.0866
<i>MAM</i>		0.1213	0.0200	0.5295**	-0.1873	-0.0923
<i>JJA</i>		0.3225**	-0.0440	-0.1450	0.0600	0.1089
<i>SON</i>		0.4331**	-0.0529	-0.0114	-0.0541	0.6956**

* - significant at less than 5%

** - significant at less than 1% (2-tailed)

The winter precipitation record for Fort Augustus (*Figure 6.27*) exhibits pronounced maxima during the years 1894, 1903, 1916, 1928, 1943, and 1957, yielding peaks at a frequency of 12.7 (76/6) years, which is close to the mean periodicity of the solar cycle (11.1 years; Currie 1994). Indeed, actual sunspot maxima occurred in 1893, 1905 (double maximum with 1907), 1917, 1928, 1938, and 1957 (*Source: NOAA, WDC-A*). The data for Inverness similarly yield maxima for winter precipitation for the years 1894, 1899, 1903, 1916, 1920, 1925, 1937, 1950, 1957, 1975, and 1990, most of which coincide with periods of maximum solar activity. This connection has also been reported by several other researchers, and from other locations (for example Currie, 1994; Thomas, 1993) and merits investigation into possible periodicity of forcing mechanisms prevalent at Loch Ness, which will be discussed in *Section 6.8*.

6.6.2 Comparison of precipitation with streamflow

Comparison between discharge (m^3s^{-1}) of the River Ness at UK National Grid reference NH26458425 (Highland River Purification Board, Inverness, 1995), and precipitation (mm) at Fort Augustus (*Figure 6.12*), generates a highly significant correlation coefficient at the 0.1% level (0.961, $\nu=21$).

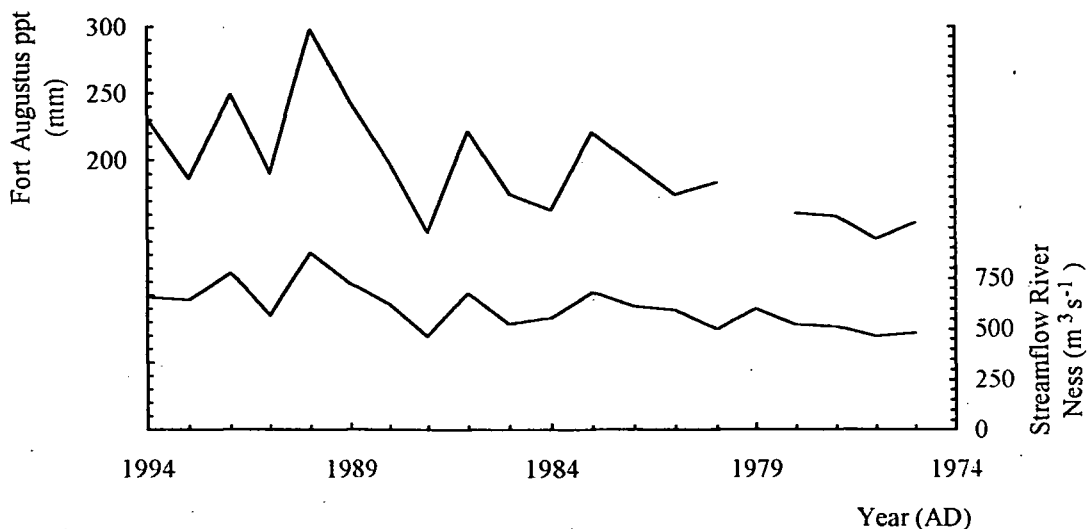


Figure 6.12 Comparison of precipitation at Fort Augustus with streamflow on the River Ness, 1974-1994

6.6.3 Occurrence of floods

Studies into the recurrence of flooding within the catchment, undertaken by the Consulting Engineers Mott McDonald (1991), reveal no trend in river flow over the period 1929-present, although many of the data for the 1960's are absent. Flooding at Inverness has, however, occurred at regular intervals over the past 200 years (Mott McDonald, 1991) including the years 1815, 1829, 1834, 1849, 1868 (two separate events: high rainfall in January, tidal flooding in February), 1892, 1920, 1977 (tidal), 1989 and 1990. Of these, only the 1868 flood is recorded in the sediments with any certainty (V.I.Jones *et al.*, 1997) and only that of 1990 is marked by an extreme in the precipitation record for Inverness (Meteorological Office, Scotland). These data may therefore indicate that precipitation records are not fully indicative of sediment influx to the loch. The hypothesis that the sedimentary record is indicative of precipitation is, however, reinforced by the observations by R.I.Jones *et al.* (1996), of amounts of seston collected by sediment traps over a year, compared with the record of monthly rainfall at Fort Augustus over the same period of time (Figure 6.13).

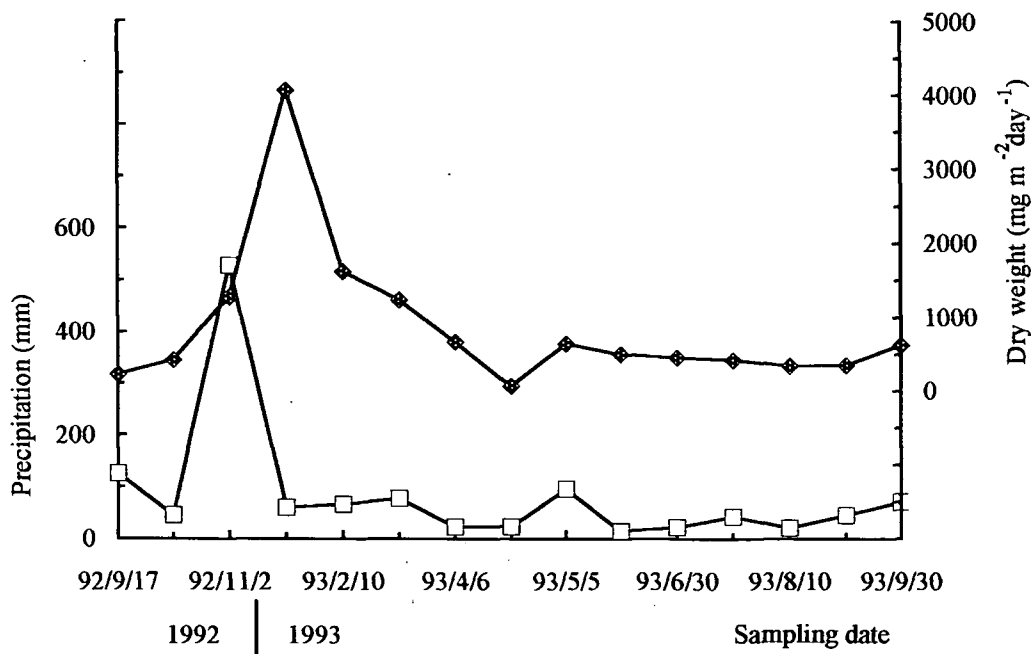


Figure 6.13 Comparison of monthly rainfall, Fort Augustus, 1992-1993, with amounts of seston collected by sediment traps (After R.I.Jones *et al.*, 1996).

6.7 The sedimentary record as a proxy of climatic variation

6.7.1 Comparison of the sediment record with precipitation

Correlation of lamination thickness of core *LNRI* with precipitation data from Fort Augustus for the period 1886-1963 reveals, however, no significant long-term relationship ($-0.158, \nu=78$). Analysis of seasonal precipitation data similarly produces little correlation (*Table 6.7*). Analysis of similar data from Inverness for the period 1890 to 1963 (*Figure 6.11*) yields a correlation of -0.0655 , not significant with $\nu=74$, with a further lack of evidence for relationships between seasonal data and lamination thickness from core *LNRI* (*Table 6.8*).

Table 6.7 Correlation of annual lamination thickness from core *LNRI* with seasonal precipitation record, Fort Augustus, 1886-1963 ($\nu=78$).

	<i>DJF</i>	<i>MAM</i>	<i>JJA</i>	<i>SON</i>	<i>Ann. ppt.</i>
<i>LNRI</i>	-0.0640	-0.1168	-0.1680	-0.1125	-0.1576

* - significant at less than 5% ** - significant at less than 1%

Errors in the dating of this core may explain the lack of correlation between precipitation and lamination thickness. This may be especially relevant owing to the lack of prominent marker, or other easily datable, horizons within this core. As will be noted later, however, other climatic indices *do* yield significant correlations with the sedimentary record, thus indicating that the chronology may be substantially correct.

Table 6.8 Correlation of annual lamination thickness from core *LNRI* with seasonal precipitation record, Inverness, 1890-1963 ($v=74$).

	<i>DJF</i>	<i>MAM</i>	<i>JJA</i>	<i>SON</i>	<i>Ann. ppt.</i>
<i>LNRI</i>	-0.0260	-0.1079	-0.0224	-0.0128	-0.0655

* - significant at less than 5% ** - significant at less than 1%

6.7.2 Comparison of the sediment record with temperature

Data on mean annual temperature for Fort Augustus (Meteorological Office, Scotland), for the period 1914-1995, are displayed in *Figure 6.10*. As with the precipitation record, gaps in the data are apparent. Correlation with the lamination thickness record from core *LNRI*, over the period 1914-1963, yields a coefficient of 0.180 ($v=47$, not significant)

Comparison between the sediment record from core *LNRI*, and mean annual temperature for Inverness, (*Figure 6.11*), over the period 1914 to 1963, produces little correlation ($r=0.0638$, $v=51$, not significant). When carried out on a seasonal basis, however, the relationship is slightly stronger for winter ($r=-0.2192$, not significant), and summer ($r=0.228$, not significant), than for spring and autumn.

6.7.3 The sediment record as a climatic proxy

It would appear, therefore, lamination thickness in core *LNRI* directly reflects neither precipitation, as recorded at Fort Augustus and Inverness, or temperature. Other studies, notably those by Dean *et al.* (1994; Elk Lake, Minnesota), Desloges (1994; Ape,

Berg & Nostetuko Lakes, Canada), Hardy *et al.* (1996; Taconite Inlet Lakes, Canada), Itkonen & Salonen (1994; Lakes Pääjärvi, Paijanne, and Pyhäjärvi, Finland), Leeman & Niessen (1994; Oeschinensee, Switzerland), Leonard (1986; Hector Lake, Canada), Perkins & Sims (1983; Skilak Lake, Alaska), and Renberg *et al.* (1984; Judesjön, N. Sweden) have revealed connections between sedimentary and climatic variables (especially precipitation and temperature), although many of these sites are situated within mountainous regions or at high latitude, with consequent importance of glacial processes, ice cover, snowmelt and ice ablation. Others contain sediments high in authigenic organic content, variations in which are related to changes in insolation.

Several studies (for example, Perkins & Sims, 1983) note that multiple effects often need to be invoked in order to account for variation in lamination thickness. This observation suggests that the signal within the lamination record from the loch may not represent one single environmental variable, but the sum of several, including perhaps, precipitation, temperature, and location of storm tracks across, and origin of input of eroded material from, the catchment. These factors will achieve paramount importance where catchment or lake, or both, are spatially extensive and sediment recovery is limited. An analogy may be drawn with the study by Liu & Fearn (1993), of evidence of hurricane strikes recorded in the sediments of the coastal Lake Shelby, Alabama. Here, they conclude that lithologically distinct deposits represent only those extreme events which had passed within *ca* 50 km of the coring site.

It is not possible, from the meteorological data obtained, to distinguish between periods of intense, but brief, rainfall, which may lead to influx of large amounts of material, and those months which experience prolonged, but relatively light precipitation. In addition, in view of the contrasting topographic locations of the weather recording sites, the role of wind direction may need to be more closely considered. South-westerly airstreams (maritime, warm and wet) may predominate in the precipitation record at Fort Augustus, which may further enjoy orographic effects from the surrounding

elevated moorlands. Inverness, however, situated in a more open, coastal location, may equally be more strongly influenced by polar maritime (cold and wet) and continental (warm *and* cold, but drier) airflows. Furthermore, comparisons between climatic and sediment records are limited to that period of time where anthropogenic effects may have affected the discharge characteristics of the catchment. These effects may not be generally significant, however, owing to the relatively small area of cultivated land existing in the catchment (Mott McDonald, 1991).

In spite of these caveats there remains the indication, especially from the study by R.I. Jones *et al.* (1996), that the amount of material recovered from sediment traps in the water column of the loch *is* dependent on seasonal variation in rainfall and streamflow. It is thus believed that lamination thickness may still be considered a proxy for climate over the Loch Ness catchment, although the connection would appear to be more complex than those applicable to some other sites.

6.8 Correlation with other time series

Time series compiled from data collected from one site, represent the response of that site to palaeoenvironmental variations. Comparison of these with similar series collected from other sites, enables an overview of change over a wide area to be synthesised (Goslar *et al.*, 1993). In addition, other well-established time series may be utilised for the purposes of comparison, in order that consistent temporal assignment of environmental events within a region (for example, Goslar *et al.*, 1995) may be carried out. Again, the differences between proxy records from comparatively recent times and the signal derived from Loch Ness sediments may be due to an increasing anthropogenic influence upon its catchment, which may have acted to decrease its sensitivity to climatic variations, possibly to the exclusion of all but the most severe, or most local, events.

6.8.1 Other proxy palaeoclimate records

The record of lamination thickness in the sediments of Loch Ness may also be compared with other proxy climatic time series from regions influenced by the North Atlantic Ocean. Of particular interest are those derived from measurements of the persistence of sea ice in North Atlantic waters, the location of the NAPF, the phase of the NAO, and dendrochronological and stable isotope studies.

6.8.1.1 Sea ice, sea surface temperature (SST), NAO, and other climatic indices

The persistence of sea ice in northern waters is an indication of sea surface temperature and location of the NAPF (Lowe, 1993). Two time series, from the coast of Iceland, and from the Danish Sound, have been considered (Lamb, 1977a). Correlations between these and the sedimentary record for core *LNRI* have been calculated. In addition, these indices have been further compared with North Atlantic SST data (Lamb, 1987), in order to ascertain whether or not there may be a link between all three. The results are presented in *Table 6.9* and the relevant data plotted in *Figures 6.14* to *6.16*.

When 5-year moving averages are considered, strong correlations between the sedimentary record of core *LNRI*, the number of ice days observed from the coast of Iceland (*Figure 6.14*; 0.5234, significant at <1%), and the Danish Sound (*Figure 6.15*; 0.5853, significant at < 1%), are observed. These results would seem to indicate that there exists a strong influence by the NAPF on deposition within the loch, presumably by varying the path of weather systems across the North Atlantic Ocean, and hence Northern Scotland (Taylor & Yates, 1967). No such correlation exists between the sediment record and NA SST, however, which may indicate that the area of ocean over which temperatures were measured (the Southwestern Approaches; 45-50°N, 5-10°W; Lamb, 1977a) remained substantially unaffected by movements of the NAPF, and thus inappropriate for this type of analysis.

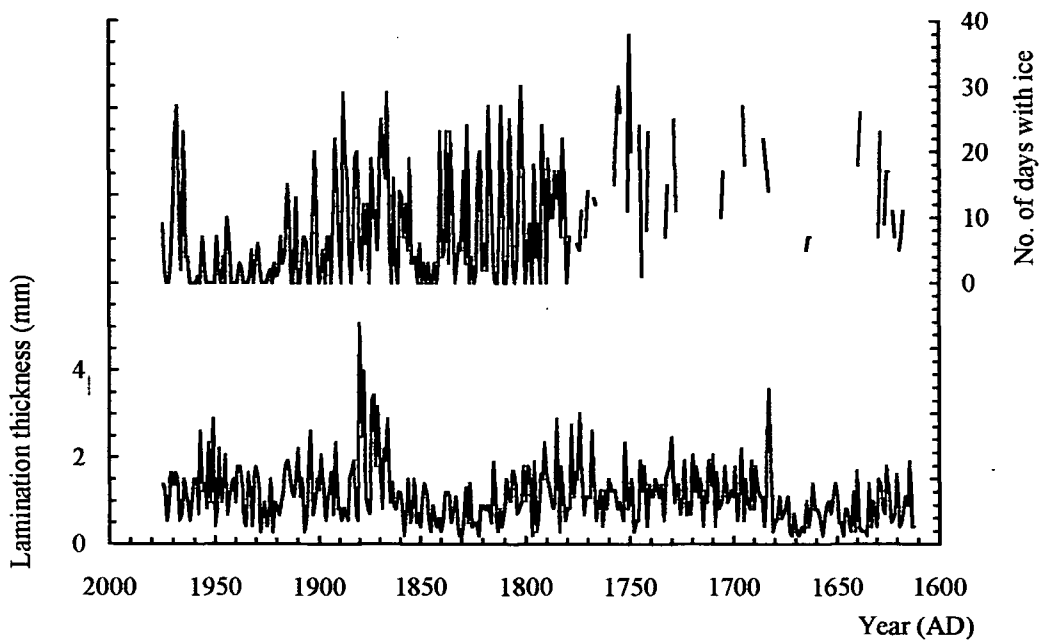


Figure 6.14 Annual lamination thickness in core *LNRI*, compared with the number of days sea ice was observed off the coast of Iceland over the period 1610 to 1963.

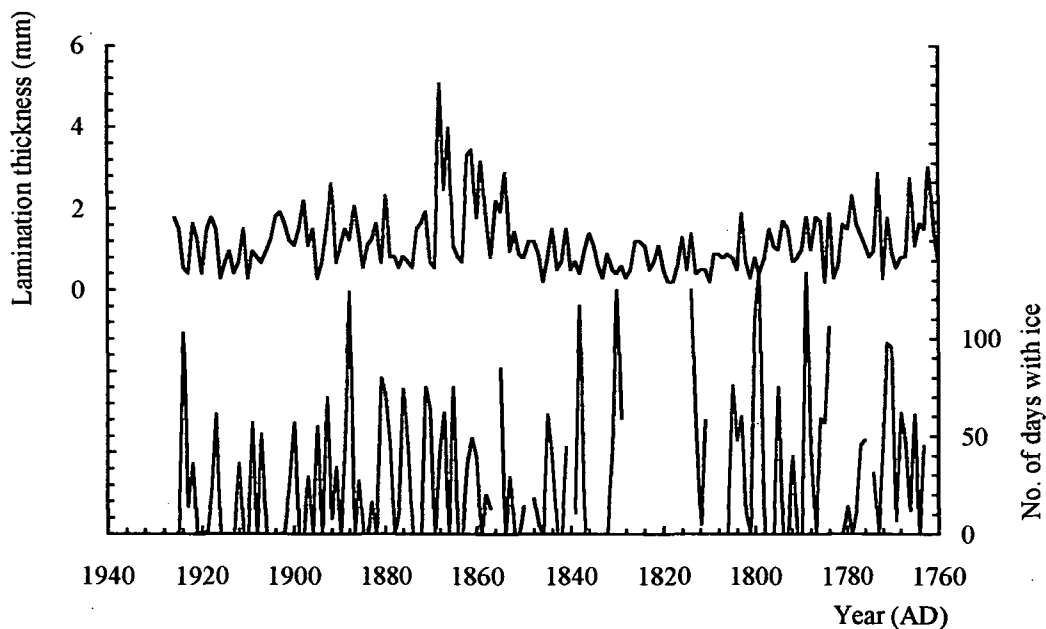


Figure 6.15 Annual lamination thickness from core *LNRI* compared with the number of days when sea ice was observed in the Danish Sound, over the period 1764 to 1930.

Table 6.9 Correlation between lamination thickness from core *LNRI*, North Atlantic sea surface temperature, and the persistence of sea ice around the coast of Iceland and in the Danish Sea.

	<i>DIce</i>	<i>DIce5</i>	<i>NA_SST</i>	<i>LNRI</i>	<i>L1_Av5</i>	<i>IIce</i>	<i>IIce5</i>
<i>DIce</i>	-	0.3960**	-0.0207	0.0374	0.0888	0.0470	0.3202**
<i>DIce5</i>	-	-	0.0808	0.1111	0.3078*	0.4518**	0.5853**
<i>NA_SST</i>	-	-	-	0.1543	0.0641	0.1169	0.1246
<i>LNRI</i>	-	-	-	-	0.6097**	0.2835*	0.3419**
<i>L1_Av5</i>	-	-	-	-	-	0.3643**	0.5234**
<i>IIcece</i>	-	-	-	-	-	-	0.5321**
<i>IIce5</i>	-	-	-	-	-	-	-

* - significant at less than 5%

** - significant at less than 1%

DIce:- number of days with ice in the Danish Sound. *DIce5*:- 5-yearly averages.

NA_SST:- average North Atlantic Sea Surface Temperature over the area 45-50°N, 5-10°W.

LNRI:-lamination thickness from core *LNRI*. *L1_Av5*:- 5-yearly averages.

IIce:- number of days with ice off the coast of Iceland. *IIce5*:- 5-yearly averages

Comparison of the same sedimentary record with data on the annual index of the North Atlantic Oscillation (NAO) index, representing the period 1890 to 1963, has been carried out (*Figure 6.17*). Positive values of NAO index are indicative of periods when the atmospheric low pressure system over Iceland deepens, which acts to induce a northward movement in the path of moisture-rich westerly airstreams over the Atlantic Ocean (Moulin *et al.*, 1997).

Comparison of both sets of data reveals that both are close to average except during the interval 1902 to 1929, when lamination thickness declined from *ca* 1.3 mm to *ca* 0.5 mm while NAO index generally changed from negative to positive, except for a

brief return to negative values around 1917. More striking comparisons may be observed when seasonal NAO data are considered. *Table 6.10* illustrates that significant correlations are generated when comparing decadal-averaged seasonal NAO data with the lamination thickness record from core *LNRI*. *Figures 6.18* and *6.19* compare lamination thickness from core *LNRI*, with those three-monthly NAO indices which yielded the largest coefficients of correlation, as displayed in *Table 6.10*.

Table 6.10 Results of correlation analysis between three-monthly-resolved NAO index and lamination thickness from core *LNRI* (decadal averages).

	<i>LNRI</i>
<i>DJF</i>	-0.2874**
<i>JFM</i>	-0.3616**
<i>FMA</i>	-0.3253**
<i>MAM</i>	-0.3386**
<i>AMJ</i>	-0.0506
<i>MJJ</i>	0.3160**
<i>JJA</i>	0.5229**
<i>JAS</i>	0.3125**
<i>ASO</i>	0.1270
<i>SON</i>	0.0597
<i>OND</i>	0.0247

*indicates significance at 5% level, ** significant at 1% level (two-tailed)

Significant negative correlations may be observed with NAO indices averaged over winter months, especially January, February and March, and positive correlations for summer indices, especially June, June and August. Further analysis of correlations between NAO index and precipitation at Fort Augustus and Inverness yielded the results displayed in *Tables 6.11* and *6.12*.

Table 6.11 Correlation between monthly NAO index (N), and precipitation data for Fort Augustus (F), 1890 to 1993 ($n=103$).

	<i>NJan</i>	<i>NFeb</i>	<i>NMar</i>	<i>NApr</i>	<i>NMay</i>	<i>NJun</i>
<i>FJan</i>	0.7364**	0.2486*	0.1395	0.1791	-0.2147*	-0.1044
<i>FFeb</i>	0.1690	0.7099**	0.2317*	0.1582	-0.1091	-0.0476
<i>FMar</i>	0.1516	0.2063*	0.7041**	0.0886	0.0375	0.1096
<i>FApr</i>	0.0037	-0.1061	-0.0621	0.4509**	0.0053	0.0187
<i>FMay</i>	0.0537	0.1087	-0.0069	-0.0443	0.2305*	0.0403
<i>FJun</i>	-0.0293	0.0181	0.1016	0.1878	-0.1037	0.2207*
<i>FJul</i>	-0.1045	-0.1035	-0.1517	-0.0902	-0.1591	-0.0720
<i>FAug</i>	0.0554	0.0615	0.0507	-0.0163	-0.0780	-0.1203
<i>FSep</i>	-0.0389	-0.1170	-0.1266	-0.0643	-0.1416	-0.1858
<i>FOct</i>	0.0961	-0.0063	-0.0501	-0.1286	-0.1443	-0.0778
<i>FNov</i>	-0.1170	0.0035	0.1542	-0.1985	0.0910	0.1848
<i>FDec</i>	-0.0635	-0.1357	0.0775	0.1068	0.0504	-0.0383
	<i>NJul</i>	<i>NAug</i>	<i>NSep</i>	<i>NOct</i>	<i>NNov</i>	<i>NDec</i>
<i>FJan</i>	0.0365	0.0805	-0.1196	0.1186	0.0651	-0.0142
<i>FFeb</i>	-0.0079	0.1302	-0.1377	-0.0577	0.0578	-0.0539
<i>FMar</i>	-0.0479	0.0732	-0.1220	-0.0639	0.1297	0.0032
<i>FApr</i>	-0.0198	-0.2387*	0.0558	-0.0514	-0.0540	-0.1005
<i>FMay</i>	0.0445	-0.0811	-0.0214	0.0876	0.1560	0.0161
<i>FJun</i>	-0.0965	-0.0755	0.0938	-0.0305	0.0415	0.0562
<i>FJul</i>	0.1198	0.0646	0.0269	-0.0264	0.0190	0.0720
<i>FAug</i>	-0.0262	0.0710	0.0688	0.0022	0.0366	0.1381
<i>FSep</i>	-0.0221	0.1873	0.4576**	0.0610	-0.1216	-0.0873
<i>FOct</i>	0.0846	0.1161	0.0845	0.5036**	0.0022	-0.0624
<i>FNov</i>	0.0706	-0.0993	-0.0086	0.1354	0.5207**	0.1189
<i>FDec</i>	-0.0145	-0.0953	-0.0512	0.0381	0.0205	0.5427**

*indicates significance at 5% level, ** significant at 1% level (two-tailed)

Table 6.12 Correlation between monthly NAO index (N), and precipitation data for Inverness (I), 1890 to 1993 ($\nu=103$).

	<i>NJan</i>	<i>NFeb</i>	<i>NMar</i>	<i>NApr</i>	<i>NMay</i>	<i>NJun</i>
<i>IJan</i>	0.5652**	0.1557	0.1134	0.1422	-0.2199*	-0.1527
<i>IFeb</i>	0.2391*	0.4728**	0.0788	0.1617	-0.1241	-0.0384
<i>IMar</i>	0.1896	0.1875	0.4688**	0.1137	-0.0354	-0.0261
<i>IApr</i>	0.0056	-0.0089	-0.0517	0.0649	-0.1198	-0.0634
<i>IMay</i>	0.0578	0.0212	-0.1290	0.0240	-0.1340	-0.0873
<i>IJun</i>	-0.1333	-0.0944	0.1126	0.1338	-0.0397	-0.0050
<i>IJul</i>	-0.1070	-0.0565	-0.1827	-0.2131*	0.0178	-0.0867
<i>IAug</i>	-0.0574	-0.0021	-0.0083	-0.0087	0.0103	-0.0312
<i>ISep</i>	0.0816	-0.0898	-0.1581	0.0750	-0.1222	-0.0638
<i>IOct</i>	0.0378	-0.0038	0.0405	-0.2097*	-0.1794	0.0032
<i>INov</i>	-0.1011	0.0349	-0.0455	-0.0153	0.0701	0.0875
<i>IDec</i>	-0.0208	-0.1159	-0.0745	0.0489	-0.0353	-0.1376
	<i>NJul</i>	<i>NAug</i>	<i>NSep</i>	<i>NOct</i>	<i>NNov</i>	<i>NDec</i>
<i>IJan</i>	0.0559	0.0051	-0.0853	-0.0024	0.0788	0.0141
<i>IFeb</i>	0.0387	0.0339	-0.0856	-0.0595	-0.0799	-0.1857
<i>IMar</i>	-0.0179	0.0489	-0.1721	-0.0902	0.0245	-0.0622
<i>IApr</i>	0.1161	-0.1371	0.1090	0.0250	-0.1378	-0.1408
<i>IMay</i>	0.0657	-0.0470	-0.0673	0.0296	0.0400	-0.0609
<i>IJun</i>	-0.0770	-0.1590	-0.0601	-0.0606	0.0317	0.0689
<i>IJul</i>	-0.0554	0.0104	-0.0244	-0.0247	0.0231	0.0771
<i>IAug</i>	0.0156	-0.1224	0.1314	0.0118	0.0420	0.1637
<i>ISep</i>	0.0290	0.0539	0.1541	0.0576	-0.1538	-0.1165
<i>IOct</i>	0.1916	0.1258	0.0881	0.1731	0.0699	-0.1278
<i>INov</i>	-0.0563	-0.0863	0.1578	0.1397	0.1588	0.1221
<i>IDec</i>	-0.0783	-0.0488	-0.0987	0.0225	0.0196	0.3745**

*indicates significance at 5% level, ** significant at 1% level (two-tailed)

Correlations between monthly NAO index and precipitation at Fort Augustus are positive and mostly highly significant (at the 1% level). They range from *ca* 0.45 in April and September, to *ca* 0.73 in January. Data for the summer months (May to August) are not as significant. Positive correlations are recorded between NAO index and Inverness precipitation data from December to March (*ca* 0.4 to 0.6, significant at 1%). Analysis of the remaining months yields both positive and negative, but non-significant, results.

In addition, there exist striking similarities between annual lamination thickness in core *LNRI* and the NAO (*Figure 6.19*), when the index for the quarter-year June to August is plotted. It would thus appear that lamination thickness may be influenced by the occurrence of westerly airflows, originating from the North Atlantic Ocean, but that these are negatively correlated in winter and positive in summer. Hence, the occurrence of wet summers may be a significant factor in the formation of laminae.

The recent sedimentary record was also compared qualitatively with winter severity indices for Paris and London (Lamb, 1977a). There, it is noted that warm conditions existed during the late 15th century and that many winters during the 16th and 17th centuries were cold. An amelioration occurred around AD 1700 which has persisted to the present, although with a brief return to more severe conditions around AD 1800. This record is similar to that of core *LNRI*, in that thick laminae occur throughout most of the 15th century (especially in the latter half), and again after *ca* AD 1660. Prolonged periods, during which thinner laminations were deposited, took place from *ca* AD 1520 to AD 1660, and around AD 1800. Studies of glacier movements throughout Iceland also indicate warmer conditions during the 18th century, followed by a readvance in the early 1800s (Lamb, 1977a).

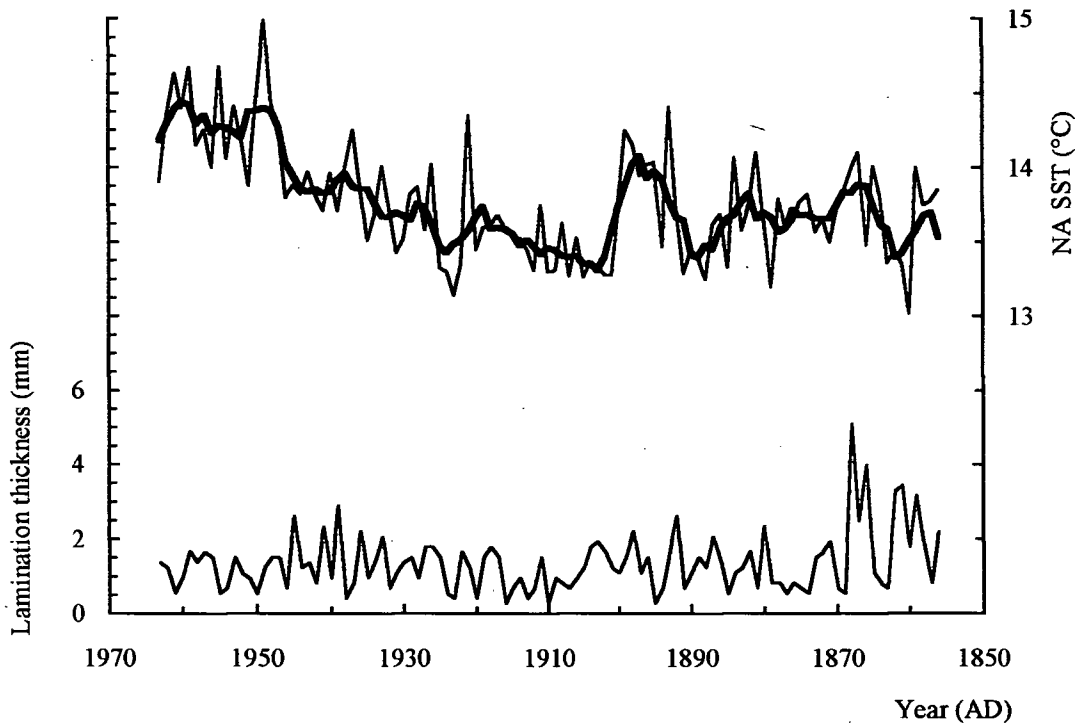


Figure 6.16 Annual lamination thickness from core *LNR1* compared with North Atlantic Sea Surface Temperature (NA SST), over the period 1864 to 1963.

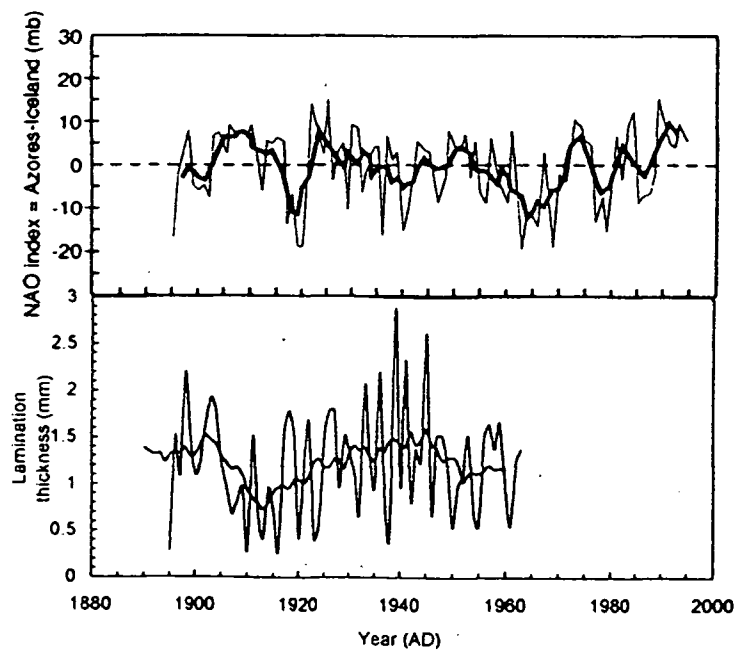


Figure 6.17 Comparison of the North Atlantic Oscillation index (*top*, after Mann & Lazier, 1996) with lamination thickness from core *LNR1* (*bottom*), over the period 1890 to 1963.

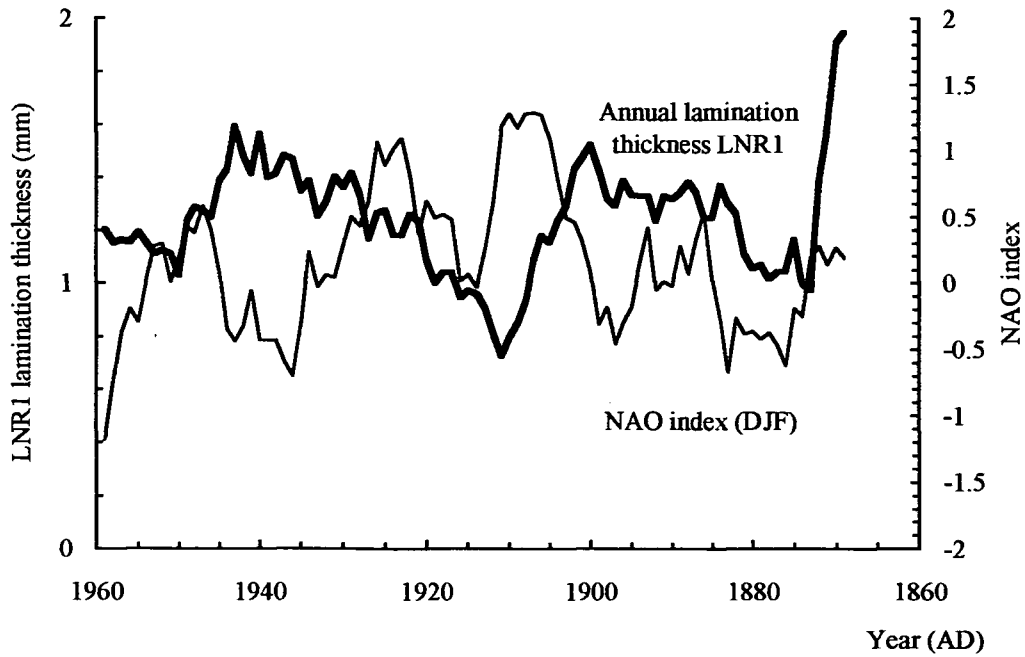


Figure 6.18 Comparison of annual lamination thickness from core *LNR1* with winter (DJF) NAO index (decadal averages).

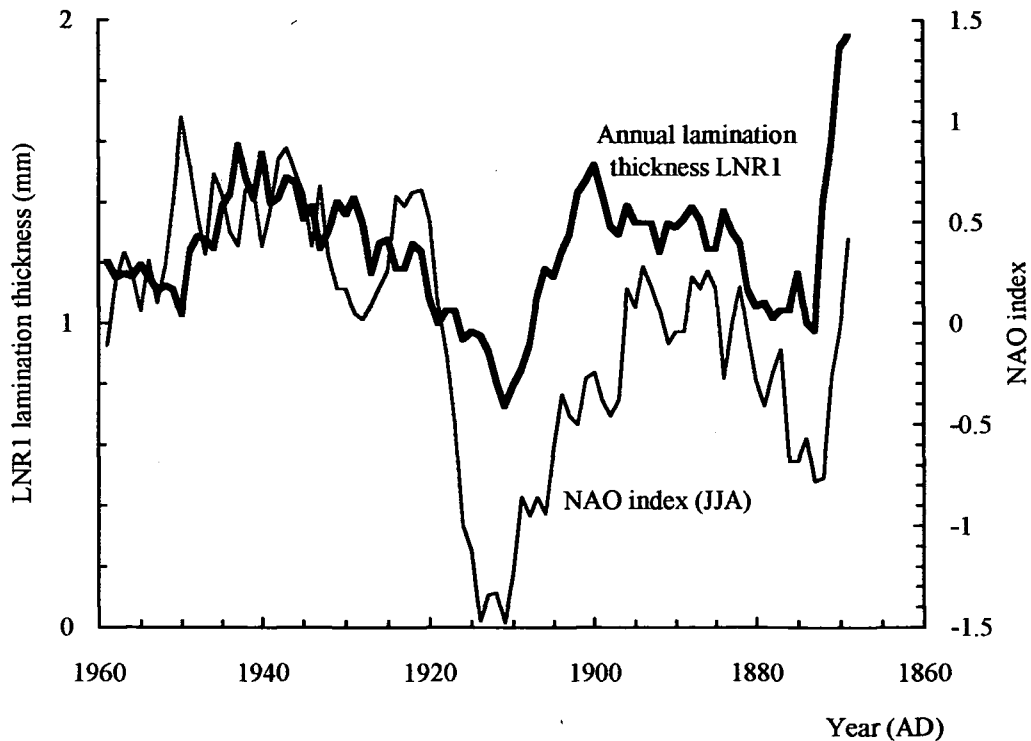


Figure 6.19 Comparison of annual lamination thickness from core *LNR1* with summer (JJA) NAO index (decadal averages).

6.8.1.2 Dendrochronological studies

Several chronologies based upon tree ring records have been considered for comparison with time series derived from measurements on Loch Ness sediments. Series are derived from studies of one site, in addition to averaged data representing entire regions. Professor M.G.L. Baillie, of the Queen's University Belfast, has kindly provided three regional chronologies, representative of Ireland, Scotland, and the English Midlands, for comparison with the record from core *LNR1* (Figure 6.20).

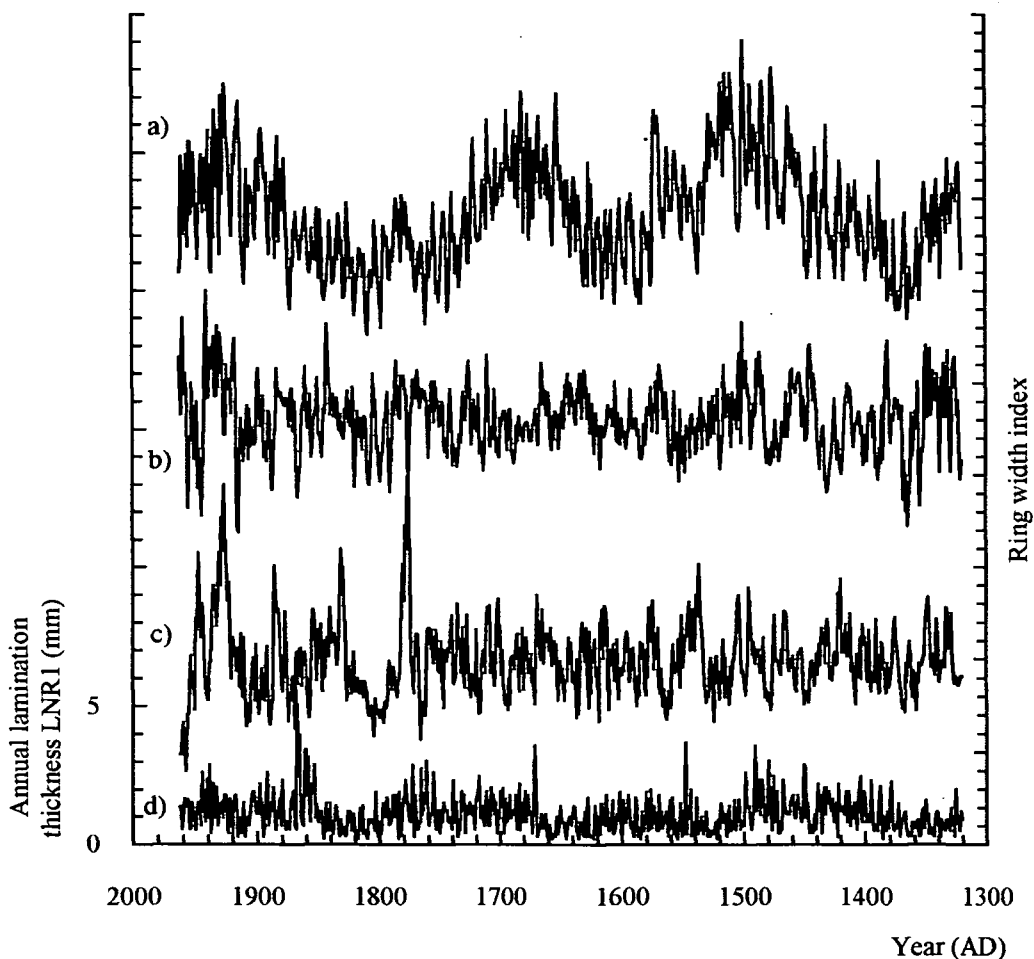


Figure 6.20 Regional tree ring records, AD 1300-1963. a) the English Midlands, b) Scotland, and c) Ireland. (After Baillie; *pers comm*, 1977a, 1977b), compared with lamination thickness from core *LNR1* (d). All dendrochronological series are plotted to the same scale, but offset for clarity.

Visually, the three tree ring series have little in common with each other, although statistically all correlations between them are positive and significant at less than the 1% level (*Table 6.13*). Each exhibits a brief increase in ring width value just prior to 1800, and marked decreases during the late 14th century, and around 1820. Correlation with data from core *LNR1* is also included in *Table 6.13*, and indicates that comparison with the English Midland time series yields a coefficient significant at less than the 1% level.

Table 6.13 Correlation between tree ring data from Ireland, the English Midlands, Scotland and lamination thickness from core *LNR1*.

	<i>Bel</i>	<i>Bel11</i>	<i>Mid</i>	<i>Mid11</i>	<i>Sco</i>	<i>Sco11</i>	<i>LNR1</i>	<i>LNR11</i>
<i>Bel</i>	-	0.7308**	0.1024**	0.1147**	0.0252	0.1719**	0.0134	0.0594
<i>Bel11</i>	-	-	0.1266**	0.1543**	0.1453**	0.2788**	0.0541	0.0682
<i>Mid</i>	-	-	-	0.7678**	0.1095**	0.1803**	0.1025**	0.1321**
<i>Mid11</i>	-	-	-	-	0.1300**	0.2265**	0.0848*	0.1726**
<i>Sco</i>	-	-	-	-	-	0.6082**	-0.0100	0.0032
<i>Sco11</i>	-	-	-	-	-	-	0.0131	0.0534
<i>LNR1</i>	-	-	-	-	-	-	-	0.4934**
<i>LNR11</i>	-	-	-	-	-	-	-	-

*indicates significance at 5% level, ** significant at 1% level (two-tailed).

Bel- Belfast chronology

Bel11- Belfast chronology, 11-year running mean

Mid- English Midlands chronology

Mid11- English Midlands chronology, 11-year running mean

Sco - Scottish chronology

Sco11- Scottish chronology, 11-year running mean

LNR1- Sediment record, core *LNR1*

LNR11- Sediment record, core *LNR1*, 11-year running mean

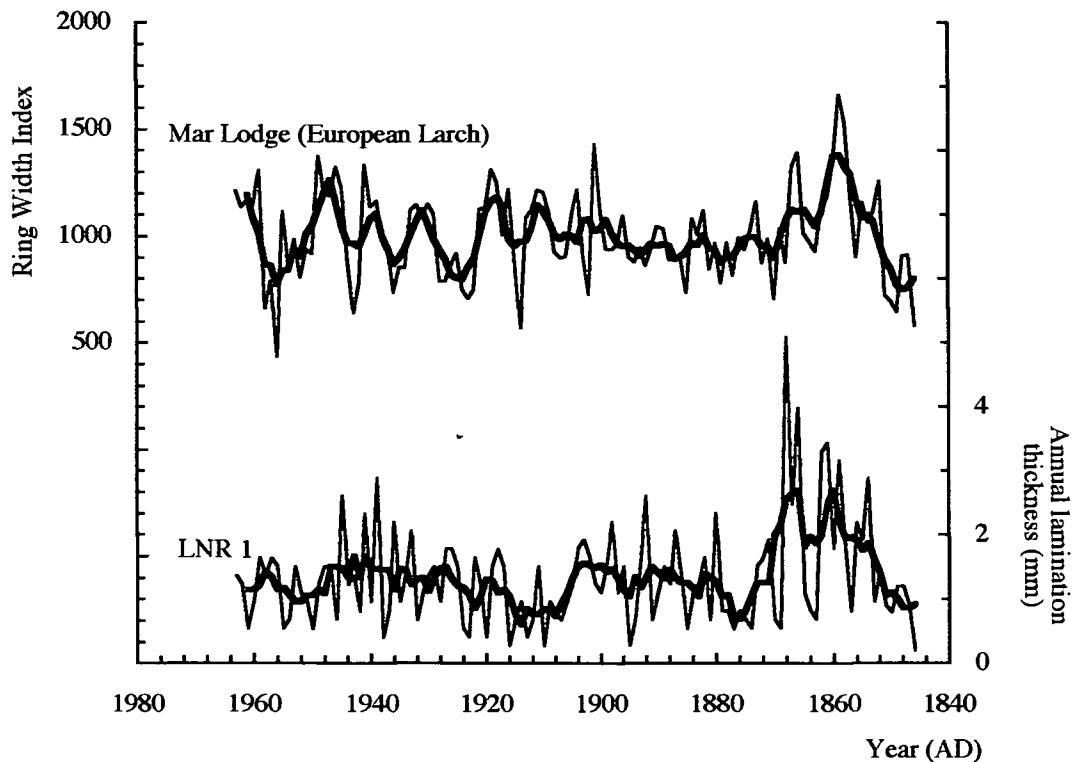


Figure 6.21 Record of normalised ring widths from European Larch (*Larix decidua* Miller) located at Mar Lodge, Highlands (Analyst F.Schweingruber. Source NOAA, WDC-A), compared with annual lamination thickness from core LNR1.

Figure 6.21 (top) illustrates a time series derived from analysis of ring widths of European Larch (*Larix decidua* Miller; analyst F.Schweingruber; source NOAA, WDC-A) growing at Mar Lodge, Deeside, Scottish Highlands (latitude 57° N, longitude $3^{\circ} 30'$ W), some 85 km SE of Loch Ness. This sequence spans *ca* 140 years, and may be compared with annual lamination thickness in core LNR1 (*Figure 6.21, bottom*). Some similarities may be observed, especially around the period of the intense 1868 flood in the Loch Ness catchment, when both series exhibit large variations from the mean (core LNR1: *ca* + 4 sd; dendro: *ca* + 2 sd). Overall, a correlation of 0.2676 is exhibited between these curves, rising to 0.477 when smoothed by a 5-yr moving window. For 115 data points the value for the raw data is significant at less than 1%, while that for

smoothed data is significant at the 0.1% level.

Data from dendrochronological studies carried out within continental Europe may also be compared with lamination thickness sequences in order to explore the spatial extent of climatic influence. Schweingruber (1988) highlights the existence of significant correlations between tree ring series derived from a wide area of West, Central and Southern Europe (Figure 6.22). Figure 6.23 plots a German Oak (*Quercus petraea* L.) chronology developed by Huber & Giertz-Siebenlist (Lamb, 1977a), originating from the Spessart Forest area of Central Germany (latitude $50^{\circ} 10' N$, longitude $9^{\circ} 20' E$) and lamination thickness in core *LNR1*. Correlation coefficients for the entire sequence are low (0.0325 for raw data; -0.0008 for 11-yr averages; -0.0075 for 22-yr averages), although extremes, such as those prevalent during part of the Little Ice Age (the 17th Century; Lamb, 1977a), but admittedly of different duration, are well represented in both. Of note is the period of both increased sedimentation *and* ringwidth after AD 1650, and by the decrease in both signals during the early 19th Century. From then to recent times the records diverge substantially, with the extreme events in core *LNR1* for the late AD 1860s not replicated in the tree-ring data.

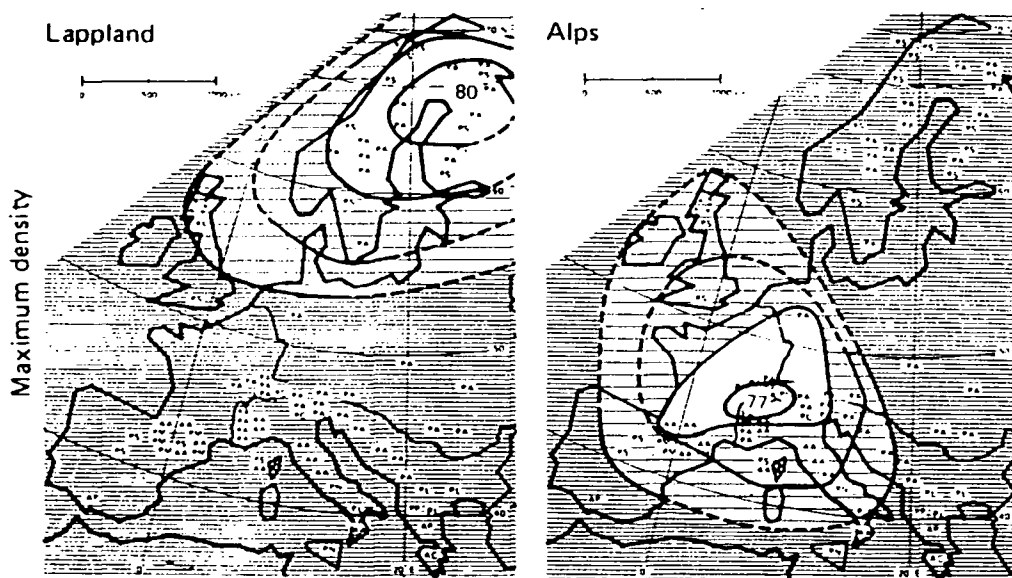


Figure 6.22 Spatial extent of correlation between dendrological datasets in Europe.

(After Schweingruber, 1988).

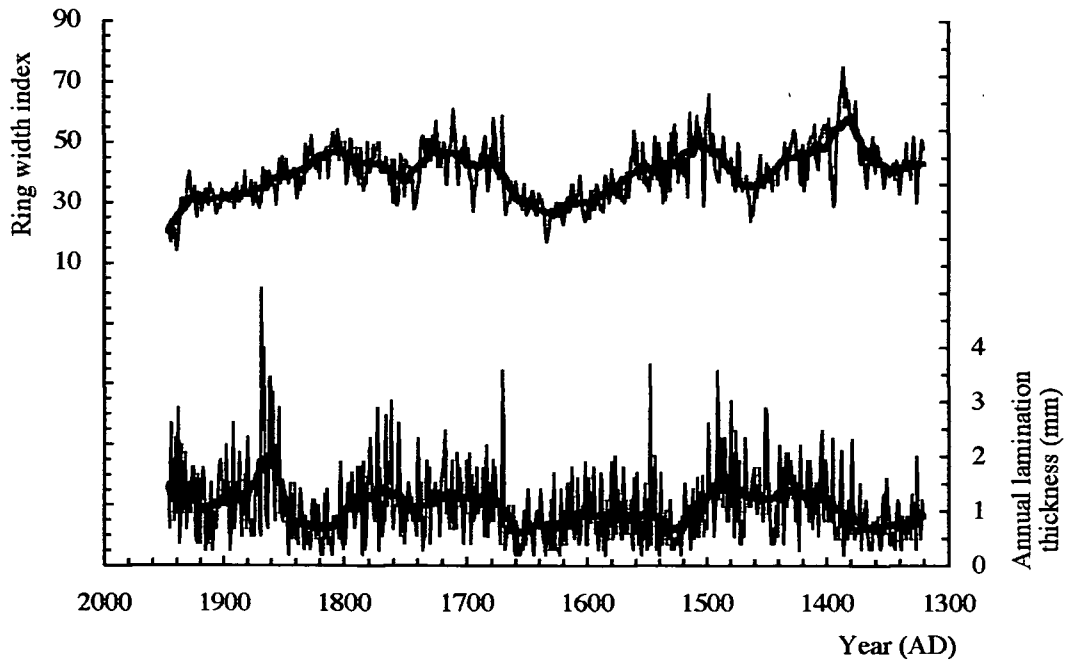


Figure 6.23 Tree-ring chronology, 1945 AD to 1320 AD, derived from German Oak (*Quercus petraea* L.) growing in the Spessart Forest, Germany (After Huber & Giertz-Siebenlist (Lamb, 1977a), upper), compared with annual lamination thickness from core LNRI (lower).

Many other studies have utilised tree-ring records in order to determine indications of palaeoclimate over the North Atlantic region. Two will be briefly mentioned here, and their results compared to the record from Loch Ness.

Briffa *et al.* (1990b) have employed both ring-width and latewood density of living and fossil Scots pine (*Pinus sylvestris* L.) sampled within the Torneträsk region of Sweden in order to reconstruct summer temperatures in Fennoscandia over the past 1400 years. Events such as the Medieval Warm Period and Little Ice Age do not figure prominently in their interpretation, and they conclude that these episodes were not as pronounced in that region, as reported from the rest of Europe. Their record suggests that the LIA lasted only from *ca* AD 1570 to AD 1650 and that the MWP was confined only to the latter half of the twelfth century. The record of lamination thickness from core LNRI

exhibits low values from *ca* AD 1510 until AD 1650, which may correspond to an LIA signal on the basis of warm-wet/cold-dry climatic model. In addition, they note that “the proxy evidence for spatially coherent century-timescale climate fluctuations around the North Atlantic basin is relatively weak” (p 439).

Over a timescale comparable to that spanned by the long sediment cores from Loch Ness, Bridge *et al.* (1990) examined the abundance of fossil Scots pine in peat hags. They identified a number of reductions in abundance of trees around 5700-5250 a BP, 3800-3500 a BP, and post-3250 a BP, which they attribute to deteriorating climate, in that pine was probably more prolific during warm, dry conditions, and peat accumulation increased at times of cold, wet weather. Their selection of these three periods seems arbitrary, however, since their data also exhibit similar dearths of trees around 6.3 and 4.8 ka BP. The record from core *Ness 3* displays an increase in lamination thickness around *ca* 6200, 4800, and 3500 a BP, but not during the other periods mentioned.

6.8.1.3 Stable isotope record

Analysis of variations in isotopic composition of water contained in ice cores has been shown to provide a proxy for temperature at the time of deposition (Dansgaard *et al.*, 1984). Studies of $\delta^{18}\text{O}$ in material recovered from the Greenland Ice Sheet, especially by the GRIP team, have furnished data which enable the construction of a proxy temperature record for the past 200,000 years. Examination of the record from 10 ka BP to the present may indicate, amongst other processes, variations in location of the North Atlantic Polar Front, and also storm tracks across the Atlantic Ocean.

Figure 6.24 illustrates a comparison between lamination thickness in long core *Ness 3*, and the $\delta^{18}\text{O}$ isotope record from the GRIP core (*source: NOAA, WDC-A*). Owing to the fragmented nature of the lamination thickness data, it is difficult to compare the curves fully, although weak maxima in both series occur at *ca* 7600, 5200, and 2700

BP, and minima at around 7100 and 5000 BP. In addition, however, deviations of opposite sign may be noted in both signals around 8700 BP. The correlation coefficient between the oldest and longest continuous section of the lamination thickness curve (*ca* 6300 to 9000 BP), and the comparable section of the GRIP curve is -0.237, hardly significant at any level with $\nu=14$. Comparison of lamination thickness in core *LNRI*, and variations in $\delta^{18}\text{O}$ from Camp Century, Greenland (*Figure 6.25*), reveals contemporaneous low values in both records during the periods *ca* AD 1500, AD 1580 to AD 1660, and *ca* AD 1830 (Johnsen *et al.*, 1970; Moseley-Thompson, 1993).

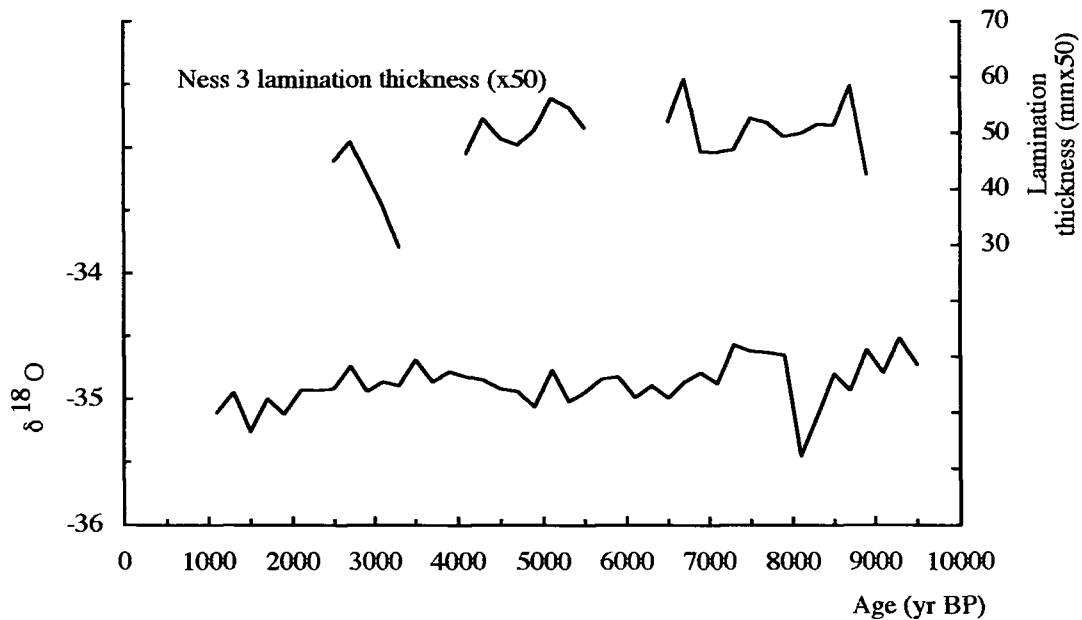


Figure 6.24 GRIP $\delta^{18}\text{O}$ record compared with lamination thickness data from core *Ness 3*.

6.8.1.4 Other isotope records

In *Figure 6.26*, are shown comparisons of grey level, derived from digital images of both long cores (*Ness 3* and *4*), variations in $\delta^{18}\text{O}$ from the GRIP ice core (*source: NOAA, WDC-A*), and atmospheric ^{14}C concentrations (Stuiver and Reimer, 1993). All curves are smoothed by calculating *ca* 200-yr averages, in order to match the sampling frequency of the GRIP data. Correlations are displayed in *Table 6.14*.

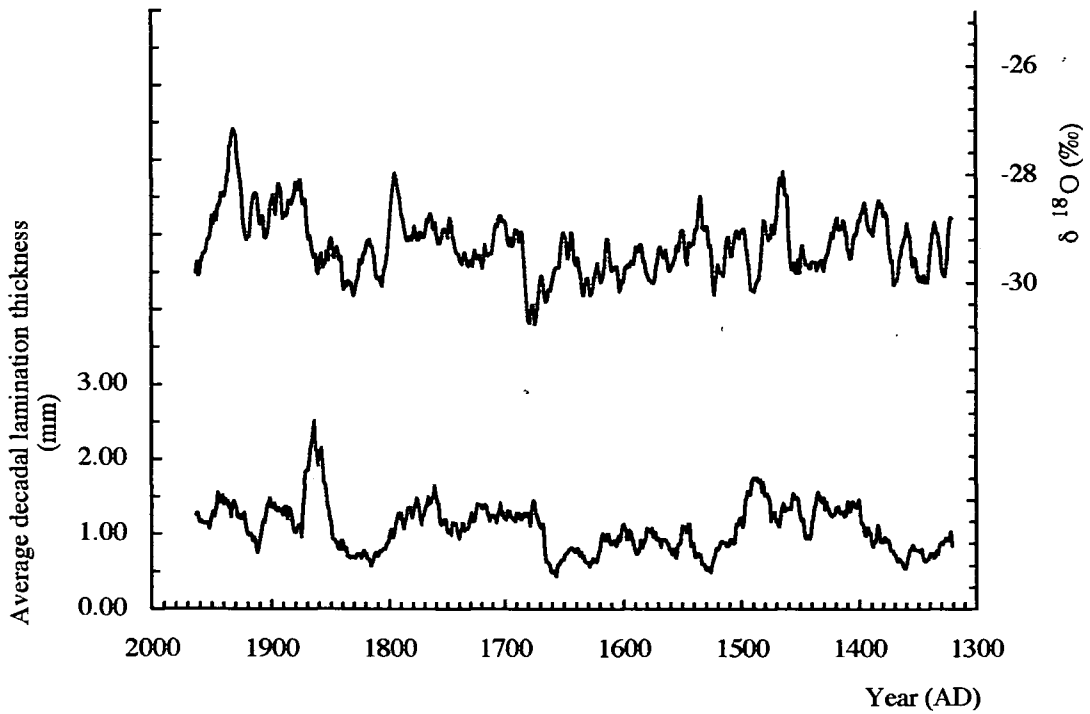


Figure 6.25 Camp Century $\delta^{18}\text{O}$ record compared with lamination thickness data from core LNRI. (Decadal averages; Source www.ngdc.noaa.gov/paleo/icecore/greenland/gisp/campcentury/campc_data.html)

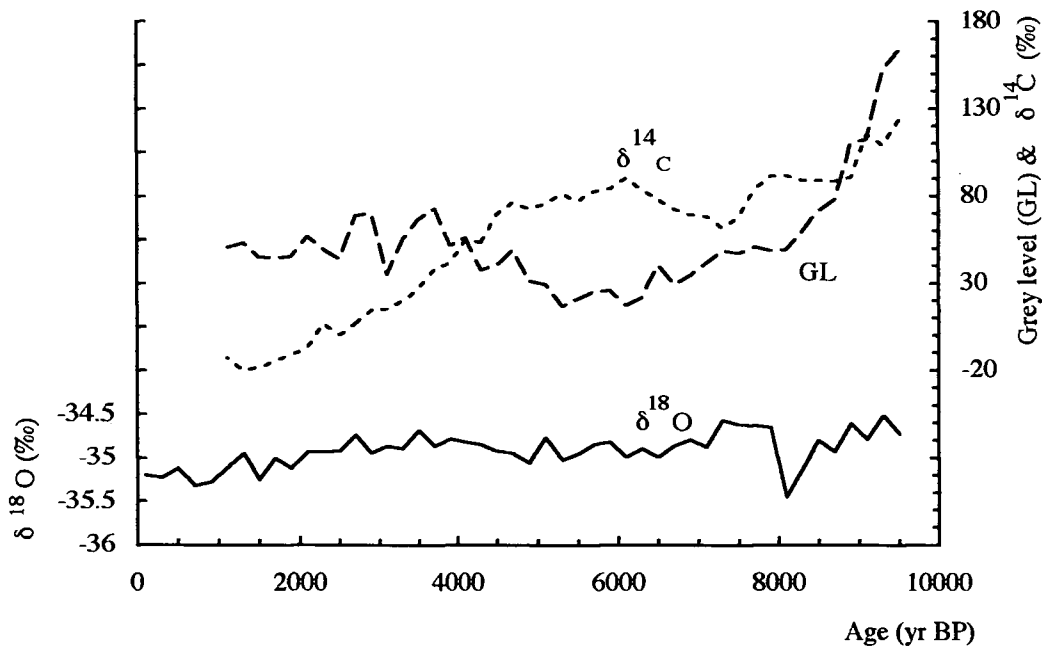


Figure 6.26 Comparison of grey level in long core Ness 3, atmospheric $\delta^{14}\text{C}$, and $\delta^{18}\text{O}$ in the GRIP ice core.

Table 6.14 Pearson correlation coefficients for data plotted in Figure 6.26

	<i>Ness 3 GL</i>	$\delta^{14}C$	$\delta^{18}O$
<i>Ness 3 GL</i>	-	0.2442†	0.3807*
$\delta^{14}C$	-	-	0.3114*
$\delta^{18}O$	-	-	-

*indicates significance at 5% level ,** significant at 1% level (two-tailed).

† a correlation coefficient of 0.242 has been obtained when comparing these data, utilising non-smoothed data. This is significant at the 1% level for $\nu=506$ in the original data set.

The record of $\delta^{18}O$ variations from an ice core indicates the temperature prevailing at the time of formation (Jouzel *et al.*, 1997). More positive values indicate warmer, and more negative values colder, conditions. Positive correlation between these data and grey level, which generally indicates the type of sediment deposited rather than lake productivity, would seem to imply that warm episodes on the Greenland ice cap correspond to an increase in deposition of paler silts, and cooler conditions by the predominance of darker clay/*gyttja*. Pale, silty material is washed into the loch during late winter (R.I.Jones *et al.*, 1997), so that a preponderance of such material suggests increased storminess over Loch Ness and Northern Scotland. This observation reinforces the earlier conclusion that the long-term climate history of the region was characterised by alternating cold/dry and warm/wet phases.

Atmospheric $\delta^{14}C$ is a measure of the amount of that isotope produced by solar (short term) and geomagnetic (long term) variations (Siegenthaler & Beer, 1988). Over the last 10 ka, the long term trend in this record has indicated that production of atmospheric ^{14}C briefly declined around 7.5 ka BP, increased to a maximum at 6 ka BP before decaying to a minimum during the last millenium. A small increase to the present

has also occurred. Positive correlation between GL data and $\delta^{14}\text{C}$ time series is, however, difficult to explain only in terms of geomagnetic field variation. Changes in solar output may further lead to variation in lake productivity, producing darker *gyttja*-rich sediments at periods of higher, and paler, silt rich deposits during times of lower radiation output. This is not borne out, however, by the observation that many periods of increased solar activity may be correlated with episodes of higher rainfall (*Figure 6.27*), which result in the influx of a greater proportion of silt-rich material to the loch, producing paler-coloured sediments possessing high GLs. In addition, primary productivity in the modern loch is low, the majority of the organic matter in the sediment originating from allochthonous terrestrial material (R.I.Jones *et al.*, 1997). It is unlikely, therefore, that variation in solar output would produce significant changes in sediment type, and by implication, colour.

6.8.1.5 Other records

Comparison of records of winter precipitation over Fort Augustus with sunspot indices reveals that local maxima in the rainfall data have tended to fall at or near times of maximum sunspot activity (*Figure 6.27*). Correlation of these data, utilising a 5-yr running average to smooth the precipitation figures, yields a coefficient of 0.202, significant at the 5% level, $v=104$. Although the correlation between lamination thickness and precipitation has been demonstrated to be slight, comparison of sunspot record and lamination thickness from core *LNR1* yields a correlation coefficient of 0.32, significant at the 1% level, $v=202$ (*Figure 6.28*).

Tinsley (1988), complementing the research of Labitzke & van Loon (1990), determined that during the period AD 1921 to AD 1976, relative to their positions at solar minimum, storm tracks over the North Atlantic Ocean were displaced, on average, 2.5° in latitude to the south during periods of maximum solar activity. When using the methods of Labitzke & van Loon, who separated data according to the directional phase of the QBO, Tinsley further noted that storm tracks across the North Atlantic could vary by

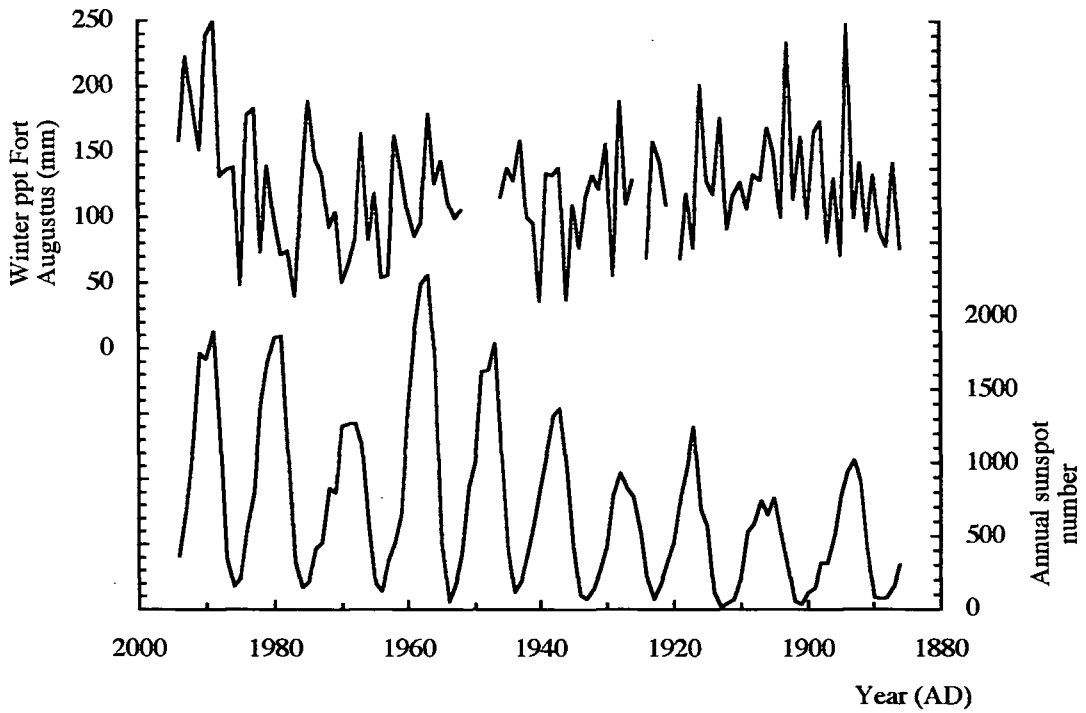


Figure 6.27 Fort Augustus winter precipitation record (*upper*) compared with sunspot number (*lower*), AD 1884 to AD 1994.

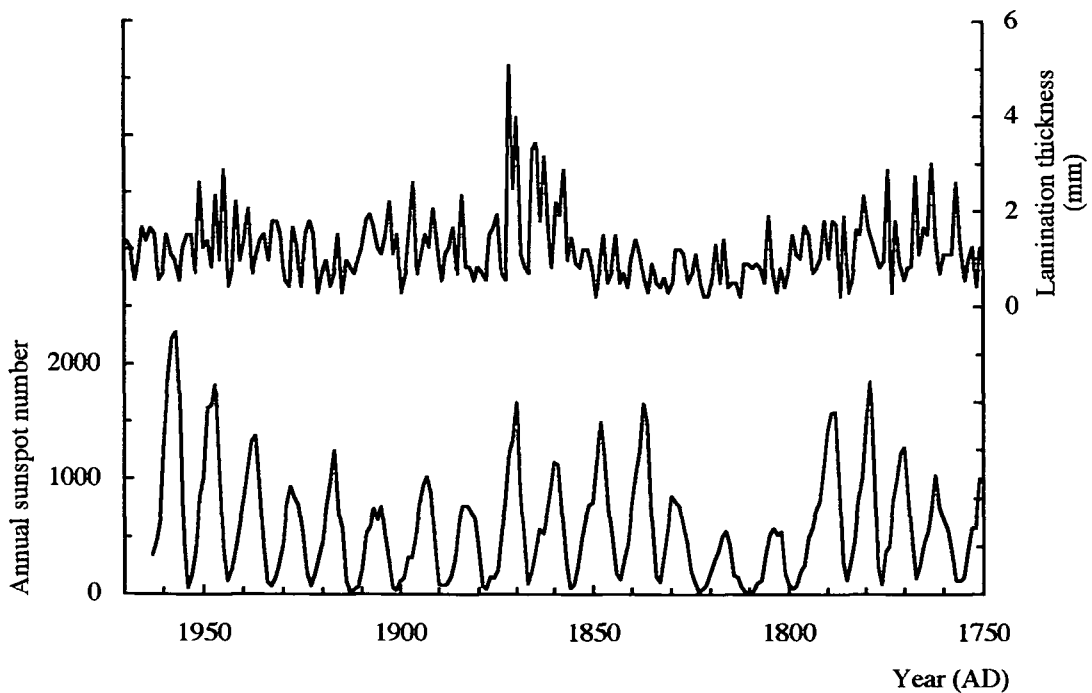


Figure 6.28 Comparison of lamination thickness record from core *LNR1* (*upper*), with annual sunspot number (*lower*), AD 1750 to AD 1963.

up to 8° latitude during its west phase. He suggested that this movement of storm tracks might be mediated by changes in position of the jet stream above the North Atlantic Ocean owing to variations in planetary wave dynamics and possibly by the further strengthening of the dynamic coupling between stratosphere and troposphere. These mechanisms may be employed to explain variation of precipitation over Loch Ness with the solar cycle.

6.9 Spectral analysis

Comparison of the sedimentary record with other periodic time series, such as the solar cycle, suggests that there may exist elements of cyclicity within the varve thickness data from Loch Ness. Fast Fourier Transform spectral analysis has been employed in order to investigate whether or not external climatic and extraterrestrial forcing events have influenced sedimentation through the time period represented by the long and short cores.

Spectral analysis of lamination thickness data from a range of sites and locations reveals periodicities which occur within many of the frequency bands associated with climatic forcing agents. Data display a diversity of outcomes when subjected to this analysis. Sonnett *et al.* (1992) report a cyclicity of deposition of riverine varves, possibly influenced by the Quasi-Biennial Oscillation (QBO), which is detected at periods of *ca* 2.2 to 2.8 years, or 0.45 to 0.35 cycles per year (Burroughs, 1992). Other studies may also be considered, particularly those of Renberg *et al.* (1984) at Judesjön, Sweden, who report periodicities of 11, *ca* 20 and *ca* 37 years, and Zolitschka (1992) at Holzmaar, where periodicities of *ca* 3 and 11 years have been observed.

6.9.1 Spectral analysis of precipitation records

The results of spectral analyses of seasonal and annual precipitation records for Fort Augustus and Inverness are presented in *Figures 6.29* and *6.30*. Of immediate

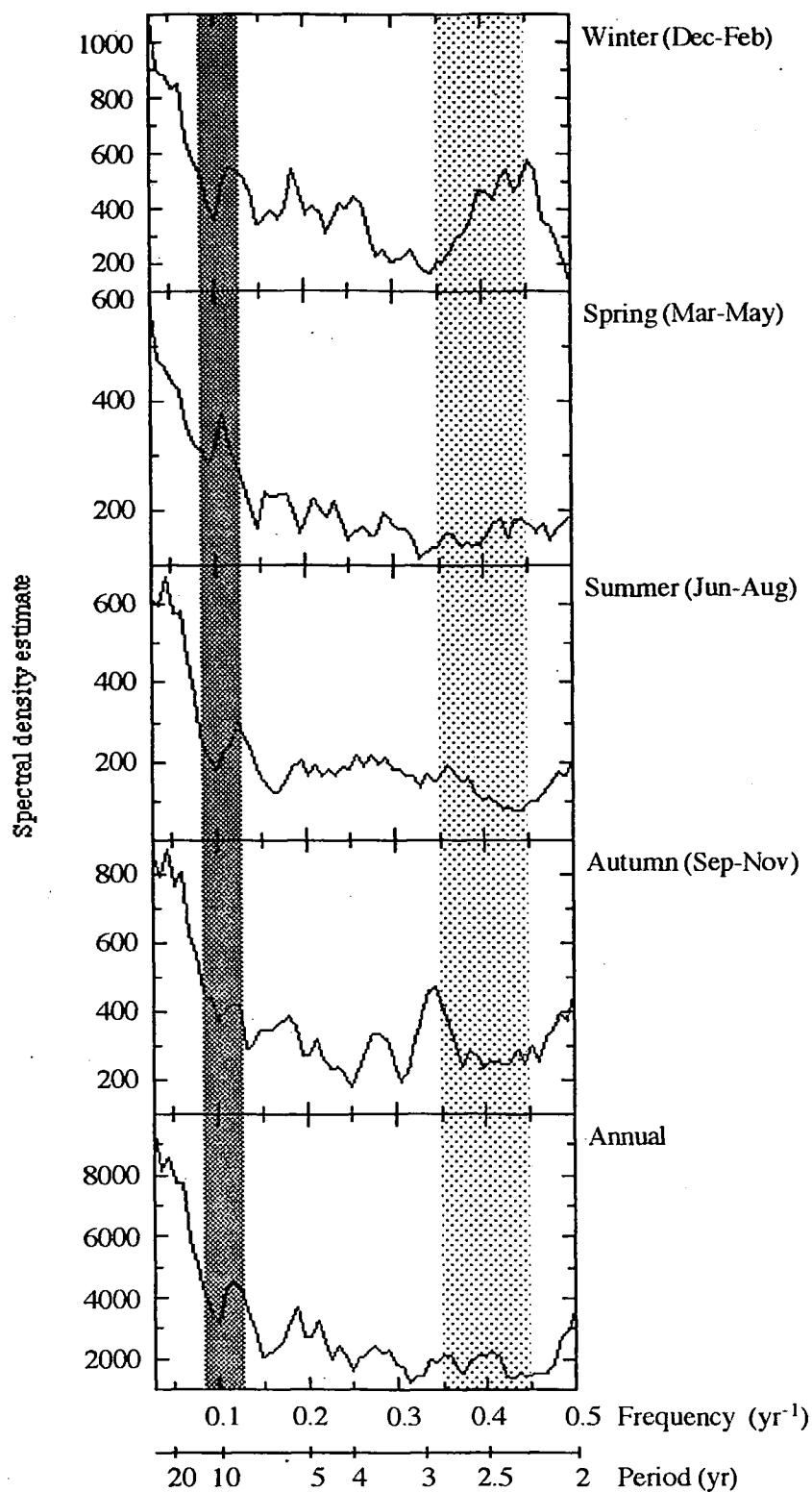


Figure 6.29 Fast Fourier Transform spectra of seasonal and annual precipitation. Fort Augustus, 1886-1994. Dark shading indicates periodicities in the solar cycle frequency band, and light shading those attributable to the QBO.

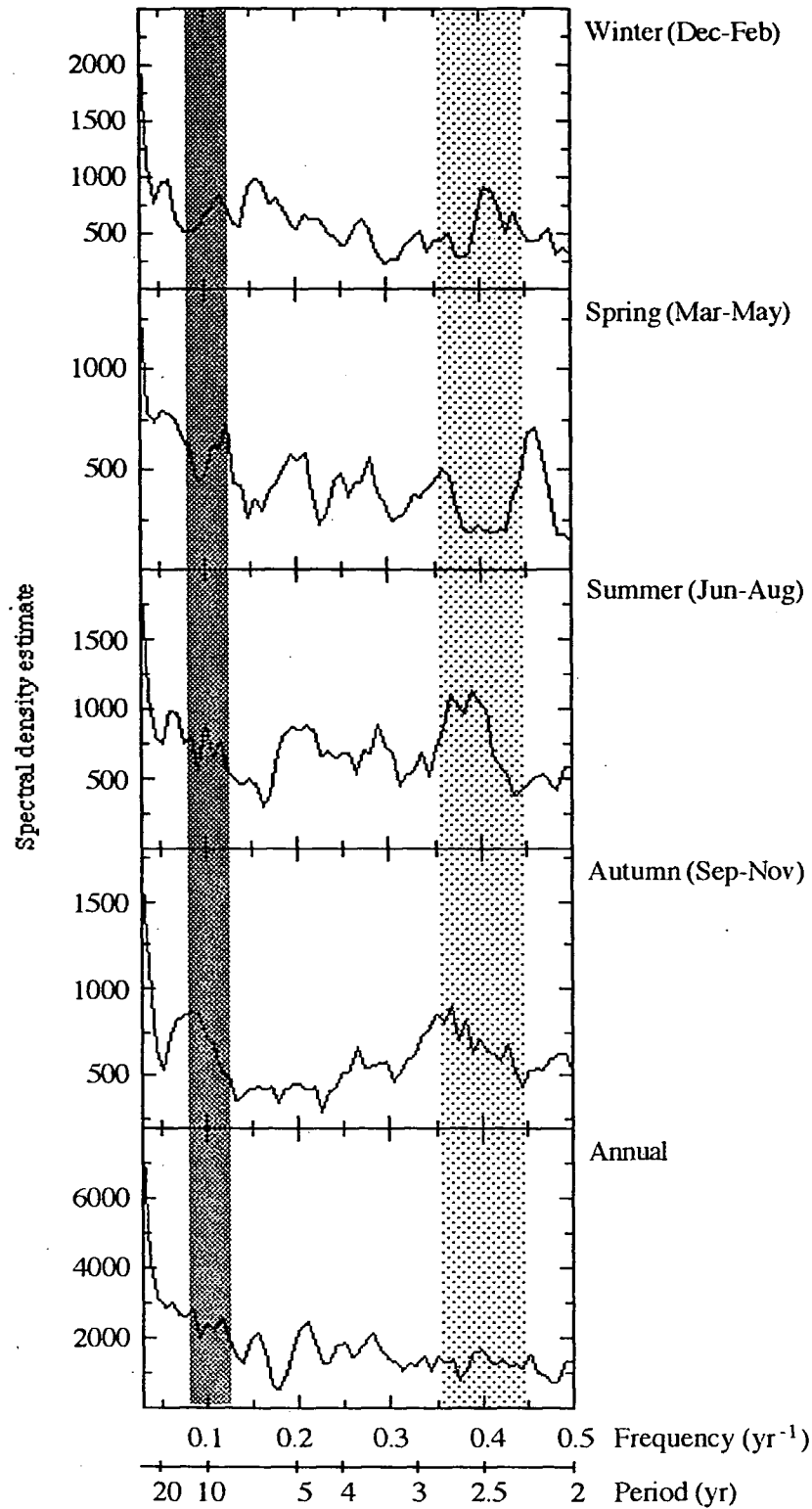


Figure 6.30 Fast Fourier Transform spectra of seasonal and annual precipitation. Inverness, 1890-1994. Dark shading indicates periodicities in the solar cycle frequency band, and light shading those attributable to the QBO.

note is the multiplicity of peaks generated, and the general low level of significance of most of them.

In detail, all spectra generated in this study possess high density at low frequency, particularly around 0.05 cycles per year (20-year periodicity), which may be associated either with the 22-year Hale solar, or the 18.6-year Luni-solar (the *Saros*), cycles (for example Currie, 1994a,b,c,d; Nicholson, 1985). This periodicity is apparent in many climatic time series, and is the second most common cycle reported, after the QBO (Burroughs, 1992). In addition, a peak at *ca* 0.12 cycles per year (8.3-year period) appears common, and may be a higher harmonic of the solar cycle. Spectral power at mid-range frequencies are not consistent through all analyses. Some, such as the Fort Augustus summer record, are almost featureless. High frequency periodicity is well displayed in the Fort Augustus winter and autumn records, however, where significant peaks appear at 0.45 cycles (winter; 2.2-year cycle), and 0.35 cycles (autumn; 2.9-year cycle) per year. Both of these fall within that frequency range ascribed to the QBO.

6.9.2 Spectral analysis of the sediment record

Fast Fourier Transform analysis has also been performed on the record of lamination thickness from both long cores, and from short core *LNRI*. Many spectra exhibit large noise components which serve to decrease resolution, spreading spectral estimates over neighbouring frequency bands. Spectra displaying some 'peaks' around the 11-year frequency band typical of solar activity may clearly be observed, however, in addition to higher frequencies possibly indicative of the QBO. Spectral analysis of decadal totals of lamination thickness was employed in order to enhance longer-period variations.

6.9.2.1 Core Ness 3

The three sections of this core for which distinct lamination images were

obtained by X-radiography, were analysed individually. Each yielded quite different spectra. For brevity the sections will be denoted by *Ness 3/1*, *Ness 3/2* and *Ness 3/3*. *Ness 3/1* represents recent sediments and *Ness 3/3* those at the base of the core.

Analysis of *Ness 3/1* (Figures 6.31 and 6.32) yielded many signals, most of little significance. Periodicities were indicated at : 342, 205, 147, 31, 22, 18, 8, and 6 years, in addition to a plethora of signals within the 2-3 year band. Clearly, little of any certainty may be discussed when such multiple periodicities are observed, but the detection of those signals at 205-, 22-, 18-, and sub 3-year periods, is of some interest. These periodicities have been identified in many proxy time series and have been attributed, respectively, to oceanic influences, the solar Hale cycle, lunar nodal cycle, and the QBO phenomenon. The strong signal at *ca* 6 years is situated within a frequency band often attributed to a harmonic of the solar cycle (Burroughs, 1992).

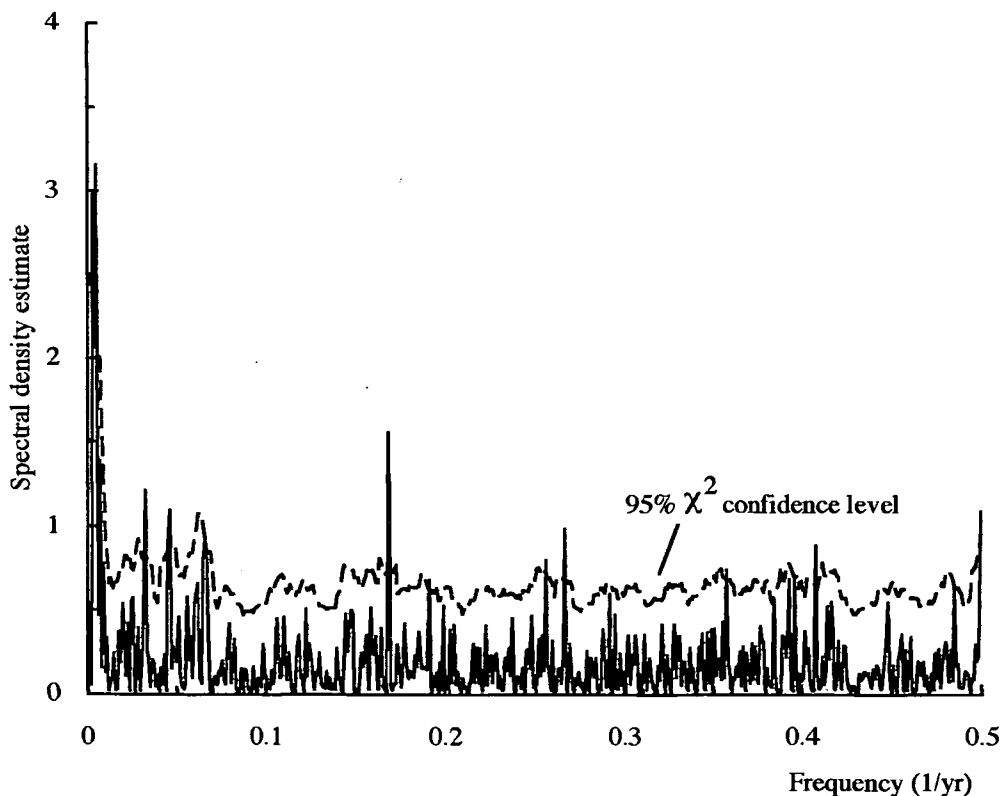


Figure 6.31 Fast Fourier Transform spectrum of lamination thickness data, core *Ness 3*, section 1 (*ca* 2.5 ka to 3.2 ka BP).

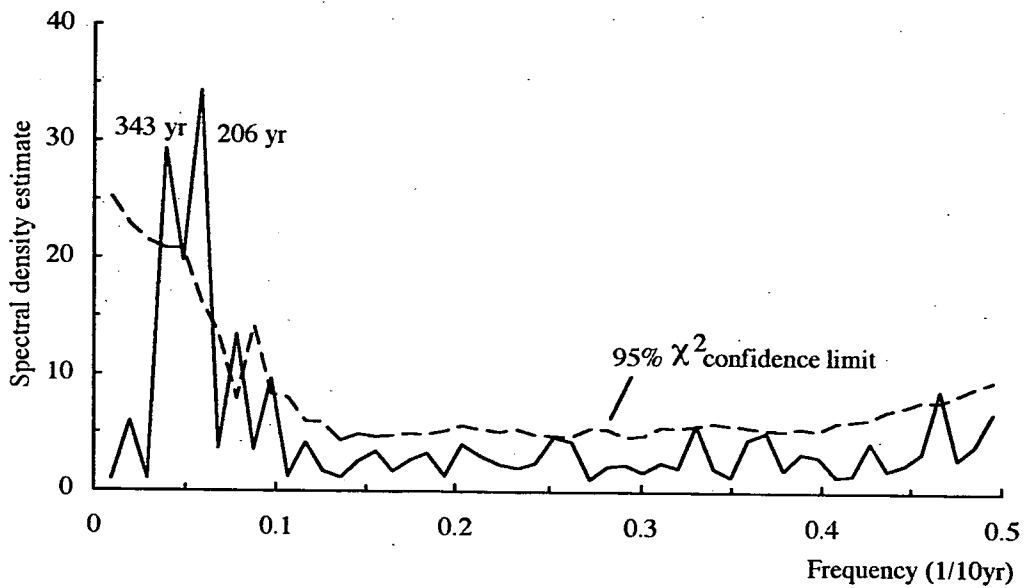


Figure 6.32 Fast Fourier Transform spectrum of decadal totals of lamination thickness, core *Ness 3*, section 1.

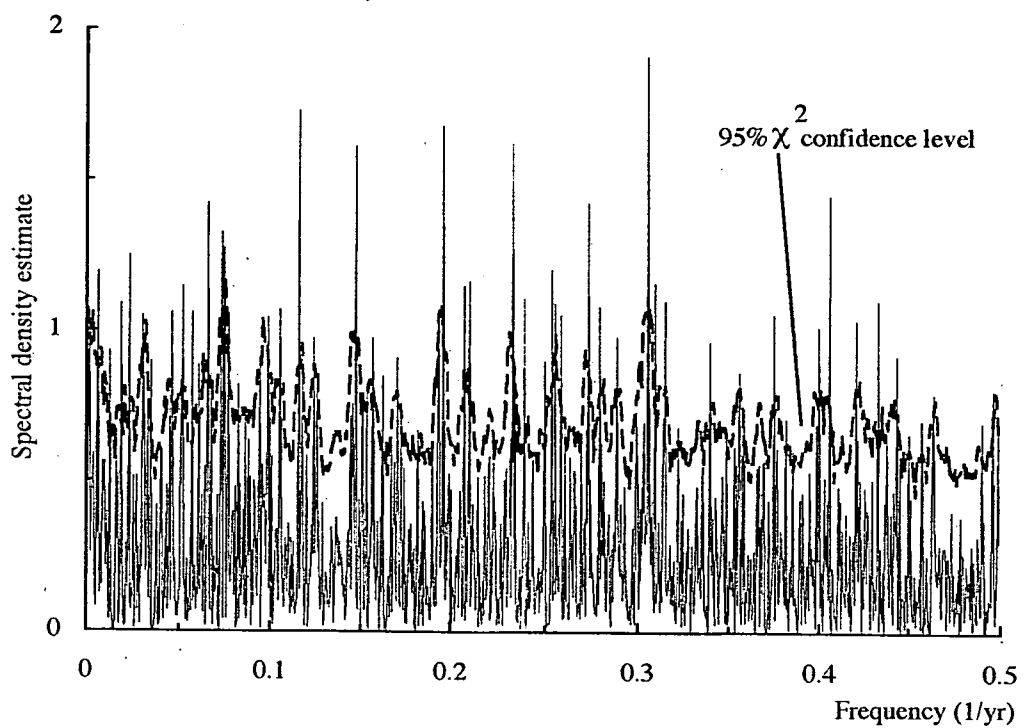


Figure 6.33 Fast Fourier Transform spectrum of lamination thickness data, core *Ness 3*, section 2 (ca 3.2 ka to 4.9 ka BP).

Analysis of *Ness 3/2* (Figure 6.33) results in a spectrum exhibiting a great number of peaks, none of which appear significant. The largest signals are situated between the periods of 3 and 10 years and may represent, if genuine, a weak response to atmospheric forcing processes such as the QBO, or else harmonics of lower frequency events. Consideration of decadal totals (Figure 6.34) produces significant peaks at ca 33 and 22 years.

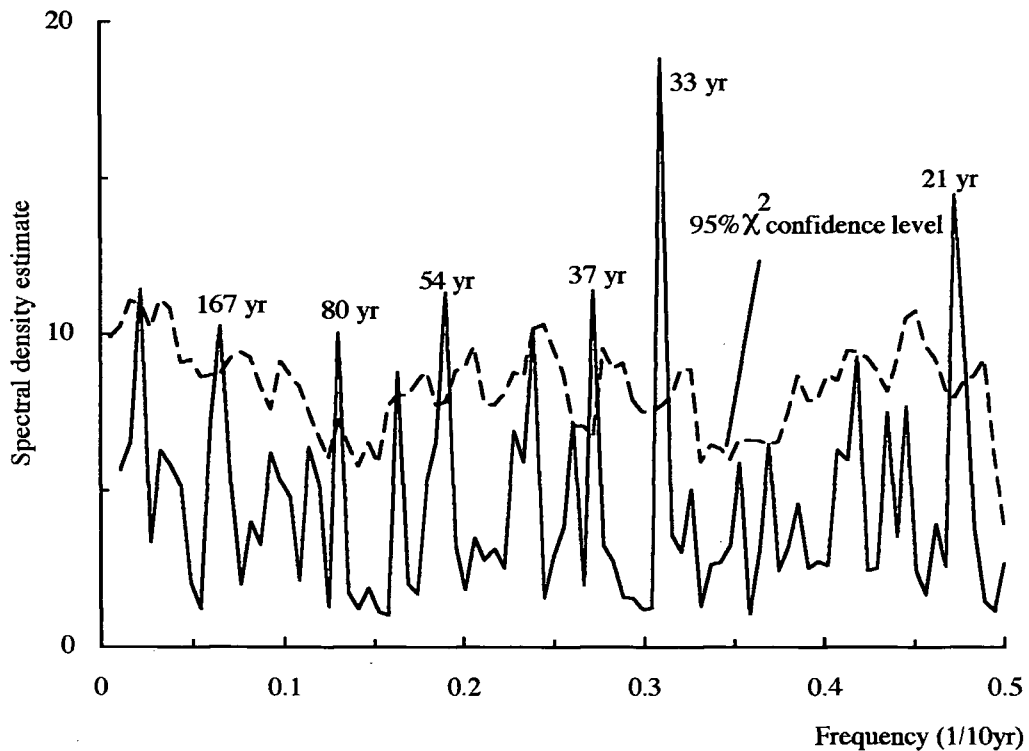


Figure 6.34 Fast Fourier Transform spectrum of decadal totals of lamination thickness, core *Ness 3*, section 2.

The time series derived from *Ness 3/3* (Figure 6.35) represents the longest sequence within core *Ness 3* to be analysed and consists of some 1200 Fourier frequencies. It is not surprising, therefore, that this FFT spectrum also exhibits many peaks. Analysis of decadal totals does little to clarify the spectrum (Figure 6.36), although several peaks, representing periods of ca 160, 45, 36, 33 and 28 years, become statistically significant. Many can be explained as possible harmonics of an 11- or 22 year period.

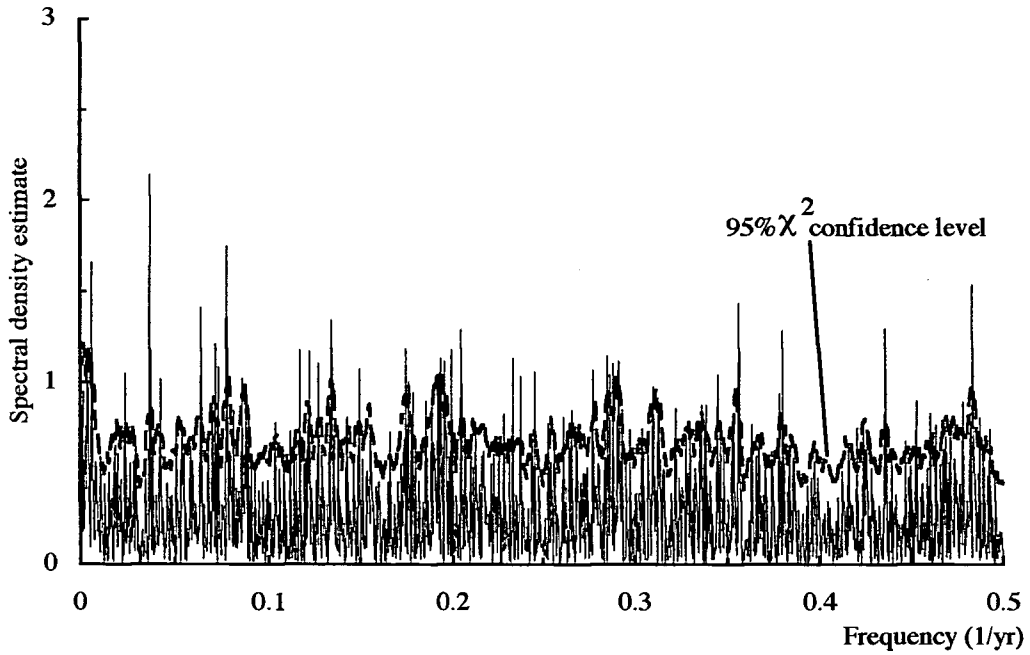


Figure 6.35 Fast Fourier Transform spectrum of lamination thickness data, core *Ness 3*, section 3 (ca 5.9 ka to 8.7 ka BP).

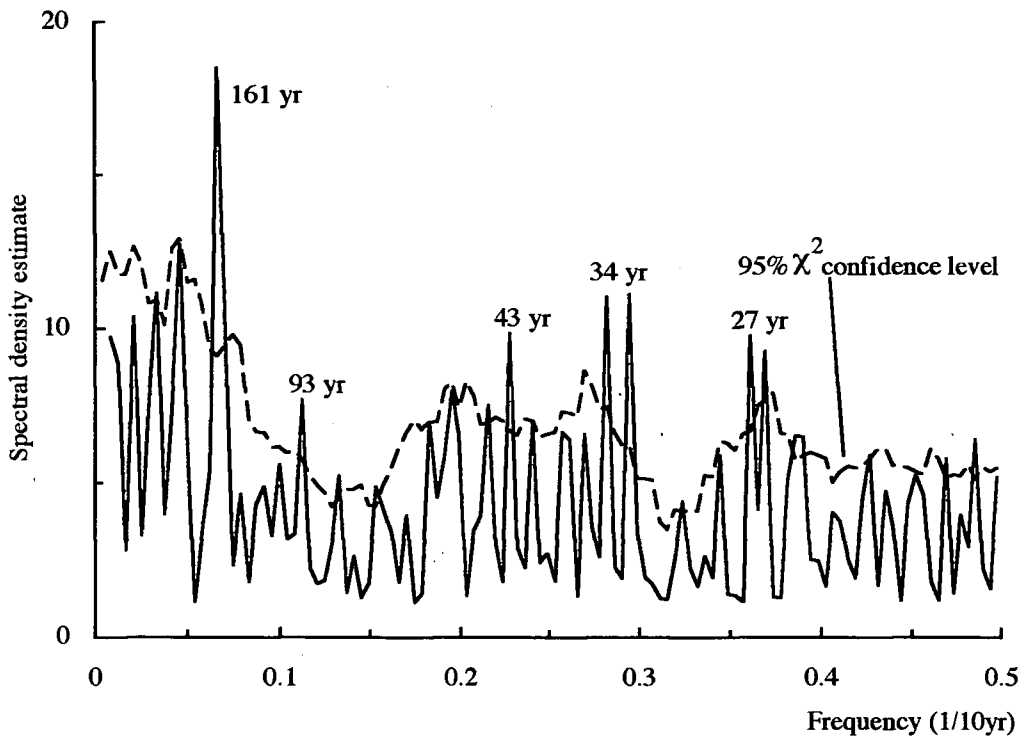


Figure 6.36 Fast Fourier Transform spectrum of decadal totals of lamination thickness, core *Ness 3*, section 3.

6.9.2.2 Core Ness 4

Analysis of the time series of lamination thickness for this core does not present conclusive evidence of any significant cyclicity (*Figure 6.37*). However, assuming that the data represent a continuous series of annual layers, this is the only core to exhibit very long periodicities, of the order of 2200 years. While caution must be exercised in its interpretation, it may be of interest to note that Bond *et al.* (1997) have identified cyclicities of 1470 years in Glacial and Holocene climatic data sets compiled from locations throughout the North Atlantic region, and Barber *et al.* (1994) have commented on an implied *ca* 800-year cycle of variation in moisture in cores from a raised bog near Carlisle (Cumbria, UK). The extreme length of the series from core *Ness 4* (6651 data points) may act to blur any periodic behaviour, since many forcing processes have been discovered to vary in phase through time, thus decreasing the spectral power contribution and resolution of each component (Currie, 1994a). In addition, the integrity of the record is in doubt, and the absence of laminae, or presence of extra ones, will render the analysis unreliable.

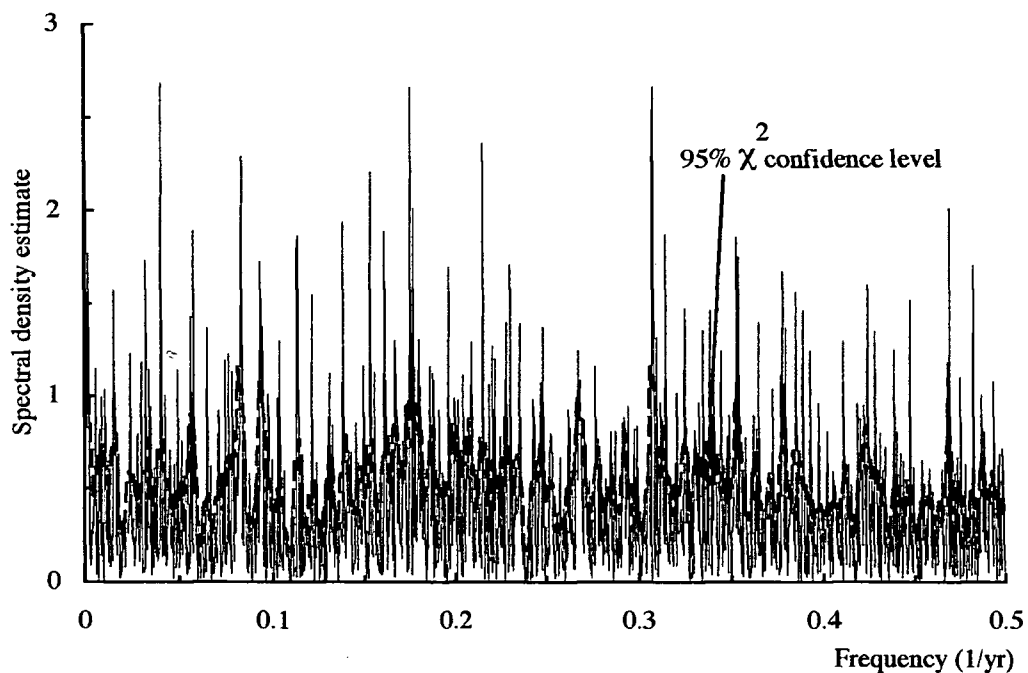


Figure 6.37 Fast Fourier Transform spectrum of lamination thickness data, core *Ness 4*.

 6.9.2.3 Core LNRI

Fast Fourier Transform analysis of the entire time series derived from core LNRI indicates that long period variations in lamination thickness predominate (Figure 6.38). A particularly intense signal is observed at *ca* 90 years, within the frequency band for the solar Gleissberg cycle (*ca* 88 years). This has also been detected in a number of other records, including the Central England temperature series (Burroughs, 1992; Manley, 1974). A further comparable peak in the spectrum is that for a period of 214 years, which is again observed in many series including the Bristlecone pine chronology (Burroughs, 1992; Libby & Pandolfi, 1977; Suess & Linick, 1990), sunspot series, and lunar tidal data (Burroughs, 1992). Aaby (1976) has detected a similar periodicity in the stratigraphy of Danish bogs (*ca* 260 years), as have Johnsen *et al.* (1970; 78 and 181 years) in data from the Camp Century, Greenland, ice cores and Stuiver (1994) from

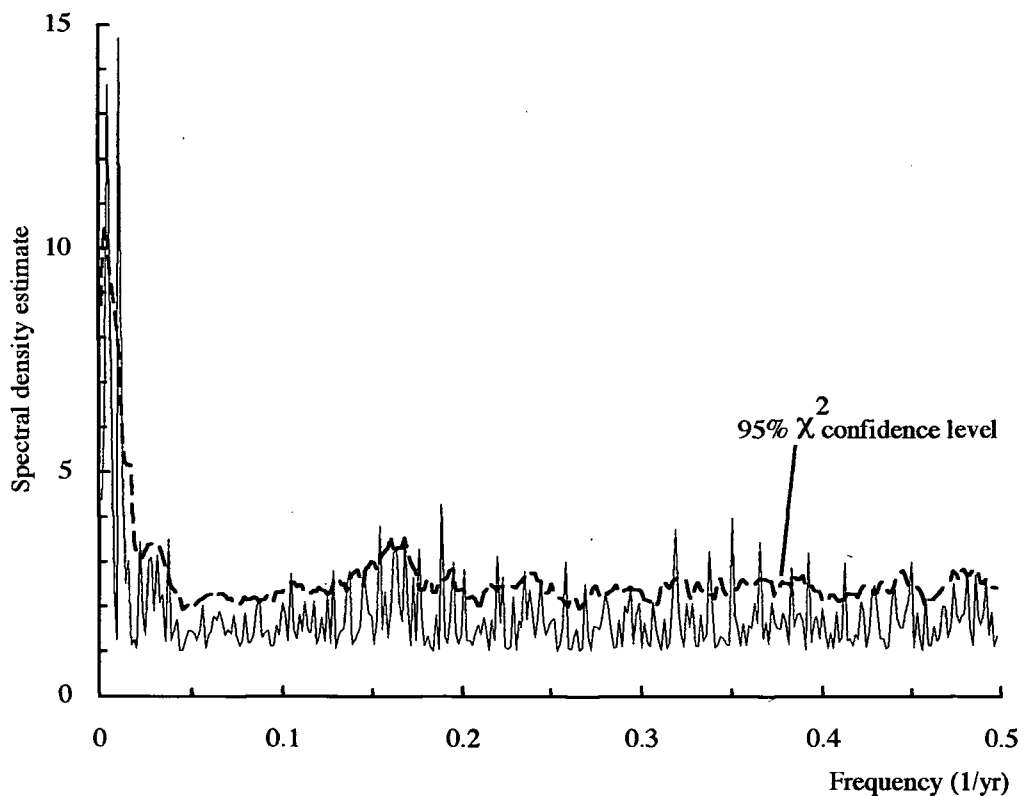


Figure 6.38 Fast Fourier analysis of lamination thickness from core LNRI, over the period 1321-1963 AD.

analysis of the spectrum of abundance of radiocarbon in the atmosphere (87 and 206 year periods). Variation in concentration of calcium ions in the GISP2 core (Mayewski *et al.*, 1993a) also displays *ca* 55 and *ca* 160 year periodicities, which are considered to indicate changes in atmospheric circulation or cycles of continental erosion. Lamination thickness in sediments from Lake Turkana, from 4000 a BP to present, have also been found to exhibit 78- and 200-year periodicities (Halfman & Johnson, 1988), as have varved sediments from Holzmaar, Germany (Vos *et al.*, 1997). Signals of shorter period from core *LNRI* lack the spectral power of these long period cyclicities.

6.9.2.4 Spectral characteristics of the NAO signal and its comparison with precipitation and lamination thickness records

In view of the strong correlation between lamination thickness from core *LNRI*, NAO activity, and precipitation over Fort Augustus and Inverness (*section 6.6*), spectral analysis of annual NAO index was performed, in order to further investigate the possibility that this phenomenon may be considered a forcing agent of climate, leading to variations in deposition (*Figure 6.39*). Analysis of monthly NAO index revealed no coherent seasonal pattern. A periodicity of *ca* 66 years is apparent in late winter/early spring and again in July, and one of *ca* 44 years, again in spring, and in November. Cyclicities typical of the double Hale solar cycle (*ca* 22 to 26 years) are detected. Periods indicative of the Luni-solar cycle (18.6 years; Currie, 1994) are sparse, occurring only in April (*ca* 16 years), September (*ca* 19 years), and October (*ca* 16 years). The 11-year solar cycle may be represented by periods of around 8 to 11 years which are apparent in NAO indices for February, April to August, and for December. Short period (QBO-like) cyclicities are noted within each monthly data series.

The FFT spectrum obtained from core *LNRI* was compared with that obtained from the NAO index (*Figure 6.40*), although exact comparisons of Fourier periods were not possible, owing to differences in sizes of the data sets. Similarities were noted in the

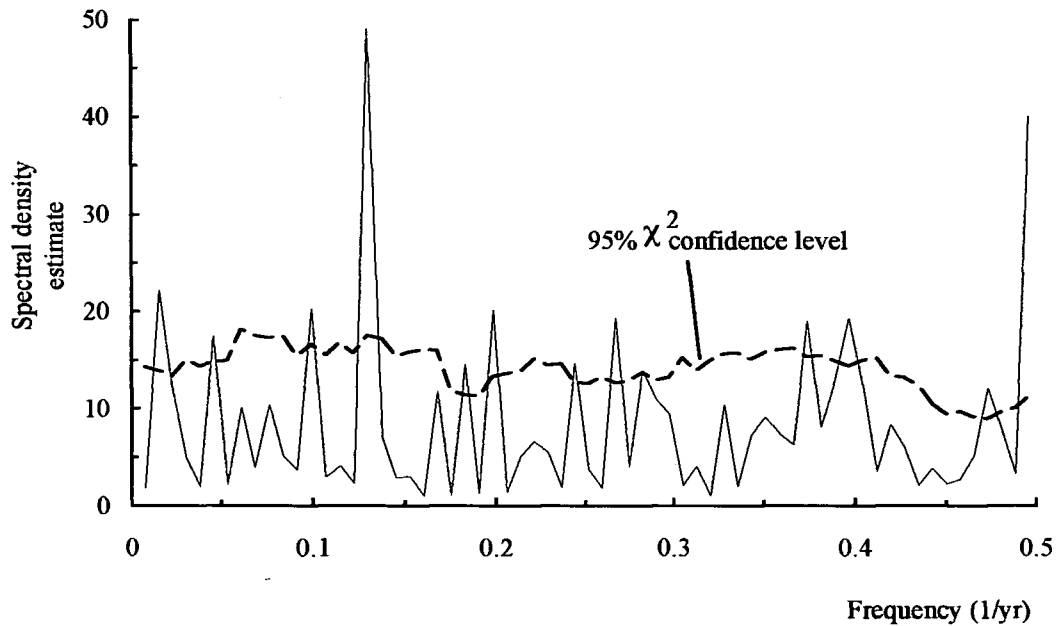


Figure 6.39 Fast Fourier Transform spectrum of the annual NAO index, 1876-1996.

ca 40-year period (LNR1: 46 yr, NAO: 44 yr), ca 25-year (27 yr, 26 yr) and the solar cycle period (9.5 yr, 9-12 years). Although not conclusive, the results suggest that the NAO may indeed have been influential in the variation of deposition within the loch over the past 600 years.

6.9.2.5 Evolutive spectral analysis (Figures 6.41 to 6.43)

Analysis performed on time series derived from lamination measurements from cores *Ness 3* and *Ness 4* reveal very little information, since spectral power is generally very low, and features are indistinct. Of note is the trend for periodicities to shift from longer to shorter timescales. It is not certain whether this effect is an artefact of data processing or a genuine phenomenon representing, perhaps, the ability of the system, in recent times, to respond more rapidly to change. Data derived from a small set of proxy temperature reconstructions spanning the period 1750-1950 AD (Mann *et al.* 1995) also display this type of frequency shift when analysed by evolutive spectral analysis. The drift in periodicity is noted, but not explained.

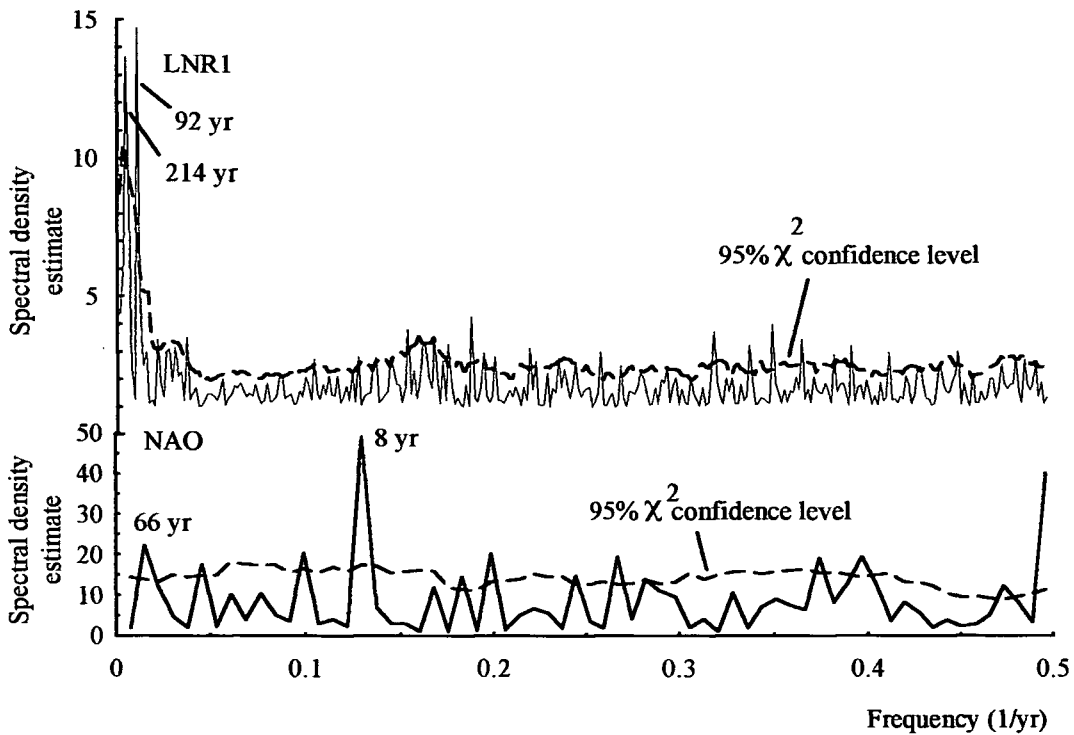


Figure 6.40 FFT spectrum from core *LNR1* (upper) compared with that from analysis of the annual NAO index (lower).

The FFT spectrum from core *LNR1* suggests that analyses performed upon shorter sequences of lamination thickness highlight periodicities inherent in the data better than those which involve series consisting of many thousands of measurements. This may be caused by changes in phase of periodic elements over time, which will act to blur any signal they produce (Currie, 1994a; Mayewski *et al.*, 1993a). In order to investigate the temporal variation of any periodic behaviour in lamination thickness, evolutive spectral analysis was performed over consecutive periods of 128 years. The maximum Fourier period, 64 years, is well represented throughout, especially in the period 1321-1447 AD, where it is accompanied by a slightly weaker signal at 4.9 years and a very strong one at 3.8 years, both of which may be higher harmonics of an 11-year period. Short cycles, of two to five years, are observed in all time slices and may represent response to QBO forcing. Medium-period cyclicities seem only to be observed during the time periods

1450-1575, and 1835-1963 AD. Thus, it may be observed, that throughout the periods analysed, at no time do these signals persist, and they are, in addition, occasionally weak in terms of spectral density. These analyses, however, are difficult to reconcile with that derived from the whole series, since the Fourier frequencies are calculated differently, and periods longer than 64 years will be summed into that frequency. Thus, there exists a need to balance temporal and frequency resolutions, since the greater the number of time slices analysed, the better the understanding of variation of cyclic behaviour, but at a reduced frequency resolution.

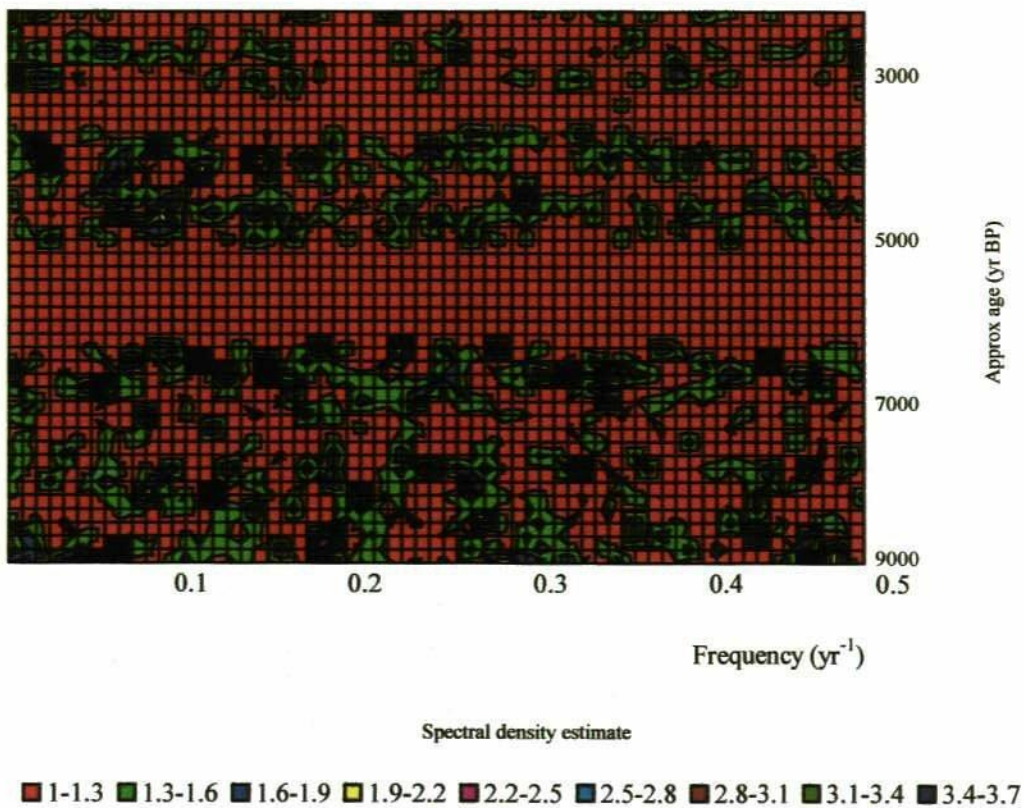


Figure 6.41 Evolutive Fourier spectrum of elements of periodicity contained within core Ness 3.

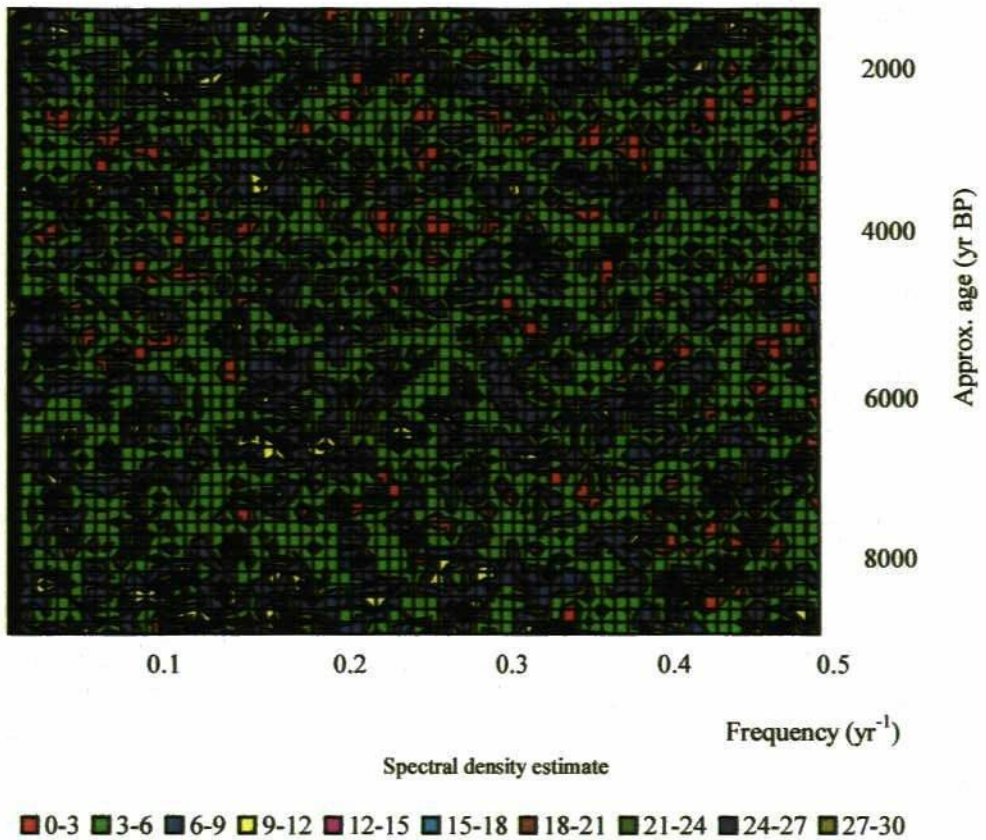


Figure 6.42 Evolutive Fourier spectrum of elements of periodicity contained within core *Ness 4*.

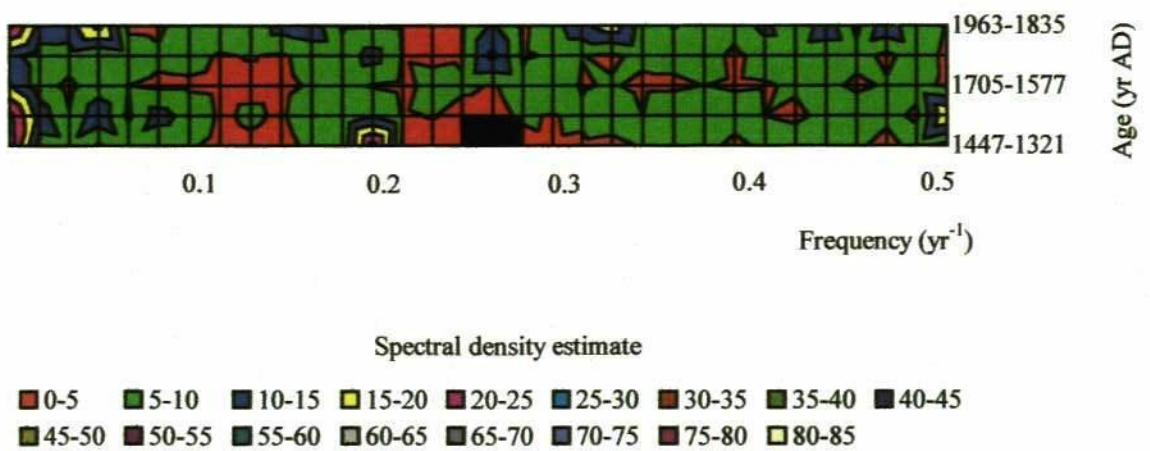


Figure 6.43 Evolutive Fourier spectrum of elements of periodicity contained within core *LNRI*.

6.10 Summary of analyses

The average value for loss on ignition was determined to be 25% in core *Ness 3* and almost 40% in core *Ness 4*. Both cores exhibit low values of %LOI from early Holocene sediments, but the record derived from core *Ness 4* was noted to be more complex than that obtained from core *Ness 3*.

Grey level varied throughout each 'long' core, with paler sediments occurring in the lower sections and darker material from about two to three metres. Recent sediments were noted to be paler than those from the mid-Holocene.

Microolithological examination revealed differences between pale and dark layers, and identified four styles of lamination, although EDS failed to resolve differences in elemental composition. It was thus concluded that the variation in sedimentation was derived primarily from the alternating deposition of clay- and silt-rich material, both of which are derived from catchment material.

Comparison of time series was performed with varying degrees of success. Local meteorological records did not provide significant coefficients of correlation with lamination thickness, although precipitation was well correlated with streamflow in the River Ness ($r=0.961$; signif 0.1%). Data on the deposition of seston from the water column (R.I Jones *et al.*, 1996) exhibits a close similarity to variations in precipitation.

Regional palaeoclimatic datasets yielded some significant correlations with lamination thickness, indicating that some climatic forcing processes may be implicated in sedimentation in the loch. The incidence of sea ice around Iceland, and in the Danish Sound, which is indicative of the movement of the NAPF, was found to be significantly correlated ($r=0.5234$ and 0.5853 respectively; signif <1%) with lamination thickness. Summer NAO index was highly significantly correlated with lamination thickness in core

LNRI ($r=0.5229$; signif 1%) while winter NAO index was negatively correlated ($r=-0.3253$; signif 1%), indicating that NAO may be instrumental in providing a substantial forcing component to sedimentation.

Comparison of both lamination thickness and grey level with ^{14}C and ^{18}O records revealed similarities between lamination thickness in core *LNRI* and $\delta^{18}\text{O}$ from the Camp Century ice core, which further reinforces the premise that sedimentation in the loch is partially driven by NAPF movement. Correlation of solar output, via the ^{14}C record indicates that at times of increased insolation, paler silts tend to be deposited, possibly through increased precipitation, since periods of maximum rainfall tend to coincide with increased sunspot number, most likely via movement of storm tracks by the QBO.

Spectral analysis of the sediment record reveals the presence of long period (214 -and 90- year) variations in core *LNRI* and comparable 342-, 205-, 147- and 6- year periodicities from the upper part of core *Ness 3*. Many of these periods have been observed in other proxy time series, and indicate that they may be widespread in climatic processes and that sedimentation in Loch Ness is a system able to record them.

6.11 Estimation of errors

At every stage of an analysis, errors may be introduced and certain assumptions made. It is important to be able to quantify these, in order to estimate the overall accuracy of the analysis, and to ascertain whether or not these errors and assumptions have added significant distortion to any conclusions drawn. In this study, the topics which have been identified as possibly having some significant effect on the results are presented in *Table 6.15*.

Table 6.15 Stages of analysis during which significant errors may have occurred

Photography and X-radiography
Image analysis
Determination of lamination position and thickness
Compilation of chronology
Suitability of coring site and understanding of mechanisms of deposition of sediment

6.11.1 Photography and x-radiography

Both techniques are reliant upon both the quality and amount of radiation employed for illumination, and on the quality of the recording medium and associated developing and printing processes. Careful setting-up of the photographic stage enabled uniform illumination to be obtained, and developing and printing was undertaken by the same, skilled individual (Ms Betty Fox) each time. X-radiography was carried out utilising plates from one production batch and employing constant conditions of exposure, which were electronically controlled. This operation was, however, performed over a considerable period of time, and utilised a machine which was used by other researchers, and may thus have suffered variation in performance during the period of study. Gross changes, in terms of resolution or uniformity of illumination were, however, not noticed upon examination of X-ray plates. It is thus considered that operations performed on photographs and X-radiographs will suffer negligible errors.

6.11.2 Image analysis

Efforts to minimise errors within this step are achieved by averaging images at each stage of analysis. Thus, random errors are effectively eliminated. The techniques chosen in order to enhance images are co-ordinate invariant, and hence do not affect the relative positions of lamination boundaries within an image. Grey level determinations are

constant for each image and errors have been determined by the repeated acquisition and analysis of the same x-radiograph, under identical conditions. In addition, the same camera and lens combination was employed for every analysis, further ensuring reproducibility.

Calibration of the image analyser was performed at the beginning of each session, employing an engraved steel ruler as a standard measure. Calibration data were stored within each file of Grey Level measurements. Linearity of measurement within the image field was ascertained by determining the number of pixels between millimetre divisions of the engraved ruler. The results are presented in *Table 6.16* and *Figure 6.44*

The process of digitisation does, however, incur a penalty when analysing images which contain details with dimensions close to the limit of optical resolution. Here, small changes in size may result in measurement errors of ± 1 pixel, resulting, in this case, in errors in lamination thickness of, perhaps, $\pm 100\%$. The effect of such variations may be considerable when comparisons between cores are considered.

Table 6.16 Linearity of image field of Quantimet 570 image analyser

Initial pixel position: $x=279$ $y=111$; Calibration= 0.099 mm pixel⁻¹

ruler mark (mm)= 21.0	y= 111	(mm) =20.2	y= 191
20.9	121	20.1	201
20.8	131	20.0	211
20.7	141	19.9	221
20.6	151	19.8	230
20.5	161	19.7	241
20.4	171	19.6	250
20.3	181	19.5	260

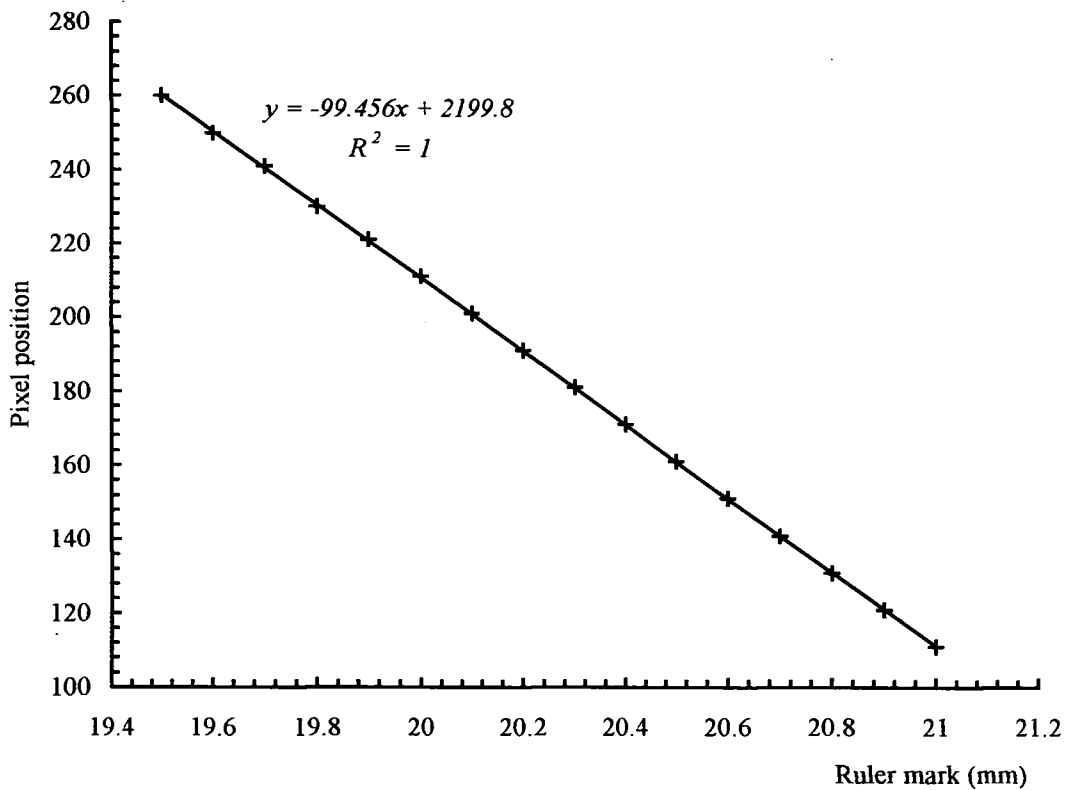


Figure 6.44 Graphical presentation of the linearity of the image field of the Quantimet image analyser.

6.11.3 Computer program

Errors in the determination of lamination boundaries by computer algorithm are a function of the correct location and form of the boundary itself, usually marked by a rapid change in grey level and of the estimation of the 'noise' inherent in the image of the sediment. This influences the selection of a threshold over which it is certain that a change in grey level represents a lamination boundary.

The algorithm utilised for this study represents, however, a rather simplistic estimation of lamina properties, but addresses the question of errors above. Consideration of signal noise within an image is achieved by determining an average grey level for the image under consideration and adjusting, on the basis of this, the minimum change in grey

level which will be accepted as representing a boundary. Laminae which record a constant gradation from one to another are located by determining pixel positions mid-way between a 'peak' and subsequent 'trough' in the grey level signal. The algorithm is configured to consider only laminae which are assumed to represent varved sediments, in that they correspond to the classical '2 laminae per varve' type.

6.11.4 Chronology

Errors in counting may arise as a result of limitations in the image analysis method and from sedimentological processes which may produce laminae with indistinct boundaries. In addition, there are laminations which are deposited by extreme events, such as sublacustrine slumping or by seismic disturbance, within the water body. These 'extraordinary' laminae will remain undetected by x-radiography if their properties resemble those of 'normal' layers and may only be recognised upon analysis of thin sections by microscopy.

Differences between cores *Ness 4* and *Ness 3* are presently under study, grey scale data from both being compared by utilisation of tree-ring correlation software under the supervision of Dr. Martin Bridge, at University College London, and by Dr. Christopher Ramsey at the University of Oxford, by 'wobble matching' lamination thickness data using the software program **Oxcal** (Ramsey, 1995). The nature of the differences are uncertain, since prominent laminae may be identified in images of both cores, although at different locations. It is thought that small scale differences between cores, owing to variation in lamination thickness and structure, may be due to their being recovered from slightly different locations, where contrasting sedimentary regimes may prevail.

6.11.5 Suitability of coring site

The location of the coring site, and the rationale for its situation, was outlined within *Section 3.4*. The results of an acoustic survey (Shine & Martin, 1988), indicated the suitability of the site for the recovery of sediment cores owing to its remoteness from riverine inputs and from the steep sides of the loch. It is, however, located at the base of the slope to the northern outflow, and a recent sonar survey, carried out at high resolution by the Department of Oceanography at the University of Southampton, UK, now indicates that the site may not be ideal in terms of sublacustrine profile. It may be useful, therefore, in the light of this recent evidence, to discuss processes which may be considered to inhibit or alter the formation of annual laminations.

The littoral zones of the longitudinal shores of Loch Ness plunge quickly into the profundal with an average slope of 33%. The northern outlet of the loch rises somewhat more gently, from -200 m to 10 m AOD over a distance of about 7300 m, a slope of 2.9% (Ordnance Survey, 1993). The severity of the gradients on each side of the loch poses questions as to the stability of sediments accumulating there, especially during episodic flooding, and in the event of tectonic movements (Mirecki, 1996; Shilts & Clague 1992), of which there is a long record (British Geological Survey. Seismic Activity Reports). In fact, it is postulated that the chaotically-structured sediments observed in the upper sections of both 4.5 m cores may be derived from such an event, by causing older laminated sediments, deposited in a quasi-stable location on the steep flanks of the loch, to slide downslope onto younger ones. This problem is also discussed by Digerfeldt (1979), Shilts & Clague (1992), and is described in detail by Bennett (1986), for sediments recovered from Hall Lake, Canada. Evidence from the Loch Ness record for this mechanism includes pollen analytical data which display changes in arboreal pollen taxa, including a large increase in *Pinus*, a taxon much more abundant during the early Holocene, associated with the chaotic zone (S.M.Peglar, unpubl.). Investigations by submarine sampling of such sediments indicates that two main types exist, a brown *gyttja*

overlying a yellow/ochre clay (A.J.Shine, unpubl.).

The coring site is situated to the north-east of Urquhart Bay (Grid Reference 530295), which receives riverine inputs from the rivers Coiltie and Enrick. Both rivers drain the Balmacaan Forest, an area of high moorland (mean elevation, *ca* 450 m) of some 148 km², while the Enrick additionally receives material from high ground (mean elevation *ca* 280 m, area *ca* 64 km²) to the north of Glen Urquhart. The River Enrick also passes through Loch Meiklie, at Grid Reference 435302, which may act as a sediment trap (McManus & Duck, 1988), although no data are available to support this hypothesis. The sublacustrine structure of Urquhart Bay has been determined by sonar studies, which indicate the presence of a delta dissected by channels from the two rivers previously described (Shine & Martin, 1988). Thus it is thought that both sediment deposition and erosion occur within the delta, which may have implications for the integrity of the temporal sequence of sedimentation on the profundal plain.

Coring has taken place towards the northern end of the loch, which has a long fetch owing to the predominantly southwesterly direction of the prevailing winds. These influence both water and seston movement within the loch (R.I.Jones *et al.*, 1995; Thorpe, 1971), generating a net flow of both towards the north, although sediment close to the floor of the loch may not be transported across the profundal rise at Foyers. Material already present in the northern basin may, however, be driven upslope towards the outflow and then be transported by eddy flow back into the loch, to be deposited over an unquantified timespan at unknown locations. Under strong wind conditions, material entering the loch from Urquhart Bay will be transported at an angle to right of the wind direction owing to the Coriolis force (Horne & Goldman, 1994), which, at depth, may be as great as 45°.

The large fetch is also responsible for the initiation of the well-documented internal wave or seiche within the loch, which induces a 'rocking' motion of the

thermocline, in both longitudinal and latitudinal axes, with a periodicity of some 54 hours (Mortimer, 1974; Thorpe, 1977). As a result, water in the hypolimnion undergoes a reversal in its direction of motion every half-period, with possible implications for the disturbance and resuspension of previously settled material, especially fine clay particles. This observation must be tempered by highlighting that data concerning water movement over the profundal plain of the loch are scarce. Further investigation may be needed if the mechanism of lamination formation in the sediments of Loch Ness is fully to be understood.

7. Conclusions

This section will present conclusions as to the nature of the sediment recovered from Loch Ness, the accuracy of the chronology postulated, its suitability for the study of the palaeoclimate of the region, and of elements of periodicity which may be contained within it.

7.1 Factors influencing the formation of laminations in the sediments of Loch Ness

It is now established that sediments from the north basin of Loch Ness consist of fine laminae, alternating dark and pale brown in colour. Pale layers are rich in silt, while the darker laminations are clay-rich and contain more organic matter. These are occasionally interspersed with thicker pale layers which have been determined, by their internal structure, to represent deposition by major floods (Dean, unpublished). It is believed that the fine pale laminae are deposited during late winter and early spring and that the darker layers represent sedimentation throughout the rest of the year.

Several factors seem implicated in the formation of the laminations:

- a) The Loch is unproductive, and organic matter, which is mainly found in the fine, dark laminae, is almost entirely allogenic (R.I. Jones *et al.*, 1997).
- b) The amount of sediment present in the water column has been correlated with precipitation (R.I. Jones *et al.*, 1996).
- c) Precipitation over the region is correlated with the NAO index, and this phenomenon is undoubtedly instrumental in the formation of the signal observed, in recent sediments at least.
- d) Storm tracks over the region are influenced by the location of the NAPF (Taylor & Yates, 1967) and are additionally linked to solar activity via the

QBO (Tinsley, 1988). These would, therefore, be expected to influence the frequency and distribution of the thick pale layers observed in the sediment record.

e) Wind direction is also affected by the NAO. A high index signifies predominantly moist, southwesterly airstreams, while a low index indicates drier easterly ones (Hurrell, 1995).

f) Distribution of seston within the water column has been determined to be affected by wind stress (R.I. Jones *et al.*, 1995), with some materials settling out evenly across the bed of the Loch, while others are preferentially deposited in the northern basin.

Further factors, which may influence the pattern of sediment deposition, include the presence of deep currents in the profundal of the Loch (Wedderburn & Watson, 1909). In addition, large scale movement of water in the basin takes place during storms (Thorpe, 1977), which may lead to sediment being lost at the outflow of the Loch before deposition can occur. The presence of seiche may also affect sedimentation, especially of fines held above the thermocline (Thorpe, 1971).

Analysis of cores by image processing techniques has allowed the classification of sediments in terms of Grey Level (GL). 'Storm layers' (thick, silt-rich laminae) possess high GL values, whereas darker, clay-rich laminations are assigned low GLs. Thus GL datasets which have been derived from whole core images indicate variations in the predominant sediment type with depth.

When these data are compared with palaeoclimatic and extraterrestrial records several points follow. The high GL values observed in sediments of the early Holocene probably indicate input of fresh, minerogenic, glacially-derived material. Then, in the mid-Holocene, there is an increase in the deposition of dark clay-rich *gyttja*. GL of cores has been demonstrated to be positively correlated with $\delta^{18}\text{O}$ from the GRIP core, and also

with atmospheric $\delta^{14}\text{C}$ (Stuiver & Reimer, 1993). There exists, therefore, a strong indication that during periods of warm climate, for example during the mid-Holocene, there is an increase in the deposition of dark clay-rich *gyttja*. Furthermore, during these periods $\delta^{14}\text{C}$ values are low, indicating increased solar activity, with a greater intensity of radiation incident on the Earth. This may, in turn, have acted to increase the amount of allochthonous organic material in the water column, possibly through an increase in temperature, *and precipitation*. It is not possible to determine the effect on GL of the distribution of individual storm layers, owing to insufficient resolution of the images used in this analysis.

Taken together, consideration of both lamination thickness and GL indicates that the mechanism of deposition of material in the Loch is influenced by the location of the NAPF, by insolation, and more recently, by the configuration of the NAO, especially during summer. The preceding discussion may be summarised as a flow chart (*Figure 7.1*).

It may thus be suggested that the sediment record consists of a 'continuum' of alternating fine silt, and allochthonous organic carbon and clay-sized layers deposited through the year, and which is infrequently punctuated by large influxes of eroded material brought in by severe storms. The amount of sediment deposited has been, in recent times, primarily affected by the action of the NAO during the summer and, to a lesser degree, by insolation, although during the early Holocene insolation may have been the prevalent agent. Since recent sedimentation appears to be correlated with the NAO, anthropogenic forcing of sedimentary processes within the Loch may still be negligible.

7.2 Summary

It is believed that the laminated sediments recovered from the profundal plain of Loch Ness are composed of clastic varves. Thin, pale layers are deposited during the

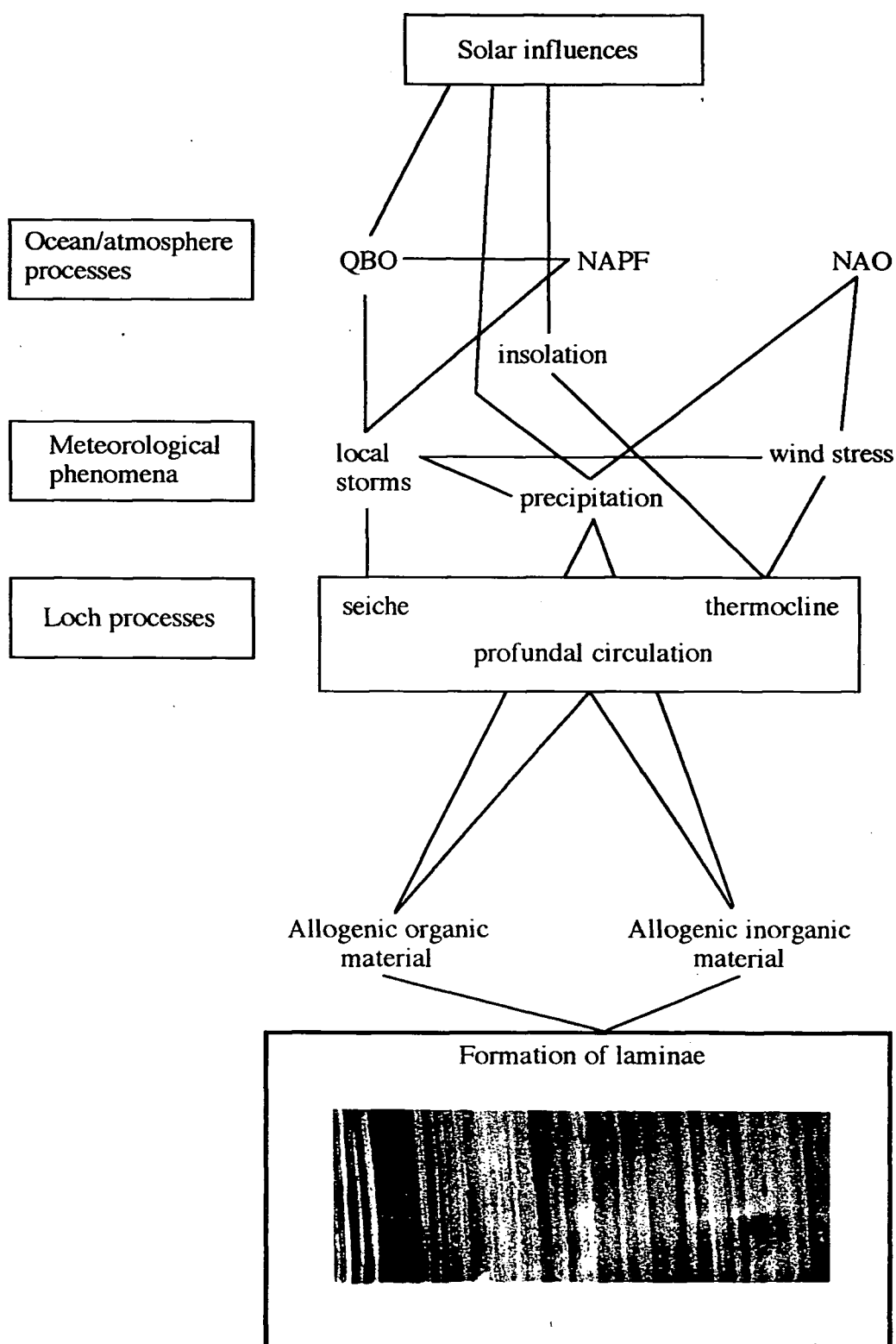


Figure 7.1 Flow chart summarising the factors influencing the formation of annually laminated sediments in the north basin of Loch Ness.

late winter and spring, with darker clay-rich laminae representing material sedimented throughout the rest of the year. Examination of X-radiographs and BSEI/SEM images reveals no reason to reject the hypothesis that only two laminae are produced each year, although annual examination of the sediment/water interface has not been carried out in order to test this. Results from radiocarbon dating of sediments appear to substantiate the assumption that lamination pairs are annual. Varve counting has produced a similar age/depth relationship to that obtained by ^{14}C dating, especially in sediment representing the Middle to Late Holocene.

Time series derived from lamination thickness measurements may not solely represent the effect of one climatic variable, but may be the product of several. Only weak correlations were found between lamination thickness and local climatic indices. The signal contained within time series derived from lamination thickness measurements, however, exhibits elements of periodicity which suggest that external forcing processes may affect sedimentation within the Loch. This is further borne out by the correlation between summer NAO index and lamination thickness from core *LNRI*, and by correlation of sunspot index and precipitation at Fort Augustus over the last century.

It has been demonstrated that the utilisation of image transforms may be employed in this type of study, enabling rapid characterisation and enumeration of laminated sediments. It is recognised, however, that more traditional types of analysis may still be more amenable and that image analysis be considered as a useful adjunct to them.

It is finally suggested that the north basin of Loch Ness be utilised as a site for the further recovery of annually laminated sediments, as these appear to exhibit a response to variations in climate within the North Atlantic region. This response has also been correlated with other climatically-dependent time series.

8. Further work

Further study will be necessary in order to clarify and expand upon the many questions raised by this investigation. In general, it is considered that the dynamic processes acting in the profundal environment of Loch Ness are poorly understood on all scales, and in particular, that a recent acoustic survey has highlighted possible shortcomings inherent in the present coring site.

Clearly, the dynamics of a system of such dimensions cannot be fully addressed by the study of two or three sediment cores from one location. Indeed, Håkanson & Jansson (1983), suggest that the minimum number of cores (n) required in such an investigation may be expressed as

$$n = 2.5 + 0.5 \sqrt{a \cdot f} \quad (8.1)$$

where a represents the area of the water body in km^2 , and f is a factor indicating the degree of shoreline development. Substituting the dimensions of the Loch into this equation, six cores are deemed to be necessary, and probably this number may be considered sufficient only to study processes acting in the immediate vicinity of the coring site.

The utilisation of the initial sediment core to be recovered, core *Ness 3*, may be criticised, since it eventually became clear that the quality of laminae is variable and many distortions and defects are present. Study of this material by diatom and pollen analyses may be justified by considering that problems encountered with coring at that time, cast doubt on the possibility of ever recovering further material. It was thus decided to utilise this core. It is recognised, however, that the chronology so far obtained needs to be extended, expanded and converted into a fixed timescale in order that a complete time series can be constructed for further analysis. Further scope also exists for the continuation of the chronology into the Late Pleistocene, for it is believed that *ca* 40 m of

sediment exist at the bottom of the Loch (Shine, pers. comm.).

Little is understood of the processes taking place in Loch Ness, especially those concerned with the deposition and resuspension of material in profundal areas. Influences of riverine inputs, wind stress and of circulation patterns have not been studied in detail and their effects on sediment deposition may only be estimated. The correlation between precipitation and seston deposition highlighted by R.I.Jones *et al.* (1996) does not directly imply that the thickness of sediment deposited in the profundal of the Loch be similarly correlated, since no studies of year-on-year variations at the SWI have been performed. In addition, erosion of surficial sediment has been assumed, for convenience, to have been constant, or even absent, throughout the seasons and throughout the time period represented by the cores, which is most probably not the case.

Thus, it is recommended that further study of sedimentation processes be attempted on an annual or sub-annual basis and these results correlated with climatic variables measured over the same time period. Further, investigation into processes acting at the sediment/water interface need to be fully understood, with special attention being focused upon variation of rates of erosion on a seasonal level and the effect of large volumes of water input to the Loch over short time periods, for example during flood events. The effect of sediment input from flooding in remote areas of the catchment may also require study in order to ascertain whether or not the *thick*, pale, silt-rich laminae (such as that produced by the 1868 flood) represent only *local* storm events.

Recovery of further material from the Loch may be considered of paramount importance in order to complete and verify the chronology derived from lamination counting. The utilisation of annually laminated sediments in the verification of radiocarbon dating has already been mentioned. Furthermore, it has been demonstrated that fractionation of the various forms of organic carbon within sediments may be performed, in order that these may be dated separately and the results analysed to ascertain which

fraction yields the date closest to that obtained by lamination counting (Eglinton *et al.*, 1998). Loch Ness may be an important site within the UK from which to proceed with this type of investigation, in addition to its rôle as an archive of the palaeoclimate of the region.

9. References

- Aaby B. 1976. Cyclic climatic variations in climate over the past 5,500 yr reflected in raised bogs. *Nature*. **263**. 281-284.
- Alapieti T. & Saarnisto M. 1981. Energy Dispersive X-Ray Microanalysis of Laminated Sediments from Lake Valkiajärvi, Finland. *Bulletin of the Geological Society of Finland*. **53**. 3-9.
- Algeo T.J., Phillips M., Jaminski J. & Fenwick M. 1994. High-resolution x-radiography of laminated sediment cores. *Journal of Sedimentary Research*. **A64**. 665-669.
- Alley, R.B., Mayewski P.A., Sowers T., Stuiver M., Taylor K.C. & Clark P.U. 1997. Holocene climate instability: A prominent, widespread event 8200 yr ago. *Geology*. **25**. 483-486.
- Allison T.D. & Moeller R.E. 1989. Organic laminations and detailed chronology for Holocene sediment at Pout Pond, New Hampshire, USA. *Archiv für Hydrobiologie*. **116**. 161-180.
- Allison T.D., Moeller R.E. & Davis M.B. 1986. Pollen in laminated sediments provides evidence for a Mid-Holocene forest pathogen outbreak. *Ecology*. **67**. 1101-1105.
- Anderson R.Y. 1993. The varve chronometer in Elk Lake: record of climatic variability and evidence for solar-geomagnetic-¹⁴C-climate connection. In Bradbury J.P. & Dean W.E. (eds) 1993. *Elk Lake, Minnesota: Evidence for rapid climate change in the North-Central United States*. USGS Special Paper 276. United States Geological Survey. 45-67.

-
- Anderson R.Y., Dean W.E., Bradbury J.P. & Love D. 1985. *Meromictic Lakes and Varved Sediments in North America*. U.S. Geological Survey Bulletin 1607. US Government Printing Office, Washington.
- Anderson R.Y., Linsley B.K. & Gardner J.V. 1990. Expression of seasonal and ENSO forcing in climate variability at lower than ENSO frequencies: evidence from Pleistocene marine varves off California. *Paleogeography, Paleoclimatology, Paleoecology*. **78**. 287-300.
- Anderson R.Y. & Dean W.E. 1988. Lacustrine Varve Formation Through Time. *Paleogeography, Paleoclimatology, Paleoecology*. **62**. 215-235.
- Anderson R.Y., Dean W.E. & Bradbury J.P. 1993. Elk Lake in perspective. In Bradbury J.P. & Dean W.E. (eds) 1993. *Elk Lake, Minnesota: Evidence for rapid climate change in the North-Central United States*. USGS Special Paper 276. United States Geological Survey. 1-6.
- Andrews J.T., Erlenkeuser H., Tedesco K., Aksu A.E. & Jull A.J.T. 1994. Late Quaternary (Stage 2 and 3) Meltwater and Heinrich Events, Northwest Labrador Sea. *Quaternary Research*. **41**. 26-34.
- Anthony R.S. 1977. Iron-rich rhythmically laminated sediments in the Lake of the Clouds, northeastern Minnesota. *Limnology and Oceanography*. **22**. 45-54.
- Appleby P.G., Oldfield F., Thompson R., Huttunen P. & Tolonen K. 1979. ^{210}Pb dating of annually laminated lake sediments from Finland. *Nature*. **280**. 53-55.
- Appleby P.G., Richardson N., Nolan P.J. & Oldfield F. 1990. Radiometric dating of the United Kingdom SWAP sites. *Philosophical Transactions of the Royal Society of*
-

London. **B327**. 233-238.

- Appleby P.G., Richardson N., Smith J. 1993. The use of radionuclide records from Chernobyl and weapons test fallout for assessing the reliability of ^{210}Pb in dating very recent sediments. *Verhandlungen der Internationalen Vereinigung für Theoretische and Angewandte Limnologie*. **25**. 266-269.
- Arslanov K.A. & Svezhentsev Y.S. 1993. An Improved Method for Radiocarbon Dating Fossil Bones. *Radiocarbon*. **35**. 387-391.
- Assel R.A. 1998. The 1997 ENSO event and implication for North American Laurentian Great Lakes winter severity and ice cover. *Geophysical Research Letters*. **25**. 1031-1033.
- Axelsson V. 1983. The use of X-Ray radiographic methods in studying sedimentary properties and rates of sediment accumulation. *Hydrobiologia*. **103**. 65-69.
- Bailey-Watts A.E. & Duncan P. 1981. Chemical characterisation-a one-year comparative study. In Maitland P.S. (ed.) *The Ecology of Scotland's Largest Lochs. Lomond, Awe, Ness, Morar and Shiel. Monographiae Biologicae*. **44**. Dr.W.Junk Publishers, The Hague. 67-87.
- Baillie M.G.L. 1977a. An Oak Chronology for South Central Scotland. *Tree-Ring Bulletin*. **37**. 33-44.
- Baillie M.G.L. 1977b. The Belfast Oak Chronology to AD 1001. *Tree-Ring Bulletin*. **37**. 1-12.

-
- Baillie M.G.L. & Munro M.A.R. 1988. Irish tree rings, Santorini and volcanic dust veils. *Nature*. **332**. 344-346.
- Baker A., Smart P.L., Edwards R.L. & Richards D.A. 1993. Annual growth banding in a cave stalagmite. *Nature*. **364**. 518-520.
- Baker A., Smart P.L., Barnes W.L., Edwards R.L. & Farrant A. 1995. The Hekla 3 volcanic eruption recorded in a Scottish speleothem? *The Holocene*. **5**. 336-342.
- Barber K.E., Chambers F.M., Maddy D., Stoneman R. & Brew J.S. 1994. A sensitive high-resolution record of late Holocene climatic change from a raised bog in northern England. *The Holocene*. **4**. 198-205.
- Barnola J.M., Raynaud D., Korotkevich Y.S. & Lorius C. 1987. Vostok ice core provides 160,000 year record of atmospheric CO₂. *Nature*. **329**. 408-414.
- Barnston A.G. 1996. Time-scales of variability of the atmosphere. *International Journal of Climatology*. **16**. 499-535.
- Barry R.G. & Chorley R.J. 1992. *Atmosphere, Weather and Climate*. Routledge, London and New York. 392 pp.
- Battarbee R.W. 1991. Recent paleolimnology and diatom-based environmental reconstruction. In Shane L.C.K. & Cushing E.J. (eds) *Quaternary Landscapes*. Belhaven Press, London. 129-174.
- Battarbee R.W. & Allott T.E.H. 1994. Palaeolimnology. In Maitland P.S., Boon P.J. & McLusky D.S. (eds) *The Fresh Waters of Scotland: A National Resource of International Significance*. J. Wiley & Sons Ltd. 113-130.
-

-
- Battarbee R.W., Flower R.J., Stevenson A.C., Jones V.J., Harriman R. and Appleby P.G. 1988. Diatom and chemical evidence for reversibility of acidification of Scottish lochs. *Nature*. **332**. 530-532.
- Baumgartner T.R., Michaelson J., Thompson L.G., Shen G.T., Soutar A. & Casey R.E. 1989. The recording of interannual climatic change by high-resolution natural systems: Tree-rings, coral bands, glacial ice layers and marine varves. In Peterson D.H. (ed.) *Aspects of climate variability in the Pacific and the western Americas. Geophysical Monograph 55*. American Geophysical Union, Washington, USA. 1-14.
- Beer J., Joos L., Lukaczyk C., Mende W., Rodriguez J., Siegenthaler U. & Stellmacher R. 1994. ^{10}Be as an indicator of solar variability and climate. In Nesme-Ribes E. (ed.) *The Solar Engine and its Influence on Terrestrial Atmosphere and Climate. NATO ASI Series. 125*. Springer-Verlag Berlin. 221-233.
- Belasco J.E. 1952. Characteristics of air masses over the British Isles. *Geophysical Memoirs*. 11. (87). Meteorological Office, London. 34pp.
- Bender M., Sowers T., Dickson M.-L., Orchardo J., Grootes P., Mayewski P.A. & Meese D.A. 1994. Climate correlations between Greenland and Antarctica during the past 100,000 years. *Nature*. **372**. 663-666.
- Bennett K.D. 1986. Coherent slumping of early postglacial lake sediments at Hall Lake, Ontario, Canada. *Boreas*. **15**. 209-215.
- Bennett K.D. 1995. Post-glacial dynamics of Pine (*Pinus sylvestris* L.) and pinewoods in Scotland. In Aldhous J.R. (ed.) *Our Pinewood Heritage*. Forestry Commission, Royal Society for the Protection of Birds and Scottish Natural Heritage. 23-39.
-

-
- Bennett S. 1992. *Pattern and process of sedimentation in Loch Ness*. BSc. (Hons) dissertation. University of Staffordshire. UK.
- Bennett S. & Shine A.J. 1993. Review of current work on Loch Ness sediment cores. *Scottish Naturalist*. **105**. 55-63.
- Berger A. 1977. Power and limitation of an energy-balance climate model as applied to the astronomical theory of paleoclimates. *Paleogeography, Paleoclimatology, Paleoecology*. **21**. 227-235.
- Berger A. 1989. The spectral characteristics of Pre-Quaternary climatic records, an example of the relationship between the astronomical theory and geo-sciences. In Berger A., Schneider S. & Duplessy J.-C. (eds) *Climate and Geo-Sciences. A Challenge for Science and Society in the 21st Century. NATO ASI Series C: Mathematical and Physical Sciences*. **285**. Kluwer Academic Publishers, Dordrecht. 47-76.
- Berger W.H. & Labeyrie L.D. 1987. Abrupt climatic change- an introduction. In Berger W.H. & Labeyrie L.D. (eds) *Abrupt Climatic Change. NATO ASI Series C. Mathematical and Physical Sciences*. **216**. D.Reidel Publishing Company, Dordrecht. 3-22.
- Berger A., Mélice J.L., Van Der Mersch I. 1990. Evolutive spectral analysis of sunspot data over the past 300 years. *Philosophical Transactions of the Royal Society of London*. **A330**. 529-541.
- Berger W.H., Burke S. & Vincent E. 1987. Glacial-Holocene transition: climate pulsations and sporadic shutdown of NADW production. In Berger W.H and Labeyrie L.D. (eds) *Abrupt Climatic Change. NATO ASI Series C: Mathematical*
-

-
- and Physical Sciences*. **216**. D.Reidel Publishing Company, Dordrecht. 279-297.
- Beukens R.P. 1992. Radiocarbon accelerator mass spectrometry: background, precision and accuracy. In Taylor R.E, Long A. & Kra R.S. (eds). *Radiocarbon After Four Decades. An Interdisciplinary Perspective*. Springer-Verlag, New York. 230-239.
- Birks H.H. 1972. Studies in the vegetational history of Scotland III. A radiocarbon-dated pollen diagram from Loch Maree, Ross and Cromarty. *New Phytologist*. **71**. 731-754.
- Birks H.J.B. 1996. Great Britain-Scotland. In Berglund B.E., Birks H.J.B., Ralska-Jasiewiczowa M. and Wright H.E. (eds) *Palaeological Events During the Last 15,000 Years: Regional Syntheses of Palaeoecological Studies of Lakes and Mires in Europe*. John Wiley and Sons Ltd. Chichester, UK. 95-143.
- Bishop W.W. & Coope G.R. 1977. Stratigraphical and faunal evidence for late glacial and early Flandrian environments in South West Scotland. In Gray J.M & Lowe J.J. (eds) *Studies in Scottish Late Glacial Environments*. Pergamon Press, Oxford. 61-88.
- Bjerkness J. 1969 Atmospheric teleconnections from the equatorial Pacific. *Monthly Weather Review*. **97**. 163-72.
- Björck S., Sandgren P. & Holmquist B. 1987. A magnetostratigraphic comparison between ^{14}C years and varve years during the Late Weichselian, indicating significant differences between the time-scales. *Journal of Quaternary Science*. **2**. 133-140.
-

-
- Björck S., Kromer B., Johnsen S., Bennike O., Hammarlund D., Lemdahl G., Possnert G., Rasmussen T.L., Wohlfarth B., Hammer C.U. & Spurk M. 1996. Synchronized terrestrial-atmospheric deglacial records around the North Atlantic. *Science*. **274**. 1155-1160.
- Bodbacka L. 1985. Annually laminated sediments in two basins of Lake Mälaren (Lilla Ullfjärden and Stora Ullfjärden) studied by X-ray radiography. *Geografiska Annaler*. **67A**. 145-150.
- Boespflug X., Long B.F.N. & Occhietti S. 1995. CAT-scan in marine stratigraphy: a quantitative approach. *Marine Geology*. 122: 281-301.
- Bond G.C & Lotti R. 1995. Iceberg discharges into the North Atlantic on millennial time scales during the last glaciation. *Science*. **267**. 1005-1010.
- Bond G., Showers W., Cheseby M., Lotti R., Almasi P., deMenocal P., Priore P., Cullen H., Hajdas I. & Bonani G. 1997. A pervasive millennial-scale cycle in North Atlantic Holocene and Glacial climates. *Science*. **278**. 1257-1266.
- Boulton G.S., Peacock J.D. & Sutherland D.G. 1991. Quaternary. In Craig G.Y. (ed.) *The Geology of Scotland*. 3rd edition. The Geological Society, London. 503-541.
- Boutton T.W. 1991. Stable Carbon isotope ratios of natural materials: II. Atmospheric, terrestrial, marine, and freshwater environments. In Coleman D. & Fry B. (eds) *Carbon Isotope Techniques*. Academic Press Inc., New York. 173-185.
- Boyle J. 1993. The Swedish varve chronology-a review. *Progress in Physical Geography*. **17**. 1-19.
-

-
- Boyko-Diakonow M. 1979. The laminated sediments of Crawford Lake, southern Ontario, Canada. In Schlüchter C. (ed.) *Moraines and varves. Origins/ Genesis/ Classification*. Balkema, Rotterdam. 303-307.
- Bradbury J.P. & Dean W.E. (eds). 1993. *Elk Lake, Minnesota: Evidence for rapid climate change in the North-Central United States. USGS Special Paper 276*. United States Geological Survey. 336 pp.
- Bradbury J.P. & Dieterich-Rurup K.V. 1993. Holocene diatom paleolimnology of Elk Lake, Minnesota. In Bradbury J.P. & Dean W.E. (eds) *Elk Lake, Minnesota: Evidence for rapid climate change in the North-Central United States. USGS Special Paper 276*. United States Geological Survey. 215-238.
- Bradley R.S. 1994. Perspectives on the climate of the last 500 years. In Nesme-Ribes E. (ed.) *The Solar Engine and its Influence on Terrestrial Atmosphere and Climate. NATO ASI Series. 125*. Springer-Verlag, Berlin. 437-447.
- Bradley R.S. & Jones P.D. (eds) 1995. *Climate since A.D. 1500*. 2nd Edition. Routledge, London. 706 pp.
- Bradley R.S., Retelle M.J., Ludlam S.D., Hardy D.R., Zolitschka B., Lamoureux S.F. & Douglas M.S.V. 1996. The Taconite Inlet Lakes Project: a systems approach to paleoclimatic reconstruction. *Journal of Paleolimnology*. **16**. 97-110.
- Breeze D.J. 1982. *The northern frontiers of Roman Britain*. St.Martin's Press Inc., New York. 188 pp.
- Bridge M.C., Haggart B.A. & Lowe J.J. 1990. The history and palaeoclimatic significance of subfossil remains of *Pinus sylvestris* in blanket peats from
-

Scotland. *Journal of Ecology*. **78**. 77-99.

- Briffa K.R. 1994. Grasping at shadows? A selective review of the search for sunspot-related variability in tree rings. In Nesme-Ribes E. (ed.) *The Solar Engine and its Influence on Terrestrial Atmosphere and Climate*. NATO ASI Series. **125**. Springer-Verlag, Berlin. 417-435.
- Briffa K.R., Jones P.D. & Schweingruber F.H. 1988. Summer Temperature Patterns over Europe: A Reconstruction from 1750AD. Based on Maximum Latewood Density Indices of Conifers. *Quaternary Research*. **30**. 36-52.
- Briffa K.R., Jones P.D. & Kelly P.M. 1990a. Principal component analysis of the Lamb catalogue of daily weather types: part 2, seasonal frequencies and update to 1987. *International Journal of Climatology*. **10**. 549-563.
- Briffa K.R., Jones P.D. & Schweingruber F.H. 1988. Summer Temperature Patterns over Europe: A Reconstruction from 1750AD. Based on Maximum Latewood Density Indices of Conifers. *Quaternary Research*. **30**. 36-52.
- Briffa K.R., Bartholin T.S., Eckstein D., Jones P.D., Karlén W., Schweingruber F.H. & Zetterberg P. 1990b. A 1,400-year tree-ring record of summer temperatures in Fennoscandia. *Nature*. **346**. 434-439.
- Brodie I. & Kemp A.E.S. 1994. Variation in biogenic and detrital fluxes and formation of laminae in late Quaternary sediments from the Peruvian coastal upwelling zone. *Marine Geology*. **116**. 385-398.
- Broecker W. S. 1994. Massive iceberg discharges as triggers for global climate change. *Nature*. **372**. 421-424.

-
- Broecker W.S. & Denton G.H. 1990. The role of ocean-atmosphere reorganisations in glacial cycles. *Geochimica et Cosmochimica Acta*. **53**. 2465-2501.
- Broecker W.S. & van Donk. 1970. Insolation changes, ice volumes and the ^{18}O record in deep-sea cores. *Review of Geophysics and Space Science*. **8**. 169-198.
- Broecker W.S., Bond G., Klas M., Clark E. & McManus J. 1992. Origin of the northern Atlantic's Heinrich events. *Climate Dynamics*. **6**. 265-273.
- Broecker W.S., Andree M., Wolfli W., Oeschger H., Bonani G., Kennett J. & Peteet D. 1988. The chronology of the last deglaciation: implications to the cause of the Younger Dryas event. *Paleoceanography*. **3**. 1-19.
- Burroughs W.J. 1992. Weather cycles. Real or imaginary? Cambridge University Press. Cambridge, UK. 210 pp.
- Callaway J.C., Delaune R.D. & Patrick W.H. 1996. Chernobyl Cs-137 used to determine sediment accretion rates at selected Northern European coastal wetlands. *Limnology and Oceanography*. **41**. 444-450.
- Canning J.C., Henney P.J., Morrison M.A., van Calsteren P.W.C., Gaskarth J.W. & Swarbrick A. 1998. The Great Glen Fault: a major vertical lithospheric boundary. *Journal of the Geological Society*. **155**. 425-428.
- Castagnoli G.C. & Bonino G. 1988. Solar imprint in sea sediments: the thermoluminescence profile as a new proxy record. In Stephenson F.R and Wolfendale A.W. (eds) *Secular Solar and Geomagnetic Variations in the Last 10,000 Years*. NATO ASI series C. Mathematical and Physical Sciences. **236**.
-

Kluwer Academic, Dordrecht. 341-348.

- Castleden R. 1992. *Neolithic Britain: new stone age sites of England, Scotland and Wales*. Routledge, London. 432 pp.
- Cave M.A., Eshel G. & Buckland R.W. 1994. Forecasting Zimbabwean maize yield using eastern equatorial Pacific sea surface temperature. *Nature*. **370**. 204-205.
- Chatfield C. 1989. *The analysis of time series. An introduction*. 4th edition. Chapman & Hall, London. 241 pp.
- Churski Z., Marszelewski W. & Szczepanik W. 1993. The dynamic and conditions of sedimentation in Lake Gosciaz. In Ralska-Jasiewiczowa M. (ed) *Polish Botanical Study. Guidebook Series* . **8**. 15-28.
- Clark J.S. 1993. Fire, climate, and forest processes during the past 2000 years. In Bradbury J.P. & Dean W.E. (eds) *Elk Lake, Minnesota: Evidence for rapid climate change in the North-Central United States. USGS Special Paper 276*. United States Geological Survey. 295-308.
- Cline W.R. 1992. *Global Warming: Estimating the economic benefits of abatement*. OECD. Paris. 69 pp.
- Coldstream J.I., Newbury D.S., Echlin P., Joy D.C., Romig A.D., Lyman C.E., Fiori C. & Lifshin E. 1992. *Scanning Electron Microscopy and X-ray analysis*. Plenum Press. New York. 2nd edition. 820 pp.
- Coope G.R. 1977. Fossil coleopteran assemblages as sensitive indicators of climatic changes during the Devensian (Last) cold stage. *Philosophical Transactions of the*

Royal Society of London. B280. 313-337.

- Coope G.R. 1987. Fossil beetle assemblages as evidence for sudden and intense climatic changes in the British Isles during the last 45,000 years. In Berger W.H. and Labeyrie L.D. (eds) *Abrupt Climatic Change. NATO ASI Series C. Mathematical and Physical Sciences*. D. Reidel Publishing Company, Dordrecht. **216**. 147-150.
- Coope G.R. and Brophy 1972. Late glacial environmental changes indicated by coleopteran succession from North Wales. *Boreas*. **1**. 97-142.
- Cooper M.C. 1998. The Use of Image Analysis techniques in the study of laminated sediments. *Journal of Paleolimnology*. **19**. 33-40.
- Cooper M.C., O'Sullivan P.E. & Shine A.J. The record of climatic variability in the Holocene laminated sediments of Loch Ness, Scotland. Paper presented at the 2nd annual workshop of the European Lakes Drilling Program, Kraków, Poland. 23-26 October 1997. Submitted to *Quaternary International*.
- Cooper M.C., O'Sullivan P.E., Harkness D.D., Lawson E.M., Bull D.J., Kemp A.E.S., Peglar S.M., Matthews N.M., Jones R.I. & Shine A.J. 1998. Radiocarbon dating of laminated sediments from Loch Ness, Scotland. Paper presented at the XVIth International Radiocarbon Conference, Groningen, The Netherlands. 16-20th June, 1997. *Radiocarbon*. **40**. 781-793.
- Cooper M.C., O'Sullivan P.E., Shine A.J., Peglar S.M., Matthews N.M., Salter N.C.J., Henon D.N., Jones V.J., Williams T.S.C., Nicholson M.J., Sandford R.E. & Morris A. (In press) The environmental record in the Holocene laminated sediments of Loch Ness, Scotland- an outline. Submitted to *Journal of*

Paleolimnology.

- Creer K.M. 1988. Geomagnetic Field and Radiocarbon Activity through Holocene time. In Stephenson F.R and Wolfendale A.W. (eds) *Secular Solar and Geomagnetic Variations in the Last 10,000 Years. NATO ASI series C. Mathematical and Physical Sciences.* **236**. Kluwer Academic, Dordrecht. 381-397.
- Currie R.G. 1994a. Luni-solar 18.6- and solar cycle 10-11-year signals in USA air temperature records. *International Journal of Climatology.* **13**. 31-50.
- Currie R.G. 1994b. Luni-solar 18.6- and 10-11-year solar cycle signals in South African rainfall. *International Journal of Climatology.* **13**. 237-256.
- Currie R.G. 1994c. Luni-solar 18.6- and 10-11-year solar cycle signals in H.H. Lamb's Dust Veil Index. *International Journal of Climatology.* **14**. 215-226.
- Currie R.G. 1994d. Variance contribution of Luni-solar and Solar cycle signals in the St. Lawrence and Nile river records. *International Journal of Climatology.* **14**. 843-852.
- Currie R.G. 1995. Luni-solar 18.6- and Solar cycle 10-11-Year signals in Chinese Dryness-Wetness Indices. *International Journal of Climatology.* **15**. 497-515.
- Curry R.G., McCartney M.S. & Joyce T.M. 1998. Oceanic transport of subpolar climate signals to mid-depth subtropical waters. *Nature.* **391**. 575-577.
- Cwynar L.C. 1978. Recent history of fire and vegetation from laminated sediment of Greenleaf Lake, Algonquin Park, Ontario. *Canadian Journal of Botany.* **56**. 10-21.

-
- Damon P.E. & Jirikowic J.L. 1992. Solar Forcing of Global Climate Change? In Taylor R.E., Long A. & Kra R.S. (eds) *Radiocarbon After Four Decades. An Interdisciplinary perspective*. Springer-Verlag. New York. 117-129.
- Dansgaard W. & Oeschger H. 1989. Past environmental long-term records from the Arctic. In Oeschger H. & Langway C.C. (eds) *The Environmental Record in Glaciers and Ice Sheets. Report of the Dahlem Workshop, Berlin 1988, March 13-18. Research report 8*. J.Wiley & Sons, Chichester, UK. 287-318.
- Dansgaard W., Clausen H.B., Gundestrup N., Hammer C.U., Johnsen S.F., Kristinsdottir P.M. & Rech N. 1984. A new Greenland deep ice core. *Science*. **218**. 1273-1277.
- D'Arrigo R.D., Cook E.R., Jacoby G.C. & Briffa K.R. 1993. NAO and Sea Surface Temperature Signatures in Tree-Ring records from the North Atlantic Sector. *Quaternary Science Reviews*. **12**. 431-440.
- Dartnell P and Gardner J.V. 1993. Digital imaging of sediment cores for archives and research. *Journal of Sedimentary Petrology*. **63**. 750-752.
- Davis R.E. & Benkovic S.R. 1994. Spatial and temporal variations of the January Circumpolar Vortex over the Northern Hemisphere. *International Journal of Climatology*. **14**. 415-428.
- Dean J.M. (unpubl.) PhD thesis. University of Southampton. UK. (In preparation).
- Dean W.E., Bradbury J.P., Anderson R.Y., Ramirez Bader L., & Dieterich-Rurup K. 1994. *A High-Resolution Record of Climatic Change in Elk Lake, Minnesota for the Last 1500 Years. US Geological Survey Open-file Report 94-578*. USGS,
-

Denver, USA. 127 pp.

- Dean W.E., Bradbury J.P., Anderson R.Y. & Barnosky C.W. 1984. The variability of Holocene climate change: evidence from varved lake sediments. *Science*. **226**. 1191-1194.
- de Beaulieu J.L, Pons A. and Reille M. 1982. Recherches pollenanalytiques sur l'histoire de la végétation de la bordure Nord du massif du Cantal (France). *Pollen et Spores*. **24**. 251-300.
- Denton G.H. & Hendy C.H. 1994. Younger Dryas Age Advance of Franz Josef Glacier in the Southern Alps of New Zealand. *Science*. **264**. 1434-1437.
- Desloges J.R. 1994. Varve deposition and the sediment yield record at 3 small lakes of the southern Canadian Cordillera. *Arctic and Alpine Research*. **26**. 130-140.
- Desloges J.R. & Gilbert R. 1995. The sedimentary record of Moose Lake: implications for glacier activity in the Mount Robson area, British Columbia. *Canadian Journal of Earth Science*. **32**. 65-78.
- de Vernal A., Hillaire-Marcel C. & Bilodeau G. 1996. Reduced meltwater outflow from the Laurentide ice margin during the Younger Dryas. *Nature*. **381**. 774-777.
- Devine T.M. 1988. *The Great Highland Famine*. John Donald, Edinburgh.
- Diaz H.F. & Markgraf V. (eds). 1992. *El Niño. Historical and Paleoclimatological Aspects of the Southern Oscillation*. Cambridge University Press. 476 pp.
- Dickman M.D. 1979. A Possible Varving Mechanism for Meromictic Lakes. *Quaternary*

Research. **11.** 113-124.

- Digerfeldt G., Battarbee R.W. & Bengtsson L. 1975. Report on annually laminated sediment in lake Järlasjön, Nacka, Stockholm. *Geologiska Föreningens i Stockholm Förhandlingar.* **97.**29-40.
- Druffel E.R.M. & Griffin S. 1993. Large variations of surface ocean radiocarbon - evidence of circulation changes in the Southwestern Pacific. *Journal of Geophysical Research-Oceans.* **98.** 20249-20259.
- Drury S.A. 1993. *Image Interpretation in Geology.* 2nd edition. Chapman & Hall, London. 283 pp.
- Dugmore A. 1989. Icelandic volcanic ash in Scotland. *Scottish Geographical Magazine.* **105.** 168-172.
- Dunbar R.B., Wellington G.M., Colgan M. & Glynn P.W. 1994. Eastern Pacific climate variability since AD 1600: stable isotopes in Galapagos corals. *Paleoceanography.* **9.** 291-315.
- Duplessy J.C., Delibrias G., Turon J.L., Pujol C. & Duprat J. 1981. Deglacial warming of the northeastern Atlantic ocean: correlation with the paleoclimatic evolution of the European continent. *Palaeogeography, Palaeoclimatology, Palaeoecology.* **35.** 121-144.
- Dwyer G.S., Cronin T.M., Baker P.A., Raymo M.E., Buzas J.S. & Corrège T. 1995. North Atlantic Deepwater temperature change during Late Pliocene and Late Quaternary climatic cycles. *Science.* **270.** 1347-1351.

-
- Eastman Kodak Company. 1972. *Infrared and Ultraviolet photography. First Combined edition. Kodak Technical Publication No. M-27/28-H*. Kodak Technical Publications, Rochester, New York. USA. 88 pp.
- Edwards C. 1996. Wavelet analysis transforms data processing. *Scientific Computing World*. June. 19-24.
- Edwards K.J. 1993. Human impact on the prehistoric environment. In Smout T.C. (ed.). *Scotland since Prehistory. Natural change and human impact*. Scottish Cultural Press, Edinburgh. 17-27
- Edwards R.L., Cheng H., Murrell M.T. & Goldstein S.J. 1997. Protoactinium-231 dating of carbonates by Thermal Ionization Mass Spectrometry: Implications for Quaternary climate change. *Science*. **276**. 782-786.
- Edwards R.L., Beck J.W., Burr G.S., Donahue D.J., Chappell J.M.A., Bloom A.L., Druffel E.R.M. & Taylor F.W. 1993. A Large Drop in Atmospheric $^{14}\text{C}/^{12}\text{C}$ and Reduced Melting in the Younger Dryas, Documented with ^{230}Th Ages of Corals. *Science*. **260**. 962-968.
- Eglinton G., Bradshaw S.A., Rosell A., Sarnthein M., Pflaumann U. & Tiedemann R. 1992. Molecular record of secular sea surface temperature changes on 100-year timescales for glacial terminations I, II, and IV. *Nature*. **356**. 423-426.
- Eglinton T.I., Benitez-Nelson B.C., Pearson A., McNichol A.P., Bauer J.E. & Druffel E.R.M. 1997. Variability in the radiocarbon ages of individual organic compounds from marine sediments. *Science*. **277**. 796-799.
- Eglinton T.I., Pearson A., Benitez-Nelson B.C., McNichol A.P., Ertel J.R., Bauer J.E.
-

-
- & Druffel E.R.M. 1998. ^{14}C measurements of individual sedimentary organic compounds: a tool for developing refined sediment chronologies and understanding source inputs. *Radiocarbon*. **39/40**. (In press).
- Eisenhauer A., Zhu Z.R, Collins L.B, Wyrwoll K.W. & Eichstatter R.. 1996. The last interglacial sea-level change-new evidence from the Abrolhos Islands, West Australia. *Geologische Rundschau*. **85**. 606-614.
- Ely L.L., Enzel Y., Baker V.R. & Cayan D.R. 1993. A 5000-Year Record of Extreme Floods and Climate Change in the Southwestern United States. *Science*. **262**. 410-412.
- Engstrom D.R. & Wright H.E. 1984. Chemical stratigraphy of lake sediments as a record of environmental change. In Haworth E.Y. & Lund J.W.G. (eds). *Lake Sediments and Environmental History*. Leicester University Press. 11-69.
- Farr K.M., Jones D.M., O'Sullivan P.E., Eglinton G., Tarling D.H. & Hedges R.E.M. 1990. Paleolimnological studies of laminated sediments from the Shropshire-Cheshire meres. *Hydrobiologia*. **214**. 279-292.
- Feng X. & Epstein S. 1995. Climatic temperature records in δD data from tree rings. *Geochimica et Cosmochimica Acta*. **59**. 3029-3037.
- Firth C.R. 1989. Raised shorelines and ice limits in the inner Moray Firth, northern Scotland. *Boreas*. **18**. 5-21.
- Firth C.R. 1993. Inverness area (Dores). In Gordon J.E and Sutherland D.G. (eds) *Quaternary of Scotland*. Chapman and Hall, London. 196-199.
-

-
- Flohn H. and Fantechi R. 1984. *The Climate of Europe: Past Present and Future. Natural and man-induced climatic changes. A European perspective*. D. Reidel, Dordrecht.
- Flower R.J., Mackay A.W., Rose N.L., Boyle J.L., Dearing J.A., Appleby P.G., Kuzmina A.E. & Granina L.Z. 1995. Sedimentary records of recent environmental change in Lake Baikal, Siberia. *The Holocene*. **5**. 323-327.
- Fraedrich K. 1994. An ENSO impact on Europe? A review. *Tellus*. **46**. 541-552.
- Fraedrich K. & Müller K. 1992. Climatic anomalies in Europe associated with ENSO extremes. *International Journal of Climatology*. **12**. 25-31.
- Friis-Christensen E. & Lassen K. (1991). Length of the solar cycle: an indicator of solar activity closely associated with climate. *Science*. **254**. 698-700.
- Fritts H. 1976. *Tree rings and climate*. Academic Press, London, UK. 567 pp.
- Fritz S.C., Juggins S., Battarbee R.W. & Engstrom D.R. 1991. Reconstruction of past changes in salinity and climate using a diatom-based transfer function. *Nature*. **352**. 706-708
- Fromm E. 1980. An estimation of errors in the Swedish varve chronology. In Ollsson I.U. (ed.) *Nobel Symposium 12, Radiocarbon Variations and Absolute Chronology*. Wiley Interscience, New York. 163-172.
- Gale S.J., Haworth R.J. & Pisanu P.C. 1995. The ^{210}Pb chronology of Late Holocene deposition in an eastern Australian lake basin. *Quaternary Science Reviews*
-

-
- (*Quaternary Geochronology*). **14**. 395-408.
- Gasse F. & Van Campo E. 1994. Abrupt post-glacial climate events in West Asia and North Africa monsoon domains. *Earth and Planetary Science Letters*. **126**. 435-456.
- Gasse F., Arnold M., Fontes J.C., Fort M., Gilbert E., Huc A., Bingyan L., Yuanfang L., Qing L., Melieres F., Van Campo E., Fubao W. & Qingsong Z. 1991. A 13,000-year climate record from western Tibet. *Nature*. **353**. 742-745.
- Gerety E.J., Wallace J.M. & Zerefos C.S. 1977. Sunspots, geomagnetic indices and the weather: across spectral analysis between sunspots, geomagnetic activity and global weather data. *Journal of Atmospheric Science*. **34**. 673-678.
- Glasbey C.A & Horgan G.W. 1995. *Image Analysis for the Biological Sciences*. John Wiley and Sons. Chichester, UK. 218 pp.
- Godwin H. 1975. *The History of the British Flora*. Cambridge University Press, Cambridge.
- Goodess C.M., Palutikof J.P. & Davies T.D. 1992. *The Nature and Causes of Climate Change*. Belhaven Press, London. 248 pp.
- Gordon D., Smart P.L., Ford D.C., Andrews J.N., Atkinson T.C., Rowe P.J. & Christopher N.J. 1989. Dating of Late Pleistocene interglacial and interstadial periods in the United Kingdom from speleothem growth frequency. *Quaternary Research*. **31**. 14-26.
- Goslar T. 1993. Varve chronology of laminated sediments of Lake Gosciadz. In
-

-
- Ralska-Jasiewiczowa M. (ed.) *Polish Botanical Study. Guidebook Series*. **8**. 105-119.
- Goslar T., Arnold M. & Pazdur M.F. 1995. The Younger Dryas cold event- was it synchronous over the North Atlantic region? *Radiocarbon*. **37**. 63-70.
- Goslar T., Kuc T., Pazdur M.F., Ralska-Jasiewiczowa M., Rózanski K., Szeroczynska K., Walanus A., Wicik B., Wieckowski K., Arnold M. & Bard E. 1992. Possibilities for Reconstructing Radiocarbon Level Changes During the Late Glacial by using a laminated sequence of Gosciąz Lake. *Radiocarbon*. **34**. 826-832.
- Goslar T., Kuc T., Ralska-Jasiewiczowa M., Rózanski K., Arnold M., Bard E., Van Geel B., Pazdur M.F., Szeroczynska K., Wicik B., Wieckowski K. & Walanus A. 1993. High-resolution lacustrine record of the Late Glacial/Holocene transition in Central Europe. *Quaternary Science Reviews*. **12**. 287-294.
- Goudie A.S. & Brunsden D. 1994. *The Environment of the British Isles. An Atlas*. Clarendon Press, Oxford. 184 pp.
- Grant A. & Bhattacharyya P.K. 1985. Application of derivative spectroscopy to the determination of chromatographic peak purity. *Journal of Chromatography*. **347**. 219-235.
- Grönlund E. 1991. Sediment characteristics in relation to cultivation history in two varved lake sediments from East Finland. *Hydrobiologia*. **214**. 137-142.
- Grootes P.M., Stuiver M., White J.W.C., Johnsen S. & Jouzel J. 1993. Comparison of oxygen isotope records from the GISP2 and GRIP Greenland ice cores. *Nature*. **366**. 552-554.
-

Grove J.M. 1988. *The Little Ice Age*. Routledge, London. 498 pp.

Guiot J. 1992. The combination of historical documents and biological data in the reconstruction of climate variations in space and time. In Pfister C. and Glaser B. (eds) *European Climate Reconstructed From Documentary Data: methods and results*. ESF project "European Climate and Man". **Special Issue 2**. G. Fischer, Stuttgart, Jena, New York. 93-104.

Guiot J., Pons A., de Beaulieu J.L. & Reille M. 1989. A 140,000 year continental climate reconstruction from two European pollen records. *Nature*. **338**. 309-313.

Hajdas I., Ivy S.D., Beer J., Bonani G., Imboden D., Lotter A.F., Sturm M. & Suter M. 1993. AMS radiocarbon dating and varve chronology of Lake Soppensee: 6000 to 12000 ¹⁴C years BP. *Climate Dynamics*. **9**. 107-116.

Hajdas I., Zolitschka B., Ivy-Ochs S.D., Beer J., Bonani G., Leroy S.A.G., Negendank J.W., Ramrath M. & Suter M. 1995. AMS radiocarbon dating of annually laminated sediments from Lake Holzmaar, Germany. *Quaternary Science Reviews*. **14**. 137-143.

Håkanson L. & Jansson M. 1983. *Lake Sedimentology*. Springer-Verlag, Berlin. 316 pp.

Halfman J.D. & Johnson T.C. 1988. High-resolution record of cyclic climatic change during the past 4ka from Lake Turkana, Kenya. *Geology*. **16**. 496-500.

Hammer C.U. 1980. Acidity of Polar Ice Cores in Relation to Absolute Dating, Past Volcanism, and Radio-echoes. *Journal of Glaciology*. **25**. 359-372.

-
- Hammer C.U. 1989. Dating by Physical and Chemical Seasonal variations and Reference Horizons. In Oeschger H. & Langway C.C. (eds) *The Environmental Record in Glaciers and Ice Sheets. Report of the Dahlem Workshop, Berlin 1988, March 13-18. Research report 8*. J.Wiley & Sons, Chichester, UK. 99-121.
- Harding A.F. (ed.) 1982. *Climatic Change During Later Prehistory*. Edinburgh University Press, Edinburgh.
- Hardy D.R., Bradley R.S. & Zolitschka B. 1996. The climatic signal in varved sediments from Lake C2, northern Ellesmere Island, Canada. *Journal of Paleolimnology*. **16**. 227-238.
- Harris A.L. 1991. The growth and structure of Scotland. In Craig G.Y. (ed.) *Geology of Scotland*. The Geological Society. London. 3rd edition. 1-24.
- Hay W.H. 1993 The role of polar deep water formation in global climate change. *Annual Review of Earth and Planetary Science*. **21**. 227-254.
- Hays J.D., Imbrie J & Shackleton N.J. 1976. Variations in the earth's orbit: Pacemaker of the ice ages. *Science*. **194**. 1121-1131.
- Hazen R. & Trefil J. 1991. Sciences greatest hits take their lumps. *Science*. **251**. 1308-1309.
- Hedges R.E.M. 1992. Sample treatment strategies in radiocarbon dating. In Taylor R.E, Long A. & Kra R.S. (eds). *Radiocarbon After Four Decades. An Interdisciplinary Perspective*. Springer-Verlag. New York. 165-183.
- Hedges R.E.M. 1995. Problems in recovering information from archaeological bone.
-

Abstracts of papers of the American Chemical Society. **209.** 17.

Hedges R.E.M., Leethorp J.A. & Tuross N.C. 1995. Is tooth enamel carbonate a suitable material for radiocarbon dating? *Radiocarbon.* **37.** 285-290.

Henderson-Sellers A. & Robinson P.J. 1987. *Contemporary Climatology.* Longman, Harlow, UK. 439 pp.

Heiarnielsen S., Conradsen K., Heinemeier J., Knudsen K.L., Nielsen H.L., Rud N. & Sveinbjornsdottir A.E. 1995. Radiocarbon dating of shells and foraminifera from the Skogen-core, Denmark-evidence of reworking. *Radiocarbon.* **37.** 119-130.

Heine J.T.. 1993. A Reevaluation of the Evidence for a Younger Dryas Climatic Reversal in the Tropical Andes. *Quaternary Science Reviews.* **12.** 769-779.

Hinnov L.A. & Goldhammer R.K. 1991. Spectral analysis of the Middle Triassic Latemar Limestone. *Journal of Sedimentary Petrology.* **61.** 1173-1193.

Hoang C.T., Dalongeville R. & Sanlaville P. 1996. Stratigraphy, tectonics and paleoclimatic implications of Uranium-series-dated coral-reefs from the Sudanese coast of the Red Sea. *Quaternary International.* **31.** 47-51.

Holcombe T.L. 1989. Paleoclimate data for studies of global climate change and Earth system science. In Berger A., Schneider S. & Duplessy J.-C. (eds) *Climate and Geo-Sciences. A Challenge for Science and Society in the 21st Century.* NATO ASI Series C: Mathematical and Physical Sciences. **285.** Kluwer Academic Publishers, Dordrecht. 173-177.

Hooghiemstra H., Melice J.L., Berger A. & Shackleton N.J.. 1993. Frequency-spectra

-
- and paleoclimatic variability of the high-resolution 30-1450 ka Funza I pollen record (Eastern Cordillera, Colombia). *Quaternary Science Reviews*. **12**. 141-156.
- Horne A.J. & Goldman C.R. 1994. *Limnology*. 2nd Edition. McGraw-Hill, Inc., New York. 576 pp.
- Hoyt D.V., Schatten K.H. & Nesme-Ribes E. 1994. A new reconstruction of solar activity, 1610-1993. In Nesme-Ribes E. (ed.) *The Solar Engine and its Influence on Terrestrial Atmosphere and Climate*. NATO ASI Series. **125**. Springer-Verlag, Berlin. 57-69.
- Huntley B. & Birks H.J.B. 1983. *An Atlas of Past and Present Pollen Maps for Europe, 0-13000 Years Ago*. Cambridge University Press, Cambridge.
- Huntley B. & Prentice I.C. 1988. July temperatures in Europe from pollen data - 13000 yr BP to present. *Science*. **241**, 687-689.
- Hurrell J.W. 1995. Decadal trends in the North Atlantic Oscillation, regional temperatures and precipitation. *Science*. **269**. 676-679.
- Imbrie J. & Imbrie K.P. 1986. *Ice Ages: solving the mystery*. Harvard University Press, Cambridge, USA. 2nd edition. 224 pp.
- Imbrie J., McIntyre A. & Mix A. 1989. Oceanic response to orbital forcing in the late Quaternary: Observational and experimental strategies. In Berger A., Schneider S., Duplessy J.-C. (eds) *Climate and Geo-Sciences. A Challenge for Science and Society in the 21st Century*. NATO ASI Series C: *Mathematical and Physical Sciences*. **285**. Kluwer Academic Publishers, Dordrecht. 121-164.
-

-
- Ingram M.J., Underhill D.J. & Farmer G. 1981. The use of documentary sources for the study of past climates. In Wigley T.M.L., Ingram M.J. & Farmer G. (eds) *Climate and History*. Cambridge University Press, Cambridge. 180-213.
- Innocent C., Fagel N., Stevenson R.K. & Hillaire-Marcel C. 1997. Sm-Nd signature of modern and Late Quaternary sediments from the northwest North Atlantic: Implication for deep current changes since the Last Glacial Maximum. *Earth and Planetary Science Letters*. **146**. 607-625.
- Itkonen A. & Salonen V.-P. 1994. The response of sedimentation in three varved lacustrine sequences to air temperature, precipitation and human impact. *Journal of Paleolimnology*. **11**. 323-332.
- Jaakkola T., Tolonen K., Huttunen P. & Leskinen S. 1983. The use of fallout ^{137}Cs and $^{239,240}\text{Pu}$ for dating of lake sediments. *Hydrobiologia*. **103**. 15-19.
- Jain A.K. 1989. *Fundamentals of digital image processing*. Prentice-Hall Inc. New Jersey, USA. 569 pp.
- Jansen E. & Veum T. 1990. Evidence for two-step deglaciation and its impact on North Atlantic deep-water circulation. *Nature*. **343**. 612-616.
- Jenkins P.H. 1993. Loch Ness sediments: a preliminary report. *The Scottish Naturalist*. **105**. 65-86.
- Johnsen S.J., Clausen H.B., Dansgaard W., Gundestrup N.S., Hammer C.U. & Tauber H. 1995. The Eem stable isotope record along the GRIP ice core and its interpretation. *Quaternary Research*. **43**. 117-124.
-

-
- Johnsen S.J., Dansgaard W., Clausen H.B., Langway C.C. 1970. Climatic oscillations 1200-2000 AD. *Nature*. **227**. 482-483.
- Johnson F.G. 1994. Hydro-electric Generation. In Maitland P.S., Boon P.J. & McLusky D.S. (eds) *The Fresh Waters of Scotland: A National Resource of International Significance*. John Wiley & Sons Ltd. Chichester, UK. 297-316.
- Johnson T.C. (ed) 1993. *IDEAL: An International Decade for the East African Great Lakes. Science and implementation plan. PAGES Working Report series 93-2*. 39 pp.
- Jones P.D., Hulme M. & Briffa K.R. 1993. A comparison of Lamb circulation types with an objective classification scheme. *International Journal of Climatology*. **13**. 655-663.
- Jones R.I. & Ilmavirta V. 1978. Vertical and seasonal variation of phytoplankton photosynthesis in a brown-water lake with winter ice cover. *Freshwater Biology*. **8**. 561-572.
- Jones R.I., Fulcher A.S., Jayakody J.K.U., Laybourn-Parry J., Shine A.J., Walton M.C. & Young J.M. 1995. The horizontal distribution of plankton in a deep, oligotrophic lake - Loch Ness, Scotland. *Freshwater Biology*. **33**. 161-170.
- Jones R.I., Young J.M., Hartley A.M. & Bailey-Watts A.E. 1996. Light limitation of phytoplankton development in an oligotrophic lake - Loch Ness, Scotland. *Freshwater Biology*. **35**. 533-543.
- Jones R.I., Laybourn-Parry J., Walton M.C. & Young J.M. 1997. The form and distribution of carbon in a deep, oligotrophic lake (Loch Ness, Scotland).
-

-
- Verhandlungen der Internationalen Vereinigung für Theoretische and Angewandte Limnologie.* **26.** 330-334.
- Jones R.I., Grey J., Sleep D. & Quarmby C. 1998. An assessment, using stable isotopes, of the importance of allochthonous organic carbon sources to the pelagic food web in Loch Ness. *Proceedings of the Royal Society of London.* **B 256.** 105-111.
- Jones V.J., Flower R.J., Appleby P.J., Natkanski J., Richardson N., Rippey B., Stevenson A.C. & Battarbee R.W. 1993. Palaeolimnological evidence for the acidification and atmospheric contamination of lochs in the Cairngorm and Lochnagar areas of Scotland. *Journal of Ecology.* **81.** 3-24.
- Jones V.J., Battarbee R.W., Rose N.L., Curtis C., Appleby P.J., Harriman R. & Shine A.J. 1997. Evidence for the pollution of Loch Ness from the analysis of its recent sediments. *Science of the Total Environment.* **203.** 37-49.
- Jonsson P., Carman R. & Wulff F. 1990. Laminated sediments in the Baltic- A tool for evaluating nutrient mass balances. *Ambio.* **19.** 152-158.
- Jouzel J., Lorius C., Petit J.R., Genthon C., Barkov N.I., Kotlyakov V.M. & Petrov V.M. 1987. Vostok Ice Core: A continuous isotope temperature record over the last climatic cycle (160,000 years). *Nature.* **329.** 403-408.
- Jouzel J., Alley R.B., Caffey K.M., Dansgaard W., Grootes P., Hoffmann G., Johnsen S.J., Koster R.S., Peel D., Shuman C.A., Sieivenend M., Stuiver M. & White J. 1997. Validity of temperaure reconstruction from water isotopes in ice cores. *Journal of Geophysical Research.* **O102.** 26471-26487.
- Joyce Loebel. 1985. *Image Analysis. Principles and Practice.* Joyce Loebel. Gateshead,
-

UK. 250pp.

- Keatinge T.H. and Dickson J.H. 1979 Mid-Flandrian changes in vegetation on mainland Orkney. *New Phytologist*. **82**. 585-612.
- Keigwin L.D. & Jones G.A. 1994. Western North Atlantic evidence for millennial-scale changes in ocean circulation and climate. *Journal of Geophysical Research*. **C99**. 12397-12410.
- Kellogg T.B. 1984. Late-glacial Holocene high-frequency climatic changes in deep-sea cores from the Denmark Strait. In Mörner N.-A. & Karlén W. (eds) *Climatic changes on a Yearly to Millennial Basis*. Riedel, Dordrecht.
- Kelly P.M. 1979. Solar Influence on North Atlantic Mean Sea Level Pressure. In McCormac B.M. and Seliga T.A. (eds) *Solar-Terrestrial Influences on Weather and Climate*. D.Reidel Publishing Company, Dordrecht, Holland. 297-298.
- Kelts K. & Hsü K.J. 1978. Freshwater carbonate sedimentation. In Lerman A. (ed.) *Lakes: Geology, Chemistry and Physics*. Springer-Verlag, New York. 295-323.
- Kemp A.E.S. 1990. Sedimentary fabrics and variation in lamination style in Peru continental margin upwelling sediments. In Suess E., von Heune R. *et al.* (eds) *Proceedings of the Ocean Drilling Program, Scientific Results*. **112**. 43-58.
- Kemp A.E.S. 1996. Laminated sediments as palaeo-indicators. In Kemp A.E.S. (ed.) *Palaeoclimatology and Palaeoceanography from Laminated Sediments*. Geological Society Special Publication. **116**. The Geological Society, London. vii-xii.

-
- Kemp A.E.S., Baldauf J.G. & Pearce R.B. 1996. Origins and palaeoceanographic significance of laminated diatom ooze from the eastern equatorial Pacific Ocean. In Kemp A.E.S. (ed.) *Palaeoclimatology and Palaeoceanography from Laminated Sediments*. Geological Society Special Publication. **116**. The Geological Society, London. 243-252.
- Kempe S. & Degens E.T. 1979. Varves in the Black Sea and Lake Van (Turkey). In Schlüchter C. (ed.) *Moraines and Varves*. Balkema, Rotterdam. 309-318.
- Kennedy J.A. & Brassell S.C. 1992. Molecular records of twentieth-century El Niño events in laminated sediments from the Santa Barbara basin. *Nature*. **357**. 62-64.
- Keppenne C.L. & Ghil M. 1992. Extreme weather events. *Nature*. **358**. 547.
- Kerr R.A. 1996. New dawn for Sun-Climate links? *Science*. **271**. 1360.
- Khalil M.A.K. & Rasmussen R.A. 1989. Temporal variations of trace gases in ice cores. In Oeschger H. & Langway Jr. C.C. (eds) *The Environmental Record in Glaciers and Ice Sheets. Report of the Dahlem Workshop, Berlin 1988, March 13-18*. **Research report 8**. J.Wiley & Sons, Chichester, UK. 193-205.
- Knox R.W.O'B. 1994. Tephra layers as precise chronostratigraphical markers. In Hailwood E.A. and Kidd R.B. (eds) *High Resolution Stratigraphy*. Geological Society Special Publication No.70. 169-186.
- Koç N. Jansen E. & Hafliðason H. 1993. Palaeoceanographic reconstructions of surface ocean conditions in the Greenland, Iceland and Norwegian Seas through the last 14ka based on diatoms. *Quaternary Science Reviews*. **12**. 115-140
-

-
- Koivisto E. & Saarnisto M. 1978. Conventional Radiography, Xerography, Tomography and contrast enhancement in the study of laminated sediments. Preliminary report. *Geografiska Annaler*. **60A**. 55-61.
- Koopmans L.H. 1974. *The spectral analysis of time series*. Academic Press Inc. New York, USA. 366 pp.
- Kreutz K.J., Mayewski P.A., Meeker L.D., Twickler M.S., Whitlow S.I. & Pittalwala I.I., 1997. Bipolar changes in atmospheric circulation during the Little Ice Age. *Science*. **277**. 1294-1296.
- Kromer B. & Münnich K.O. 1992. CO₂ gas proportional counting in radiocarbon dating- Review and perspective. In Taylor R.E, Long A. & Kra R.S. (eds). *Radiocarbon After Four Decades. An Interdisciplinary Perspective*. Springer-Verlag. New York. 184-197.
- Kullenberg B. 1947. The piston core sampler. *Svenska Hydrografisk-Biologiska Kommissionens Skrifter. Series 3*. 1-46.
- Kullman L. 1994. Climate and environmental change at high latitudes. *Progress in Physical Geography*. **18**. 124-135.
- Labitzke K. & van Loon H. 1990. Associations between the 11-year solar cycle, the Quasi-Biennial Oscillation and the atmosphere: a summary of recent work. In Pecker J.-C. & Runcorn S.K. (eds) *The Earth's Climate and Variability of the Sun Over Recent Millennia : Geophysical, Astronomical and Archaeological Aspects*. The Royal Society / Cambridge University Press. 179-190.
-

-
- La Marche V.C. 1974. Paleoclimatic inferences from long tree-ring records. *Science*. **183**. 1043-1048.
- LaMarche Jr. V.C. & Hirschboeck K.K. 1984. Frost rings in trees as records of major volcanic eruptions. *Nature*. **307**. 121-126.
- Lamb H.H. 1950. Types and spells of weather around the year in the British Isles: annual trends, seasonal structure of the year, singularities. *Quarterly Journal of the Royal Meteorological Society*. **76**. 393-438.
- Lamb H.H. 1965. The early medieval warm epoch and its sequel. *Palaeogeography, Palaeoclimatology, Palaeoecology*. **1**. 13-37.
- Lamb H.H. 1970. Volcanic dust in the atmosphere: with a chronology and assessment of its meteorological significance. *Philosophical Transactions of the Royal Society of London*. **A266**. 425-533.
- Lamb H.H. 1972a. *Climate Past Present and Future*. Vol I. Methuen, London. 613 pp.
- Lamb H.H. 1972b. British Isles weather types and a register of the daily sequences of circulation patterns 1861-1971. *Geophysical Memoirs*. **116**. London.
- Lamb H.H. 1977a. *Climate Past Present and Future, Climate history and the future*. Vol II. Methuen, London. 835 pp.
- Lamb H.H. 1977b. The Late Quaternary history of the climate of the British Isles. In Shotton (ed.) *British Quaternary Studies*. Clarendon Press, Oxford. 283-298.
- Lamb H.H. 1979. Climatic Variation and Changes in the Wind and Ocean Circulation:
-

-
- The Little Ice Age in the Northeast Atlantic. *Quaternary Research*. **11**. 1-20.
- Lamb H.H. 1995. *Climate, History and the Modern World*. Routledge, New York. 2nd Edition. 443 pp.
- Lane L.J., Nichols M.H. & Osborn H.B. 1994. Time Series Analyses of Global Change Data. *Environmental Pollution*. **83**. 63-68.
- Langereis C.G., Dekkers M.J., deLange G.J., Paterne M. & van Santvoort P.J.M. 1997. Magnetostratigraphy and astronomical calibration of the last 1.1 Myr from an eastern Mediterranean piston core and dating of short events in the Brunhes. *Geophysical Journal International*. **129**. 75-94.
- Lassen K. & Friis-Christensen E. 1995. Variability of the solar cycle length during the past five centuries and the apparent association with terrestrial climate. *Journal of Atmospheric and Terrestrial Physics*. **57**. 835-845.
- Leemann A. & Niessen F. 1994. Varve formation and the climatic record in an Alpine proglacial lake: calibrating annually laminated sediments against hydrological and meteorological data. *The Holocene*. **4**. 1-8.
- Legrand M. & Delmas R.J. 1987. Environmental changes during Last Deglaciation inferred from chemical analysis of the Dome C ice core. In Berger W.H and Labeyrie L.D. (eds) *Abrupt Climatic Change*. NATO ASI Series C. *Mathematical and Physical Sciences*. **216**. D.Reidel Publishing Company, Dordrecht. 247-259.
- Lehman S. 1996. True grit spells double trouble. *Nature*. **382**. 25-27.
- Leonard E.M. 1986. Varve studies at Hector Lake, Alberta, Canada, and the relationship
-

-
- between glacial activity and sedimentation. *Quaternary Research*. **25**. 199-214.
- Leonard E.M. 1995. A varve-based calibration of the Bridge River tephra fall. *Canadian Journal of Earth Sciences*. **32**. 2098-2102.
- Le Roy Ladurie E. 1972. *Times of Feast, Times of Famine: a history of climate since the year 1000*. Bray B. (translator). George Allen and Unwin, London. 428 pp.
- Levesque A.J., Mayle F.E., Walker I.R. & Cwynar L.C. 1993. The Amphi-Atlantic Oscillation: A proposed Late-Glacial climatic event. *Quaternary Science Reviews*. **12**. 629-643.
- Libby L.M. & Pandolfi L.J. 1977. Climate periods in tree, ice and tides. *Nature*. **266**. 415-417.
- Liu K. & Fearn M.L. 1993. Lake-sediment record of late Holocene hurricane activities from coastal Alabama. *Geology*. **21**. 793-796.
- Longworth I.H. 1985. *Prehistoric Britain*. British Museum Publications, London. 72 pp.
- Lorius C.J. Polar ice cores and climate. 1989. In Berger A., Schneider S., Duplessy J.-C. (eds) *Climate and Geo-Sciences. A Challenge for Science and Society in the 21st Century*. NATO ASI Series C: Mathematical and Physical Sciences. **285**. Kluwer Academic Publishers, Dordrecht. 77-103.
- Lorius C. 1990. Environmental records from polar ice cores. *Philosophical Transactions of the Royal Society of London*. **A330**. 459-462.
-

-
- Lorius C., Raisbeck G., Jouzel J. & Raynaud D. 1989. Long-term environmental records from Antarctic ice cores. In Oeschger H. & Langway C.C. (eds) *The Environmental Record in Glaciers and Ice Sheets. Report of the Dahlem Workshop, Berlin 1988, March 13-18. Research report 8*. J. Wiley & Sons, Chichester, UK. 343-361.
- Lotter A.F. 1991a. How long was the Younger Dryas? Preliminary evidence from annually laminated sediments of Soppensee (Switzerland). *Hydrobiologia*. **214**. 53-57.
- Lotter A.F. 1991b. Absolute dating of the Late-Glacial period in Switzerland using annually laminated sediments. *Quaternary Research*. **35**. 321-330.
- Lotter A.F. & Sturm M. 1994. The study of environmental dynamics by means of laminated sediments: Results from Switzerland. In Hicks S., Miller U. & Saarnisto M. (eds) *Laminated Sediments. Symposium held at the European University Centre for the Cultural Heritage, Ravello, June, 1991*. **41**. PACT Belgium, Rixensart. 15-24.
- Lowe J.J. 1993. Setting the scene: an overview of climatic change. In Smout T.C. (ed.) *Scotland since Prehistory. Natural change and human impact*. Scottish Cultural Press, Edinburgh. 1-16.
- Lowe J.J. & Walker M.J.C. 1984. *Reconstructing Quaternary Environments*. Longman, London. 389 pp.
- Ludlam S.D. 1969. Fayetteville Green Lake, New York. III. The Laminated Sediments. *Limnology and Oceanography*. **14**. 848-857.
-

-
- Ludlam S.D. 1979. Rhythmite deposition in lakes of the northeastern United States. In Schluchter C. (ed.) *Moraines and Varves. Origin/Genesis/Classification*. Balkema, Rotterdam. 295-302.
- Mackereth F.J.H. 1958. A portable core sampler for lake deposits. *Limnology & Oceanography*. **3**. 181-191.
- Mackereth F.J.H. 1969. A short-core sampler for sub-aqueous deposits. *Limnology & Oceanography*. **14**. 145-151.
- MacKie E.W. 1975. *Scotland: An Archaeological Guide*. Faber & Faber, London. 309pp.
- Maitland P.S. 1981. Introduction and catchment analysis. In Maitland P.S. (ed.) *The Ecology of Scotland's Largest Lochs. Lomond, Awe, Ness, Morar and Shiel. Monographiae Biologicae*. **44**. Dr.W.Junk Publishers, The Hague.1-27.
- Makrogiannis T.J., Bloutsos A.A. & Giles B.D. 1982. Zonal index and circulation change in the North Atlantic area, 1873-1972. *Journal of Climatology*. **2**. 159-169.
- Manley G. 1974. Central England temperatures: monthly means 1659 to 1973. *Quarterly Journal of the Royal Meteorological Society*. **100**. 389-405.
- Mann K.H. & Lazier J.R.N. 1996. *Dynamics of Marine Ecosystems: Biological-Physical Interactions in the Oceans*. 2nd edition. Blackwell Science, Boston. 394 pp.
- Mann M.E., Park J. & Bradley R.S. 1995. Global interdecadal and century-scale climate
-

-
- oscillations during the past five centuries. *Nature*. **378**. 266-270.
- Marion A. 1991. *An Introduction to Image Processing*. Chapman & Hall, London, UK. 314 pp.
- Markgraf V. 1993. Younger Dryas in Southernmost South America - An Update. *Quaternary Science Reviews*. **12**. 351-355.
- Markson R. 1981. The effect of cosmic rays on the electric field of the Earth. *Nature*. **291**. 304-308.
- Marr D. & Hildreth E. 1980. Theory of edge detection. *Proceedings of the Royal Society of London*. **B30**. 499-505.
- Martinson D.G., Pisias N.G., Hays J.D., Imbrie J., Moore jnr. T.C. & Shackleton N.J. 1987. Age dating and the Orbital Theory of the Ice Ages: Development of a high-resolution 0 to 300,000-year chronostratigraphy. *Quaternary Research*. **27**. 1-29.
- Maslin M.A., Shackleton N.J. & Plaumann U. 1995. Surface-water temperature, salinity, and density changes in the Northeast Atlantic during the last 45,000 years - Heinrich events, deep-water formation and climatic rebounds. *Paleoceanography*. **10**. 527-544.
- Mason B.J. 1976. Towards the understanding and prediction of climatic variations. *Quarterly Journal of the Royal Meteorological Society*. **102**. 473-498.
- Matsch C.L. 1976. *North America and the Great Ice Age*. McGraw Hill Inc. New York. 131 pp.
-

-
- Mayer L., Piasias N., Janacek T. & Leg 138 Shipboard Sedimentologists and Scientific Party. 1992. Color reflectance spectroscopy: a tool for rapid characterisation of deep-sea sediments. *Proceedings of the Ocean Drilling Program, Initial Reports*. **138**. 67-77.
- Mayes J.C. 1991. Regional airflow patterns in the British Isles. *International Journal of Climatology*. **11**. 473-491.
- Mayes J. 1996. Spatial and temporal fluctuations of monthly rainfall in the British Isles and variations in the mid-latitude westerly circulation. *International Journal of Climatology*. **16**. 585-596.
- Mayewski P.A., Meeker L.D., Morrison M.C., Twickler M.S., Whitlow S., Ferland K.K., Meese D.A., Legrand M.R. & Steffensen J.P. 1993a. Greenland Ice core "signal" characteristics: an expanded view of climate change. *Journal of Geophysical Research-D*. **98**. 12839-12847.
- Mayewski P.A., Meeker L.D., Whitlow S., Twickler M.S., Morrison M.C., Alley R.B., Bloomfield P. & Taylor K. 1993b. The atmosphere during the Younger Dryas. *Science*. **261**. 195-197.
- McBratney A.B., Moran C.J., Stewart J.B., Cattle S.R. & Koppi A.J. 1992. Modifications to a method of rapid assessment of soil macropore structure by image analysis. *Geoderma*. **53**. 255-274.
- McCormac F.G., Baillie M.G.L., Pilcher J.R. & Kalin R.M. 1995. Location dependent differences in the C-14 content of wood. *Radiocarbon*. **37**. 395-407.
- McElroy M.B. 1994. Climate of the Earth- An overview. *Environmental Pollution*. **83**.
-

3-21.

- McGovern J.H. 1981. The economics of extinction in Norse Greenland. In Wigley T.M.L., Ingram M.J. & Farmer G. (eds) *Climate and History*. Cambridge University Press, Cambridge, UK. 404-430.
- McIntyre M.E. 1994. The Quasi-Biennial Oscillation (QBO): some points about the terrestrial QBO and the possibility of related phenomena in the solar interior. In Nesme-Ribes E. (ed.) *The Solar Engine and its Influence on Terrestrial Atmosphere and Climate*. NATO ASI Series. **125**. Springer-Verlag Berlin. 293-320.
- McManus J. & Duck R.W. 1988. Scottish freshwater lochs and reservoirs: a physical perspective. *Scottish Geographical Magazine*. **104**. 97-107.
- Meehl G. 1994. Coupled land-ocean-atmosphere processes and South Asian monsoon variability. *Science*. **266**. 263-267.
- Meese D.A., Gow A.J., Grootes P., Mayewski P.A., Ram M., Stuiver M., Taylor K.C., Waddington E.D. & Zielinski G.A. 1994. An accumulation record from the GISP2 core as an indicator of climate change throughout the Holocene. *Science*. **266**. 1680-1682.
- Mehl J. & Merkt J. 1990. X-ray radiography applied to laminated lake sediments. In Saarnisto M. & Kahra A. (eds) *Proceedings of the Workshop at Lammi Biological Station, 4-6 June, 1990*. Geological Society of Finland Special Paper 14. 77-85.
- Merkt J. 1971. Zuverlässige Auszählungen von Jahresschichten in Seesedimenten mit Hilfe von Groß-Dünnschliffen. *Archiv für Hydrobiologie*. **69**. 145-154.

-
- Merritt J.W., Auton C.A. & Firth C.R. 1995. Ice-proximal glaciomarine sedimentation and sea-level change in the Inverness area, Scotland: A review of the deglaciation of a major ice stream of the British Late Devensian ice sheet. *Quaternary Science Reviews*. **14**. 289-329.
- Mienert J. & Chi J. 1995. Astronomical time-scale for physical property records from Quaternary sediments of the northern North Atlantic. *Geologische Rundschau*. **84**. 67-88.
- Miller U. 1994. Laminae formation in the long- and short- term perspectives. In Hicks S., Miller U. & Saarnisto M. (eds) *Laminated Sediments. Symposium held at the European University Centre for the Cultural Heritage, Ravello. June, 1991*. **41**. PACT Belgium, Rixensart. 9-11.
- Mirecki J.E. 1996. Recognition of the 1811-1812 New Madrid earthquakes in Reelfoot Lake, Tennessee sediments using pollen data. *Journal of Paleolimnology*. **15**. 183-191.
- Mitchell J.F.B., Grahame N.S. & Needham K.J. 1988. Climate simulations for 9000 years before present: seasonal variations and effect of the Laurentide Ice Sheet. *Journal of Geophysical Research D*. **93**. 8283-8303.
- Mitsuguchi T., Matsumoto E., Abe O., Uchida T. & Isdale P.J. 1996. Mg/Ca thermometry in coral skeletons. *Science*. **274**. 961-963.
- Mörner N.-A. 1993. The Maunder Minimum. In Frenzel B., Pfister C. & Glaser B. (eds) *European climate reconstructed from documentary data: methods and results*. ESF project European Palaeoclimate and Man. Special issue 2. Gustav Fischer Verlag, Stuttgart. 1-8.
-

-
- Mörner N.-A. Wallin B. 1977. A 10,000 Year Temperature Record From Gotland, Sweden. *Palaeogeography, Palaeoclimatology, Palaeoecology*. **21**. 113-138.
- Mörth H.T. & Schlamming L. 1979. Planetary Motion, Sunspots and Climate. In McCormac B.M. and Seliga T.A. (eds) *Solar-Terrestrial Influences on Weather and Climate*. D.Reidel Publishing Company. 193-207.
- Mott McDonald. 1992. *Highland region flooding incidents in the Great Glen, Loch Ness, River Ness*. Department of Water and Sewerage, Highland Regional Council.
- Moulin C. Lambert C.E., Dulac F. & Dayan U. 1997. Control of atmospheric export of dust from North Africa by the North Atlantic Oscillation. *Nature*. **387**. 691-694.
- Nesje A. & Dahl S.O. 1993. Lateglacial and Holocene Glacier Fluctuations and Climate Variations in Western Norway: A Review. *Quaternary Science Reviews*. **12**. 255-261.
- Newhall C.G. & Self S. 1982. The Volcanic Explosivity Index (VEI): an estimate of explosive magnitude for historical volcanism. *Journal of Geophysical Research*. **87**. 1231-1238.
- Nicholson I. 1982. *The Sun*. Mitchell Beazley Publishers/ Royal Astronomical Society, London. 40-41.
- Nuhfer E.B., Anderson R.Y., Bradbury J.P. & Dean W.E. 1993. Modern sedimentation in Elk Lake, Clearwater County, Minnesota. In Bradbury J.P. & Dean W.E. (eds) *Elk Lake, Minnesota: Evidence for rapid climate change in the North-Central*
-

United States. USGS Special Paper 276. United States Geological Survey. 75-96.

- Oeschger H. & Beer J. 1990. The past 5000 year history of solar modulation of cosmic radiation from ^{10}Be and ^{14}C studies. *Philosophical Transactions of the Royal Society of London*. **A330**. 471-480.
- Oldfield F., Crooks P.R.J., Appleby P.G. & Renberg I. 1994. The use of laminated sediments to test methods of dating and palaeoenvironmental reconstruction. In Hicks S., Miller U. & Saarnisto M. (eds) *Laminated Sediments. Symposium held at the European University Centre for the Cultural Heritage, Ravello. June, 1991*. **41**. PACT Belgium, Rixensart. 57-62.
- Olsson I.U., El-Daoushy F. & Vasari Y. 1983. Säynäjälampi and the difficulties inherent in the dating of sediments in a hard-water lake. *Hydrobiologia*. **103**. 5-14.
- Ordnance Survey. 1993. *Landranger Map 26*. Ordnance Survey of Great Britain. Southampton, UK.
- O'Sullivan P.E. 1974. Radiocarbon dating and prehistoric forest clearance on Speyside (East-Central Highlands of Scotland). *Proceedings of the Prehistoric Society*. **40**. 206-208.
- O'Sullivan P.E. 1976. Pollen analysis and radiocarbon dating of a core from Loch Pityoulish, Eastern Highlands of Scotland. *Journal of Biogeography*. **3**. 293-302.
- O'Sullivan P.E. 1983. Annually-laminated lake sediments and the study of Quaternary environmental changes - a review. *Quaternary Science Reviews*. **1**. 245-313.

-
- O'Sullivan P.E. 1994a. Slide shown at the Inaugral meeting of IGCP 374. University of Southampton. 7-9 September.
- O'Sullivan P.E. 1994b. Improving the accuracy of radiocarbon dates using annually laminated sediments. In Hicks S., Miller U. & Saarnisto M. (eds) *Laminated sediments. Symposium held at the European University Centre for Cultural Heritage, Ravello. June, 1991.* 41. PACT Belgium, Rixensart. 63-88.
- O'Sullivan P.E. 1995. Palaeolimnology. In Nierenberg W.A. (ed.) *Encyclopedia of Environmental Biology.* 3. Academic Press, Inc. New York, USA. 37-58.
- O'Sullivan P.E., Cooper M.C., Shine A.J., Bull D., Kemp A.E.S., Jones R.I., Harkness D.D., Lawson E.M., Peglar S.M., Matthews N.M., Salter N.C.J., Henon D.N., Williams T.S.C., Cooke D.A. & Rowland S.J. 1996. *The holocene environmental record in the sediments of Loch Ness, Scotland.* Paper presented at the 1st Annual Workshop, European Lakes Drilling Project (ELDP), Le Bischenburg, near Strasbourg. 24-27 October, 1996.
- Overpeck J., Hughen K., Hardy D., Bradley R.S., Case R., Douglas M., Finney B., Gajewski K., Jacoby G., Jennings A., Lamoureux S., Lasca A., MacDonald G., Moore J., Retelle M., Smith S., Wolfe A. & Zielinski G. 1997. Arctic environmental change of the last four centuries. *Science.* 278. 1251-1256.
- Parker D.E., Legg T.P. & Folland C.K. 1992. A new daily Central England Temperature series, 1772-1991. *International Journal of Climatology.* 12. 317-342.
- Peglar S.M., Fritz S.C., Alapieti T., Saarnisto, M. & Birks H.J.B. 1984. Composition
-

-
- and formation of laminated sediments in Diss Mere, Norfolk, England. *Boreas*. **13**. 13-28.
- Pennington W. 1981. Records of a lake's life in time: the sediments. *Hydrobiologia*. **79**. 197-219.
- Pennington W., Haworth E.Y., Bonny A.P. & Lishman J.P. 1972. Lake sediments in Northern Scotland. *Philosophical Transactions of the Royal Society of London*. **B264**. 191-294.
- Perkins J.A. & Sims J.D. 1983. Correlation of Alaskan varve thickness with climatic parameters, and use in paleoclimatic reconstruction. *Quaternary Research*. **20**. 308-321.
- Peterson L.C., Overpeck J.T. & Murray D.W. 1995. Anoxic basin records detailed climate history. *JOI/USSAC Newsletter*. **8**. 10-13.
- Peteet D.M., Vogel J.S., Nelson D.E., Southon J.R., Nickmann R.J. & Heusser L.E. 1990. Younger Dryas climatic reversal in northeastern USA? AMS ages for an old problem. *Quaternary Research*. **33**. 219-230.
- Pfister C. 1981. An analysis of the Little Ice Age climate in Switzerland and its consequences for agricultural production. In Wigley T.M.L., Ingram M.J. & Farmer G. (eds) *Climate and History*. Cambridge University Press, Cambridge. 214-248.
- Pike J. & Kemp A.E.S. 1996. Preparation and analysis techniques for studies of laminated sediments. In Kemp A.E.S. (ed.) *Palaeoclimatology and Palaeoceanography from Laminated Sediments*. Geological Society Special
-

Publication. **116**. The Geological Society, London. 37-48.

- Pike J. & Kemp A.E.S. 1997. Early Holocene decadal-scale ocean variability recorded in Gulf of California laminated sediments. *Paleoceanography*. **12**. 227-238.
- Pilskaln C.H. & Johnson T.C. 1991. Seasonal Signals in Lake Malawi sediments. *Limnology and Oceanography*. **36**. 544-557.
- Pinglot J.F. & Pourchet M. 1995. Radioactivity measurements applied to glaciers and lake sediments. *Science of the Total Environment*. **173**. 211-223.
- Pokras E.M. & Winter A. 1987. Variability of Holocene diatom assemblages in laminated sediments near Walvis Bay, Southwest Africa. *Marine Geology*. **76**. 185-194.
- Polach A.H. 1992. Four decades of progress in ¹⁴C dating by liquid scintillation counting and spectrometry. In Taylor R.E, Long A. & Kra R.S. (eds). *Radiocarbon After Four Decades. An Interdisciplinary Perspective*. Springer-Verlag. New York. 198-213.
- Preece R.C., Kemp R.A. & Hutchinson J.N. 1995. A Late-glacial colluvial sequence at Watcombe Bottom, Ventnor, Isle Of Wight, England. *Journal of Quaternary Science*. **10**. 107-121.
- Press W.H., Flannery B.P., Teukolsky S.A. & Vetterling W.T. 1986. *Numerical recipes in C. The art of scientific computing*. Cambridge University Press, Cambridge. 496-558.
- Price R.J. 1983. *Scotland's environment during the last 30,000 years*. Scottish Academic Press, Edinburgh. 224 pp.

QUICBasic programmers manual. 1995. Leica UK Milton Abbot, Cambridge, UK.

- Raisbeck G.M., Yiou F., Jouzel J. & Petit J.R. 1990. ^{10}Be and $\delta^2\text{H}$ in polar ice cores as a probe of the solar variability's influence on climate. In Pecker J.-C. and Runcorn S.K. (eds) *The Earth's Climate and Variability of the Sun Over Recent Millennia : Geophysical, Astronomical and Archaeological Aspects*. The Royal Society / Cambridge University Press. 65-70.
- Raisbeck G.M. & Yiou F. 1988. ^{10}Be as a proxy indicator of variations in solar activity and geomagnetic field intensity during the last 10,000 years. In Stephenson F.R. and Wolfendale A.W. (eds) *Secular Solar and Geomagnetic Variations in the Last 10,000 Years. NATO ASI series C. Mathematical and Physical Sciences*. **236**. Kluwer Academic, Dordrecht. 287-296.
- Ralska-Jasiewiczowa M. & van Geel B. 1992. Early human disturbance of the natural environment recorded in annually laminated sediments of Lake Gosciarz, Central Poland. *Vegetation History and Archaeobotany*. **1**. 33-42.
- Ralska-Jasiewiczowa M., van Geel B., Goslar T., & Kuc T. 1992. The Record of the Late Glacial/Holocene transition in the varved sediments of Lake Gosciarz, Central Poland. *Sveriges Geologiska Undersökning. Series Ca* **81**. 257-268.
- Rampino M.R., Self S. & Stothers R.B. 1988. Volcanic winters. *Annual Review of Earth and Planetary Science*. **16**. 73-99.
- Ramsey C.B. 1995. Radiocarbon calibration and the analysis of stratigraphy: The OxCal program. *Radiocarbon*. **37**. 425-430.

-
- Reasoner M.A., Osborn G. & Rutter N.W. 1994. Age of the Crowfoot advance in the Canadian Rocky Mountains: a glacial event coeval with the Younger Dryas oscillation. *Geology*. **22**. 439-442.
- Reid G.C. & Gage K.S. 1988. The climatic impact of secular variations in solar irradiance. In Stephenson F.R. & Wolfendale A.W. (eds) *Secular Solar and Geomagnetic Variations in the Last 10,000 Years. NATO ASI series C. Mathematical and Physical Sciences*. **236**. Kluwer Academic, Dordrecht.
- Reid P.C., Edwards M., Hunt H.G. & Warner A.J. 1998. Phytoplankton change in the North Atlantic. *Nature*. **391**. 546.
- Renberg I. 1981. Improved methods for sampling, photographing and varve-counting of varved lake sediments. *Boreas*. **10**. 255-258.
- Renberg I. 1986. Photographic demonstration of the annual nature of a varve type common in N. Swedish lake sediments. *Hydrobiologia*. **140**. 93-95.
- Renberg I. & Wik M. 1985. Carbonaceous particles in lake sediments- pollutants from fossil fuel combustion. *Ambio*. **4**. 161-163.
- Renberg I., Segerström U. & Wallin J.-E. 1984. Climatic reflection in varved lake sediments. In Mörner N.-A. and Karlén W.(eds) *Climatic Changes on a Yearly to Millenial Basis*. D. Reidel Publishing Company. 249-256.
- Ricketts R.D. & Johnson T.C. 1996. Climate change in the Turkana basin as deduced from a 4000 year long $d^{18}O$ record. *Earth and Planetary Science Letters*. **142**. 7-17.
-

-
- Ripepe M., Roberts L.T. & Fischer A.G. 1991. ENSO and sunspot cycles in varved Eocene oil shales from image analysis. *Journal of Sedimentary Petrology*. **61**. 1155-1163.
- Roberts A. 1993. Midges in a changing Highland environment. In Smout T.C. (ed.) *Scotland since Prehistory. Natural change and human impact*. Scottish Cultural Press, Edinburgh. 113-124.
- Rodo X., Baert E. & Comin F.A. 1997. Variations in seasonal rainfall in southern Europe during the present century: Relationships with the North Atlantic Oscillation and the El Nino Southern Oscillation. *Climate Dynamics*. **13**. 275-284.
- Rose N.L., Harlock S., Appleby P.G. & Battarbee R.W. 1995. Dating of recent lake sediments in the United Kingdom and Ireland using spheroidal carbonaceous particle (SCP) concentration profiles. *The Holocene*. **5**. 328-335.
- Ruddiman W.F. & McIntyre A. 1981. The mode and mechanism of the last deglaciation: Oceanic evidence. *Quaternary Research*. **16**. 125-134.
- Ruddiman W.F., Sancetta L.D. & McIntyre A. 1977. Glacial/Interglacial response rate of subpolar North Atlantic water to climatic change: The record in ocean sediments. *Philosophical Transactions of the Royal Society of London*. **B280**. 199-242.
- Russ J.C. 1992. *The Image Processing Handbook*. CRC Press Inc. Boca Raton, Florida, USA. 445 pp.
- Rutsch H.-J., Mangini A., Bonani G., Dittrich-Hannen B., Kubik P.W., Suter M. & Segl M. 1995. ^{10}Be and Ba concentrations in West African sediments trace productivity in the past. *Earth and Planetary Science Letters*. **133**. 129-143.
-

-
- Saarinen T. 1994. Palaeomagnetic study of the holocene sediments of Lake Päijänne (Central Finland) and Lake Paanajärvi (North-West Russia). *Geological Survey of Finland Bulletin*. **376**. 85 pp.
- Saarnisto M. 1985. Long varve series in Finland. *Boreas*. **14**. 133-137.
- Sanders G., Jones K.C. & Shine A.J. 1993. The use of a sediment core to reconstruct the historical input of contaminants to Loch Ness: PCBs and PAHs. *The Scottish Naturalist*. **105**. 87-111.
- Sandgren P. 1993. Paleomagnetic and Mineral Magnetic Investigations of the Laminated Sediments in Lake Gosciadz and the Soils in its Catchment, Central Poland. In Ralska-Jasiewiczowa M. (ed.) *Polish Botanical Study. Guidebook Series* . **8**. 127-142.
- Sandweiss D.H., Richardson J.B., Reitz E.J., Rollins H.B. & Maasch K.A. 1996. Geoarchaeological evidence from Peru for a 5000 years B.P. onset of El Niño. *Science*. **273**. 1531-1533.
- Sanger J.E. & Hay R.J. 1993. Fossil pigments in Holocene varved sediments in Elk Lake, Minnesota. In Bradbury J.P. & Dean W.E. (eds). *Elk Lake, Minnesota: Evidence for rapid climate change in the North-Central United States. USGS Special Paper 276*. United States Geological Survey. 181-188.
- Sartoretto S., Verlaque M. & Laborel J. 1996. Age of settlement and accumulation rate of submarine coralligene (-10 to -60 m) of the Northwestern Mediterranean Sea - Relation to Holocene rise in sea-level. *Marine Geology*. **130**. 317-331.
- Schaaf M. & Thurow J. 1994. A fast and easy method to derive highest-resolution time-
-

-
- series datasets from drillcores and rock samples. *Sedimentary Geology*. **94**. 1-10.
- Schäfer P, Thiede J., Gerlach S., Graf G. & Zeitzschel B. 1995. Global environmental change: the northern North Atlantic. *Geologische Rundschau*. **84**. 3-10.
- Schimmelmann A. & Lange C.B. 1996. Tales of 1001 varves: a review of Santa Barbara Basin sediment studies. In Kemp A.E.S. (ed). *Palaeoclimatology and Palaeoceanography from Laminated Sediments*. Geological Society Special Publication. **116**. The Geological Society, London. 121-141.
- Schimmelmann A., Lange C.B., Berger W.H., Simon A., Burke S.K. & Dunbar R.B. 1992. Extreme climatic conditions recorded in Santa Barbara Basin laminated sediments: the 1835-1840 *Macoma* Event. *Marine Geology*. **106**. 279-299.
- Schweingruber F.H. 1988. *Tree Rings : basics and applications of dendrochronology*. Kluwer Academic Publishers, Dordrecht, Holland. 276 pp.
- Shen G.T., Boyle E.A. & Lea D.W. 1987. Cadmium in corals: Chronicles of historical upwelling and industrial fallout. *Nature*. **328**. 794-796.
- Shilts W.W. & Clague J.J. 1992. Documentation of earthquake-induced disturbance of lake sediments using subbottom acoustic profiling. *Canadian Journal of Earth Sciences*. **29**. 1018-1042.
- Shine A.J. & Martin D.S. 1988. Loch Ness habitats observed by Sonar and underwater television. *The Scottish Naturalist*. **100**. 111-199.
- Shine A.J., Minshull J. & Shine M. 1993. Historical background and introduction to the recent work of the Loch Ness and Morar Project. *The Scottish Naturalist*. **105**. 7-
-

22.

- Shoji H. & Langway Jr. J.J. 1989. Physical property reference horizons. In Oeschger H. & Langway Jr. C.C. (eds) *The Environmental Record in Glaciers and Ice Sheets. Report of the Dahlem Workshop, Berlin 1988, March 13-18. Research report 8*. J.Wiley & Sons, Chichester, UK. 269-286.
- Shopov Y.Y., Ford D.C. & Schwarcz H.P. 1994. Luminescent microbanding in speleothems: High-resolution chronology and paleoclimate. *Geology*. **22**. 407-410.
- Shore J.S., Bartley D.D. & Harkness D.D. 1995. Problems encountered with the ^{14}C dating of peat. *Quaternary Science Reviews (Quaternary Geochronology)*. **14**. 373-383.
- Shulmeister J. & Lees B.G. 1995. Pollen evidence from tropical Australia for the onset of an ENSO-dominated climate at c. 4000 BP. *The Holocene*. **5**. 10-18
- Siegenthaler U. & Beer J. 1988. Model comparison of ^{14}C and ^{10}Be isotope records. In Stephenson F.R and Wolfendale A.W. (eds) *Secular Solar and Geomagnetic Variations in the Last 10,000 Years*. NATO ASI series C. Mathematical and Physical Sciences. **236**. Kluwer Academic, Dordrecht. 315-328.
- Simola H. 1977. Diatom succession in the formation of annually-laminated sediments in Lovojärvi, a small eutrophicated lake. *Annales Botanici Fennici*. **14**. 143-148.
- Simola H. & Tolonen K. 1981. Diurnal laminations in the varved sediment of Lake Lovojärvi, south Finland. *Boreas*. **10**. 19-26.
- Simola H. & Uimonen-Simola P. 1983. Recent stratigraphy and accumulation of

-
- sediment in the deep, oligotrophic Lake Pääjärvi in South Finland. *Hydrobiologia*. **103**. 287-293.
- Simpson J.H. & Woods J.D. 1970. Temperature microstructure in a fresh water thermocline. *Nature*. **226**. 832-834.
- Singer C., Shulmeister J. & McLea B. 1998. Evidence against a significant Younger Dryas cooling event in New Zealand. *Science*. **281**. 812-814.
- Sissons J.B. 1981. Lateglacial marine erosion and a jökulhlaup deposit in the Beaully Firth. *Scottish Journal of Geology*. **17**. 7-19.
- Sissons J.B. 1979. Catastrophic lake drainage in Glen Spean and the Great Glen, Scotland. *Journal of the Geological Society of London*. **136**. 215-224.
- Slowey N.C., Henderson G.M. & Curry W.B. 1996. Direct U-Th dating of marine sediments from the two most recent interglacial periods. *Nature*. **383**. 242-244.
- Smith I.R., Lyle A.A. & Rosie A.J. 1981. Comparative physical limnology. In Maitland P.S. (ed.) *The Ecology of Scotland's Largest Lochs. Lomond, Awe, Ness, Morar and Shiel. Monographiae Biologicae*. **44**. Dr.W.Junk Publishers, The Hague. 29-66.
- Smith K. 1995. Precipitation over Scotland, 1757-1992: Some aspects of temporal variability. *International Journal of Climatology*. **15**. 543-556.
- Smith M.B., Poynter J.G., Bradshaw S.A. & Eglinton G. 1994. High resolution molecular stratigraphy: analytical methodology. In Hailwood E.A. and Kidd R.B. (eds) *High Resolution Stratigraphy*. Geological Society Special Publication. **70**.
-

-
- The Geological Society. London. 51-63.
- Smout T.C. 1993. Woodland history before 1850. In Smout T.C. (ed.) *Scotland since Prehistory. Natural change and human impact*. Scottish Cultural Press, Edinburgh. 40-49.
- Sonett C.P., Williams C.R. & Mörner N.-A. 1992. The Fourier spectrum of Swedish riverine varves: evidence of sub-arctic quasi-biennial (QBO) oscillations. *Paleogeography, Paleoclimatology, Paleoecology (Global and Planetary Change Section)*. **98**. 57-65.
- Sowers T., Bender M., Labeyrie L., Martinson D., Jouzel J., Raynaud D., Pichon J.J. & Korotkevich Y.S. 1993. A 135,000-year Vostok-SPECMAP common temporal framework. *Paleoceanography*. **8**. 737-766.
- Sprowl D.R. 1993. On the precision of the Elk lake chronology. In Bradbury J.P. & Dean W.E. (eds) *Elk Lake, Minnesota: Evidence for Rapid Climate Change in the North-Central United States*. Special Paper 276. Geological Society of America, Boulder, Colorado. 69-73.
- Sprowl D.R. & Banerjee S.K. 1985. High-resolution paleomagnetic record of geomagnetic field fluctuations from the varved sediments of Elk Lake Minnesota. *Geology*. **13**. 531-533.
- Stauffer B. 1989. Dating of Ice by Radioactive Isotopes. In Oeschger H. & Langway C.C. (eds) *The Environmental Record in Glaciers and Ice Sheets. Report of the Dahlem Workshop, Berlin 1988, March 13-18. Research report 8*. J.Wiley & Sons, Chichester, UK. 123-139.
-

-
- Steig E.J., Brook E.J., White J.W.C., Sucher C.M., Bender M.L., Lehman S.J., Morse D.L., Waddington E.D. & Clow G.D. 1998. Synchronous climate changes in Antarctica and the North Atlantic. *Science*. **282**. 92-95.
- Stihler S.D., Stone D.B. & Beget J.E. 1992. "Varve" counting vs. tephrochronology and ^{137}Cs and ^{210}Pb dating: A comparative test at Skilak Lake, Alaska. *Geology*. **20**. 1019-1022.
- Stix M. 1991. *The Sun: an introduction*. Springer Verlag, Berlin. 2nd edition. 390 pp.
- Strömberg B. 1994. Younger Dryas deglaciation at Mt. Billingen, and clay varve dating of the Younger Dryas/Preboreal transition. *Boreas*. **23**. 177-193.
- Stuiver M. 1980a. Solar variability and climatic change during the current millenium. *Nature*. **286**. 616-617.
- Stuiver M. 1980b. Long-term C14 variations. In Olsson I.U. (ed.) *Nobel Symposium 12, Radiocarbon Variations and Absolute Chronology*. Wiley Interscience, New York. 197-213.
- Stuiver M. 1989. Dating proxy data. In Berger A., Schneider S., Duplessy J.-C. (eds) *Climate and Geo-Sciences. A Challenge for Science and Society in the 21st Century*. NATO ASI Series C: Mathematical and Physical Sciences. **285**. Kluwer Academic Publishers, Dordrecht. 39-45.
- Stuiver M. 1994. Atmospheric ^{14}C as a proxy of solar and climatic change. In Nesme-Ribes E. (ed.) *The Solar Engine and Its Influence on Terrestrial Atmosphere and Climate*. NATO ASI Series. **125**. Springer-Verlag, Berlin.
-

-
- Stuiver M. & Quay P.D. 1980. Changes in Atmospheric Carbon-14 Attributed to a Variable Sun. *Science*. **207**. 11-19.
- Stuiver M. & Reimer P.J.. 1993. Extended 14C database and revised CALIB 3.0.3e ¹⁴C calibration program. *Radiocarbon*.. **35**. 215-230.
- Sturm M. 1979. Origin and composition of clastic varves. In Schlüchter C. (*ed.*) *Moraines and varves. Origins/ Genesis/ Classification*. Balkema, Rotterdam. 281-285.
- Sturm M. & Matter A. 1972. The electro-osmotic guillotine, a new device for core cutting. *Journal of Sedimentary Petrology*. **42**. 987-989.
- Sturm M. & Matter A. 1978. Turbidites and Varves in Lake Brienz (Switzerland): Deposition of Clastic Detritus by Density Currents. In Matter A. and Tucker M.E. (*eds*) *Modern and Ancient Lake Sediments: Special Publication Number 2 of the International Association of Sedimentologists*. 147-168.
- Sudo M., Uto K., Anno K., Ishizuka O. & Uchiumi S. 1998. SORI93 biotite: a new mineral standard for K-Ar dating. *Geochemical Journal*. **32**. 49-58.
- Suess H.E. & Linick T.W. 1990. The ¹⁴C record of bristlecone pine wood of the past 8000 years based on the dendrochronology of the late C.W. Ferguson. *Philosophical Transactions of the Royal Society of London*. **A330**. 403-412.
- Sugden D.E. 1977. Did glaciers form in the Cairngorms in the seventeenth to nineteenth centuries? *Cairngorm Club Journal*. **18**. 189-201.
- Sutherland D.G. & Gordon J.E. 1993. Inverness area (Introduction). In Gordon J.E and
-

-
- Sutherland D.G. (eds) *Quaternary of Scotland*. Chapman and Hall, London. 147-152.
- Swain A.M. 1978. Environmental changes during the past 2000 years in North-Central Wisconsin: Analysis of pollen, charcoal, and seeds from varved lake sediments. *Quaternary Research*. **10**. 55-68.
- Syngé F.M. 1977. Records of sea levels during the Late Devensian. *Philosophical Transactions of the Royal Society of London*. **A280**. 211-228.
- Syngé F.M. & Smith J.S. 1980. *Inverness Field Guide*. Quaternary Research Association, Cambridge. 1-29.
- Tanaka K., Machette M.N., Crone A.J. & Bowman J.R. 1995. ESR dating of aeolian sand near Tennant Creek, Northern Territory, Australia. *Quaternary Science Reviews (Quaternary Geochronology)*. **14**. 385-393.
- Tauber H. 1980. Scandinavian varve chronology and C14. In Olsson I.U. (ed.) *Nobel Symposium 12, Radiocarbon Variations and Absolute Chronology*. Wiley Interscience, New York. 173-196.
- Taylor A.H. 1996. North-South shifts of the Gulf Stream: Ocean-atmosphere interactions in the North Atlantic. *International Journal of Climatology*. **16**. 559-593.
- Taylor A.H., Jordan M.B. & Stephens J.A. 1998. Gulf Stream shifts following ENSO events. *Nature*. **393**. 638.
- Taylor K.C., Lamorey G.W., Doyle G.A., Alley R.B., Grootes P.M., Mayewski P.A.,
-

-
- White J.W.C. & Barlow L.K. 1993. The 'flickering switch' of late Pleistocene climate change. *Nature*. **361**. 432-436.
- Taylor P.D. 1991. *Observing the Sun*. Cambridge University Press. Cambridge, UK. 159 pp.
- Taylor J.A. & Yates R.A. 1967. *British Weather in Maps*. 2nd Edition. Macmillan, London. 315 pp.
- Thomas R.G. 1993. Rome rainfall and sunspot numbers. *Journal of Atmospheric and Terrestrial Physics*. **55**. 155-164.
- Thompson L.G. 1995. Ice core evidence from Peru and China. In Bradley R.S & Jones P.D. (eds). 1995. *Climate since A.D. 1500*. 2nd Edition. Routledge, London. 517-548.
- Thompson R. 1973. Paleolimnology and Paleomagnetism. *Nature*. **242**. 182-184.
- Thorpe S.A. 1971. Asymmetry of the Internal Seiche in Loch Ness. *Nature*. **231**. 306-308.
- Thorpe S.A., Hall A. & Crofts I. 1972. The internal surge in Loch Ness. *Nature*. **237**. 96-98.
- Thorpe S.A. 1977. Turbulence and mixing in a Scottish Loch. *Philosophical Transactions of the Royal Society of London*. **A286**. 125-181.
- Tinsley B.A. 1988. The Solar Cycle and the QBO influences on the latitude of storm tracks in the North Atlantic. *Geophysical Research Letters*. **15**. 409-412.
-

-
- Tinsley H.M. & Grigson C. 1981. The Bronze Age. In Simmons I.G. & Tooley M.J. (eds). *The environment in British prehistory*. Duckworth & Co., London. 334 pp.
- Tipping R.M. 1989. Long-distance transported *Pinus* pollen as a possible chronostratigraphic marker in the early Scottish Postglacial. *Boreas*. **18**. 333-341.
- Tolonen M. 1978. Paleoecology of annually laminated sediments in Lake Ahvenainen, S. Finland. I. Pollen and charcoal analyses and their relation to human impact. *Annales Botanici Fennici*. **15**. 177-208.
- Tolonen M. 1978. Paleoecology of annually laminated sediments in Lake Ahvenainen, S. Finland. II. Comparison of dating methods. *Annales Botanici Fennici*. **15**. 209-222.
- Tolonen M. 1978. Paleoecology of annually laminated lake sediments in Lake Ahvenainen, S. Finland. III. Human influence in the lake development. *Annales Botanici Fennici*. **15**. 223-240.
- Tudhope S. 1994. Extracting High-Resolution Climatic Records From Coral Skeletons. *Geoscientist*. **4**. 17-20.
- van Geel B. & van der Hammen T. 1973. Upper Quaternary vegetational and climatic sequence of the Fuquene area (eastern Cordillera, Colombia). *Palaeogeography, Palaeoclimatology, Palaeoecology*. **14**. 9-92.
- Van Klinken G.J., Van der Plicht H. & Hedges R.E.M. 1994. Bone C-13/C-12 ratios reflect (palaeo-) climatic variations (Vol 21, pg 445, 1994). *Geophysical Research Letters*. **21**. 2867.
-

-
- Velde B. 1996. Compaction trends of clay-rich deep-sea sediments. *Marine Geology*. **133**. 193-201.
- Verosub K.L. 1988. Geomagnetic secular variation as determined from paleomagnetic studies of lake sediments and its relation to the study of the cosmic ray flux. In Stephenson F.R and Wolfendale A.W. (eds) *Secular Solar and Geomagnetic Variations in the Last 10,000 Years. NATO ASI series C. Mathematical and Physical Sciences*. **236**. Kluwer Academic, Dordrecht. 399-418.
- Vincens A., Chalié F., Bonnefille R., Guiot J. & Tiercelin J.-J. 1993. Pollen-derived rainfall and temperature estimates from Lake Tanganyika and their implication for late Pleistocene water levels. *Quaternary Research*. **40**. 343-350.
- Vos H., Sanchez A., Zolitschka B., Brauer A. & Negendank J.F.W. 1997. Solar activity variations recorded in varved sediments from the crater Lake of Holzmaar - A Maar Lake in the Westeifel volcanic field, Germany. *Surveys in Geophysics*. **18**. 163-182.
- Walanus A. & Goslar T. 1993. Komputerowe Pomiaru Grubosci Lamin. In Ralska-Jasiewiczova M.(ed.) *Polish Botanical Studies, Guidebook Series 8*. 121-125. (in Polish)
- Wedderburn E.M. & Watson W. 1909. Observations with a current meter in Loch Ness. *Proceedings of the Royal Society of Edinburgh*. **7**. 619-647.
- Werrity A., Brazier V., Gordon J.E & McManus J. 1994. Geomorphology. In Maitland P.S., Boon P.J. & McLusky D.S. (eds) *The Fresh Waters of Scotland: A National Resource of International Significance*. John Wiley & Sons, Chichester.
-

65-88.

- Wheeler L.A. Unpubl. PhD thesis. University of Wolverhampton. UK. (In preparation).
- Whitlock C., Bartlein P.J. & Watts W.A. 1993. Vegetation history of Elk Lake. In Bradbury J.P. & Dean W.E. (eds) *Elk Lake, Minnesota: Evidence for rapid climate change in the North-Central United States. USGS Special Paper 276*. United States Geological Survey. 251-274.
- Whyte I.D. 1995. *Climatic change and human society*. Arnold Publishers, London. 217 pp.
- Wigley T.M.L. & Kelly P.M. 1990. Holocene climatic change, ¹⁴C wiggles and variations in solar irradiance. *Philosophical Transactions of the Royal Society of London*. **A330**. 547-560.
- Willson R.C. & Hudson H.S. 1988. Solar luminosity variations in solar cycle-21. *Nature*. **332**. 810-812.
- Wohlfarth B., Björck S., Possnert G., Lemdahl G., Brunnberg L., Ising I., Ollsson S. & Svensson N.-O. 1993. AMS dating Swedish varved clays of the last glacial/interglacial transition and the potential/difficulties of calibrating Late Weichselian 'absolute' chronologies. 1993. *Boreas*. **22**. 113-128.
- Wood A.M., Whatley R.C., Cronin T.M. & Holtz T. 1993. Pliocene palaeotemperature reconstruction for the southern North Sea based on Ostracoda. *Quaternary Science Reviews*. **12**. 747-767.

-
- Yiou P., Ghil M., Jouzel J., Paillard D. & Vautard R. 1994. Nonlinear variability of the climatic system from singular and power spectra of Late Quaternary records. *Climate Dynamics*. **9**. 371-389.
- Yiou F., Raisbeck G.M., Bourles D., Lorius C. & Barkov N.I. 1985. Be-10 in ice at Vostok, Antarctica during the last climatic cycle. *Nature*. **316**. 616-617.
- Young I. & Shine A.J. 1993. Loch Ness bathymetry and seismic survey, December 1993. *The Scottish Naturalist*. **105**. 23-43.
- Zaitseva G.I. 1995. Chemical composition and sample preparation of archaeological wood for radiocarbon dating. *Radiocarbon*. **37**. 311-317.
- Zeeb B.A. & Smol J.P. 1993. Postglacial chrysophycean cyst record from Elk Lake, Minnesota. In Bradbury J.P. & Dean W.E. (eds) *Elk Lake, Minnesota: Evidence for rapid climate change in the North-Central United States*. USGS *Special Paper 276*. United States Geological Survey. 239-250.
- Zolitschka B. 1991. Absolute dating of late Quaternary lacustrine sediments by high resolution varve chronology. *Hydrobiologia*. **214**. 59-61.
- Zolitschka B. 1992. Climatic Change Evidence and Lacustrine Varves from Maar Lakes, Germany. *Climate Dynamics*. **6**. 229-232.
- Zolitschka B. 1996. High resolution lacustrine sediments and their potential for palaeoclimatic reconstruction. In Jones P.D., Bradley R.S and Jouzel J. (eds) *Climatic Variations and Forcing Mechanisms Over The Last 2000 Years*. NATO ASI series C. *Mathematical and Physical Sciences*. **41**. Springer Verlag, Berlin.
-

453-478.

Zolitschka B., Negendank J.F.W. & Lottermoser B.G. 1995. Sedimentological proof and dating of the early Holocene volcanic eruption of Ulmener Maar (Vulkaneifel, Germany). *Geologische Rundschau*. **84**. 213-219.

Core Ness 3 x-radiograph, 0.0-0.15 m



Core *Ness 3* x-radiograph, 0.14-0.29 m



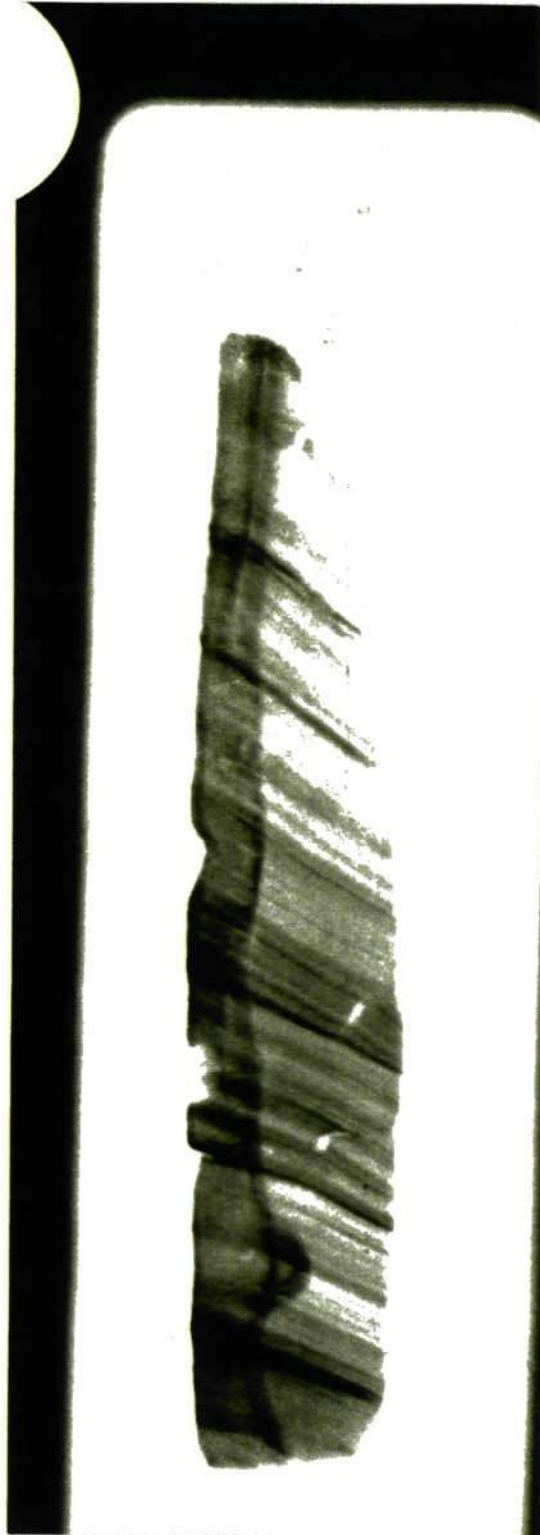
Core Ness 3 x-radiograph, 0.27-0.42 m



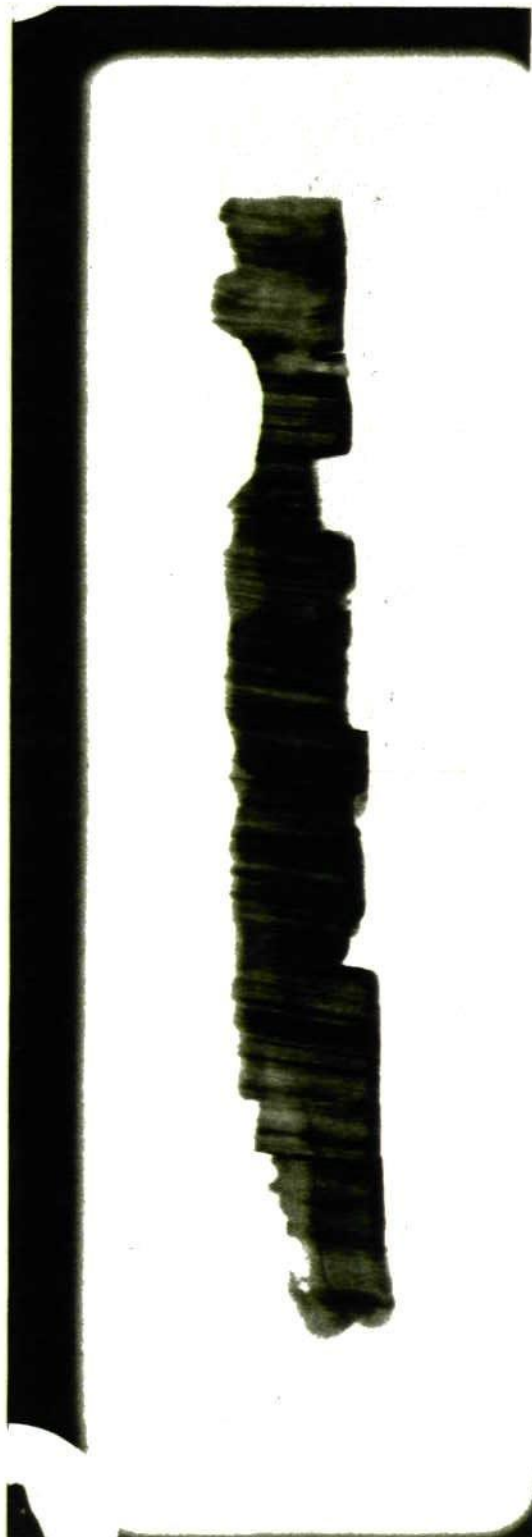
Core Ness 3 x-radiograph, 0.40-0.55 m



Core *Ness 3* x-radiograph, 0.55-0.70 m



Core Ness 3 x-radiograph, 0.69-0.84 m



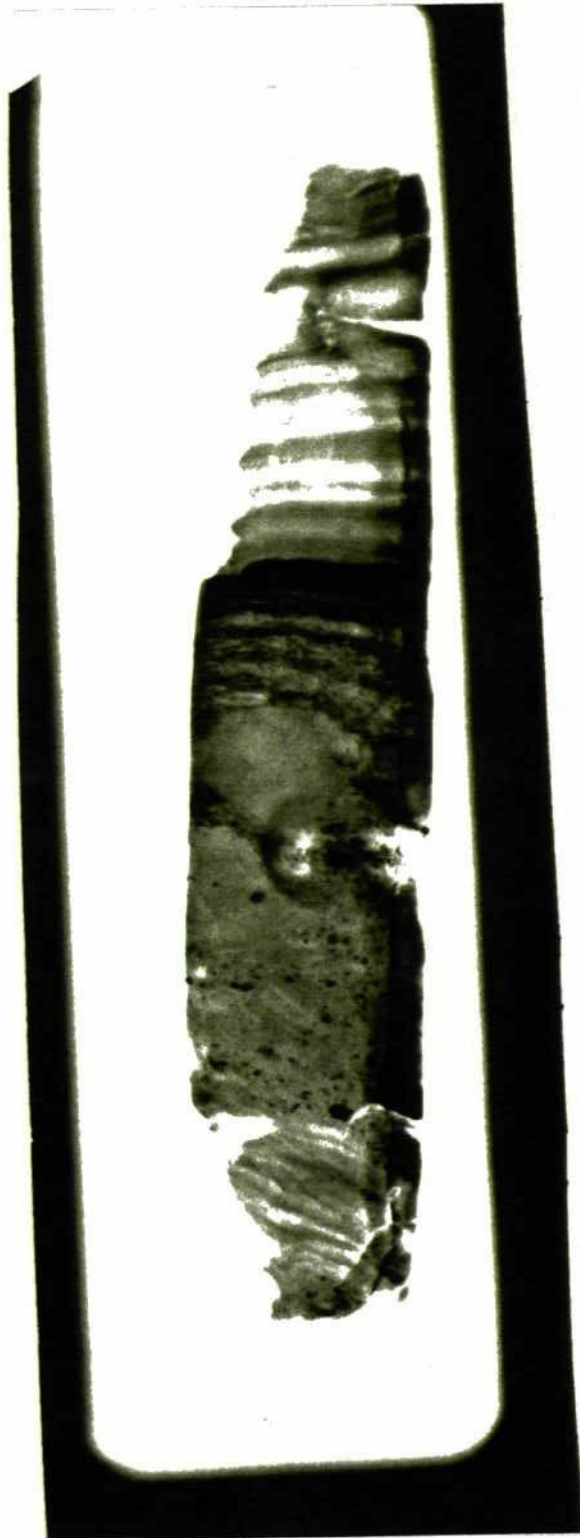
Core *Ness 3* x-radiograph, 0.83-0.98 m



Core Ness 3 x-radiograph, 0.97-1.12 m



Core *Ness 3* x-radiograph, 1.09-1.24 m



Core *Ness 3* x-radiograph, 1.18-1.33 m



Core Ness 3 x-radiograph, 1.32-1.47 m



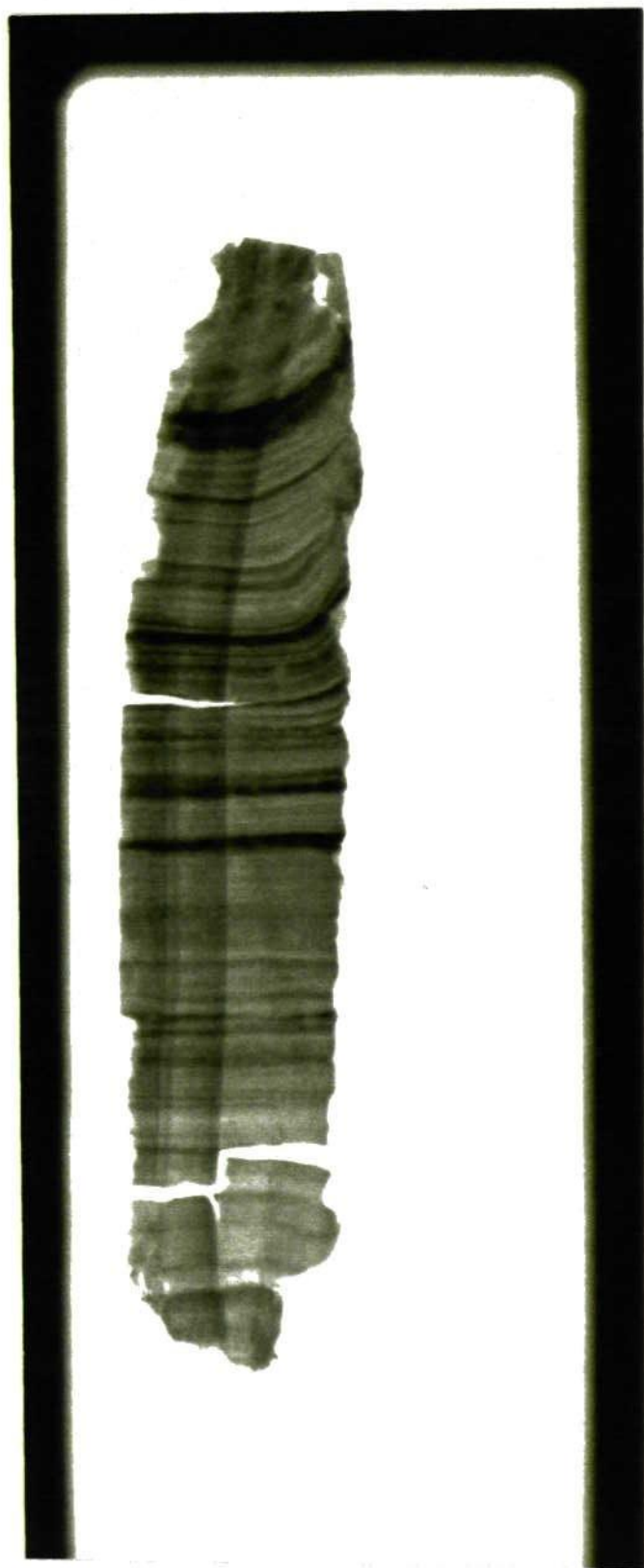
Core Ness 3 x-radiograph, 1.44-1.59 m



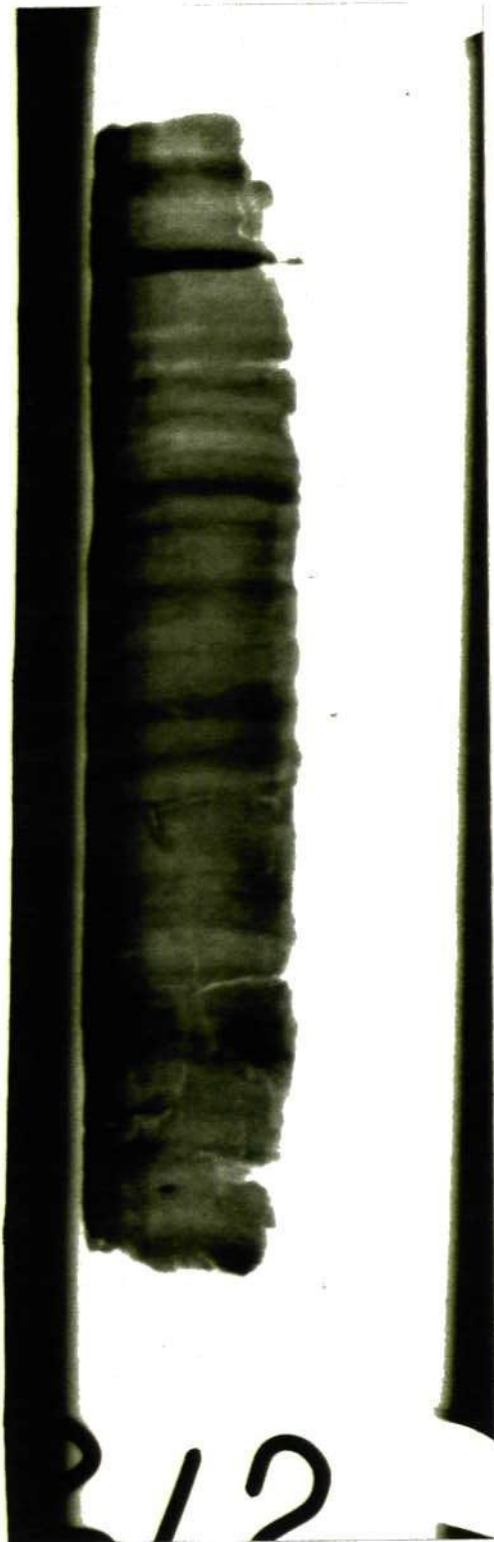
Core Ness 3 x-radiograph, 1.59-1.62 m



Core *Ness 3* x-radiograph, 1.62-1.79 m



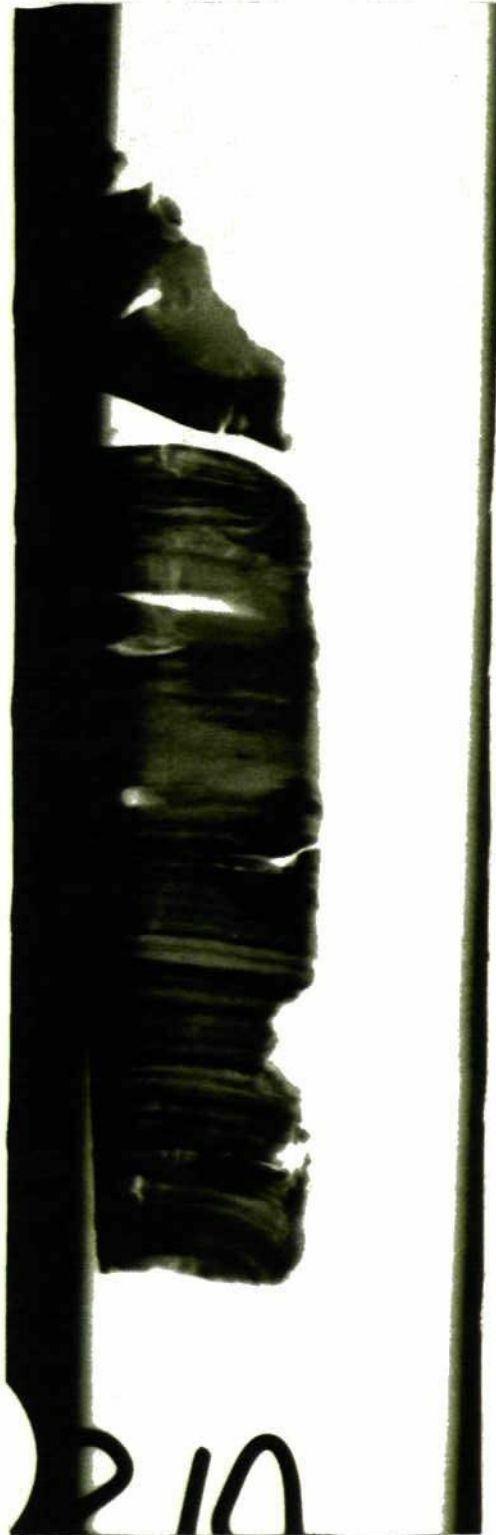
Core Ness 3 x-radiograph, 1.78-1.93 m



Core Ness 3 x-radiograph, 1.92-2.07 m



Core *Ness 3* x-radiograph, 2.05-2.20 m



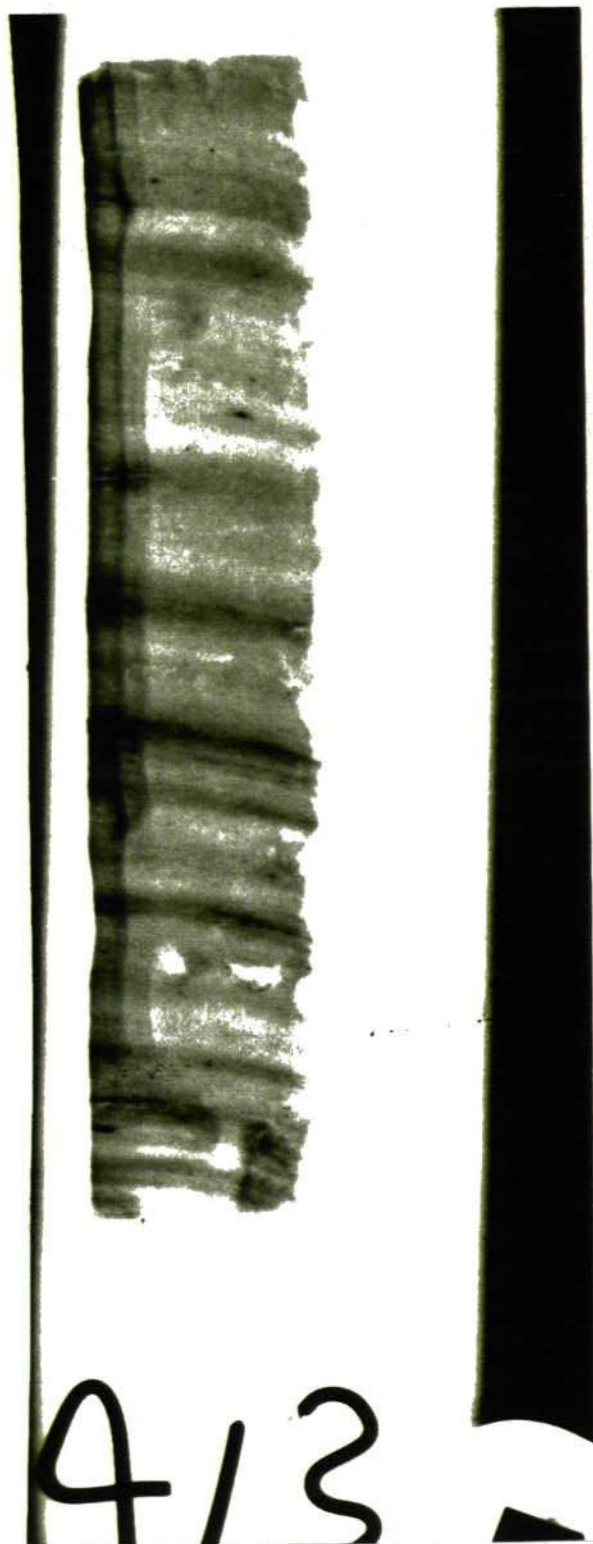
Core *Ness 3* x-radiograph, 2.20-2.35 m



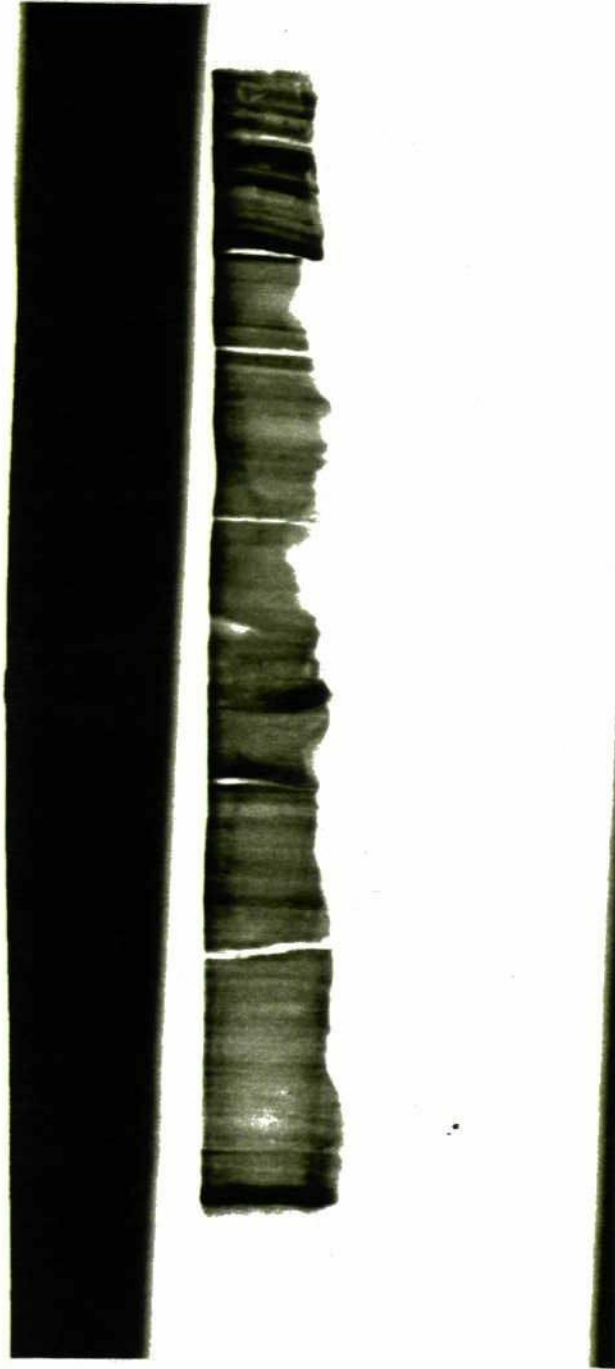
Core *Ness 3* x-radiograph, 3.32-3.47 m



Core Ness 3 x-radiograph, 3.46-3.61 m



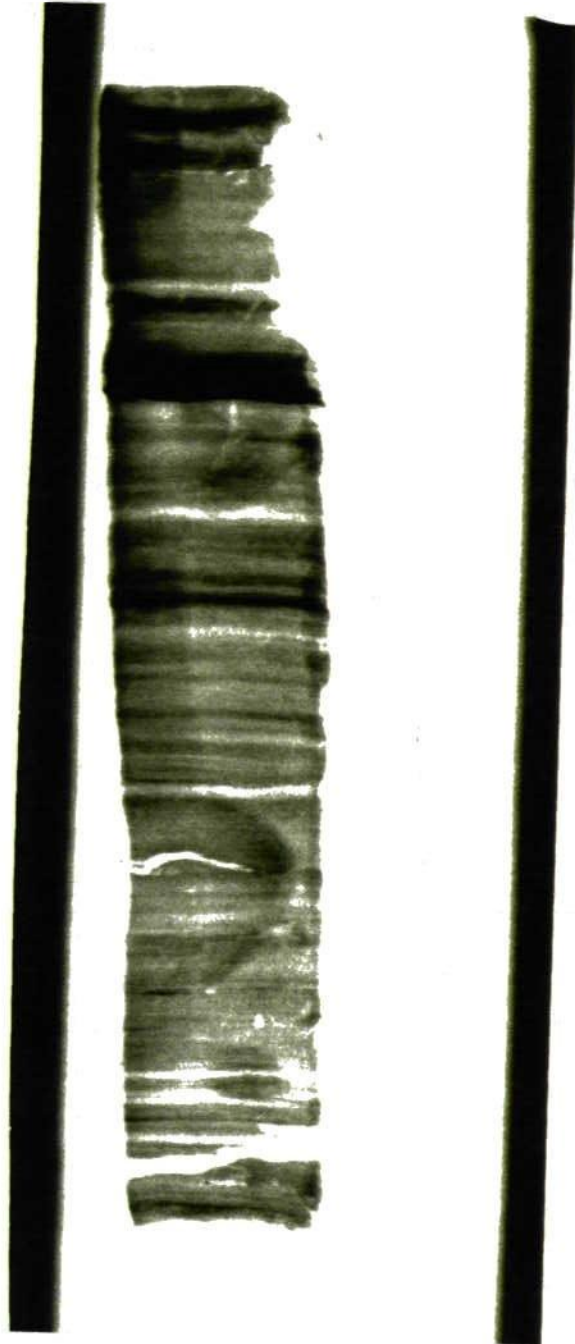
Core *Ness 3* x-radiograph, 3.59-3.74 m



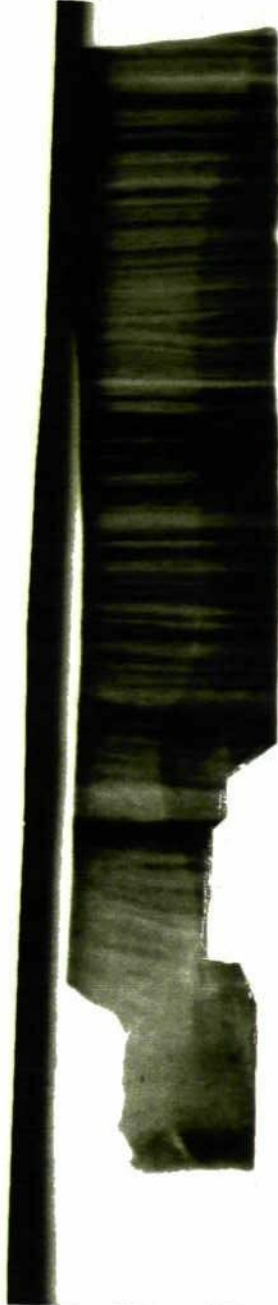
Core Ness 3 x-radiograph, 3.73-3.88 m



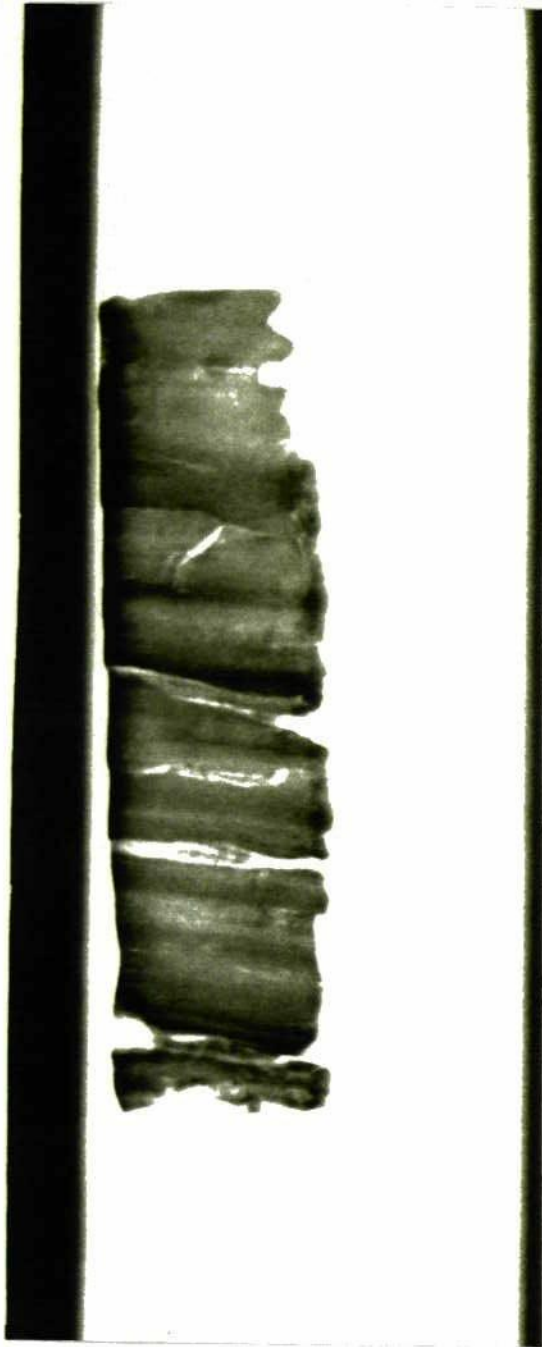
Core *Ness 3* x-radiograph, 3.86-4.01 m



Core *Ness 3* x-radiograph, 3.99-4.14 m



Core Ness 3 x-radiograph, 4.13-4.28 m



Core *Ness 3* x-radiograph, 4.23-4.38 m. Clay/*gyttja* contact. The image on the left is overexposed, illustrating laminations within the uppermost 1 cm of the clay, and the granularity of the sand layer beneath it.



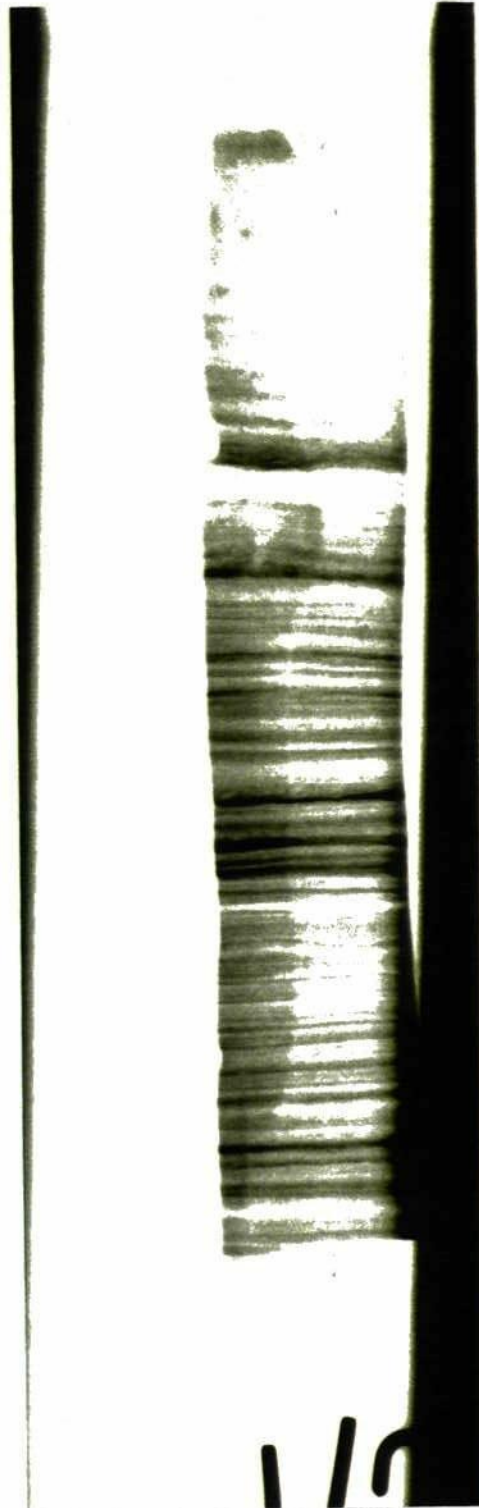
Core Ness 3 x-radiograph, 4.36-4.51 m. Unlaminated grey clay.



Core *Ness 4* x-radiograph, 0.0-0.15 m



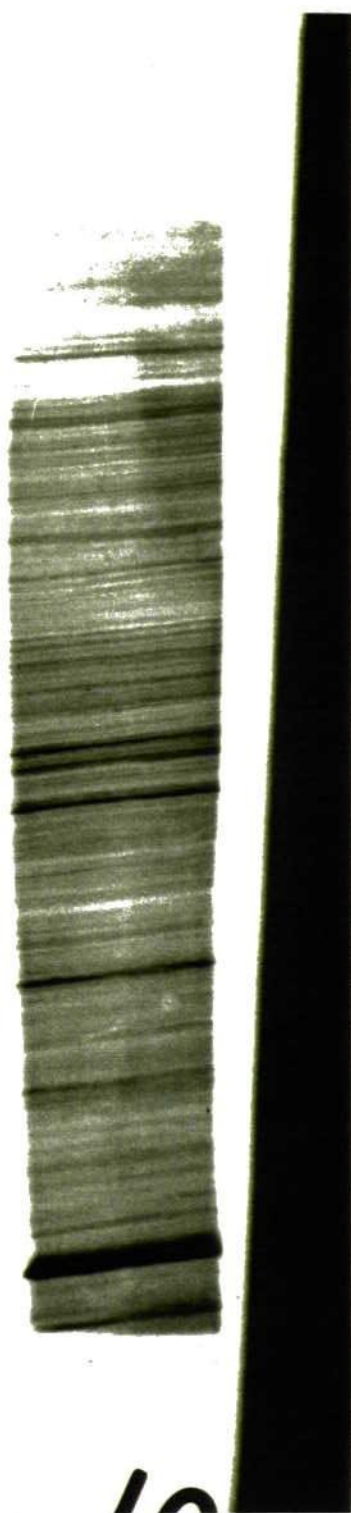
Core Ness 4 x-radiograph, 0.14-0.29 m



Core *Ness 4* x-radiograph, 0.28-0.43 m



Core Ness 4 x-radiograph, 0.42-0.58 m

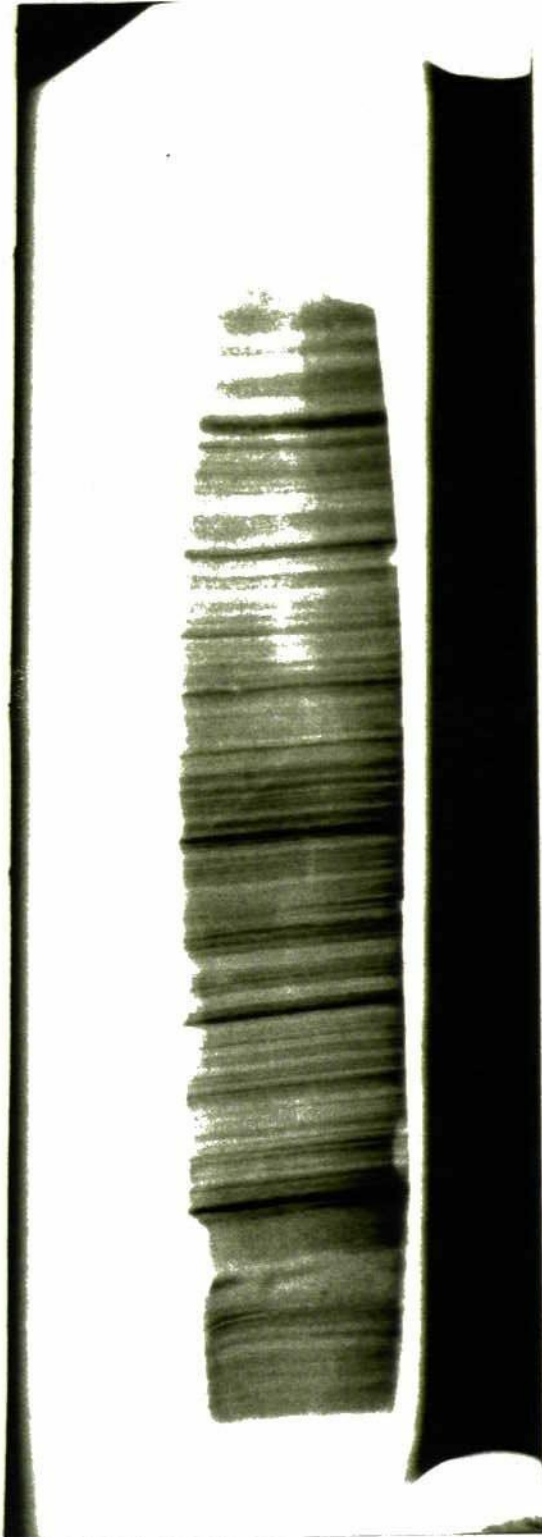


10

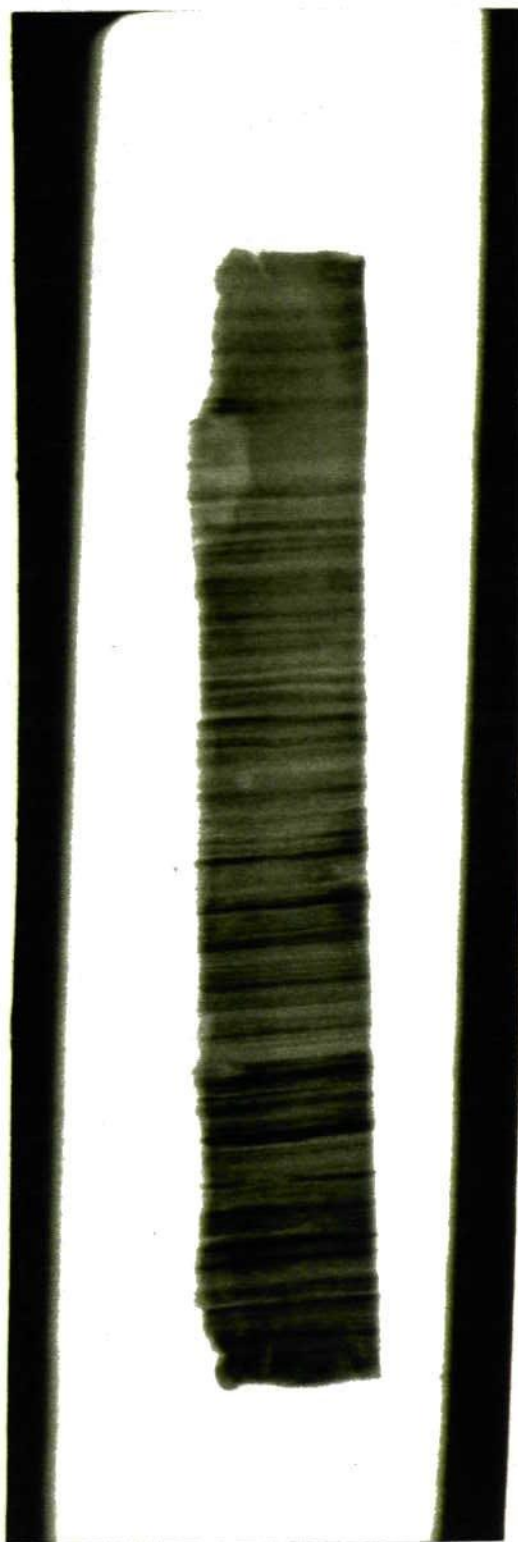
Core Ness 4 x-radiograph, 0.56-0.71 m



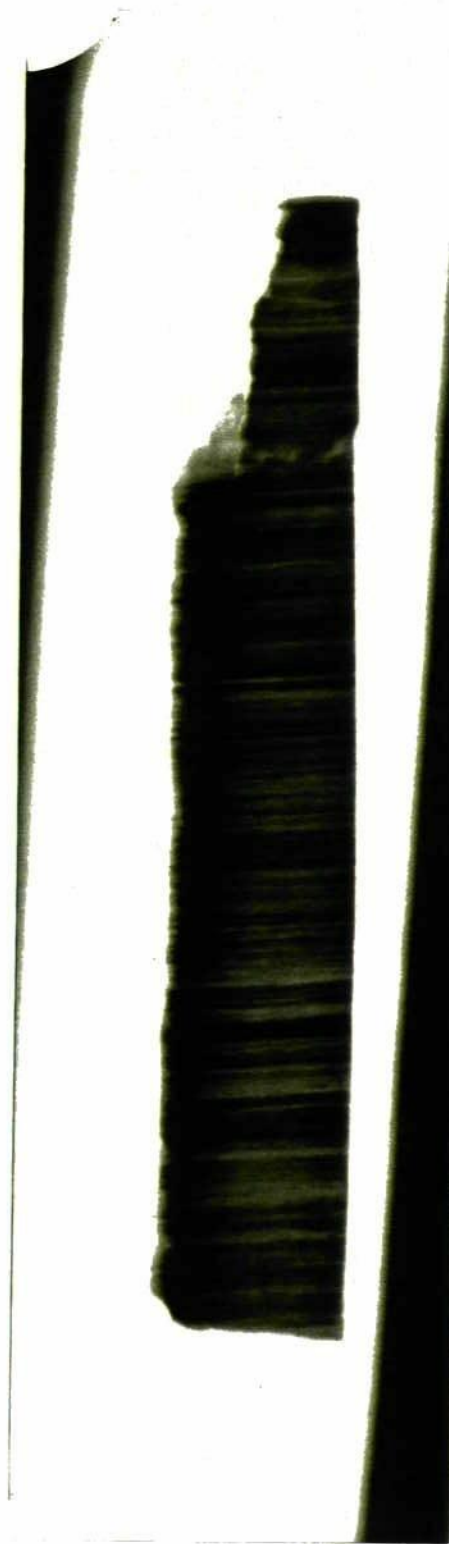
Core Ness 4 x-radiograph, 0.70-0.85m



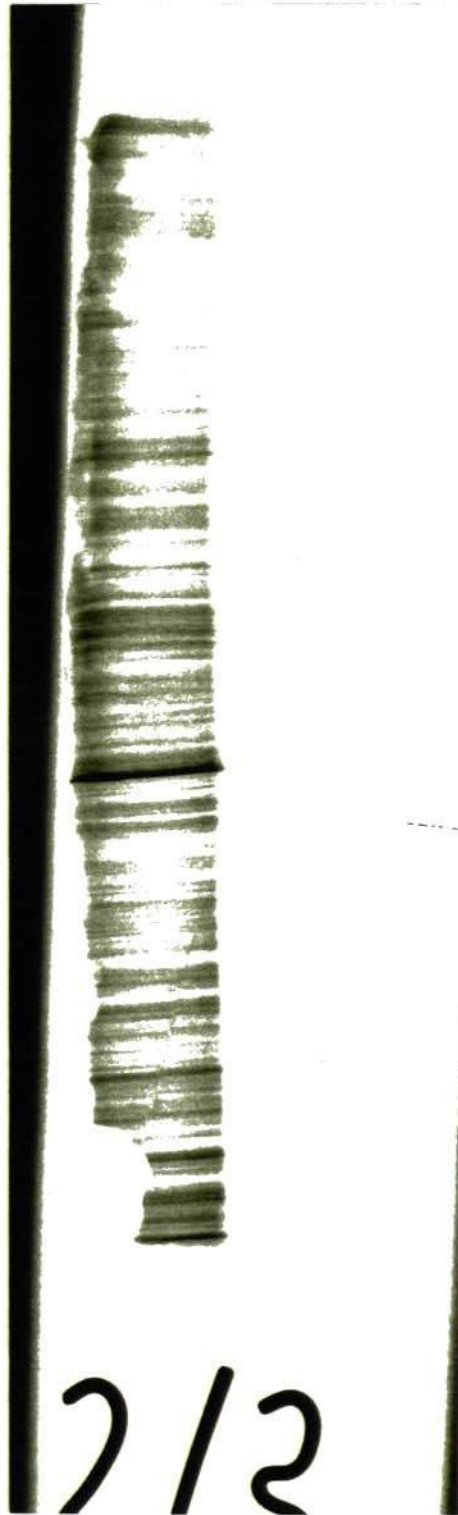
Core *Ness 4* x-radiograph, 0.85-1.00 m



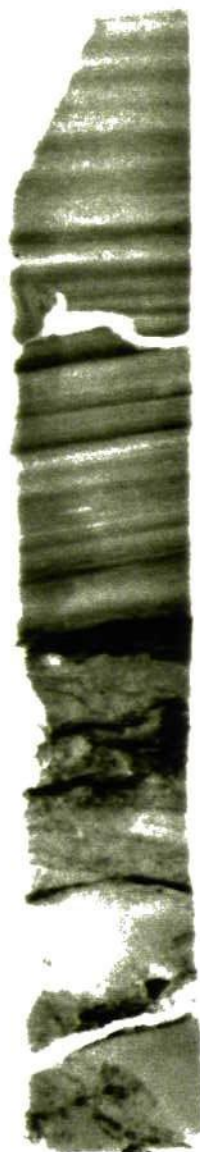
Core Ness 4 x-radiograph, 1.00-1.15 m



Core *Ness 4* x-radiograph, 1.15-1.30 m



Core *Ness 4* x-radiograph, 1.30-1.45 m



Core *Ness 4* x-radiograph, 1.42-1.57 m

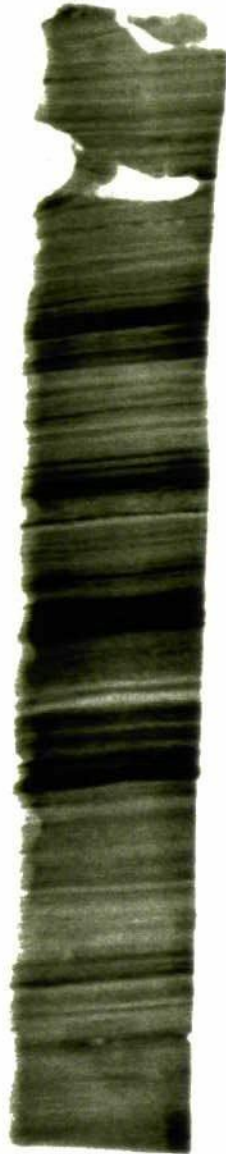


Core *Ness 4* x-radiograph, 1.57-1.72 m

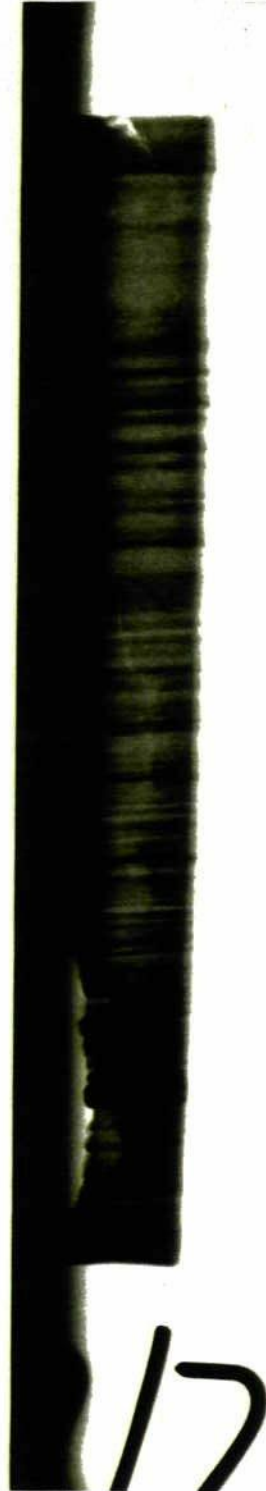


261

Core *Ness 4* x-radiograph, 1.71-1.86 m



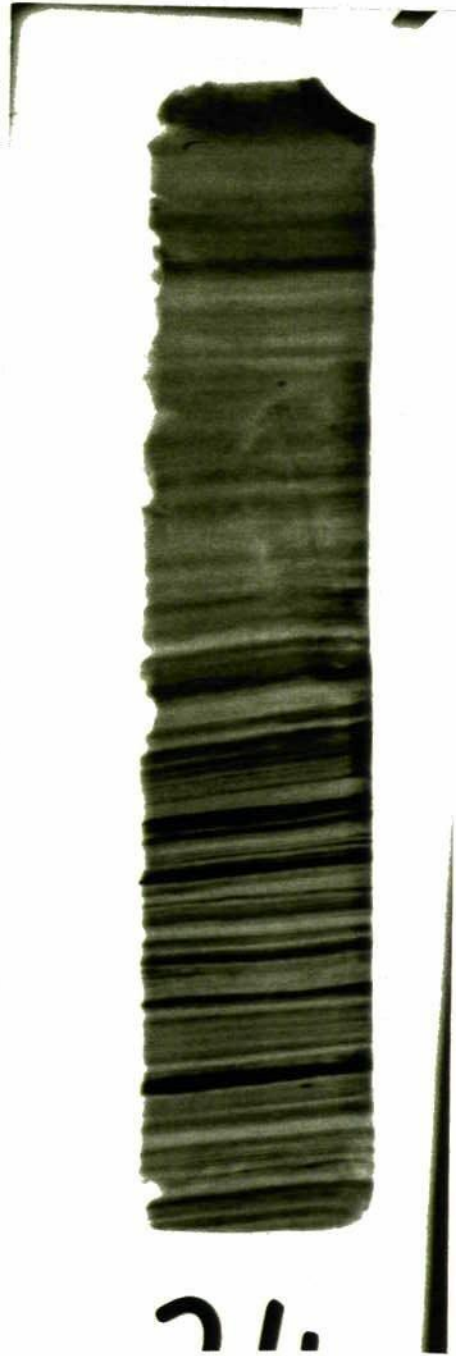
Core Ness 4 x-radiograph, 1.85-2.00 m



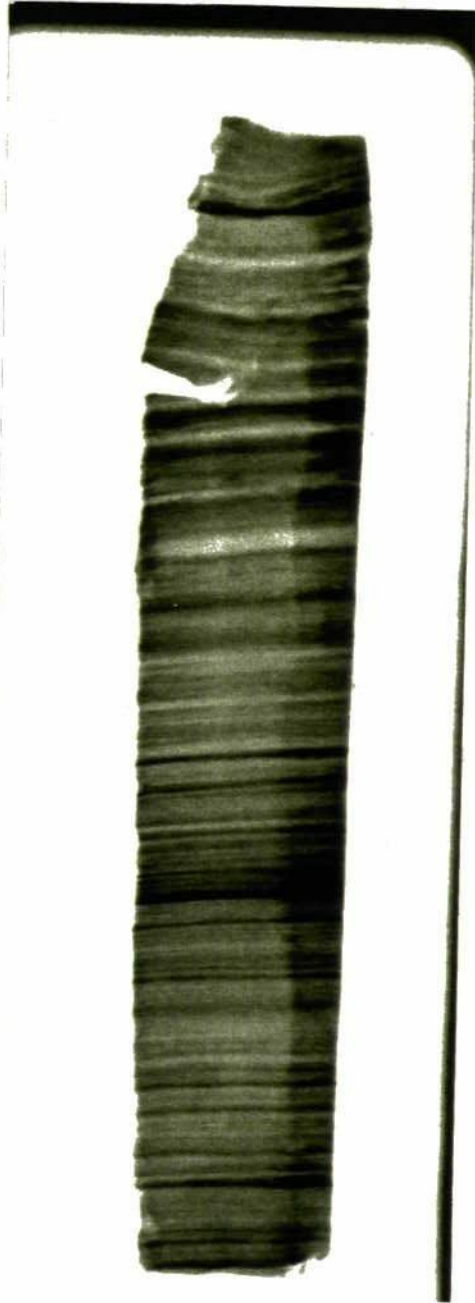
Core *Ness 4* x-radiograph, 2.00-2.15 m



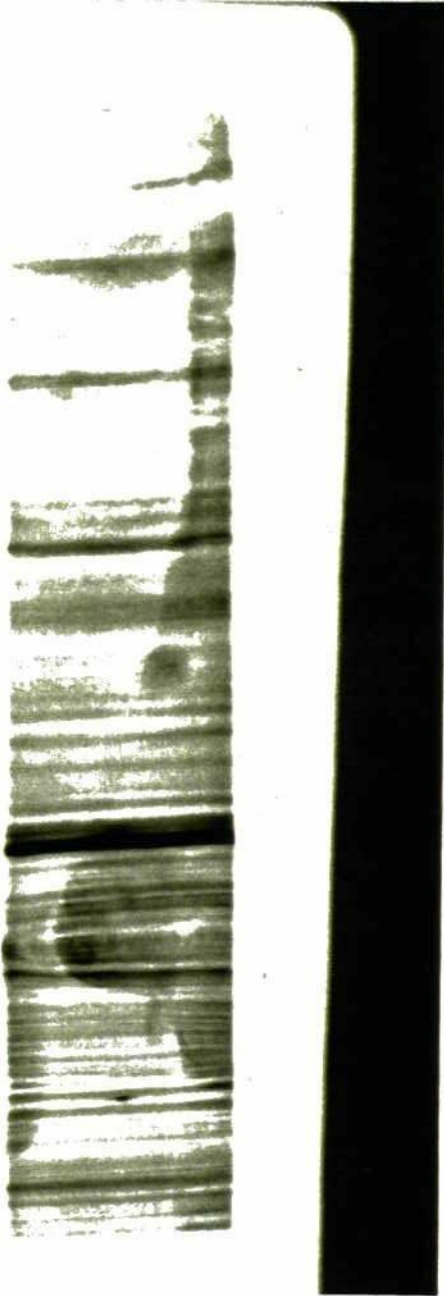
Core *Ness 4* x-radiograph, 2.14-2.29 m



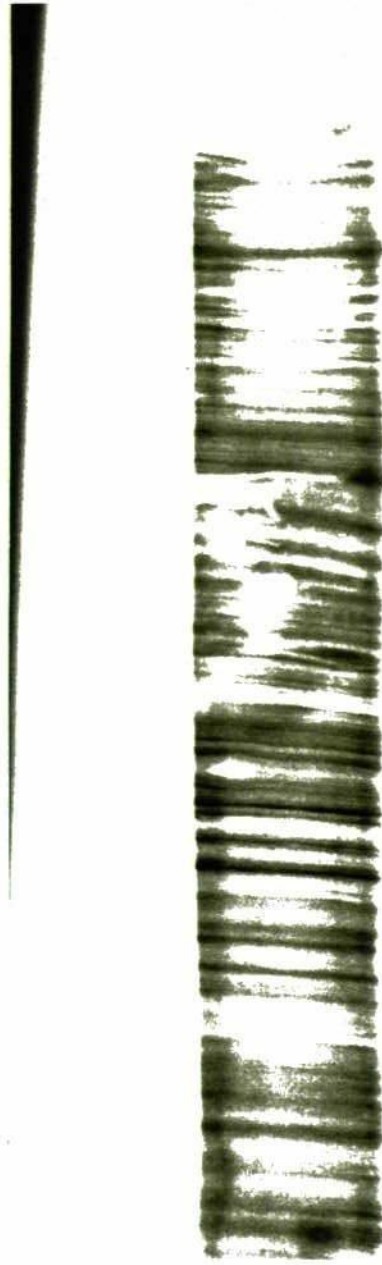
Core *Ness 4* x-radiograph, 2.28-2.43 m



Core *Ness 4* x-radiograph, 2.42-2.57 m

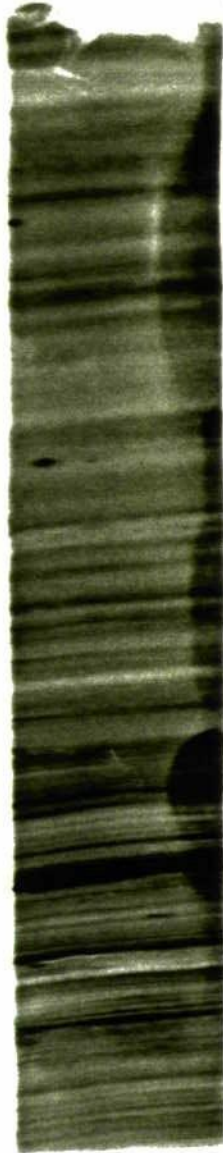


Core Ness 4 x-radiograph, 2.55-2.70 m



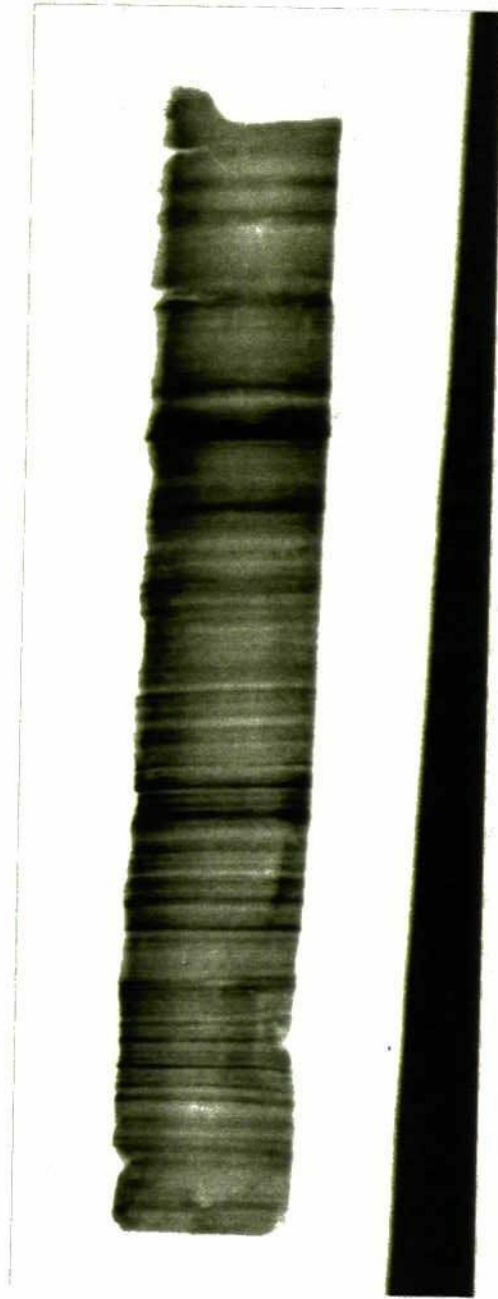
3 1/2

Core Ness 4 x-radiograph, 2.69-2.84 m



2/5

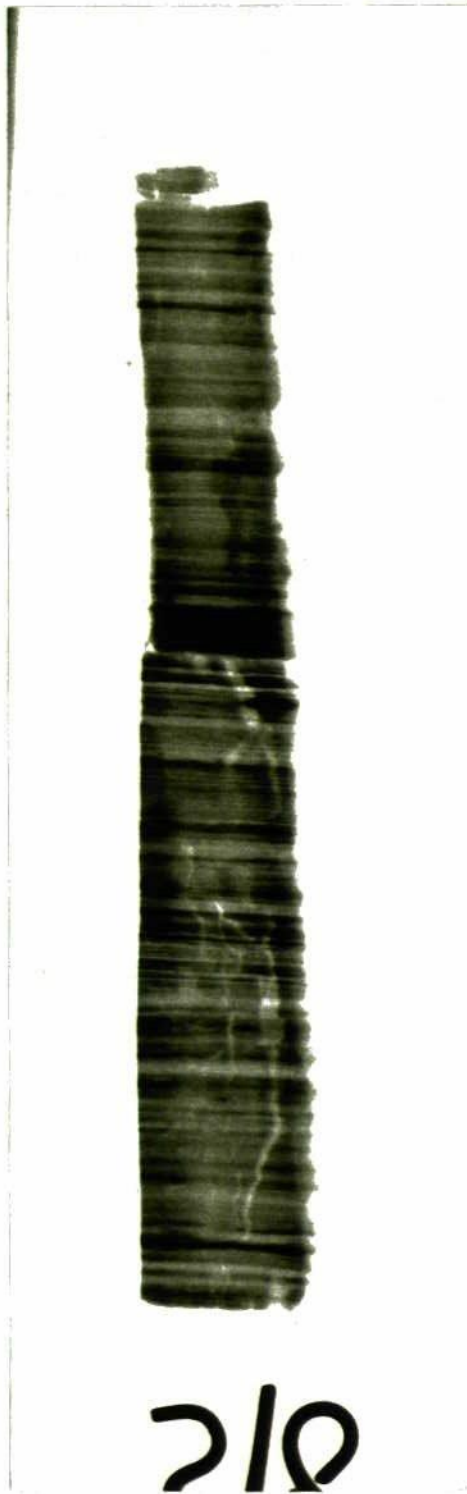
Core *Ness 4* x-radiograph, 2.83-2.98 m



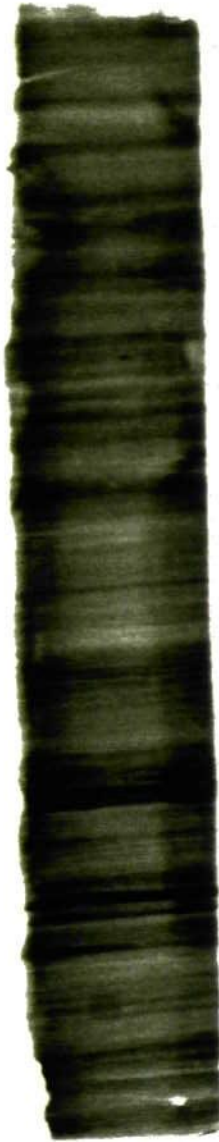
Core *Ness 4* x-radiograph, 2.97-3.12 m



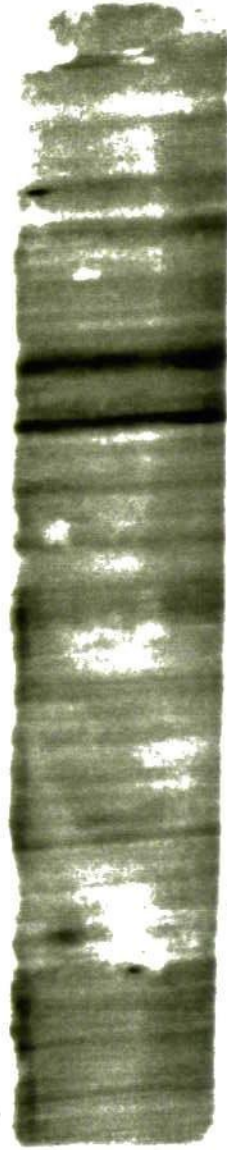
Core Ness 4 x-radiograph, 3.11-3.26 m



Core Ness 4 x-radiograph, 3.25-3.40 m

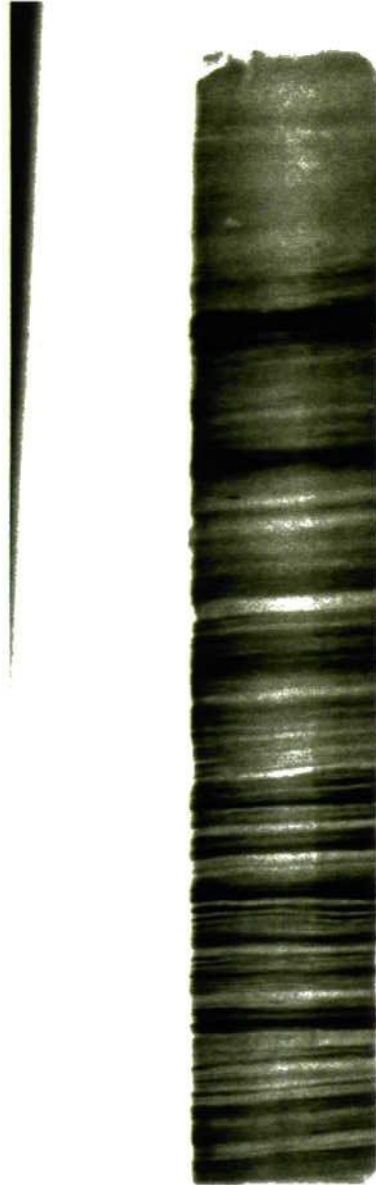


Core Ness 4 x-radiograph, 3.38-3.53 m

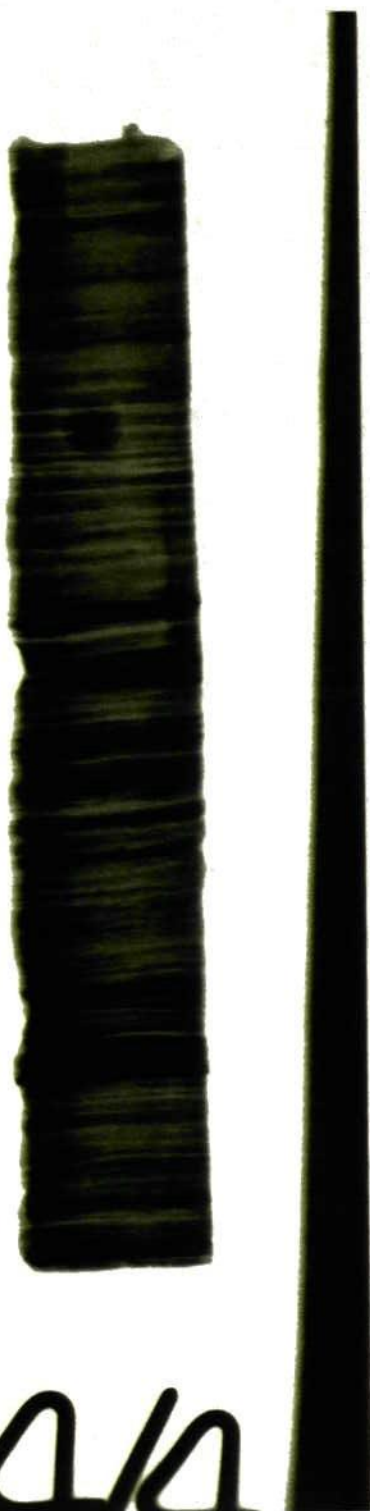


4/2

Core *Ness 4* x-radiograph, 3.52-3.67 m



Core Ness 4 x-radiograph, 3.66-3.81 m



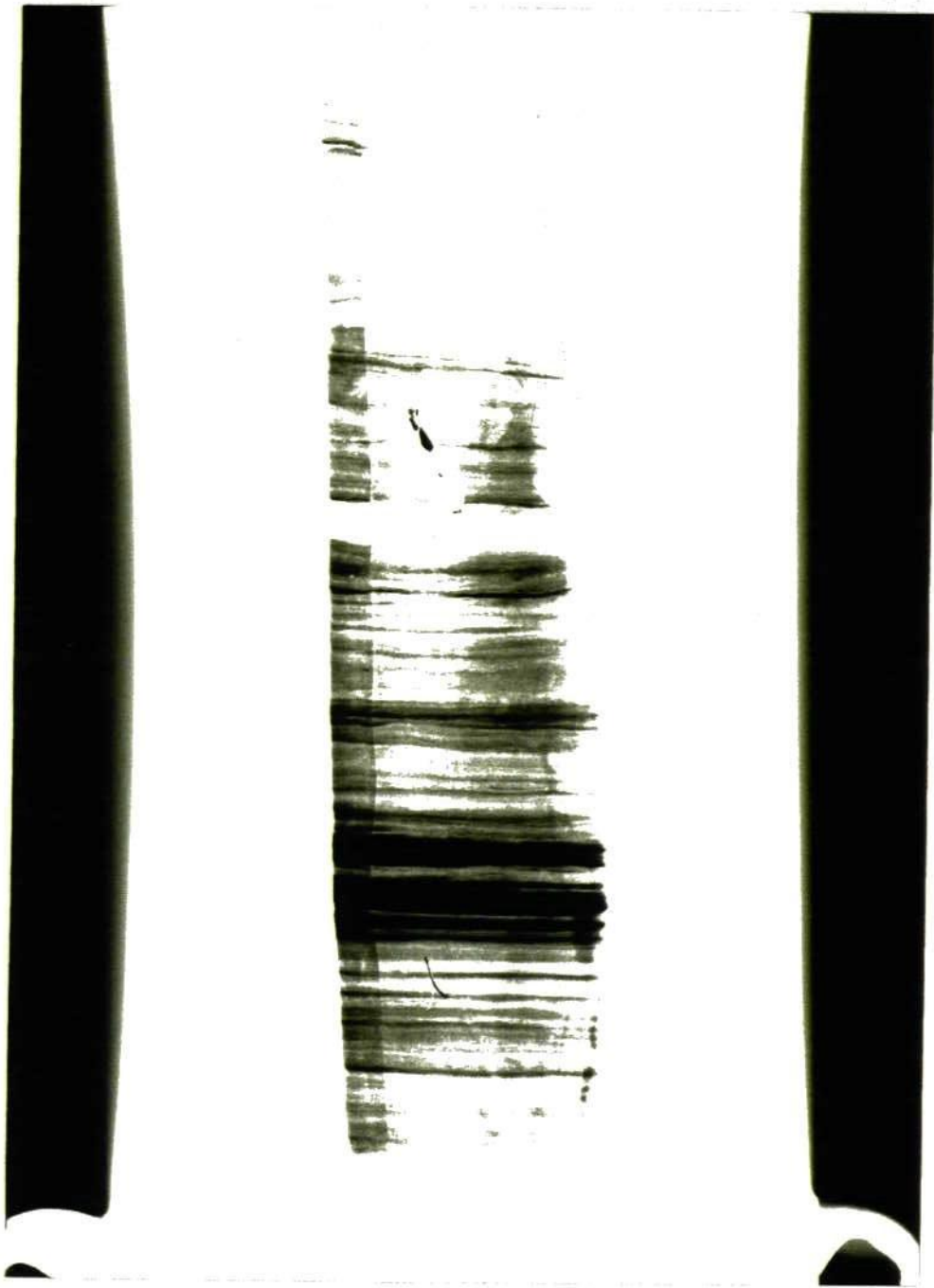
Core Ness 4 x-radiograph, 3.85-4.00 m



Core Ness 4 x-radiograph, 3.99-4.14 m. Clay/gyttja contact.

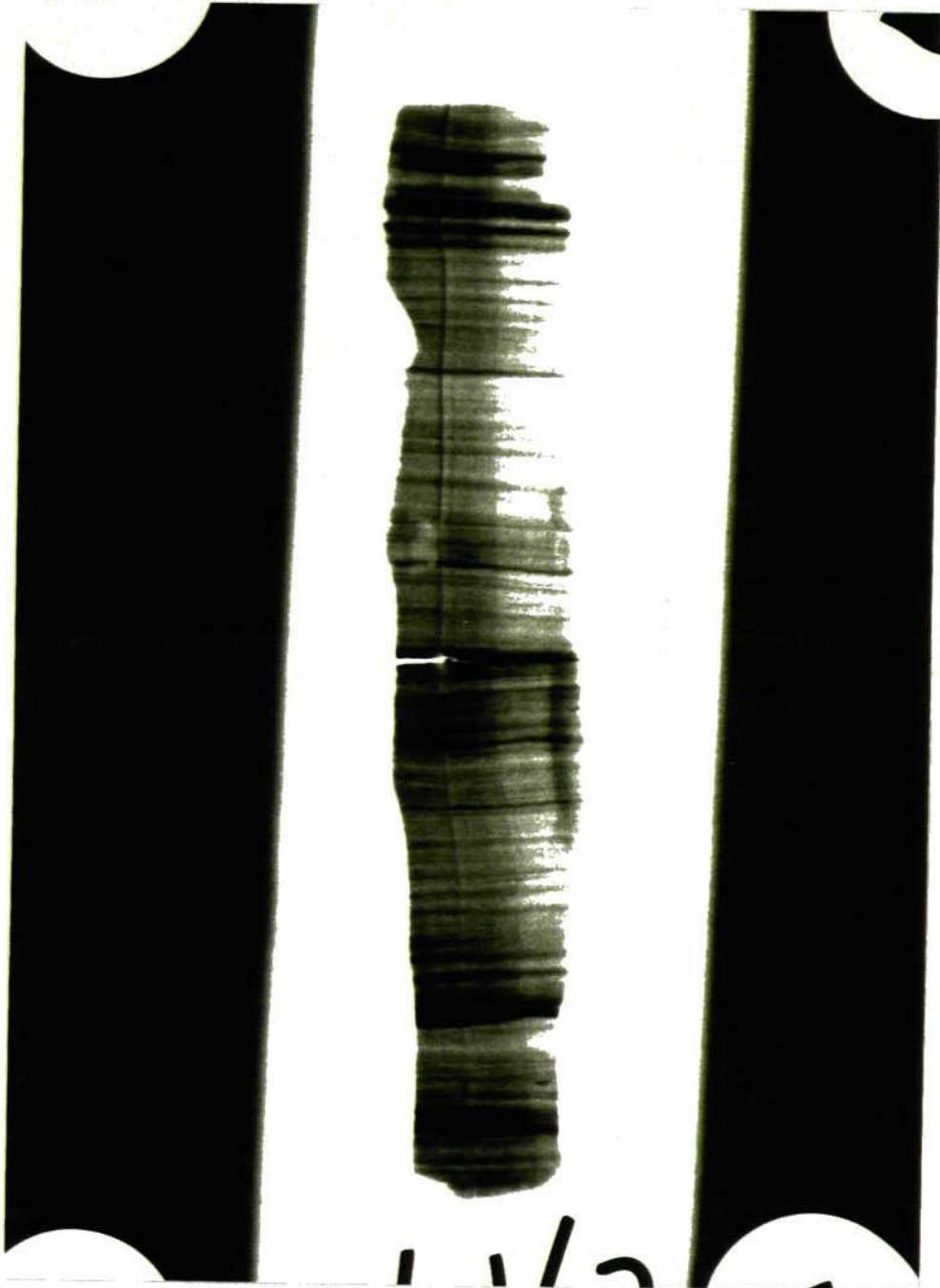


Core *LNRI* x-radiograph, 0.04-0.19 m



(X-radiograph produced by D.Bull, University of Southampton)

Core *LNR1* x-radiograph, 0.13-0.28 m

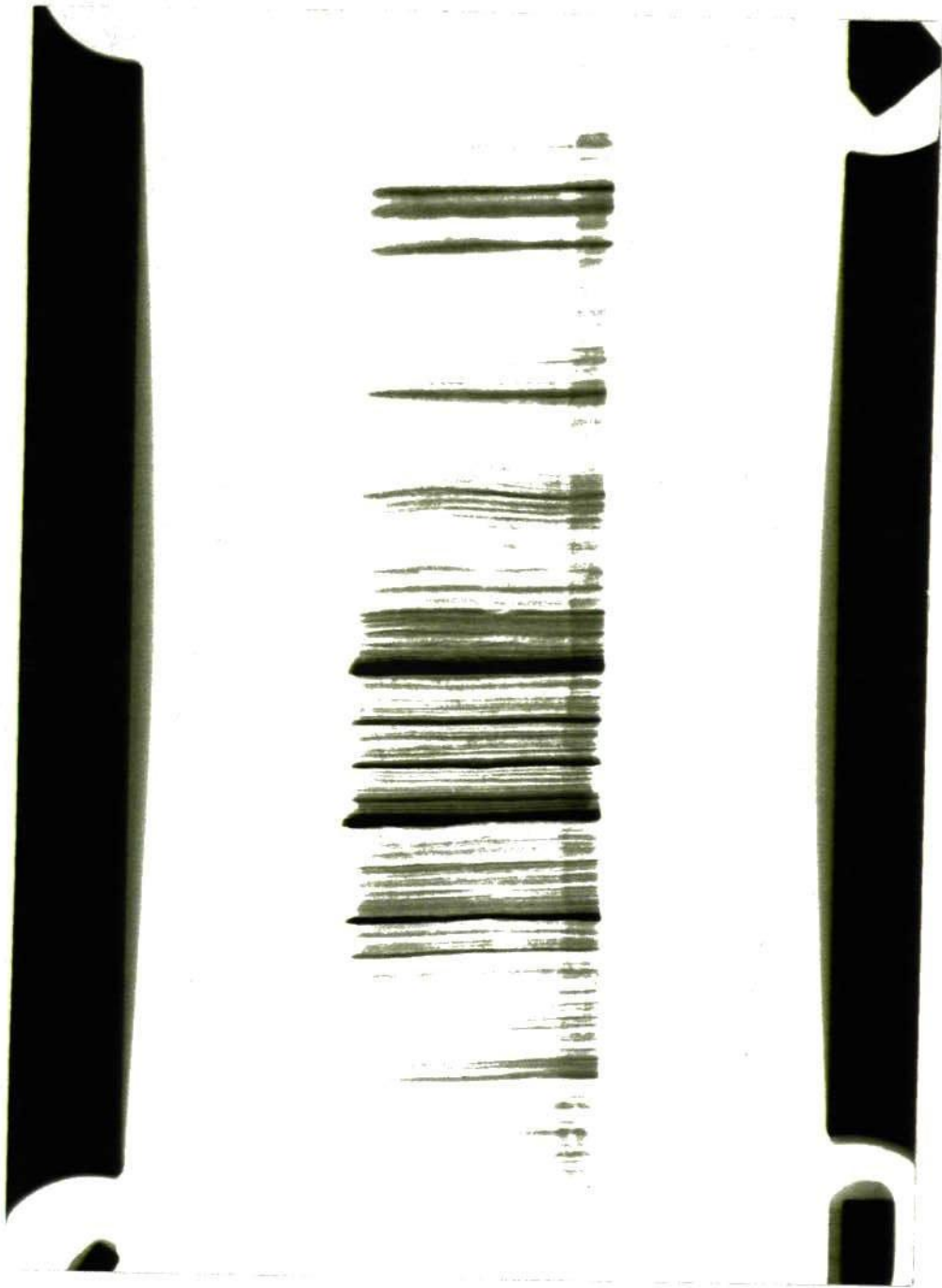


Core *LNRI* x-radiograph, 0.225-0.375 m



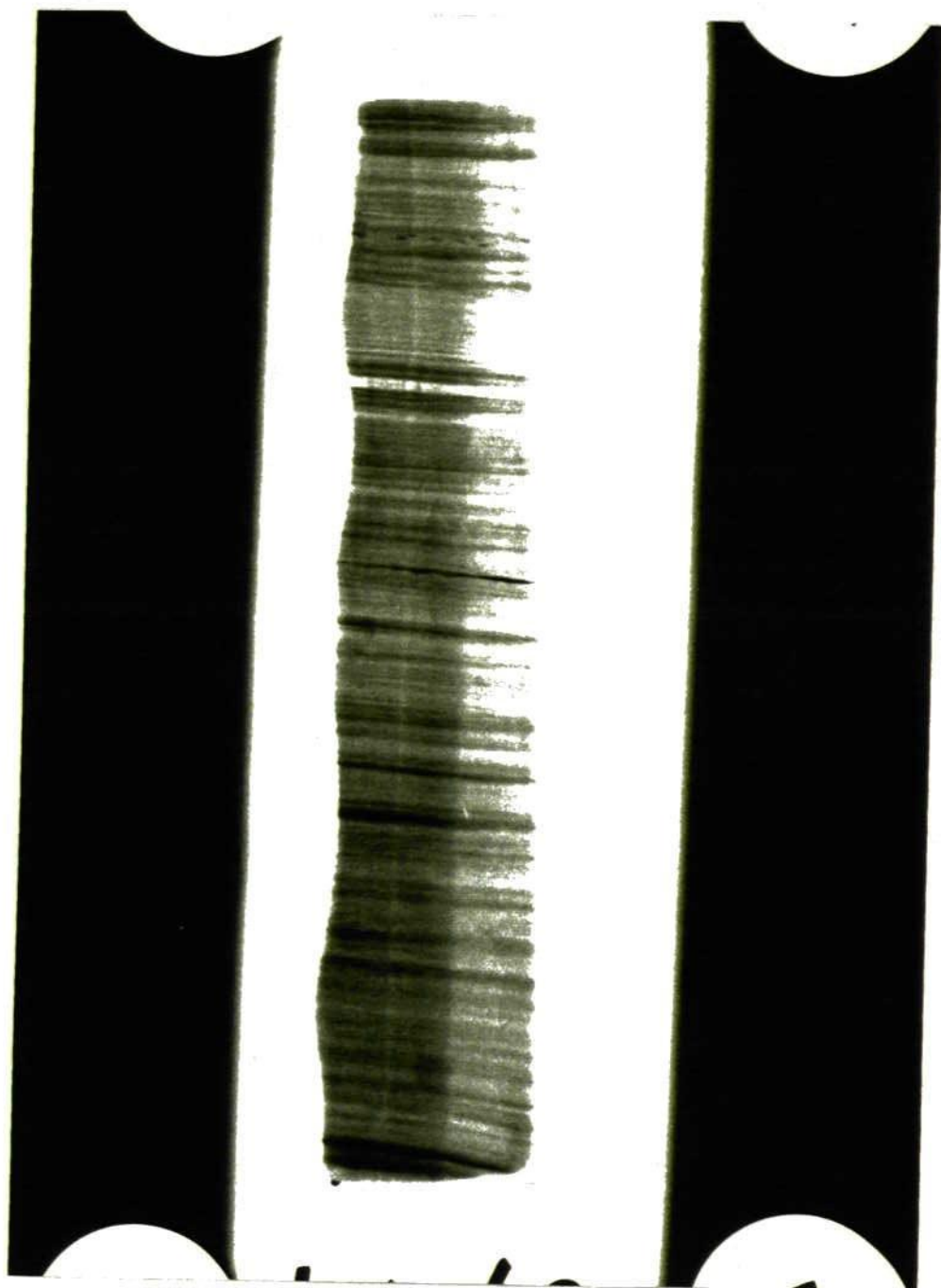
(X-radiograph produced by D.Bull, University of Southampton)

Core *LNRI* x-radiograph, 0.36-0.51 m



(X-radiograph produced by D.Bull, University of Southampton)

Core *LNRI* x-radiograph, 0.5-0.65 m



Core *LNRI* x-radiograph, 0.6-0.75m

